

AD-A129 508

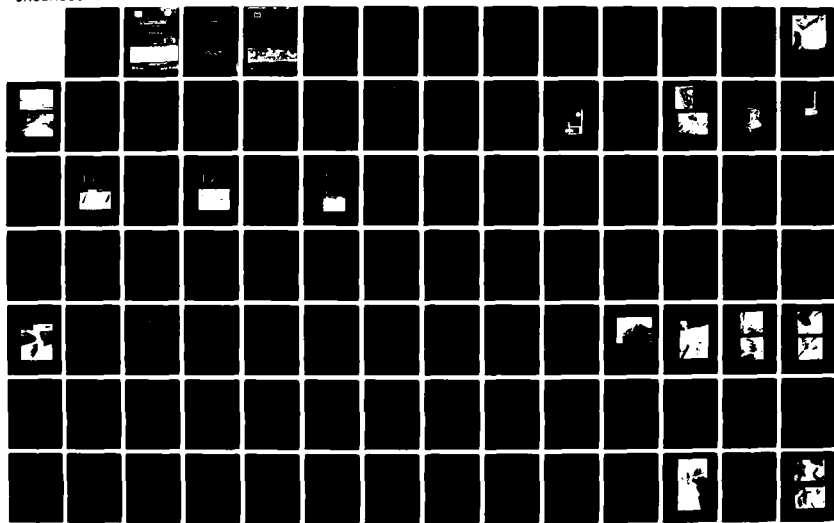
WEIR JETTY PERFORMANCE: HYDRAULIC AND SEDIMENTARY
CONSIDERATIONS(U) ARMY ENGINEER WATERWAYS EXPERIMENT
STATION VICKSBURG MS HYDRAULICS LAB W C SEABERGH
MAR 83 WES/TR/HL-83-5

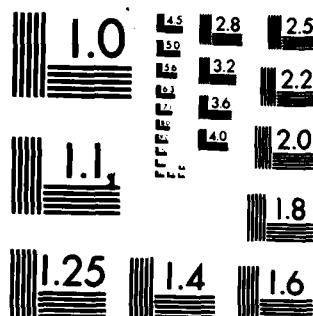
1/4

UNCLASSIFIED

F/G 13/2

NL





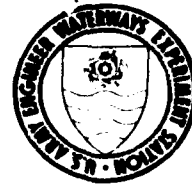
MICROCOPY RESOLUTION TEST CHART
NATIONAL BUREAU OF STANDARDS-1963-A

ADA 1 29508





12



TECHNICAL REPORT HL-83-5

ADA 129508

WEIR JETTY PERFORMANCE: HYDRAULIC AND SEDIMENTARY CONSIDERATIONS

Hydraulic Model Investigation

by

William C. Seabergh

Hydraulics Laboratory

U. S. Army Engineer Waterways Experiment Station
P. O. Box 631, Vicksburg, Miss. 39180

March 1983

Final Report

Approved For Public Release: Distribution Unlimited

DTIC
ELECTE
JUN 17 1983

A



Prepared for U. S. Coastal Engineering Research Center
Fort Belvoir, Va. 22060

DTIC FILE COPY

83 06 17 001

Destroy this report when no longer needed. Do not return
it to the originator.

The findings in this report are not to be construed as an official
Department of the Army position unless so designated
by other authorized documents.

The contents of this report are not to be used for
advertising, publication, or promotional purposes.
Citation of trade names does not constitute an
official endorsement or approval of the use of
such commercial products.

Unclassified

SECURITY CLASSIFICATION OF THIS PAGE (When Data Entered)

REPORT DOCUMENTATION PAGE		READ INSTRUCTIONS BEFORE COMPLETING FORM
1. REPORT NUMBER Technical Report HL-83-5	2. GOVT ACCESSION NO. AD-A129508	3. RECIPIENT'S CATALOG NUMBER
4. TITLE (and Subtitle) WEIR JETTY PERFORMANCE: HYDRAULIC AND SEDIMENTARY CONSIDERATIONS; Hydraulic Model Investigation		5. TYPE OF REPORT & PERIOD COVERED Final report
7. AUTHOR(s) William C. Seabergh		6. PERFORMING ORG. REPORT NUMBER
9. PERFORMING ORGANIZATION NAME AND ADDRESS U. S. Army Engineer Waterways Experiment Station Hydraulics Laboratory P. O. Box 631, Vicksburg, Miss. 39180		8. CONTRACT OR GRANT NUMBER(s)
11. CONTROLLING OFFICE NAME AND ADDRESS U. S. Army Coastal Engineering Research Center Fort Belvoir, Va. 22060		10. PROGRAM ELEMENT, PROJECT, TASK AREA & WORK UNIT NUMBERS
14. MONITORING AGENCY NAME & ADDRESS (if different from Controlling Office)		12. REPORT DATE March 1983
		13. NUMBER OF PAGES 299
		15. SECURITY CLASS. (of this report) Unclassified
		15a. DECLASSIFICATION/DOWNGRADING SCHEDULE
16. DISTRIBUTION STATEMENT (of this Report) Approved for public release; distribution unlimited.		
17. DISTRIBUTION STATEMENT (of the abstract entered in Block 20, if different from Report)		
18. SUPPLEMENTARY NOTES Available from National Technical Information Service, 5285 Port Royal Road, Springfield, Va. 22151.		
19. KEY WORDS (Continue on reverse side if necessary and identify by block number) Hydraulic models Hydraulic structures Jetties Sediment transport Tidal inlets		
20. ABSTRACT (Continue on reverse side if necessary and identify by block number) The weir jetty concept offers one alternative for jetty design at tidal inlets. Instead of impounding sand in a fillet upcoast of the jetty system where it is difficult to handle for sand bypassing, a low weir section of the jetty permits movement of the sand by wave- and tide-generated currents over the low weir into a deposition basin where it can be handled by a dredge in more protected waters.		

(Continued)

DD FORM 1 JAN 73 1473 EDITION OF 1 NOV 65 IS OBSOLETE

Unclassified

SECURITY CLASSIFICATION OF THIS PAGE (When Data Entered)

20. ABSTRACT (Continued).

> The hydraulic model investigation was performed to study important design parameters for a weir jetty system including weir length, elevation, orientation with respect to the shoreline and the conventional portion of the jetty structure, tidal currents over the weir section, flow patterns in the vicinity of the weir section, sediment movement over the weir and effects of the weir jetty on accretion, and erosion upcoast of the jetty system. The study was accomplished with a fixed-bed undistorted, 1:100 scale model. Large ocean and bay areas were reproduced in a 150-ft by 305-ft facility. Tides were reproduced in the model and two types of inlet-bay systems were simulated--one system in which the bay nearly fills (high Keulegan K value) and the other in which the bay only partially fills (low Keulegan K value). The conditions provided extremes of velocity-tidal elevation flow relationships over the weir. Sediment tracers and a movable-bed beach section provided the means to examine deposition basin filling, fillet accretion patterns for upcoast waves, and fillet removal by waves from the downcoast direction for several weir jetty orientations, including weir angles with the shoreline of 30, 45, 60, and 90 deg.

Results indicate the mean tide level weir elevation is the most practical elevation for providing wave protection for a dredge, good sediment transport across the weir, and good flood-ebb tidal flow relationships, i.e., moderate flood flow currents and little or no ebb flow. Strong ebb flow currents over the weir are not desirable as they might aid in migration of the navigation channel through the deposition basin. Jetty systems with the outer, more oceanward portions parallel to each other and at minimum spacing provide the best flow characteristics when tidal current migration through the deposition basin region is considered. Wave-generated currents upcoast of the weir jetty are not entirely captured by the weir but some current, and thus sediment, moves oceanward along the outer portion of the jetty. Also reflected waves off the jetty and weir structure combine with incident waves to form a short-crested wave field which aids in removal of sediment from the upcoast beach to various degrees, depending on the structure's angle with respect to the shoreline and the incident wave angle.

The effects of groins adjacent to the weir section were examined with regard to providing additional fillet storage and reducing the sediment movement in an oceanward direction along the jetty. Positive results were found for each variation tested.

PREFACE

Commanders and Directors of WES during the study were COL John L. Cannon, CE, COL Nelson P. Conover, CE, and COL Tilford C. Creel, CE. Technical Director was Mr. F. R. Brown.

1

CONTENTS

	<u>Page</u>
PREFACE	1
CONVERSION FACTORS, U. S. CUSTOMARY TO METRIC (SI) UNITS OF MEASUREMENT	3
PART I: INTRODUCTION	4
Background	4
Purpose of Study	8
PART II: THE MODEL	9
Design	9
Model Appurtenances	15
PART III: THE TESTING PROGRAM	21
Hydraulic Tests	21
Beach Response Tests	21
PART IV: HYDRAULIC TESTING	27
Flow Over the Weir	28
Flow Patterns for the Jetty Systems	36
PART V: BEACH RESPONSE TESTS	47
Short-Crested Wave Field and Beach Interaction	47
Preliminary Testing	65
Detailed Beach Response Testing	65
Comments on Test Conditions and Effects on Test Results . .	80
Discussion of Beach Response Tests	82
PART VI: OBSERVATIONS AND CONCLUSIONS	94
Hydraulic Testing	94
Beach Response Tests	97
Application to Weir Jetty Design	98
REFERENCES	104
TABLES 1-3	
PHOTOS 1-59	
PLATES 1-105	
APPENDIX A: TWO-DIMENSIONAL WAVE FLUME TESTS	A1
TABLE A1	
PLATES A1-A15	
APPENDIX B: NOTATION	B1

CONVERSION FACTORS, U. S. CUSTOMARY TO METRIC (SI)
UNITS OF MEASUREMENT

U. S. customary units of measurement used in this report can be converted to metric (SI) units as follows:

<u>Multiply</u>	<u>By</u>	<u>To Obtain</u>
cubic feet	0.02831685	cubic metres
cubic feet per second	0.02831685	cubic metres per second
cubic yards	0.7645549	cubic metres
cubic yards per second	0.7645549	cubic metres per second
feet	0.3048	metres
feet per second	0.3048	metres per second
feet per second per second	0.3048	metres per second per second
inches	25.4	millimetres
square feet	0.09290304	square metres

WEIR JETTY PERFORMANCE: HYDRAULIC
AND SEDIMENTARY CONSIDERATIONS
Hydraulic Model Investigation

PART I: INTRODUCTION

Background

1. Traditionally, jetties have been used to stabilize the location of a channel and to maintain channel dimensions to safely accommodate vessels of a given size. Jetties are normally constructed of quarystone and flank both sides of the desired channel alignment, extending from the shoreline to a depth usually governed by the desired depth of the entrance channel. A rule of thumb used in the past for shallower channels has been to extend the jetties to the depth contour corresponding to the entrance channel depth. However, with the advent of deeper channels for larger vessels this rule of thumb has often been disregarded due to the large expense of constructing longer jetties in much deeper water.

2. The sediment-laden coastal environment in which jetties are constructed contains the sediment-moving forces of wind waves, longshore currents, tidal currents (on the ocean coasts) or seiche currents (on lake coasts), and wind. The net result of jetty construction in this environment usually is the impoundment of sand against the jetties. If there is a net movement of sand in one direction along the coast, the impoundment on the updrift jetty side may increase until sand is able to move around the oceanward jetty tip and into the navigation channel. On the downdrift side of the jetty system erosion of the shoreline occurs, since the jetties have interrupted the normal supply of sand that is transported longshore. It must be kept in mind that the conceptual notion of upcoast and downcoast drift is quite idealized. In reality sand is transported in both directions and it is likely that a fillet will develop on both sides of the jettied inlet (the larger fillet on the updrift side), and the more nearly balanced the north and south

transport rates, the more likely that erosion can occur on both sides of the inlet.

3. One of the shortcomings of typical parallel jetties is that there is no sheltered location for a dredge to operate when it is necessary to bypass sand. One concept to overcome this shortcoming is the weir jetty system. A weir jetty is defined here as a shore-connected jetty structure, usually of rubble-mound construction, whose shoreward end is constructed to an elevation such that it acts as a weir, and water and sediment can be transported over this portion of the structure for part or all of a normal tidal cycle by tidal and wave-generated currents. The weir itself can be constructed of rubble-mound stone or, for more accurate elevation control, can be constructed of concrete or metal sheet pile. On the lee side of the weir a deposition basin may be dredged to act as a settling basin for sediments passing over the weir. The weir acts as a breakwater for waves and provides a semiprotected area for dredging of the deposition basin when it has filled. The basin is dredged to store some estimated quantity of sand moving into the basin during a given time period (i.e., storage of 6 months, 1 year, 2 years, etc.). A hydraulic dredge working in the semiprotected waters can bypass or backpass to mitigate potential beach erosion. In this way the inlet may act as a source of sand instead of a sink. The jetty system may have one weir on the updrift side of the channel which will be increasingly effective as longshore transport becomes more nearly unidirectional. For a jettied system with a near balance of longshore transport rates, consideration should be given to a weir section in both jetties.

4. This concept has been used recently with varying degrees of success. The idea originated at Hillsboro Inlet, Fla., as far as sand bypassing applications are concerned; however, weir jetties were constructed at Charleston Harbor as early as the 1800's to induce a net ebb flow in the region between the jetties (Figure 1). These weirs were at -13 ft* below low water elevation and thus the predominant ebb flow

* A table of factors for converting U. S. customary units of measurement to metric (SI) units is presented on page 3.



Figure 1. Weir jetties at Charleston Harbor

flushed channel sediments oceanward (Mason 1977). Hillsboro Inlet is bounded on the upcoast side by a rock reef which is an extension of the shoreline near the inlet (Figure 2). Longshore drift passed over the reef into a basin dredged behind it. Details of this and other weir jetty projects at Masonboro Inlet, N. C., Perdido Pass, Ala., East Pass, Fla., and Ponce de Leon Inlet, Fla., are presented in Weggel (1981). Parker (1979) also presents an informative summary of weir jetty projects. Figure 3 shows the weir jetty system at Murrell's Inlet, S. C.

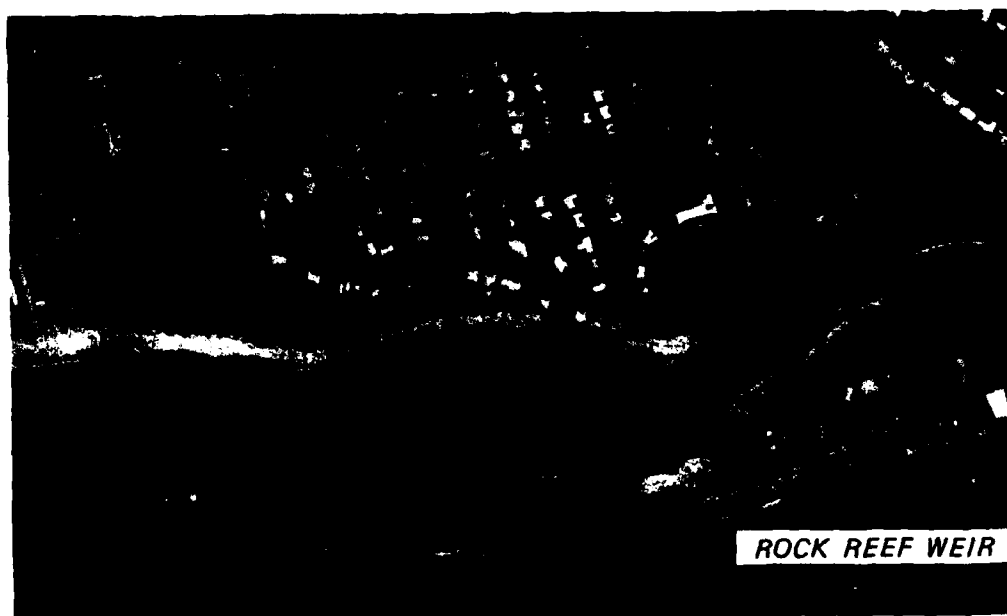


Figure 2. Hillsboro Inlet, natural weir jetty



Figure 3. Murrells Inlet weir jetty

Purpose of Study

5. This study was performed in order to evaluate the effect of the variation of a number of design parameters upon the capability of a weir jetty system to function as an efficient sediment-handling system. The experimental procedure, discussed later, was to construct a fixed-bed model of a generalized inlet entrance and to evaluate various configurations through injection of a tracer material and the simulation of tides and wind waves and their associated hydraulic currents. Important parameters to be investigated were weir orientation, weir elevation, and weir length.

PART II: THE MODEL

Design

6. Model dimensions and scale were based on reproducing realistic parameters for inlet width, bay size, jetty length, and offshore bathymetry. The model was constructed to an undistorted scale to assure simultaneous similitude of both diffraction and refraction.

7. A scale of 1:100 was selected based on model scale requirements for accurate reproduction of waves and currents and size of the area and jetty system to be modeled. Figure 4 shows the test basin with a typical jetty system layout. The inlet was shifted laterally from the center of the test basin to maximize the upcoast beach length. Any larger model scale would not have provided a sufficient upcoast shoreline nor provided a realistic bay size (in the facility used) behind the inlet. A smaller scale model would have resulted in excessive viscous friction significantly affecting wave propagation.

8. From an extensive examination of prototype inlets, dimensions considered representative of typical breadth, shallow inlet channels were selected as follows:

Maximum cross section at throat (trapezoidal channel)	21,000 ft ²
Spacing between jetties	1200 ft
Channel depth	21.5 ft
Jetty length (measured oceanward from the high water line)	2600 ft

The weir jetty was constructed in the model of sheet metal and rock to represent a prototype jetty with a concrete sheet pile weir and rubble-mound construction both landward and seaward of the weir. Elevation of the rubble portion of the jetty was +10.0 ft mean sea level (msl) and the elevation of the weir was 0.0 msl or +2.5 ft mean low water (mlw). It was decided to model a concrete sheet pile weir in the prototype (such as Masonboro Inlet, N. C., Perdido Pass, Fla., and East Pass, Fla.) instead of the rubble-mound type (such as Murrells Inlet, S. C.) in

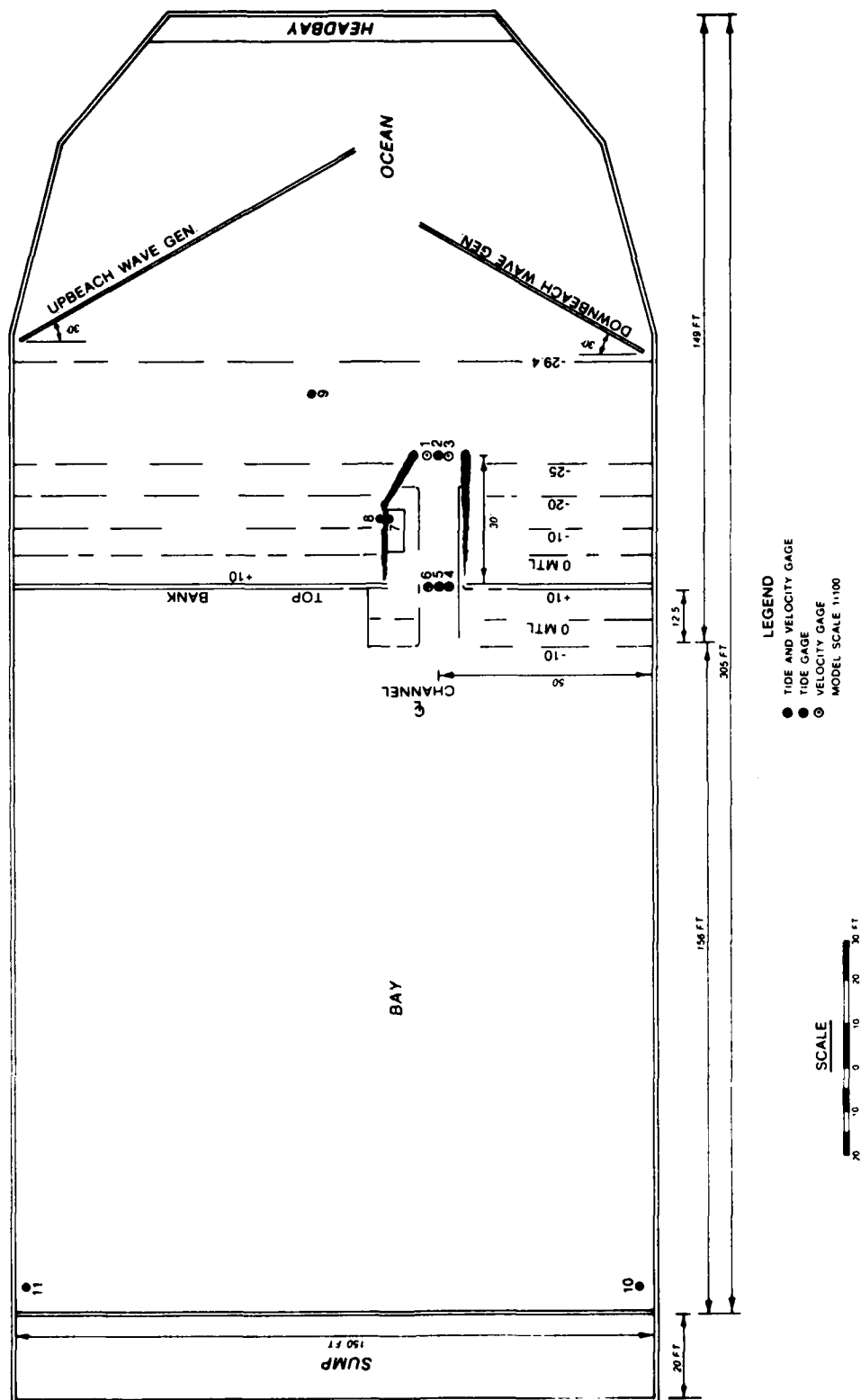


Figure 4. Model basin

order to have better control of elevation in the model which would contribute to more accurate measurements of head difference and flow across the model weir. The jetty had an impermeable core in the model so that flow through the channel and over the weir could be more accurately quantified. An average reflection coefficient of 0.30 was measured for the model jetty, a value believed to reasonably represent reflection in the prototype (Thornton and Calhoun 1972).

9. Examination of Figure 4 shows that the bathymetric contours were parallel to the shoreline. This bathymetry was chosen to maintain the same bottom slopes adjacent to various structures and to easily and cost effectively modify the structural configuration of the weir jetty system. Usually as one approaches an inlet, the bathymetric contours indicate an accumulation of sediments seaward of the inlet. Consequently, the seaward terminus of the model jetties is in relatively deeper water than the prototype might be. This difference between the model and typical prototype jetties is probably unimportant to most hydraulic tidal phenomena, but it may be important relative to wave refraction and sediment movement near the seaward terminus of the jetty structure. There will be some further discussion of this point later in the report. Idealized, parallel contours and the absence of an offshore bar made comparisons between various structural configurations easier. It might be desirable in a later study to repeat certain tests with seaward-directed bottom contours near the inlet and an offshore bar.

10. The model was designed to realistically reproduce tidal currents through the inlet and over the weir section. The bay area was sized to accommodate the expected tidal prism of an inlet with the given cross section described earlier and as related by O'Brien's (1969) empirical relationship between the equilibrium minimum cross-sectional flow area below mean sea level A_{CE}^* (ft^2), and tidal prism P (ft^3):

* For convenience, symbols and unusual abbreviations are listed and defined in the Notation (Appendix B).

$$A_{C_E} = 4.69 \times 10^{-4} P^{0.85} \text{ (for jettied inlets)} \quad (1)$$

Bay size was selected so it would fill completely, thus providing an inlet with a high Keulegan K , or repletion coefficient, where K is defined by O'Brien and Dean (1972) as:

$$K = \frac{T}{2\pi a_o} \frac{A_c}{A_b} \left(\frac{2ga_o}{F} \right)^{1/2} \quad (2)$$

in which

- T = tidal period, sec
- a_o = ocean tidal amplitude, half range, ft
- A_c = cross-sectional area of inlet, ft^2
- A_b = surface area of bay, ft^2
- g = acceleration due to gravity, ft/sec^2
- F = inlet impedance = $K_i + K_e + fL_c/4R_c$
- K_i = inlet entrance loss coefficient
- K_e = inlet exit loss coefficient
- f = Darcy-Weisbach friction coefficient
- R_c = hydraulic radius of flow area, ft
- L_c = channel length, ft

It was also desirable to model a low K value inlet because of the significant change in velocity-tidal elevation relationship with a significant change in K which would in turn produce different flow conditions at the weir section. Examining the expression for Keulegan's K , it is noted that K is inversely proportional to A_b . If all other terms in the expression for K are held constant, from a graph of a_b/a_o versus K from Dean (1971), where a_b = tide amplitude in bay shown in Figure 5, it can be found that:

$$\frac{a_b}{a_o} \approx 0.8 K^{0.75} \text{ for } 0.2 < K < 0.8 \quad (3)$$

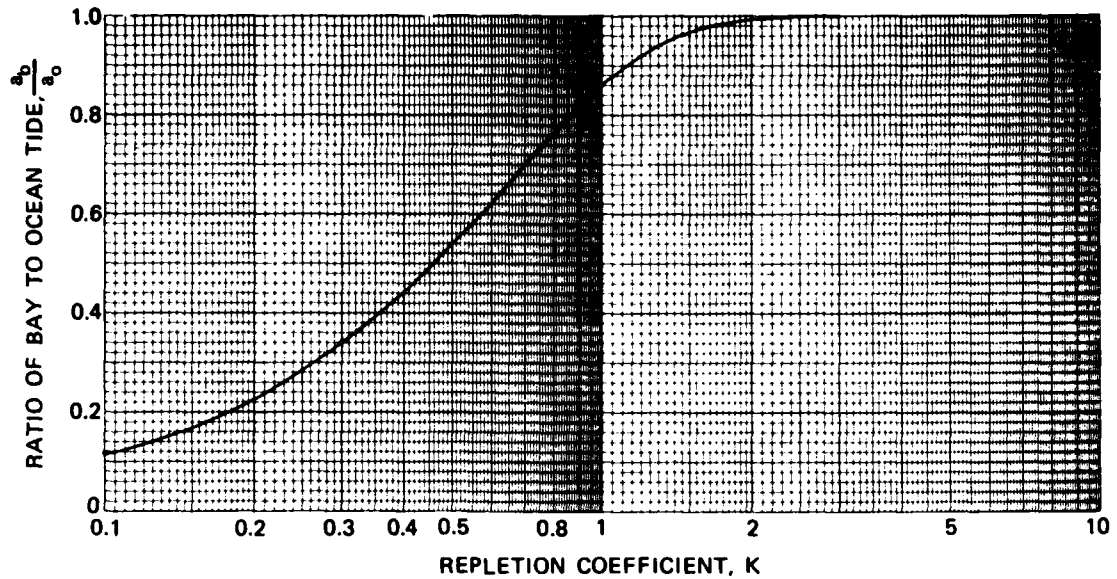


Figure 5. Ratio of bay to ocean tide amplitude versus Keulegan repletion coefficient, K

Also the tidal prism P can be defined as:

$$P = A_b \cdot a_b \quad (4)$$

Substituting in the expression for K, it can be found that

$$P \propto \frac{1}{K^{0.25}} \quad (5)$$

Therefore while trying to reduce K by increasing bay area, the tidal prism would be increased. Thus in changing from the high K value (say, 1.75) to a low K value (say, 0.2), the tidal prism would increase by a factor of 2. The increase in tidal prism would mean an increase in velocity to values double the high K velocity values (since the area, A_c , is fixed). Since the high K inlet is designed to have an area in equilibrium with its tidal prism, which in turn would have maximum velocities of 4 to 5 fps (prototype), then velocities of 8 to 10 fps would occur for the low K inlet, much too high for an equilibrium condition. In order to reduce this prism increase and its associated velocity

increase, it was felt an increase in F would be appropriate. This was performed by adding roughness bayward of the inlet throat. The entrance channel between the jetties was left as is so that physical flow relationships between the weir and entrance channel would be unchanged from the high K inlet condition.

11. The creation of the low K inlet condition required the use of a storage sump at the rear of the bay. Two pumps and two programmable flow controllers were used to remove water from the bay during flood flow and store it in the sump. The same quantity that was removed was returned to the bay during ebb flow. Thus the bay tide range was reduced (producing a smaller K value) while about the same tidal prism of the high K inlet was maintained, thus simulating a bay of greater surface area.

12. As discussed previously, a 1:100 scale was chosen for the model. From this scale the following relations were computed based on the Froudian law of similitude:

<u>Characteristic</u>	<u>Model:Prototype- Scale Relation</u>
Horizontal length	$L_H = 1:100$
Vertical length	$L_V = 1:100$
Surface area	$L_H L_H = 1:10,000$
Volume	$L_H L_H L_V = 1:1,000,000$
Velocity	$L_V^{1/2} = 1:10$
Discharge	$L_V^{3/2} L_H = 1:100,000$
Time--tidal wave	$L_H L_V^{-1/2} = 1:10$
Slope	$L_V L_H = 1:1$
Time--wind wave	$L_V L_V^{-1/2} = 1:10$

One prototype tidal cycle (semidiurnal) of 12 hr and 25 min was reproduced in the model in 74.5 min.

Model Appurtenances

13. The model was equipped with the necessary appurtenances to reproduce and measure all pertinent phenomena including tidal elevations, current velocities, waves, and sediments used in shoaling tests. Apparatus used in connection with the reproduction and measurement of these phenomena included a tide generator and recorder, velocity meters, wave generators, wave gages, and tidal gages.

Tide generator

14. The model was equipped with an automatic tide generator designed and constructed by the U. S. Army Engineer Waterways Experiment Station (WES) and is shown schematically in Figure 6. The

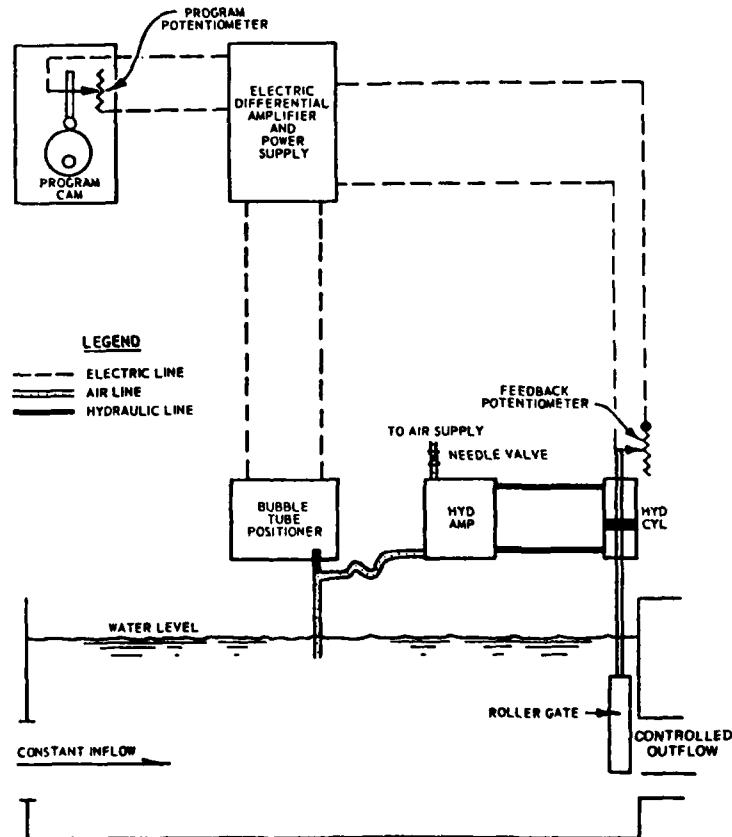


Figure 6. Automatic tide generator

five major components of the system were:

- a. The program cam.
- b. The differential amplifier and power supply.
- c. The bubble tube positioner.
- d. The hydraulic-pneumatic amplifier.
- e. The hydraulic cylinder and control gate assembly.

When the differential amplifier detected a difference between the water level sensed by the bubble tube positioner and the desired water level indicated by the program cam, a signal was transmitted to the hydraulic cylinder to alter the position of the control gate. A feedback control loop allowed time for the model to respond to the change in gate position before the next signal was accepted.

Velocity meters

15. Velocities of model tidal currents were measured with miniature Price-type current meters (Figure 7). The Price-type meter cups

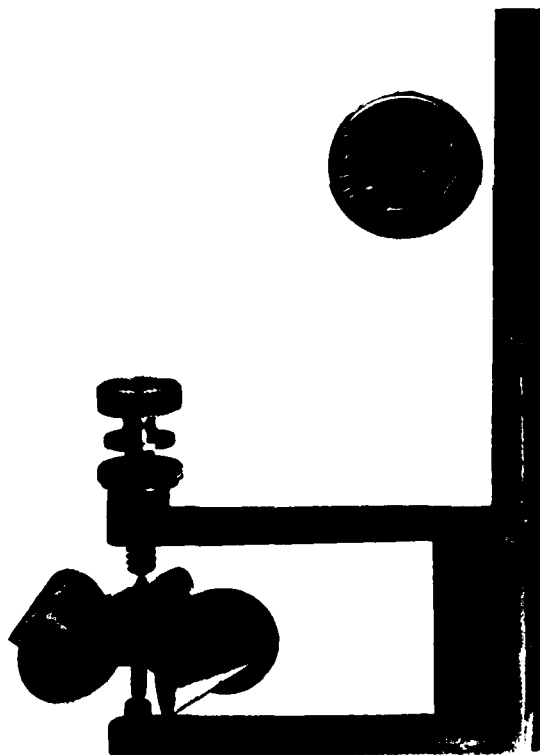


Figure 7. Miniature Price-type current meter

were about 0.04 ft in diameter, representing 4.0 ft vertically in the prototype. The center of the cup was about 0.045 ft from the bottom of the frame, representing 4.5 ft in the prototype. In a vertical plane, the entire meter occupied a space of about 3 by 7 ft when scaled to the prototype.

16. Velocities in the regions of wave-generated currents were usually measured by the use of dye since depths were shallow and the flow was turbulent. Dye movement was timed with a stopwatch over selected distances marked on the model bottom, and velocities were calculated from these measurements.

Photographic system

17. Surface current velocities were recorded photographically by a group of cameras mounted above the water surface of the model, with their shutters tripped simultaneously by an electronic timer to provide a time exposure of confetti float movement. An electronic strobe light was flashed near the end of each exposure so that a bright spot was recorded near the tip of the float streak, indicating the direction of movement. Lengths of streaks shown on the photographs can be converted to velocities when used with a scale shown below each set of photographs (Photos 1-59).

Wave generators

18. Wave action was reproduced in the model with 90-ft-long (upcoast) and 40-ft-long (downcoast) wave generators located at appropriate angles to the shoreline. Vertical plunger-type wave generators (Figure 8) were used and could be adjusted quickly to generate the wave height and wave period required.

Automated Data Acquisition and Control System (ADACS)

19. This system (designed at WES) was used to secure wave height data at selected locations in the model. Through the use of a mini-computer, ADACS recorded onto magnetic tape the electrical output of parallel-wire, resistance-type sensors (Figure 9). These sensors measured the change in water-surface elevation with respect to time. The magnetic tape output of ADACS then was analyzed by computer. A detailed



Figure 8. Vertical plunger wave generator

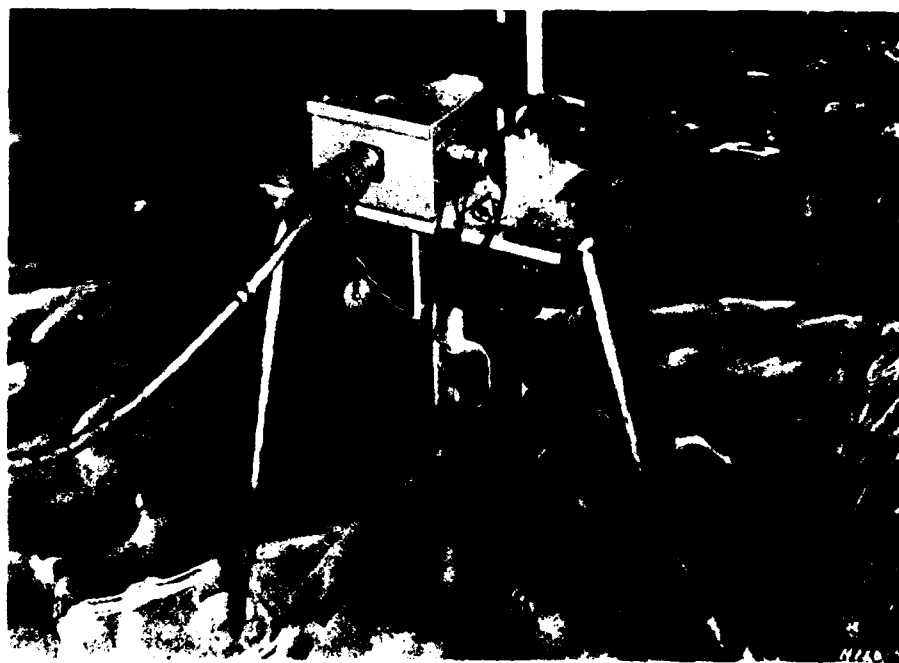


Figure 9. Wave gage

discussion of this system is found in Durham, Greer, and Whalin (1975).

Tide gages

20. Tidal-stage history was measured by the use of an electronic system consisting of a transmitter (Figure 10) and a recorder (Figure 11) with a telemetering circuit consisting of two selsyn motors, one in the transmitter and the other in the recorder, connected by an electrical cable. The tidal stage transmitter, positioned over the desired data gathering point, measured the water-surface elevation by means of an electronic sensing probe and transmitted this elevation to a recorder located in a control or instrument house. An ink pen continuously recorded the water-surface elevation on a chart that was

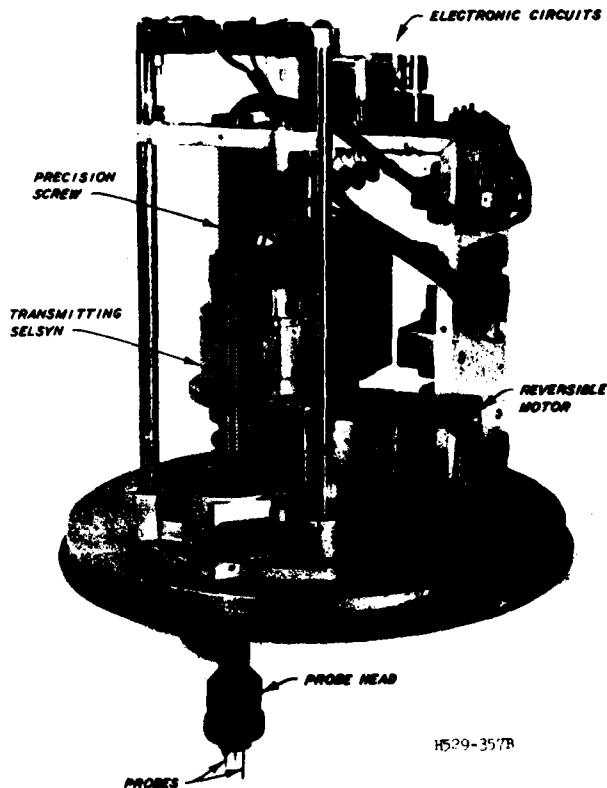


Figure 10. Water level transmitter of tide gage

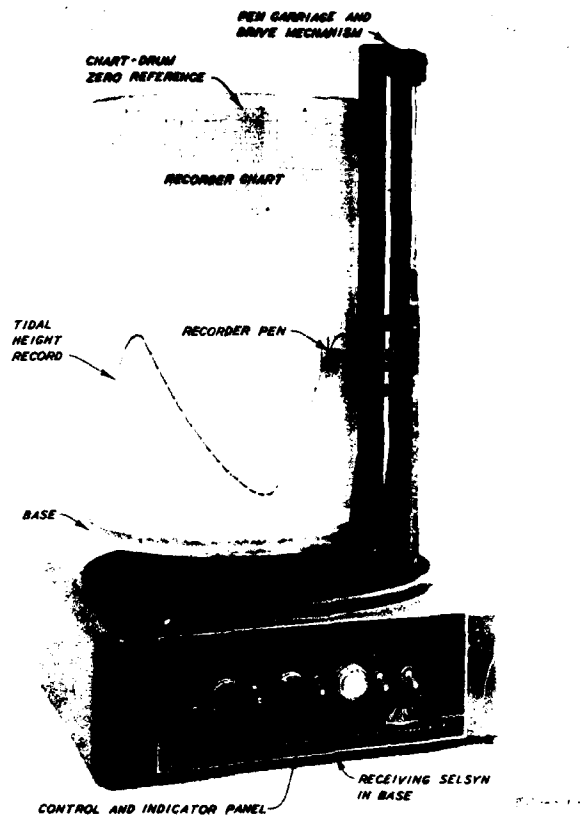


Figure 11. Water level recorder of tide gage

turned automatically at a preset rate to give a plot of water-surface elevation as a function of time. Portable point gages also were used to measure tidal elevations at other points as required.

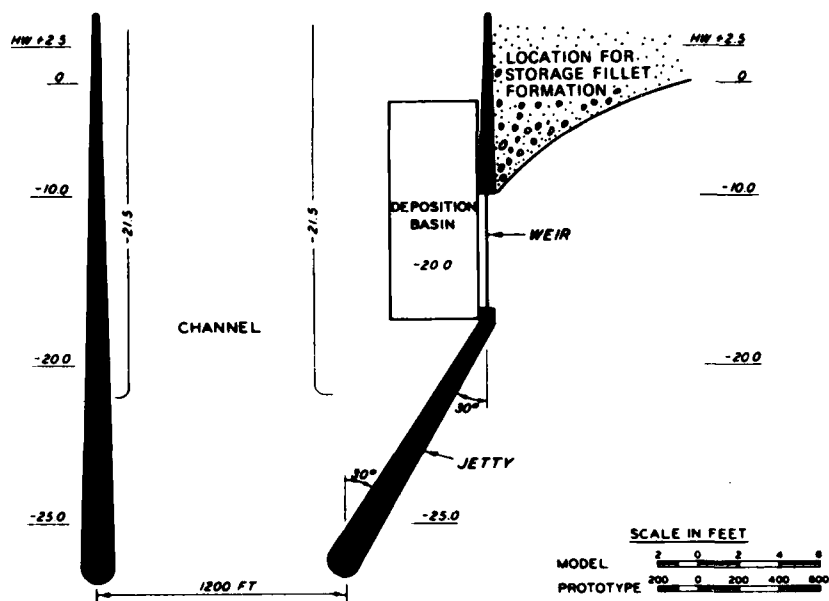
PART III: THE TESTING PROGRAM

Hydraulic Tests

21. Tests were divided into two categories. The first, hydraulic testing, focused on flow over the weir due to tidal currents. Two inlet types were modeled, as discussed in the section on model design. Head differences across the weir and velocities over the weir were measured and unit discharges and flow volumes over the weir were calculated. In order to study the effect of various entrance widths on flow over the weir, a series of tests was run in which the entrance cross-sectional area at the oceanward end of the jetty was reduced. These detailed hydraulic tests were run using the Plan 1 jetty system shown in Figures 12a and 12b. The weir was perpendicular to the shore and the 600-ft-long weir section was initiated at the minus 10-ft contour. This weir location was selected in an attempt to provide a region for a storage fillet to form upcoast of the weir section between the minus 10-ft contour and the initial water line so that when waves from downcoast occurred they could transport some material back upcoast and attempt to restrict the deposition basin to capturing as near as possible the net drift rather than the total downcoast component of drift. Also included in the hydraulic portion of testing was an examination of wave-induced currents along the upcoast jetty and shoreline for both tidal and nontidal conditions. Various upcoast jetty structures were investigated in this phase of testing.

Beach Response Tests

22. The second category of testing was beach response testing, wherein a beach composed of a tracer material was placed on the concrete model contours. The beach extended seaward to the outer limit of the breaker zone. During testing, tracer material was fed at the upcoast end of the beach, and tracer movement was observed by surveying and photographing the beach planform and measurement of transport over the



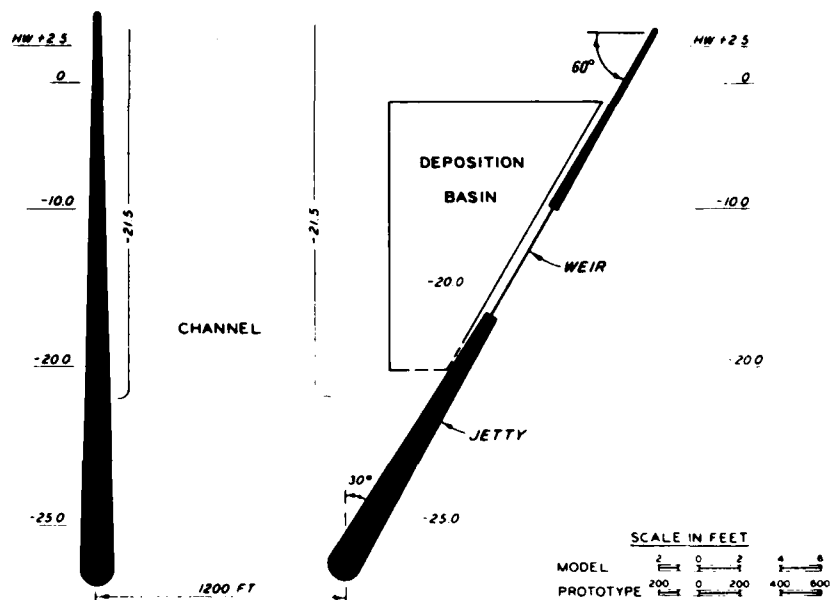
a. Schematic



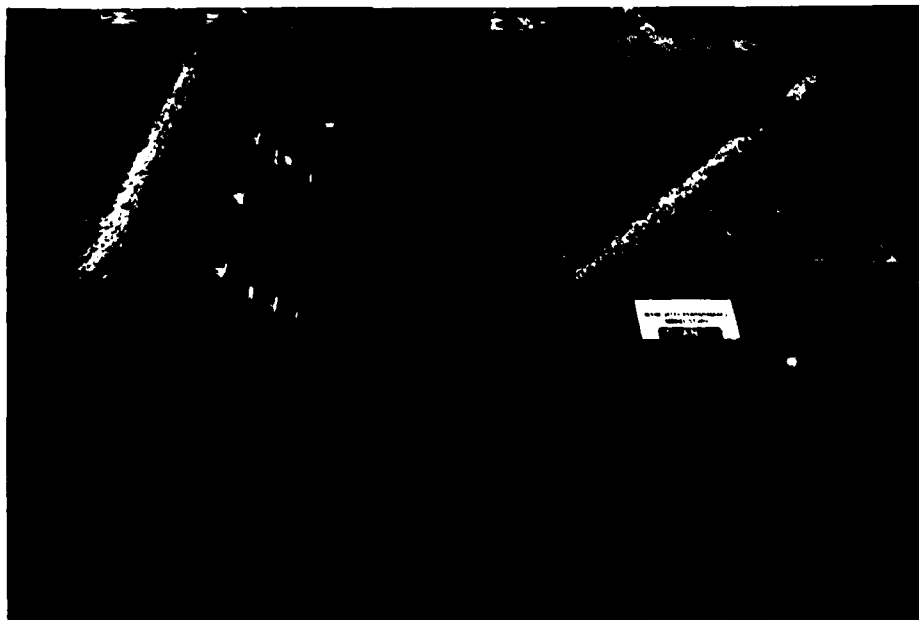
b. Model

Figure 12. Plan 1 weir jetty system

weir. Tests were run for three different jetty configurations which included four different weir section-shoreline angles. The second and third jetty configurations are seen in Figures 13a and 13b and 14a-f and are identified as Plan 2 and Plan 3. Plan 3 had five variations, including two weir angles of 30 and 45 deg. The Plan 2 weir angle was 60 deg as was the entire jetty structure. Plan 3 jetties all had an oceanward jetty trunk perpendicular to shore. This was necessary in order to accommodate such small angled weirs. A 45- or 30-deg angle the entire length of the upcoast jetty would extend too far upcoast to be practical. Thus, these combinations of weir angles and jetty trunk angles seemed appropriate in order to minimize as much as possible the upcoast extent of the jetty system. In the case of the 90- and 60-deg weir angles, it was felt that an angled oceanward jetty trunk was necessary to provide a protected region, which was offset from the channel, for the deposition basin. This would reduce wave activity in the basin resulting from waves entering between the jetties and also reduce the chance of tidal currents cutting through the basin. Plans 3A, 3B, and 3D involved spur structures, which in the case of 3A and 3B were to aid in forming a large storage fillet or in the case of 3D to attempt to reduce any tendency for material to bypass the weir and move along the jetty toward the channel.



a. Schematic



b. Model

Figure 13. Plan 2 weir jetty

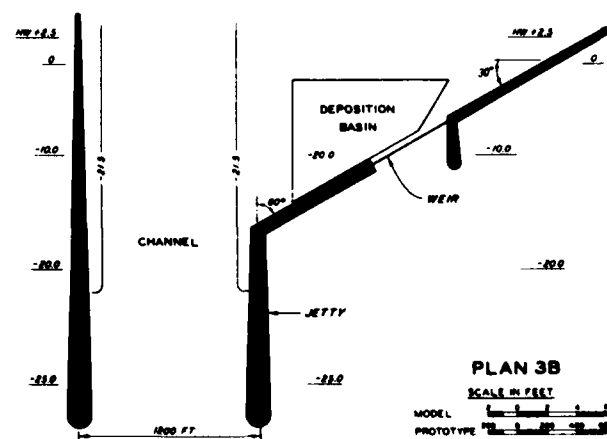
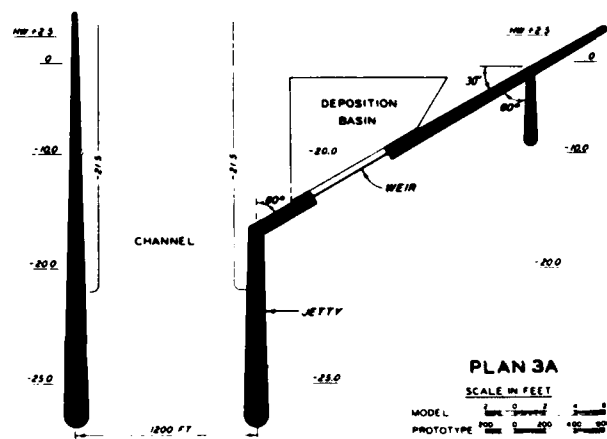
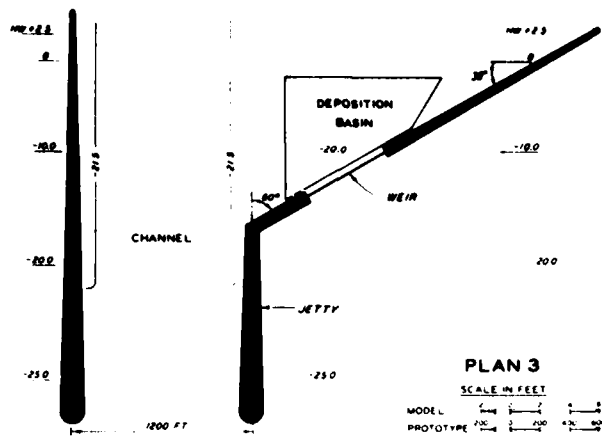


Figure 14. Plan 3 series of weir jetties
(Continued)

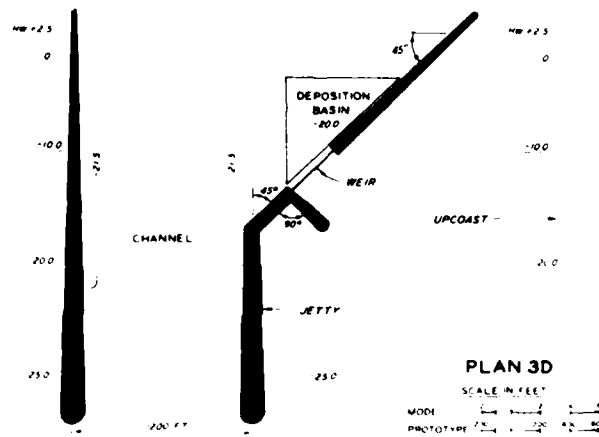
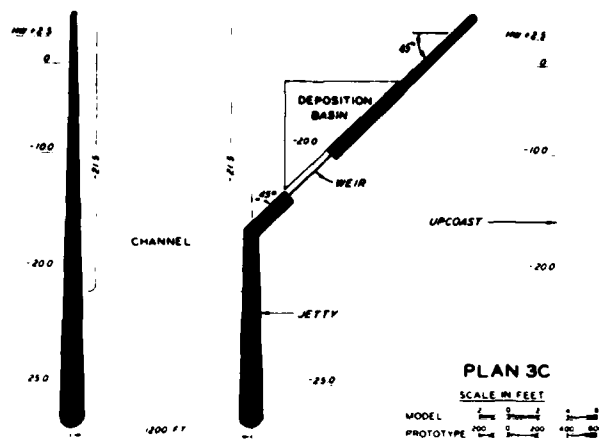


Figure 14. (Concluded)

PART IV: HYDRAULIC TESTING

23. The model was capable of reproducing the hydraulics of two types of inlets (see model design section): (a) an inlet characterized by a Keulegan K of 1.75, indicating that the bay completely fills producing a bay tide curve (compared with the ocean tide curve) as shown in Plate 1 and (b) an inlet with $K = 0.52$ indicating the bay only partially fills and produces a bay tide curve as shown in Plate 2. The importance of these two inlet types in this study lies in the different velocity-tidal elevation relationships that occur for the two different K values. For the high K inlets, the head difference between ocean and bay tides reverses near times of high and low water, and therefore the flow reverses from flood to ebb or ebb to flood at times of high and low water, respectively. Also maximum flood and ebb currents in the inlet occur at about midtide. For the low K inlet, the head difference between ocean and bay tides reverses at times closer to midtide. Maximum flood and ebb currents occur at times closer to high and low water, respectively, than for the high K inlets. Plates 3-8 show velocities taken at gage locations 1-6 (see Figure 4 for locations) in the inlet gorge and at the oceanward end of the jetties. The shift in velocity phase for the Plan 1A (low K) inlet relative to the Plan 1 (high K) inlet is shown.

24. Integration of flood and ebb velocities for the basic Plan 1 and 1A conditions indicated that the tidal prism for Plan 1A was larger than that of Plan 1 by about 29 percent. This was the result of not increasing F (inlet impedance) enough (see paragraph 10) in order to obtain a prism in equilibrium with the fixed minimum area. However, rather than continue trial and error testing to increase F , it was felt that the primary purpose of the change in K (to investigate the change in velocity phase with respect to water level) could be achieved without an exact duplication of the tidal prism. Also the testing concerning reduction in entrance channel area at the oceanward end would cause tidal prism changes which would have required extensive frictional adjustments. A means of adjusting the velocities for direct

comparison was developed and is discussed later.

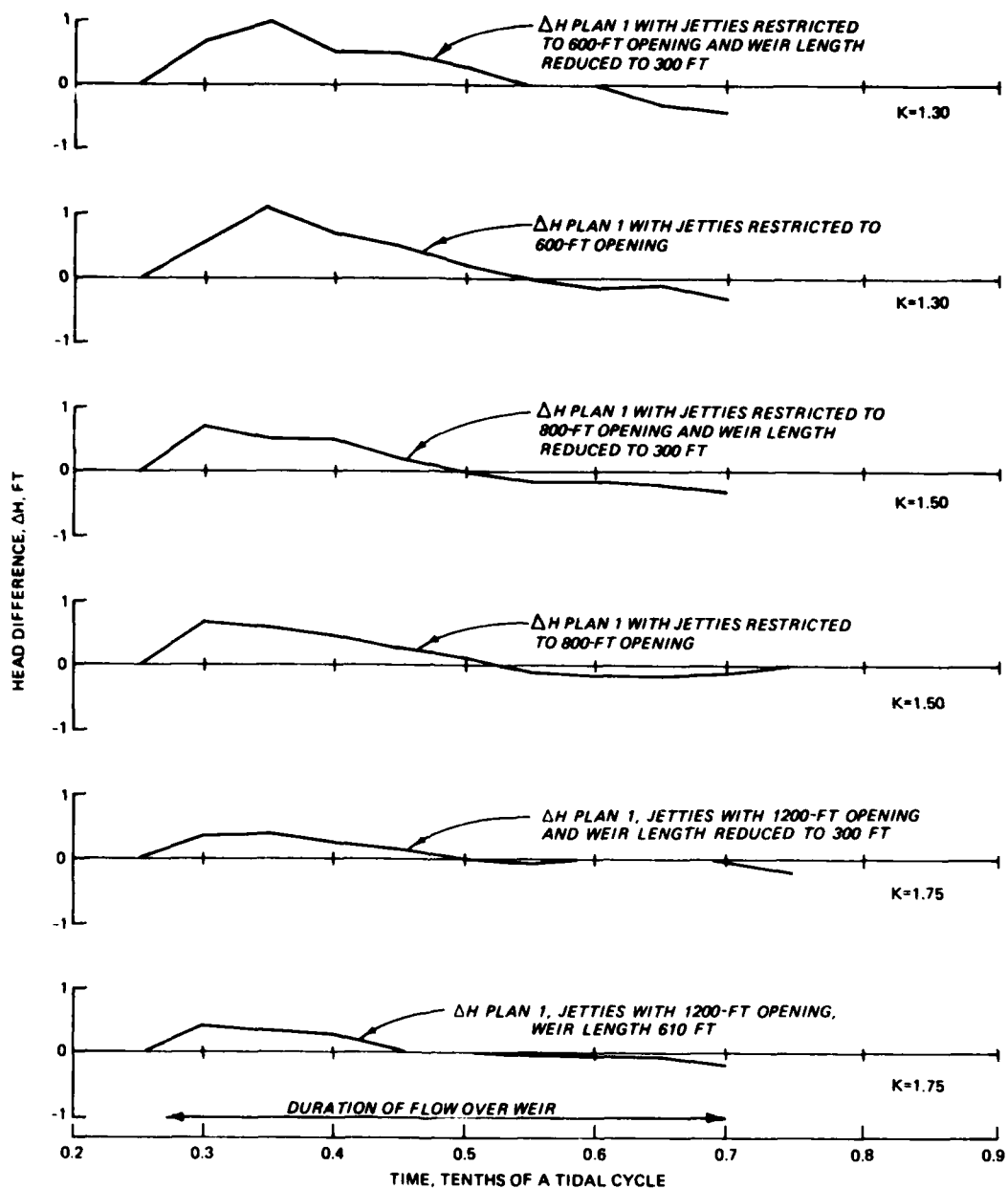
25. Plates 9, 10, and 11 show tidal elevations at various locations in the model (see Figure 4 for locations). Gages 10 and 11 show the changes in bay tides between Plans 1 and 1A. Gages 4, 5, and 6 at the inlet throat, gage 2 at the jetty tip, and gages 7 and 8 at the weir show smaller reductions for the Plan 1A condition. Gage 9, a control gage, indicates the ocean tides for the two tests were similar.

Flow Over the Weir

26. Detailed testing of flow over the weir was conducted for the Plan 1 and 1A jetty system for tidal flow conditions simulating a 5-ft ocean tide range with the weir elevations at mean tide level (mtl). Weir widths were 610 and 300 ft, with the latter achieved by closing off the oceanward side of the weir. After the initial testing for the Plan 1 and 1A conditions, the cross-sectional area at the jetty tips was reduced since there are many possibilities of various cross-sectional areas in this region of a jetty system (i.e., dependent upon shore bottom slope, existing shoals, and channel dimensions). Ratios of area at the jetty tip to the area at the inlet gorge (the minimum cross-sectional area of the entrance channel) were 1.48 (with no reduction in area at the jetty tip), 1.03, and 0.77. These reductions changed the inlet hydraulics, producing new Keulegan K values.

Tidal elevations and head differences across weir

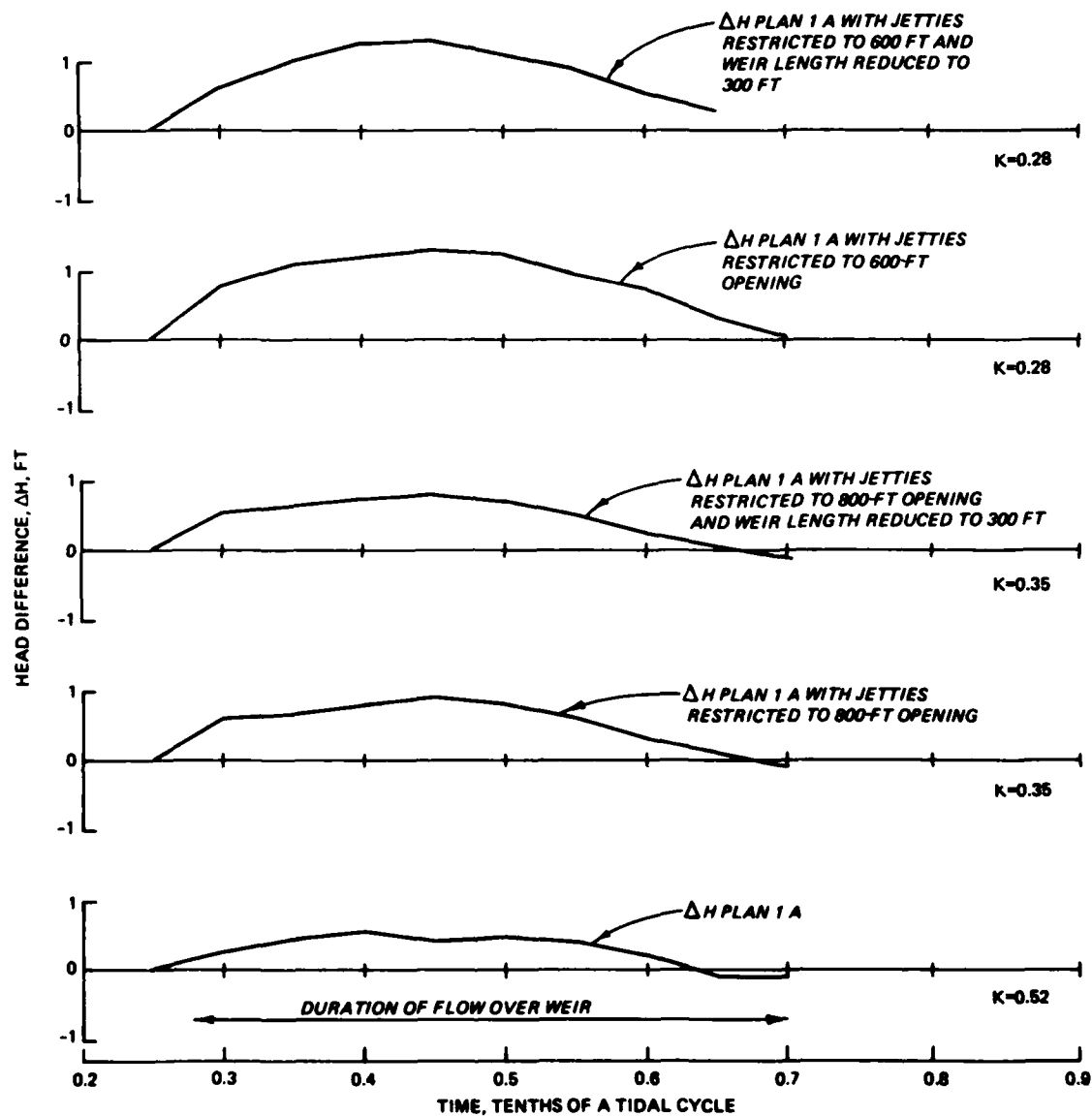
27. Tidal elevations were collected above the weir crest and at gages 7 and 8, located 100 ft (1 ft in model) on the oceanside and bay-side of the center of the weir section. Bay tides were monitored to determine the change in inlet hydraulics. Head differences across the weir between gages 7 and 8 are plotted in Figures 15 and 16 for the Plan 1 and 1A conditions, respectively. Figures 15 and 16 show that as the jetty entrance is restricted and Keulegan K reduced, the head difference across the weir is increased and occurs for a longer period. Flow over the weir starts just after 0.25 of the tidal cycle, when the tidal



NOTE: TIDE ELEVATIONS MEASURED 100 FT
OCEANWARD AND BAYWARD OF WEIR
WEIR ELEVATION AT MEAN TIDE LEVEL
TIDE RANGE = 5.0 FT

$$\Delta H = H_{\text{OCEAN SIDE}} - H_{\text{BAY SIDE}}$$

Figure 15. Head difference (ΔH) across weir, Plan 1



NOTE: TIDE ELEVATIONS MEASURED 100 FT
OCEANWARD AND BAYWARD OF WEIR
WEIR ELEVATION AT MEAN TIDE LEVEL
TIDE RANGE = 5.0 FT

$$\Delta H = H_{\text{OCEAN SIDE}} - H_{\text{BAY SIDE}}$$

Figure 16. Head difference (ΔH) across weir, Plan 1A

elevation is just above 0.0 mtl. Flow stops about 0.70, just before the ocean tidal elevation has fallen to 0.0 mtl. Table 1 shows the Keulegan K value for each condition as determined from the ratio of bay to ocean tide range in concert with Figure 5. Comparisons between Plan 1 and 1A tests (Figures 15 and 16) show that as the Keulegan K value was reduced, flood flow head differences increased in magnitude and duration while ebb flow head differences decreased in magnitude and duration. Among the individual plan tests, Plan 1 tests showed some variations indicating slight negative head increases with reduction in jetty opening. The data show that reduction in weir length did not produce significant differences in tidal elevations and head differences across the weir. In the initial discussion of velocities over the weir, the basic Plan 1 and 1A velocity conditions (i.e., no reduction in area at the jetty tips) are compared.

Tidal velocities across weir

28. Velocities across the weir were studied by use of paper floats due to the limited depth over the weir section. Velocities were measured every 100 ft (1 ft in model) along the weir. It was noted that tidal flow over the weir was uniformly distributed across the width. Figure 17 shows the average velocities and unit discharges over the weir for the basic Plan 1 and 1A conditions during the period of tidal flow over the weir. The unit discharges were calculated by multiplying the average velocity by the flow area above the weir at a given tide stage, then dividing by the length of the weir, or simplifying this, the unit discharge is equal to the average velocity multiplied by the depth over the weir crest at a given time. As implied by the previous examination of head differences, flood velocities for the high K inlet ($K = 1.75$) occurred for a period just over 0.2 of a tidal cycle, ending just after high water in the ocean. Peak average flood velocities were 3.0 fps. Ebb flow duration was 0.2 of a tidal cycle for the base high K inlet with a peak average velocity of 0.9 fps. The low K inlet velocity measurements indicated a flood current duration of 0.35 of a tidal cycle with maximum average currents of 3.6 fps. The above maximums are not directly relatable since the low K inlet had a slightly larger tidal

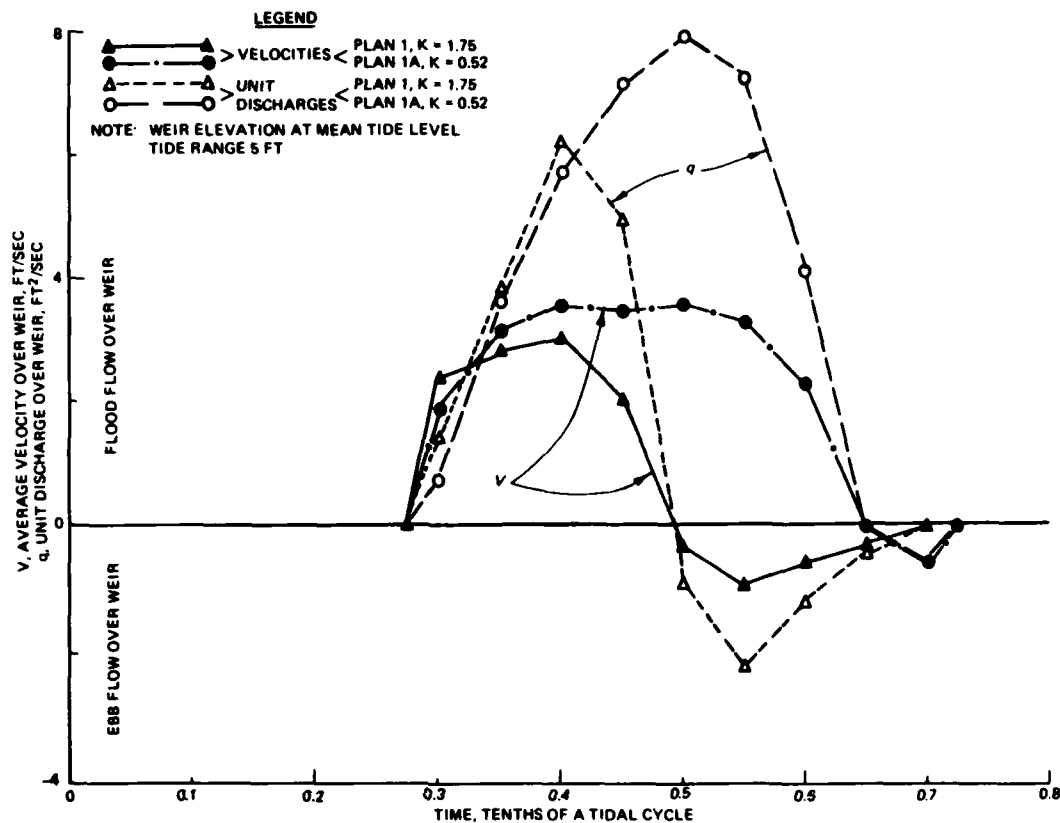


Figure 17. Average velocities and unit discharges over weir (Plans 1 and 1A)

prism than the high K inlet. An adjustment to the velocities making them directly relatable may be based on Keulegan's (1967) expression

$$\frac{TQ_m}{\pi P} = C \quad (6)$$

with

Q_m = maximum discharge, ft^3/sec

$\pi = 3.1416$

C = dimensionless number, a function of the Keulegan K

This can be written

$$V_m = \frac{C\pi P}{TA_c} \quad (7)$$

with

V_m = maximum average velocity, fps

V_m is directly proportional to P and making the assumption that V_m applies to flow over the weir as well as flow through the inlet channel, velocities can be adjusted by proportion of the measured tidal prisms. The Plan 1 velocity is used as the reference velocity since these velocities are in agreement with an equilibrium inlet. Table 1 shows the adjusted velocities for all testing. V_m for Plan 1A base condition adjusts from 3.6 fps to 2.8 fps for flood flow and from 0.6 to 0.5 fps on ebb flow.

29. The width at the jetty tips was incrementally reduced from 1200 ft to 800 ft to 600 ft producing ratios of the area at the jetty tips to the minimum cross-sectional area at the inlet gorge, bayward of the weir section, of 1.48, 1.03, and 0.77, respectively. This was done in order to simulate a reduction in entrance channel area oceanward of the weir section which might occur naturally due to shoaling or other channel area constraints. Plates 12 through 16 show the actual averaged velocity measurements over the weir during the tidal cycle for the various tests. The average velocity over the weir was determined by averaging the velocities which were taken every 50 ft (0.5 ft for the model) along the entire weir crest. Also shown are the water surface elevations at the weir crest. The plates show that as K decreases, the duration of flood flow is lengthened and ebb flow decreased. Figure 18 shows the peak average velocity plotted against Keulegan K with grouping by ebb and flood flows and by area ratios. As the area ratio is reduced, ebb and flood velocities over the weir are increased. The dependence of maximum velocity on K for given ratios seems to increase slightly as the area ratio becomes lower. A nondimensionalizing of Figure 18 in Figure 19 presents a more general and possibly more useful plot with a_o (tide amplitude) included as a variable. This graph should be used with caution since only one value of a_o was tested.

30. Figure 20 is a dimensionless plot that indicates that as soon as $A_1/A_2 \cdot a_b/a_o < 1.0$, velocities increase at a rapid rate. This is due to a change in the control cross section from the inlet gorge to the

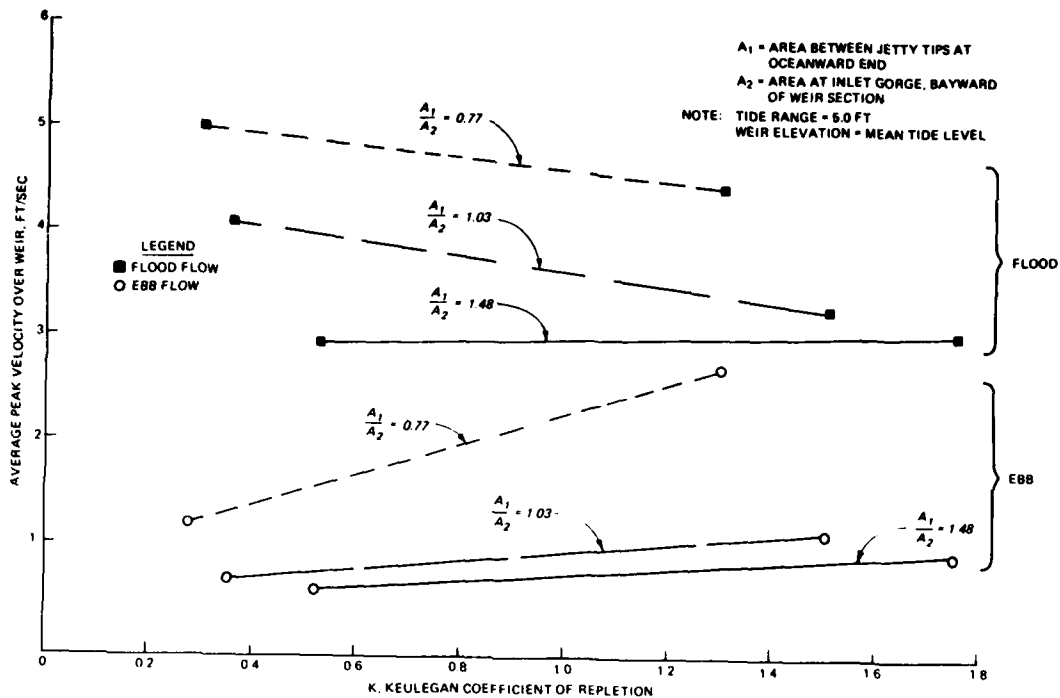


Figure 18. Average peak velocity over weir versus Keulegan K

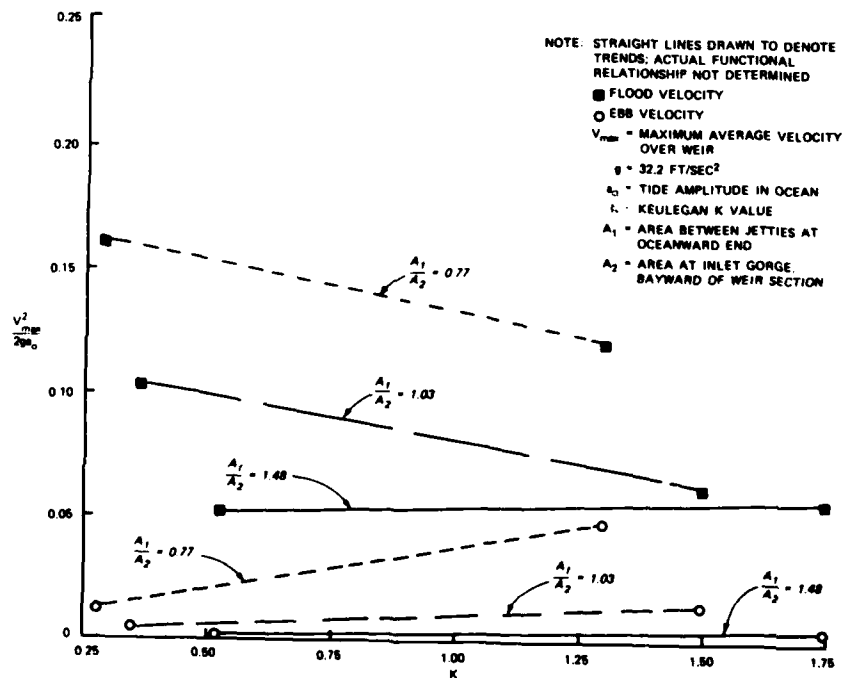


Figure 19. Nondimensionalized peak velocity over weir versus Keulegan K

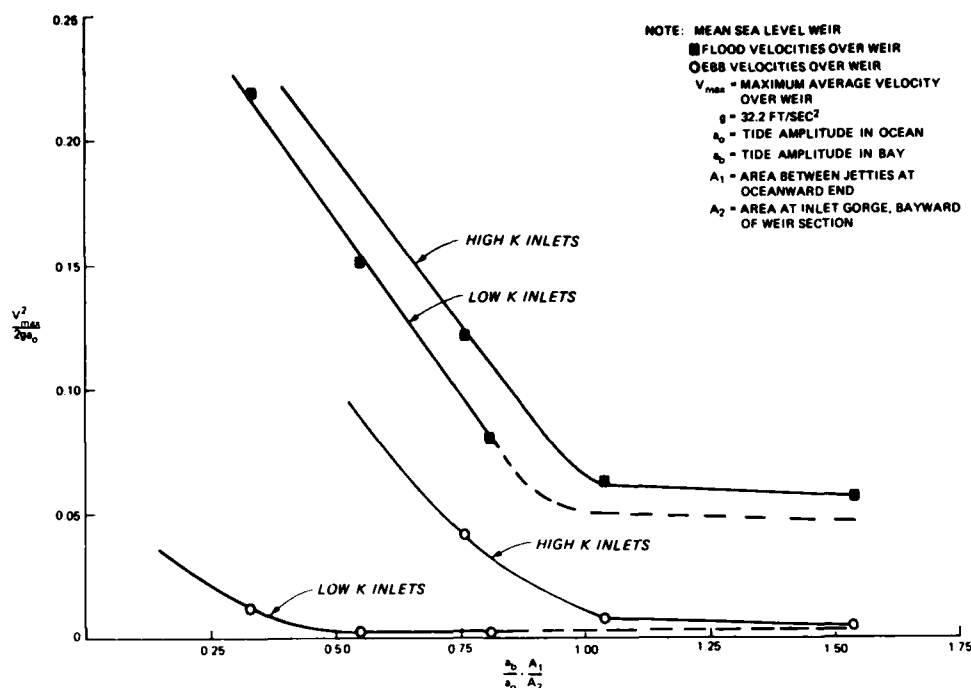


Figure 20. Nondimensionalized velocity versus tide range-flow area ratio

jetty tips. As this occurs, the region behind the weir and between the jetties responds more like the adjacent bay creating greater head differentials over the weir, thus increasing velocities.

31. Table 2 shows the peak unit discharges, q , for each test condition. These data show that for a given A_1/A_2 ratio, the lower K values have a greater flood q and a smaller ebb q than the higher K inlets (because peak flood flows for lower K inlets occur at higher water levels and peak ebb flows for lower K inlets occur at lower water levels). This translates to higher flood flow volumes over a given weir elevation for lower K inlets as seen in the table. Table 2 also shows ratios of ebb flow volumes to flood flow volumes. For the higher K inlets, as A_1/A_2 is reduced, there is greater proportion of ebb flow over the weir. This is not seen for the low K inlets since ebb flow volumes are already minimized due to their occurrence near low water in the ocean and the effect of the mean sea level weir, cutting off flow before a

maximum can be realized. Finally the last column of Table 2 shows the ratio of flood flow volume over the weir to the total tidal prism of the inlet. The maximum value is 0.047 or 4.7 percent of the tidal prism, a fairly low percentage. Other model studies at WES have shown a percentage for flood flow over the weir of 7 percent at Masonboro Inlet and 15 percent for Little River Inlet (a dual-weir design).

32. Head differences for the Plan 2 weir jetty (Figure 13) showed very little change from the basic Plan 1 measurements shown in Plate 17 and as a result, velocities were very similar (compare Plates 12 and 18). Because of this similarity, no detailed tests were conducted for the other plans since it was felt that only minor changes would occur for similar hydraulic conditions. Plate 18 also shows the effect of lowering the weir elevation to -1.0 ft below mtl for Plan 2. The peak velocity was increased from 2.9 fps to 3.8 fps, but the increased velocity only occurred over a 1-hr period, with velocities at other times close to those for the 0.0-mtl weir. An increase in flow area due to a lower weir (-1.0 mtl) contributes to increased peak unit q and total flow volume by a factor of 1.4, neglecting velocity increases.

Flow Patterns for the Jetty Systems

33. This section discusses the flow fields around the overall jetty systems due to either tidal currents or wave-generated currents or a combination of both. The flow patterns were studied in two ways. The first method used photography in which a 4-sec exposure was made of the water surface covered with confetti. This produced streaks of movement representing surface current patterns. The second method consisted of injecting dye at given locations and timing its movement over a known distance with a stopwatch. These measurements were generally considered to be at middepth of the water column and are presented graphically as velocity vectors.

34. Surface current photographs were taken at each 0.1-increment of the tidal cycle, but only photographs of 0.2, 0.4, 0.6, 0.8, and 0.0 parts of the tidal cycle are presented in this report. Low water in

the ocean was at 0.0 and high water occurred at 0.5. Each photograph indicates whether flood or ebb flow is occurring. Also, near the end of each exposure a strobe light was flashed to produce a bright spot along the trajectory of the surface float which would give an indication of direction.

35. The initial discussion focusses on tidal velocities. Photos 1-20 show surface currents for Plans 1, 1A, 2, and 3, in that order. A criterion to consider when evaluating the data is the desirability of maintaining the major portion of ebb flow and flood flow within the navigation channel in order to provide the least interference to the deposition basin where sediment should remain until dredged. If tidal flows meandered from the channel into the basin, sediment might be eroded and redeposited in the channel.

Tidal-surface currents

36. Comments concerning each photograph are listed below, after which further discussion will follow. See the photograph for test conditions.

<u>Plan</u>	<u>Photo No.</u>	<u>Comment</u>
1	1	Flood current migrated into the deposition basin before flow over weir began.
	2	Flow entering between the jetties was concentrated in the channel, as flood flow over the weir had begun. Flow over the inner one-half of the weir was directed toward the bay. Flow over the outer one-half of the weir first turned seaward, then was entrained with the channel flood current; flow approaching the jetty from upcoast was split about one-third the distance down the outer leg of the jetty. The inner third approached the weir while the outer portion entered between the jetty tips.
1	3	Early ebb flow showed no flow over the weir but a slight deflection of the ebb jet toward the inside of the upcoast jetty.
1	4	Near peak ebb flow currents were exiting fairly uniformly through the channel except for a slight deflection of the ebb jet toward the inside of the upcoast jetty.
1	5	Late in the ebb, flow was concentrated in the channel.

Plan	Photo No.	Comment
1A	6	As a result of the change in inlet hydraulics (smaller K) the Plan 1A flood velocities were just starting and concentrated near the upcoast jetty since the momentum of the ebb currents in the main channel had impeded early flood flow in that region.
1A	7	Flood flow in the main navigation channel was well aligned.
1A	8	Flood flow was well aligned with the channel and flow over weir was still occurring.
1A	9	Ebb flow was well aligned with the channel except for a small deflection toward the outer portion of the upcoast jetty. An eddy region existed over the deposition basin.
1A	10	Ebb flow was well confined to the channel.
2	11	Some movement of early flood flow toward the basin was seen, though not as much as with Plan 1 (Photo 1).
2	12	Flow over the weir had begun and tended to turn oceanward, then bayward as it became entrained with flow in the navigation channel. Ocean flow approaching the weir was similar to that of Plan 1 (Photo 2). Note low velocities along beachline.
2	13	Early ebb currents were aligned fairly well with the channel.
2	14	Ebb flow was well aligned with the channel. No movement over the basin was occurring.
2	15	Same comment as for Photo 14.
3	16	Early flood currents entered the channel uniformly.
3	17	Flow over the weir was occurring, flowing bayward into channel.
3	18	During early ebb flow some flow was diverted from the channel to the outer portion of the weir and oceanward. The outer portion of the weir was closer to the channel than the Plan 1 or 2 weir. This flow, however, occurred only in the outer corner of the deposition basin.
3	19	Ebb flow was totally confined to the main channel.
3	20	Same comment as for Photo 19.

In summary, these photographs indicate that the Plan 3 system provided the best concentration of ebb and flood currents in the channel, but was the only case where early noticeable ebb currents flowed over the

weir section since the outer portion of the weir was closer to the channel. It appears that the lower K inlet of Plan 1A shows better flow alignment than that of the Plan 1 inlet. This is easily explained for ebb velocities by the fact that ebb currents occur at lower water levels for low K inlets than high K inlets and the currents would tend to be confined more by the channel.

Surface currents
due to tide and waves

37. Photos 21-59 show both tidal currents and wave-generated currents in the vicinity of the jetty systems. Waves of 10-sec period (1 sec in model) were used in each case. Exact test conditions are listed on each photograph. The flow trajectories appear rippled due to their movement by the waves. Since the waves were 1 sec in period and the exposure was 4 sec, each streak has 4 bumps. It should be emphasized that these are surface currents. In the region of the breakers, the surface floats occasionally were caught in the breaking wave crest and did not follow the actual longshore current. Outside the breaker zone, the float trajectories are considered representative of velocity direction throughout the water column. Two wave heights of 5 ft and 10 ft (0.05 ft and 0.10 ft in model, respectively) were chosen to be reproduced for the 10-sec period. The 5-ft wave was considered a minimum height wave to reproduce for the given model scale to ensure good turbulent breaking conditions. Also the wave steepness of 0.010 (for the 10-sec, 5-ft wave) is a commonly occurring steepness on most sea-coasts representing a swell condition. While the steepness of the 10-ft, 10-sec wave of 0.20 is not considered a very steep wave by most criteria, its size should represent more stormlike conditions. Unfortunately, more wave conditions could not be reproduced due to time and budgetary limitations. Comments on the photographs follow:

<u>Plan</u>	<u>Photo No.</u>	<u>Comment</u>
1	21	There was a strong circulation pattern upcoast of the weir jetty, due to the 10-ft wave with 2- to 3-fps velocities over the weir and 3-fps currents along the oceanward face of the weir jetty. Also, the flood

<u>Plan</u>	<u>Photo</u> <u>No.</u>	<u>Comment</u>
		currents entering between the jetties were deflected toward the downcast jetty.
1	22	Surface currents along the oceanward face of the up-coast jetty were reduced slightly since the tide elevation had risen and flow over the weir was occurring. While the photograph shows few trajectories over the weir, there was significant flow. Waves breaking over the weir made it difficult to maintain surface floats in this region. There was a clockwise eddy in the nearshore upcoast region adjacent to the weir jetty.
1	23	Ebb flow had begun and there were significant offshore currents (3 to 4 fps) adjacent to the upcoast jetty. There was no deflection of ebb currents from the bay toward the deposition basin as there was for the no-wave condition; however, there was a deflection of channel currents toward the outer leg of the upcoast jetty. Also, there were velocities of 3 fps on the oceanward side of the weir flowing parallel to the weir.
1	24	Patterns for this ebb flow condition were similar to those described for Photo 23.
1	25	As the end of ebb flow neared, the ebb currents were somewhat confined to the downcoast side of the channel. Wave generated currents were still strong along the outside of the upcoast jetty.
1	26	Early in the flood flow the main channel flow was shifted toward the upcoast side of the system by the currents generated by waves from the downcoast direction and the wave-generated currents rounding the downcoast jetty and penetrating into the channel. A counterclockwise circulation cell was located upcoast of the weir jetty from the weir section shoreward. Oceanward, along the outer section of the weir jetty, surface currents were generated shoreward and gradually merged into the upcoast longshore drift.
1	27	Patterns similar to those in Photo 26 were seen for this condition, which is later during flood flow. Flow over the weir and into the basin appeared negligible (compare with Photo 2, tide-only condition).
1	28	Early ebb flow was confined against the downcoast jetty and eddying current patterns existed over the deposition basin.
1	29	Ebb flow was similar to that in Photo 28. The flow pattern upcoast of the jetty system was directed

<u>Plan</u>	<u>Photo No.</u>	<u>Comment</u>
		upcoast except at the shoreward corner of the weir jetty where a counterclockwise eddy still existed.
1	30	Late ebb flow in the channel moved close to the downcoast jetty. Slow eddy currents existed over the basin.
2	31	Upcoast waves during this early flood period increased current activity in front of the weir due to the incoming longshore current when compared with the tide-only condition (Photo 11).
2	32	Flow over the weir was directed more toward the bay entrance than for the no-wave condition (Photo 12).
2	33	Flow patterns for the 5-ft-wave condition were fairly similar to the tide-only photograph except for the longshore current in front of the weir.
2	34	As ebb flow developed, there was an offshore movement of surface currents along the oceanside of the upcoast jetty.
2	35	Late ebb flow was forced to the downcoast side of the channel. The longshore current was deflected by the upcoast jetty in the offshore direction.
2	36	The 10-ft wave created a circulation over the deposition basin from waves overtopping the weir. Channel flood flow was shifted to the downcoast side.
2	37	Strong offshore currents (3 to 4 fps) existed upcoast of the weir, even though flow over the weir had begun.
2	38	The early ebb jet was deflected downcoast. Strong currents offshore of the weir jetty still existed.
2	39	Wave overtopping of the weir created a movement toward the channel. Strong offshore currents existed upcoast of the oceanward portion of the weir jetty.
2	40	Current patterns were similar to those in Photo 39 except near the inside of the oceanward portion of the weir jetty where currents were approaching the jetty then deflecting back to the channel.
2	41	The downcoast waves nullified the surface approach flow around the upcoast jetty tip (compare with no-wave condition, Photo 12). No eddy region existed at the shoreward end of the weir jetty as it did for the Plan 1 jetty with waves (Photo 26).
2	42	Flow over the weir was directed toward the bay rather than toward the ocean before becoming entrained in channel flow (compare with Photo 12).

<u>Plan</u>	<u>Photo No.</u>	<u>Comment</u>
2	43	Early ebb flow showed a clockwise circulation over the basin, compared with none for a no-wave condition (Photo 13).
2	44	Ebb flow was more concentrated against the channel side of the weir jetty than for the no wave condition (Photo 14).
3	45	Greater current movement occurred in the deposition basin due to waves overtopping the weir than was noted for the same conditions in Plan 2.
3	46	Some of the longshore current moved past the oceanward, upcoast side of weir and decelerated one-half way seaward along the upcoast jetty. Also, currents over the deposition basin were eddylike rather than directed at the channel as in the tide-only condition (Photo 17).
3	47	Flow along the oceanward part of the upcoast jetty has decelerated. The movement of early ebb flow over the weir seen in the tide-only test (Photo 18) did not occur with tides and waves.
3	48	Current movement upcoast of the oceanward end of the jetty was somewhat erratic in pattern.
3	49	The greatest current activity was over the deposition basin for this low water time since approaching wave crests were almost parallel to the weir for this orientation.
3	50	When compared with the 5-ft wave (Photo 45), the 10-ft wave created increased currents along the entire length of the upcoast jetty. When these currents approached the jetty tip, they flowed into the channel.
3	51	Flood flow over the weir was strong, but only that portion at the oceanward end of the weir was directed into the channel.
3	52	Early ebb flow had good alignment in the channel.
3	53	Surface velocities of 4 fps occurred along the upcoast jetty.
3	54	No significant change from Photo 53, except that ebb currents were slowing.
3	55	The 5-ft downcoast wave created no eddy regions near the beach along the upcoast side of the weir.
3	56	A small eddy region occurred on the oceanward side in the bend of the weir jetty.

<u>Plan</u>	<u>Photo No.</u>	<u>Comment</u>
3	57	Slight ebb-current movement occurred over the outer end of the weir section.
3	58	Eddy currents existed over the deposition basin.
3	59	No significant change from Photo 58 was noted.

38. Waves significantly affected flow patterns along the oceanside of the upcoast weir jetty, in the deposition basin, and at the oceanward end of the navigation channel. Concerning the last item, Plan 3 showed the least effect. Flow was usually straight and almost uniform across the entrance since the parallel jetties confined the flow much more effectively than did Plan 1 or 2. On the outside of the upcoast weir jetty there was considerable flow along the outer leg of the jetty for all plans tested with the 10-ft upcoast wave. This might be significant in regard to material bypassing the weir and moving oceanward along the jetties and eventually into the channel. Plan 3 received more wave activity in the basin than did Plan 1 or 2 due to its smaller acute angle with the shoreline, but an eddylike circulation was usually maintained so that suspended materials would tend to settle in the deposition basin rather than reach the channel. Downcoast waves for Plans 2 and 3 would easily remove sediments that accumulate upcoast, adjacent to the weir section. Plan 1 showed a strong eddy region there, where the downcoast wave (30-deg deepwater angle) did not produce a longshore current in the upcoast direction. The following section will examine the flow patterns upcoast of the weir jetty in more detail.

Dye streak velocity measurements

39. In order to examine the wave-generated velocity field on the upcoast side of the weir jetty, dye was injected into the water column throughout the depth and timed as it moved over a known distance. Velocity vectors then were drawn showing location, direction, and magnitude for the individual measurements. Some measurements were made with waves only to remove any influence of tidal currents; Plates 19-32 show these data.

40. Plan 1. Plate 19 shows that for 10-ft, 10-sec upcoast waves

during flood tide, velocities of a significant magnitude (3.3 fps, prototype) flowed toward the Plan 1 jetty tip from the weir section region and around the jetty tip into the channel. There was also an oceanward directed current of 2 fps at the base of the weir section while there was flow over the weir, a variation in 90 deg in flow direction through the water column. During ebb flow, with no flow over the weir, the velocity at the base of the weir increased to 3.3 fps (Plate 20). Also velocities at the outer jetty tip were directed offshore.

41. Plate 21 shows the circulation due to a 10-ft downcoast wave for Plan 1. A counterclockwise circulation was noted at the base of the upcoast jetty. A uniform longshore current was established about 1600 ft upcoast of the jetty.

42. Plan 2. The longshore current field due to a 5-ft, 10-sec upcoast wave (no tide) is shown in Plate 22. Maximum currents were shoreward of the breaker with a peak value of 2.9 fps. Once reaching the jetty, flow was split between the weir and offshore along the jetty. Maximum currents flowing oceanward were 1.4 fps. Plate 23 shows the effect of increasing the wave height to 10 ft (no tide). Peak velocity magnitudes were 5.0 fps in the breaker zone, 4.3 fps over the weir, and 4.5 fps oceanward along the weir. As flow progressed oceanward along the jetty, velocities fell off initially but maintained maximums between 2 and 3 fps out to the jetty tip, even though depths were increasing and the flow was spreading from a width of about 600 to about 1000 ft.

43. Plate 24 shows the velocity field for a 10-ft, 10-sec downcoast wave for Plan 2. Velocities in the upcoast direction started a little over 300 ft from the jetty.

44. Plate 25 shows velocities taken during the flood tide with a 10-ft, 10-sec upcoast wave. Velocities just oceanward of the weir were slower than for the no-tide condition (Plate 23) since the tide was diverting more flow to the weir section, and further oceanward, velocities with waves plus tide were higher than the waves-only condition since the tidal flow was accelerating around the jetty tip. Plate 26, showing velocities during the ebb tide, indicated an oceanward shift in breaker

location due to lower water level and higher currents along the jetty face moving oceanward.

45. Plan 3. Plate 27 shows the upcoast velocity field for Plan 3 for a no-tide condition with 5-ft, 10-sec waves from upcoast. Currents approaching the weir were mostly between 2 and 3 fps. Movement oceanward along the jetty leg was about 1 fps. With the wave height increased to 10 ft, Plate 28 shows maximum velocities of 6 to 7 fps approaching the weir, 5 to 6 fps along the bottom adjacent and parallel to the weir, and 3 to 4 fps oceanward along the upcoast jetty.

46. A 5-ft 10-sec downcoast wave for Plan 3 produced no reversal of currents shoreward of the weir as the Plan 1 and Plan 2 jetties did (Plate 29) since the region was extended far enough out of the shadow of the jetty. There was a reversal in the current direction at the oceanward end of the weir. Currents outside the breaker were low (less than 1 fps).

47. Plate 30 shows the location of velocity stations for measurements with upcoast waves and a tide for Plan 3. Also indicated on the plate is the usual velocity direction (variation in direction was on the order of 30 deg). Plates 31 and 32 show the velocities each 0.1 of a tidal cycle for both the 5-ft and 10-ft, 10-sec upcoast waves. Velocities for the 5-ft wave tended to be fairly constant in value throughout the tidal cycle at most locations. Velocity magnitude decreased in an oceanward direction to less than 1 fps at sta F and L. The larger wave produced more variation in velocity during the tidal cycle. Sta J, K, L, M, and N showed decreases during flood flow (to about 2.5 fps) and increases during ebb (to about 5 fps), as the tide influenced flow toward the weir during flood tide and away from it on ebb. Sta D, E, F, and I, adjacent to the jetty, did not show much change during the tide but maintained velocities in the 4- to 5-fps range at all times.

48. Summary. Comparing the dye streak velocity measurements for Plans 1, 2, and 3 for 10-ft, 10-sec upcoast waves (Plan 1 wave angle was 30 deg, while Plans 2 and 3 had 40-deg waves) and a 5-ft-tide range, Plan 3 velocities were generally higher close to the oceanward portion of the upcoast jetty and parallel to the weir at its base. This should

be expected at the outer leg of the jetty due to the geometry of Plan 3 which promoted a higher concentration of longshore current at the bend of the jetty. Plans 1 and 2 permitted greater expansion of this seaward flowing current. Results also indicated that as the angle of the weir and shoreward portion of the jetty was reduced from 90 deg (i.e., Plan 1 Plan 2, then Plan 3), there was an increase in seaward flowing current at the base of the weir section.

PART V: BEACH RESPONSE TESTS

49. This phase of the study was designed to aid in interpreting the response of the beachline upcoast of the weir jetty for a variety of jetty orientations and for both an upcoast and downcoast wave direction. The response of beachlines upcoast of a groin has been studied in mathematical formulation by a number of people, the method of Pelnard-Considere perhaps being the best known. However, because of the complex boundary conditions (which include movement of material over the weir) and the ability of an undistorted physical model to reliably integrate the effects of refraction, diffraction, and wave reflection, beach response tests were performed to aid in examining relative differences in weir jetty configurations on shoreline response. Such complex situations are more reliably and more economically investigated in undistorted physical models than in numerical models at this time. As mentioned above, not only was an upcoast wave used to examine the formation of a fillet, but a downcoast wave was also used in order to note the relative ease with which material might be returned upcoast during a longshore drift reversal. This can be an extremely important factor on coasts with fairly frequent drift reversals. In such cases, drift reversals tend to reduce the amount of material accumulating in the deposition basin and thus reduce the amount of material that must be handled by dredging.

50. Before the beach response tests are discussed, an examination of a possibly important mechanism occurring in the vicinity of the weir jetty caused by the interaction of incident waves and waves reflected by the jetty will be undertaken.

Short-Crested Wave Field and Beach Interaction

51. The formation of a short-crested wave field by the interaction of incident and reflected waves and its effect on sediment transport has been studied by Silvester (1975 and 1977), Dalrymple and Lanan (1976), and Hsu (1975), among others. This study more closely compares with that of Dalrymple and Lanan in that they performed laboratory tests with

a movable-bed beach and observed the formation of beach cusps and rip currents as a result of the incident wave-reflected wave interaction with the shoreline. The weir jetty testing superimposed additional boundary conditions with the introduction of a longshore current entering the short-crested wave region from upcoast, and the weir section as a portion of the reflecting structure downcoast.

52. Figure 21 shows the formation of the short-crested wave field and its characteristic diamond pattern created by the interacting crests

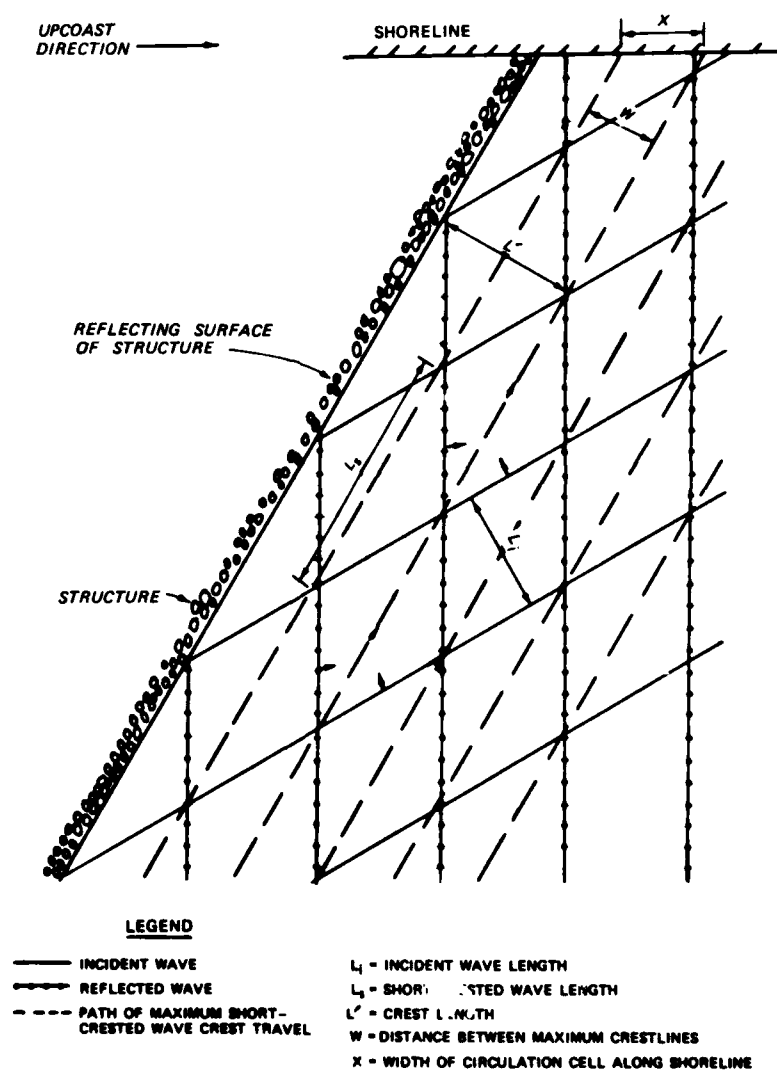


Figure 21. Short-crested wave field

of the incident and reflected waves. Figure 22 shows a short-crested wave field upcoast of the Masonboro Inlet weir during low water. By following the path of the intersecting crests in Figure 21, the direction of the short-crested wave can be noted. For a uniform flat bottom (no refraction), the path of the short-crested wave is always parallel to the structure. For the relatively straight-sloped beach of this study there was little deviation from a flat-bottomed condition in the immediate vicinity of the structure.



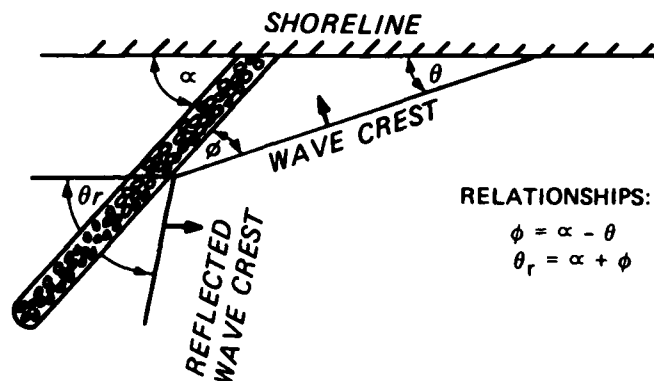
Figure 22. Short-crested wave field at Masonboro Inlet weir jetty

53. Figure 23 defines α = acute angle between structure and shoreline, θ = acute angle between wave crest and shoreline, ϕ = angle between wave crest and structure, and θ_r = angle between reflected wave crest and shoreline. Also shown are ranges of ϕ and ϕ_r for a given α and a range of θ between 0 and 25 deg, a perhaps typical range of wave angles near the shoreline. It can be shown from the geometry of the intersecting wave crests that the incident wavelength L_i and celerity C_i can be related to the short-crested wavelength L_s and celerity C_s by the expression

$$\frac{C_s}{C_i}, \frac{L_s}{L_i} = \frac{1}{\cos \phi \tan \phi} \quad (8)$$

and this relation is derived in Figure 24 and plotted in Figure 25. Using the expression from Wiegell (1964) for horizontal water particle velocity in the direction of wave propagation as derived by Fuchs for the short-crested wave and shown graphically in Figure 26, the maximum bottom velocity (which occurs under the line of crest travel) is compared with that for the incident wave in Figure 27. Two curves are shown--one for complete reflection off the structure ($K_r = 1$) and one considering only partial reflection of the wave ($K_r = 0.3$, a value measured for the model structure and a reasonable prototype value). These are linear theories and the interaction of the incident and reflected waves probably becomes a relatively nonlinear phenomenon. For usual values of θ (i.e., 0 deg < θ < 25 deg), the greater maximum bottom velocities occur for structures with larger values of α , that is, ones more perpendicular to shore. Tempering this is the Mach reflection phenomenon which indicates that for incident wave angles from 0 to 20 deg (the angle between the direction of wave advance and the reflecting surface which is equivalent to $\phi = 70$ to 90 deg) there is little or no reflection and for incident wave angles of 20 to 40 deg ($\phi = 50$ to 70 deg) there is a reduction in reflected wave height due to the formation of the "Mach stem," a wave perpendicular to the reflecting surface and from which the incident wave and reflected wave extend (Weigell 1964). Thus there is most likely some reduction in

α = ACUTE ANGLE BETWEEN STRUCTURE AND SHORELINE
 θ = ACUTE ANGLE BETWEEN WAVE CREST AND SHORELINE
 ϕ = ANGLE BETWEEN WAVE CREST AND STRUCTURE
 θ_r = ANGLE BETWEEN REFLECTED WAVE CREST AND SHORELINE



RELATIONSHIPS:

$$\phi = \alpha - \theta$$

$$\theta_r = \alpha + \phi$$

VALUES OF ϕ AND ϕ_R FOR GIVEN α AND θ

NOTE: ASSUME θ USUALLY NOT GREATER THAN 25° NEAR SHORE

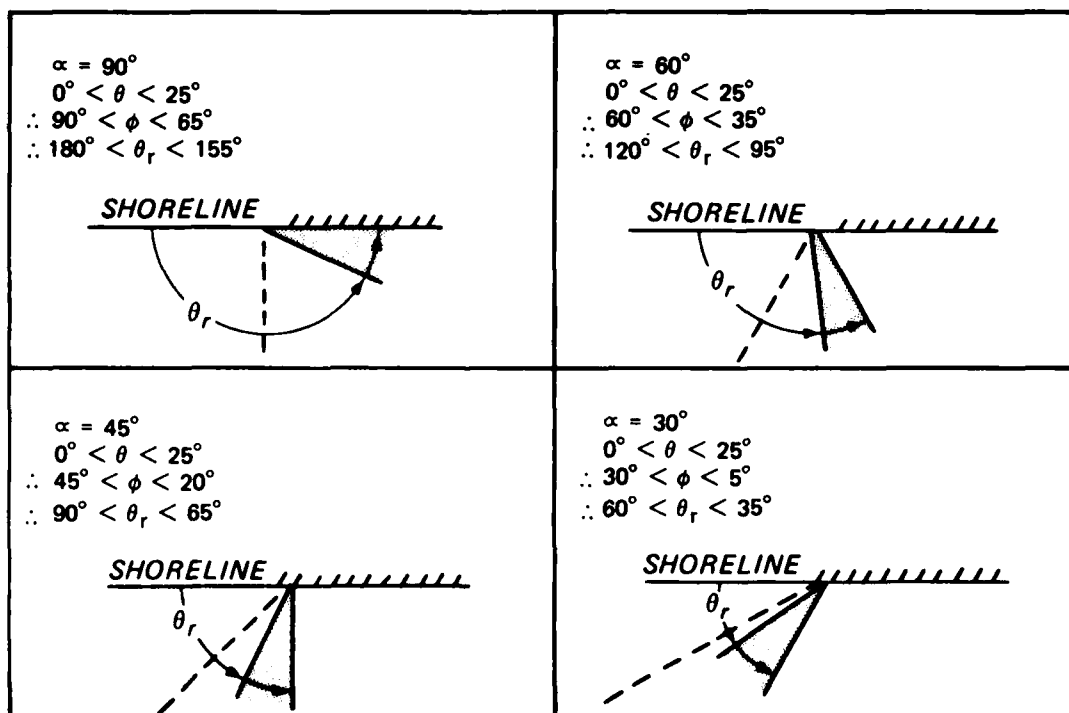
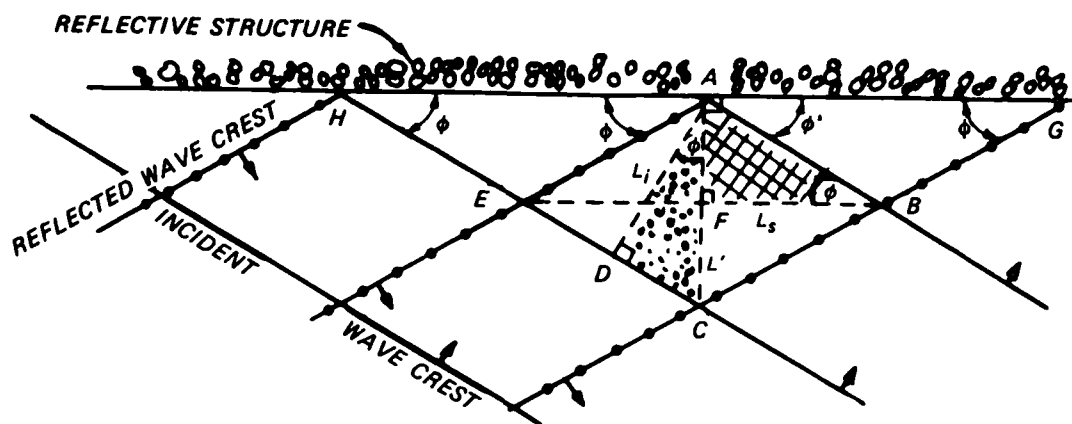


Figure 23. Angular relationships



1. From basic physics, $\angle BAG = \angle EAH = \phi$.
2. From basic geometry it can be shown that ABCE is a rhombus and it follows that BE is perpendicular to AC.
3. Also it can be shown from geometry that $\angle ABF = \angle CAD$ and that $CFA \perp HAG$.
4. DA is defined as the wavelength between two parallel wave crests and is perpendicular to the crests.
5. It follows that $\angle ABF = \angle CAD$ from basic geometry.
6. $\overline{AD} = L_i$, incident wavelength.
 $\overline{BFE} = L_s$, short-crested wavelength.
 $\overline{AFC} = L'$, crest length.

7. (a) From stippled triangle

$$\cos \phi = \frac{L_i}{L'}$$

- (b) From crosshatched triangle

$$\tan \phi = \frac{L'/2}{L_s/2} = \frac{L'}{L_s}$$

- (c) Rearranging and substituting from a and b above, eliminating L' ,

$$\frac{L_s}{L_i} = \frac{1}{\cos \phi \tan \phi}$$

8. From 7a, $\cos \phi = L_i/L'$ and from Figure 21, $L' = 2W$, then

$$\cos \phi = \frac{L_i}{2W} \text{ or } \frac{W}{L_i} = \frac{1}{2 \cos \phi}$$

Figure 24. Derivation of expression $\frac{C_s}{C_i}, \frac{L_s}{L_i} = \frac{1}{\cos \phi \tan \phi}$

$$\text{and } \frac{W}{L_i} = \frac{1}{2 \cos \phi}$$

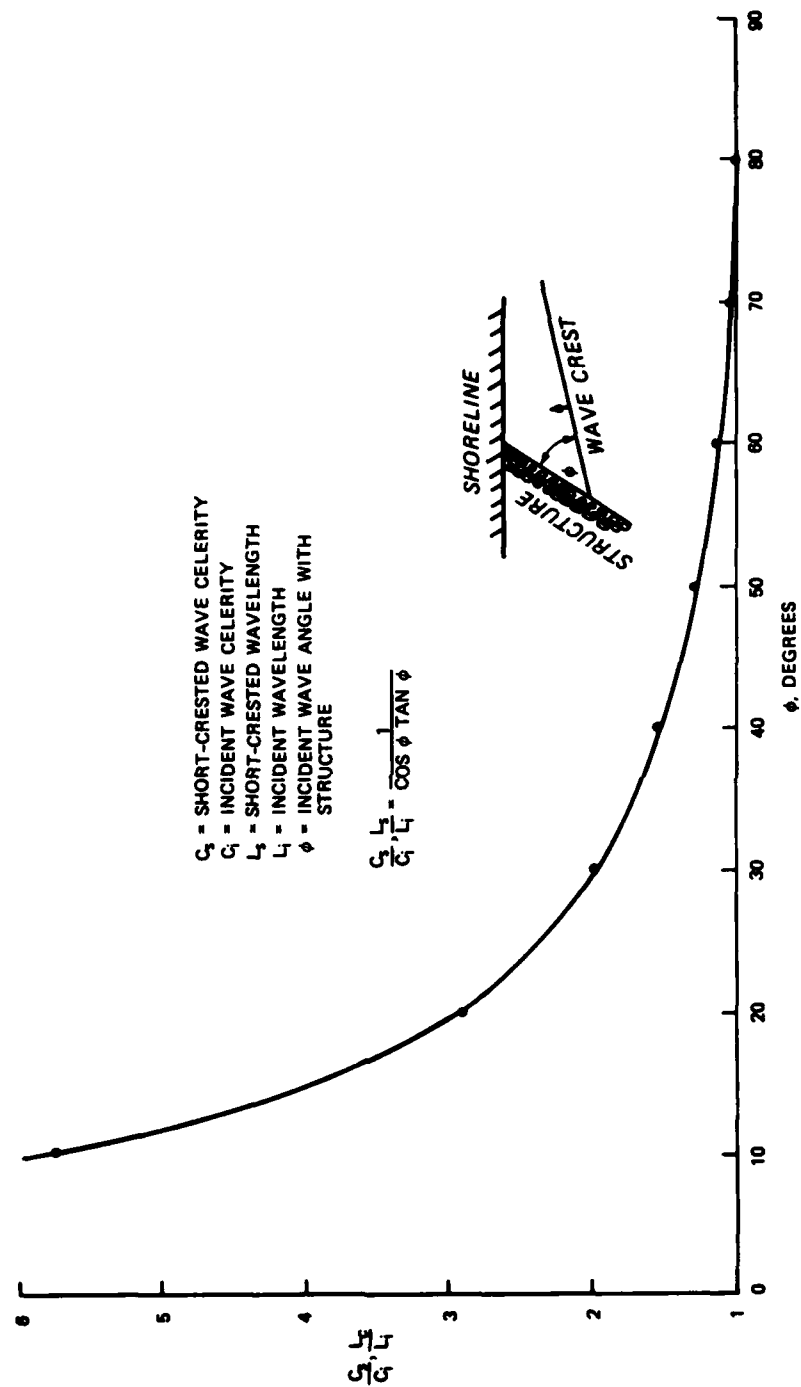


Figure 25. Ratio of short-crested to incident wave celerities, short-crested to incident wavelengths versus ϕ

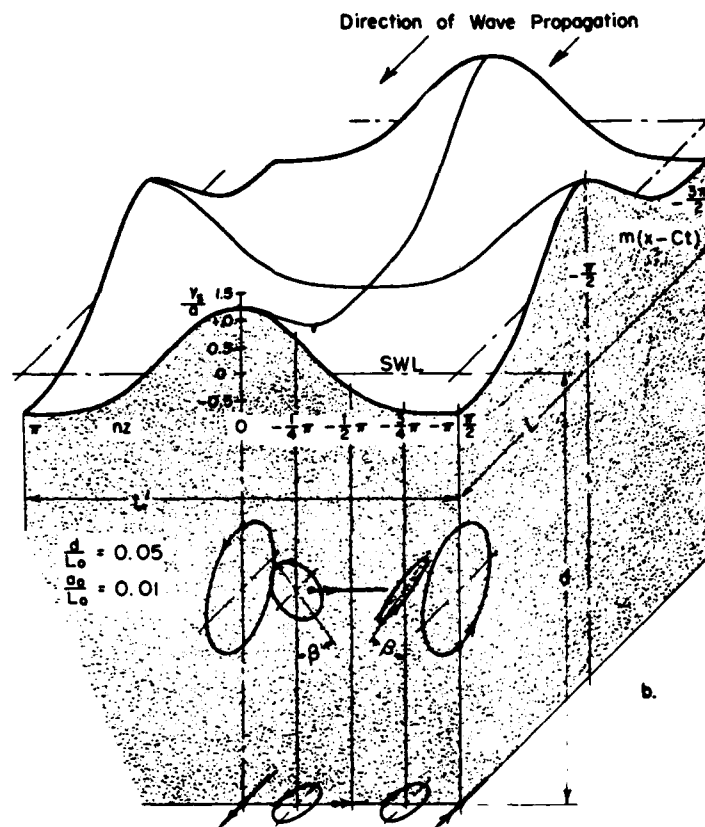


Figure 26. Short-crested wave contours and particle velocity orbits (from Wiegel 1964, after Fuchs 1952)

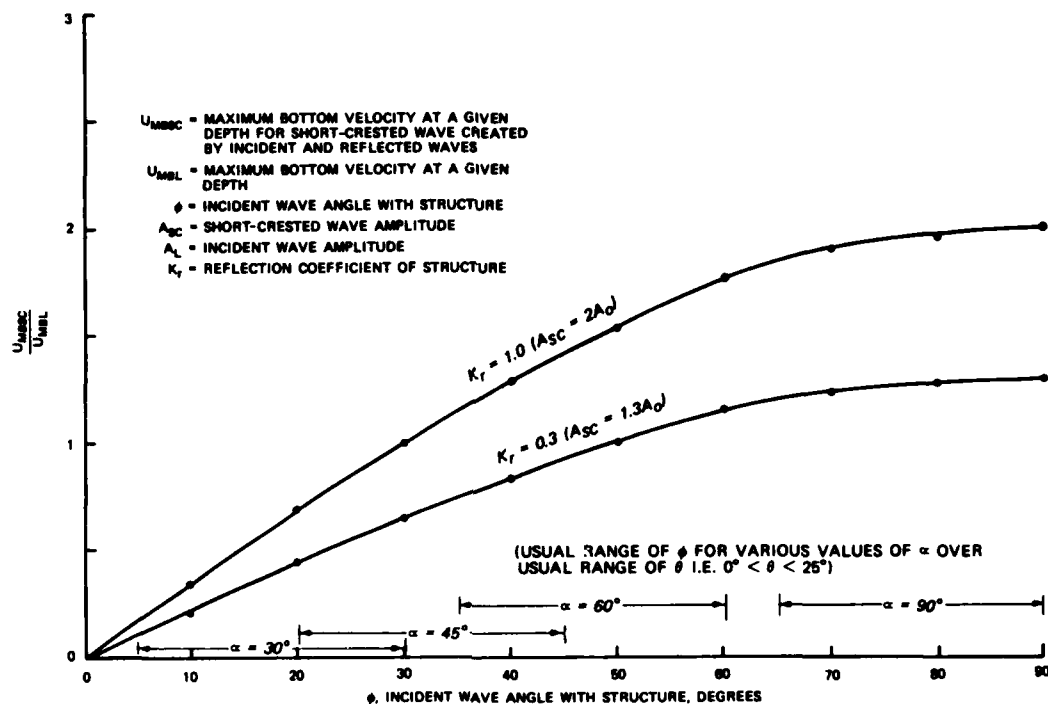


Figure 27. Ratio of maximum bottom velocity of short-crested and incident waves versus ϕ

the velocity field of the short-crested wave, and the $\alpha = 90$ deg structure probably does not produce significantly higher velocities than the $\alpha = 60$ deg structure. Also the Mach-stem effect does not occur for the $\alpha = 30$ deg and 45 deg structures when waves are from the upcoast direction since ϕ is usually less than 50 deg.

54. From geometrical considerations,

$$\frac{W}{L_1} = \frac{1}{2 \cos \phi} \quad (9)$$

where W , shown in Figure 21, is the distance between crestlines in the short-crested wave field. Figure 28 shows that for $0 < \phi < 25$ deg, the smaller α (the acute angle between this structure and the shoreline) the closer the wave crest spacing. Figure 29 presents the same information in terms of θ . In terms of spacing of the intersection of the crestlines with the shoreline, Figures 30 and 31 show spacing X ,

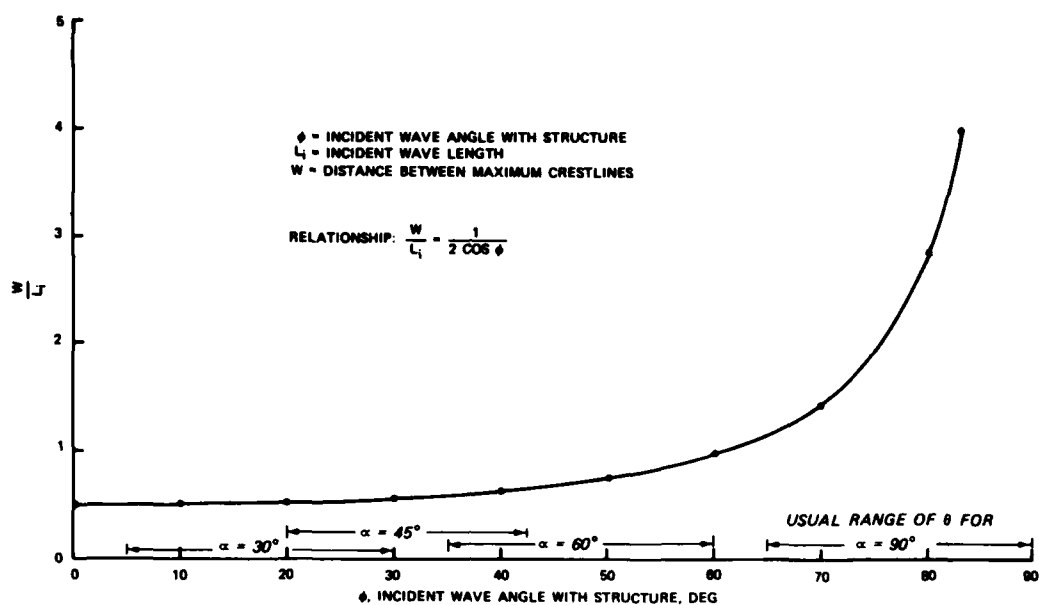


Figure 28. W/L_i versus ϕ

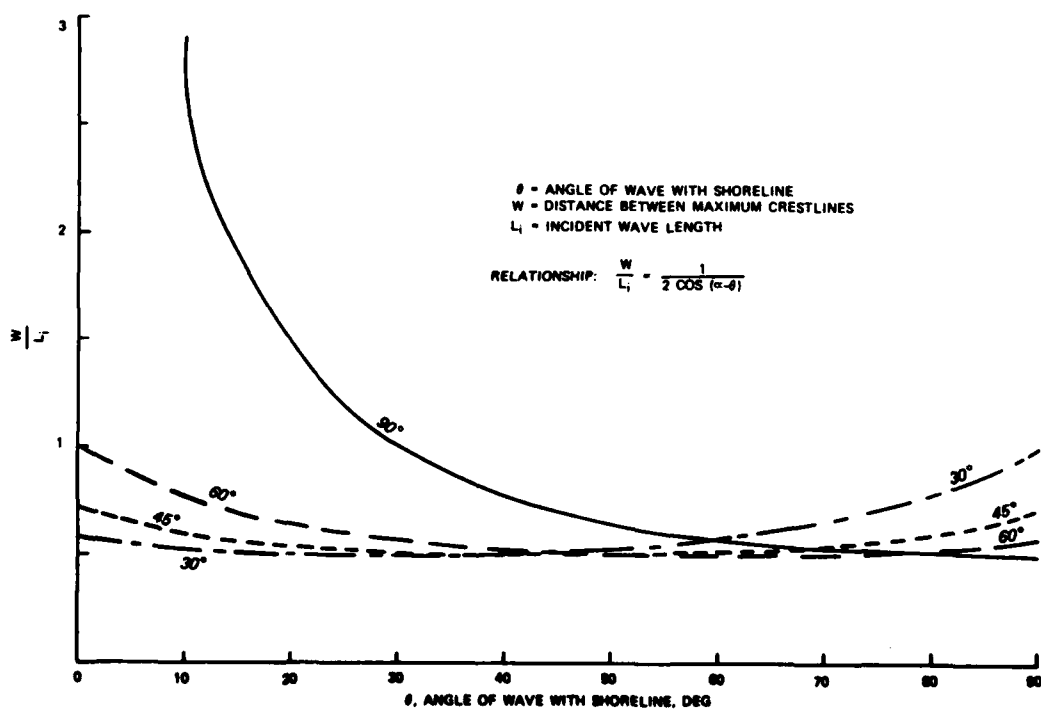


Figure 29. W/L_i versus θ

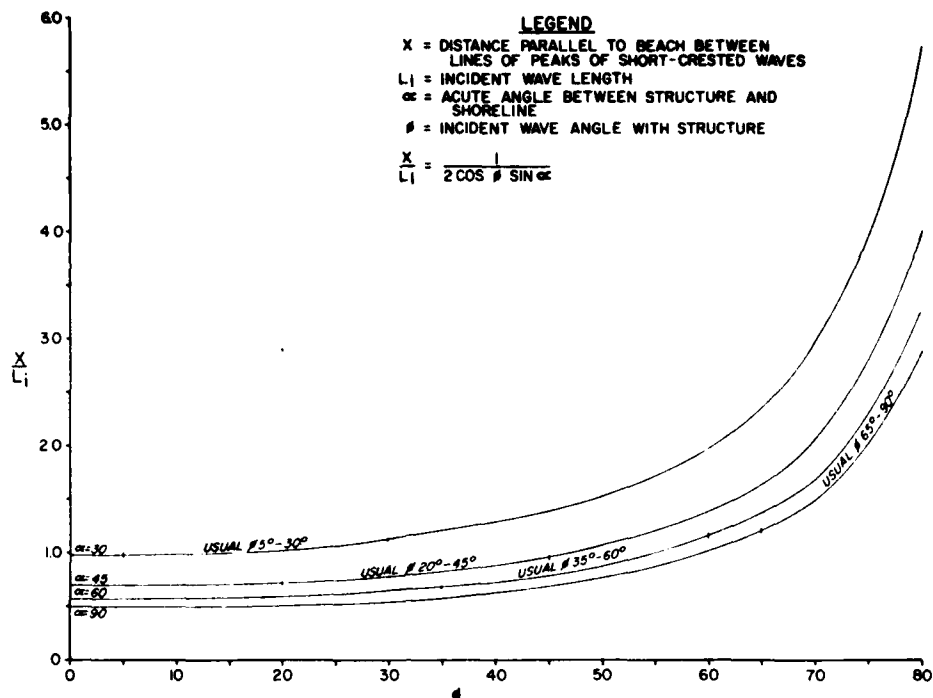


Figure 30. X/L_i versus ϕ

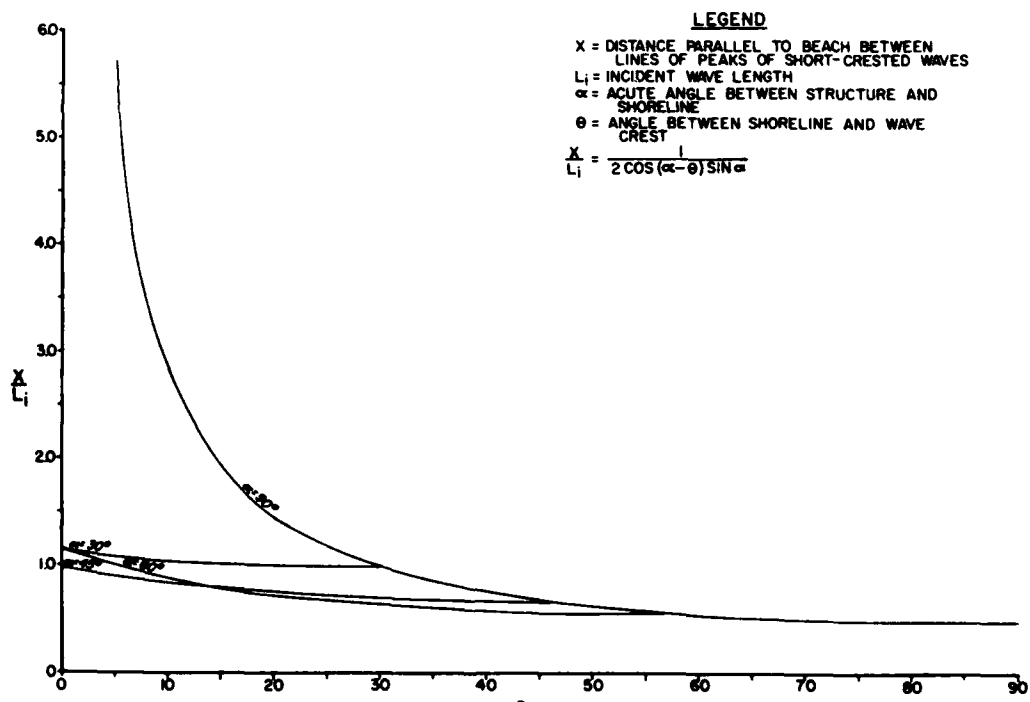


Figure 31. X/L_i versus θ

defined in Figure 21, relative to incident wave length L_1 in terms of ϕ (Figure 30) and θ (Figure 31). Figure 30 shows that the spacing of the intersection of crestlines with the beach is closer together for smaller values of ϕ . Figure 31 shows that the closest spacing of crest intersection with the beach for a given α (structure's angle with the shoreline) is at that angle of θ which approaches α . When $\theta > \alpha$, the wave is reflected seaward and the short-crested wave field does not intersect the beach. The effect of the intersection of these crests and the shoreline follows.

55. Assuming that the incident wave is from the upcoast direction, inducing a longshore current toward the upcoast jetty, the short-crested wave field approaches the shoreline in the vicinity of the structure as shown in Figure 32. The velocity field along the bottom across a short-crested wave front shows that, under the crest, velocities are in an

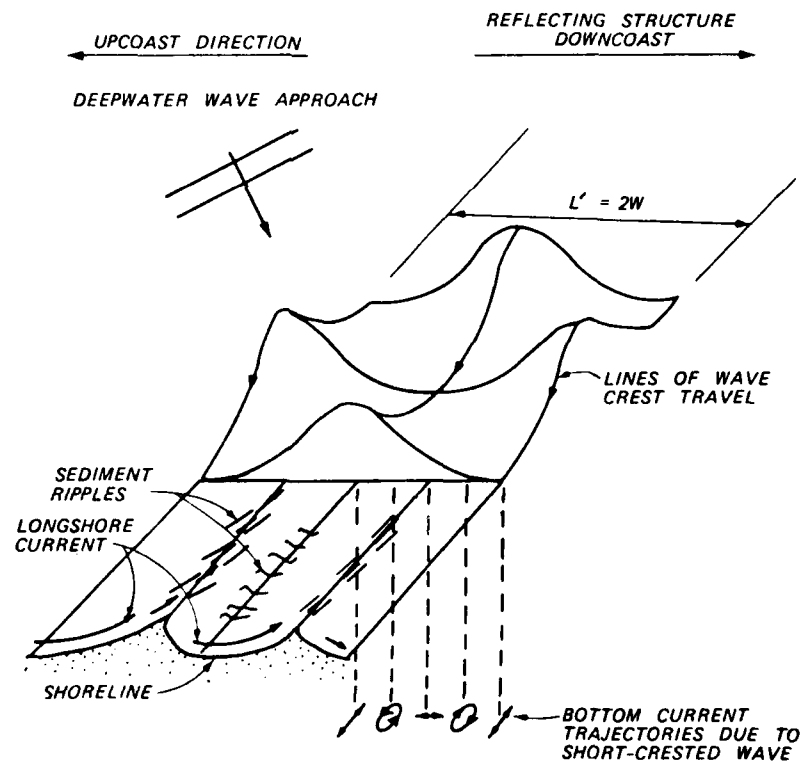


Figure 32. Interaction of short-crested wave field, longshore current, and beachline

onshore-offshore direction, and the ripple lines, perpendicular to these velocities, also indicate this. Between one crestline and the next, the bottom velocities vary from elliptical to alongshore to elliptical then to onshore-offshore under the next crest. Figure 33 shows the ripple

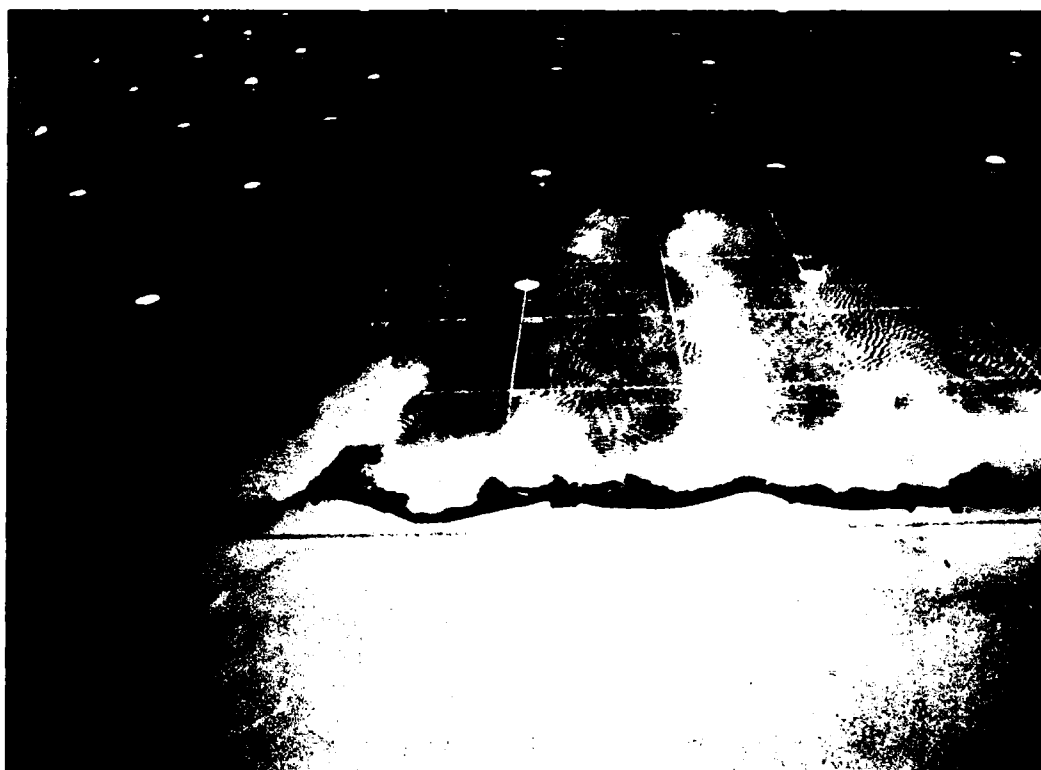


Figure 33. Shoreline upcoast of Plan 1 jetty system for test 8

pattern for a glass bead test of Plan 1 just upcoast of the jetty similar to the schematic diagram of Figure 32 where the alternating direction of ripples can be noted. The actual transport of material is brought about when the longshore current is superimposed on the short-crested wave field. Circulation cells are formed because the short-crested wave height varies along a line parallel to shore. Therefore, the higher part of the wave along the crestline breaks earlier and moves shoreward, creating a circulation flow to the zone of the lower breaker area similar to that described by Bowen (1969). The flow is to the downcoast side of

the cell due to the flow of the longshore current in that direction. The result is the creation of a cusp. As the longshore current approaches the upcoast jetty structure, it is deflected oceanward so sediment tends to follow the lines of this circulation, and examples are shown in Figures 34-38 from testing performed with coal from the Plans 1-3 tests.

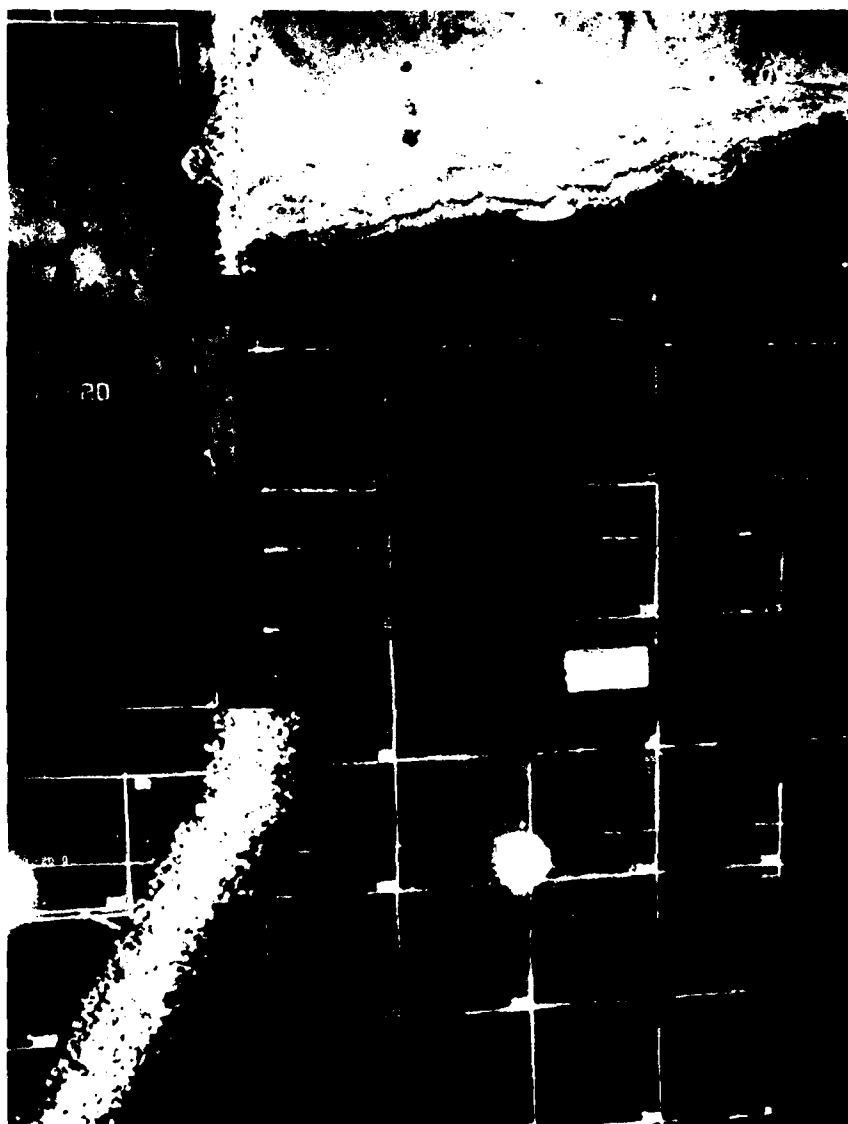


Figure 34. Offshore movement due to 5-ft, 10-sec
30-deg wave, Plan 1, test 3

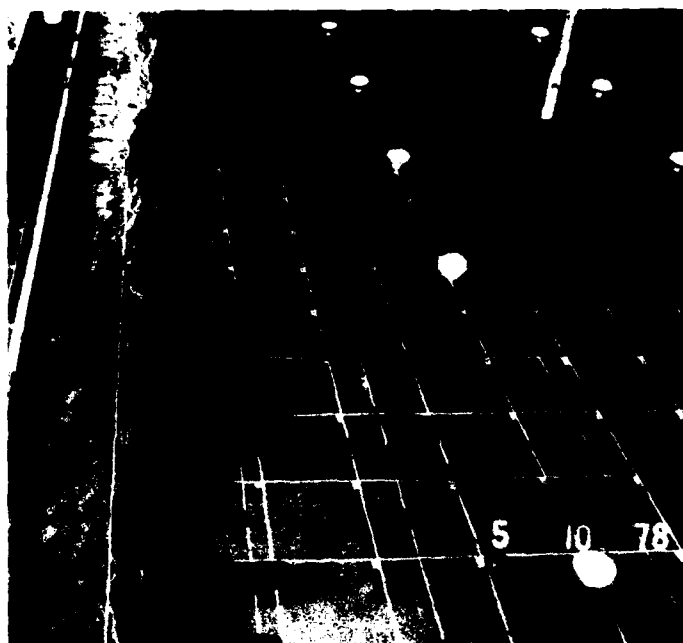


Figure 35. Offshore movement upcoast for Plan 1, test 10

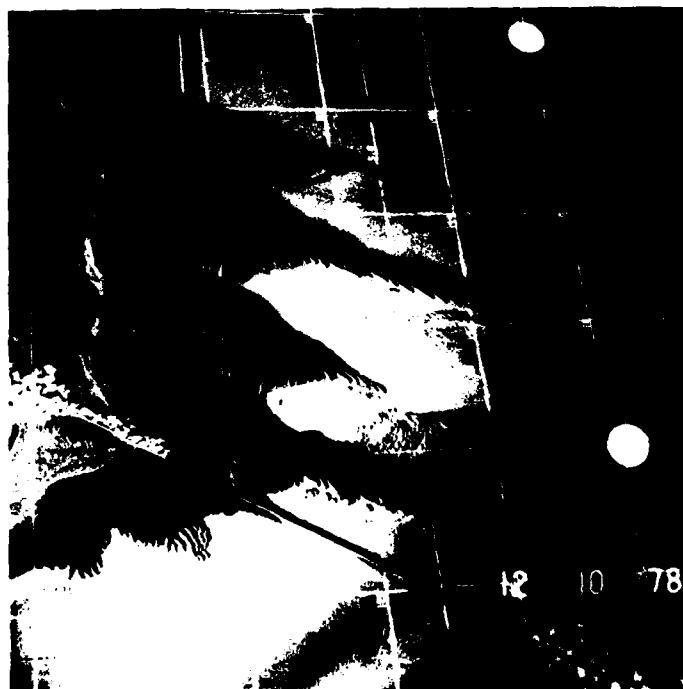


Figure 36. Offshore movement for Plan 2, test 11



Figure 37. Offshore movement for Plan 3, test 12



Figure 38. Offshore movement for Plan 3C, test 18

In each case the line of movement is parallel to the reflecting surface which is causing the short-crested wave field. This offshore movement can extend farther upcoast than the location where the main portion of the longshore current is deflected seaward by the structure so that the circulation cells are fairly strong. The spacing of the circulation cells are governed by the distance between crestlines, W , and can be determined by finding X in Figure 30 or Figure 31 for various values of ϕ or θ and β .

56. Plates 33-105 show results of the beach response test, most of which will be discussed later. For the present discussion. Plates 100 and 101 show sketches of the offshore movement of the tracer sediment for Plans 1 and 2 for the smaller 5-ft, 10-sec wave condition. There are locations where the parallel fingers of sediment intersect or join together. These are locations where there is some lateral transfer of tracer from one finger to another. Plate 55 (a test for the beads and a 10-ft, 10-sec wave) shows the fingers paralleling the outer leg of the Plan 1 jetty. The material in all these fingers originated from tracer moving offshore along the weir then gradually laterally transferring upcoast from one finger to the next due to the reflected wave energy off the jetty, although some of the tracer continued migrating oceanward along a given sediment tracer finger. Therefore, in this region of reflected wave energy, there was offshore-upcoast transport of sediment. Figures 36 and 37 also show this mechanism of sediment movement.

57. Plates 102-105 show the approximate upcoast limits of the short-crested wave field for the four basic jetty configurations studied. The reflected wave has been refracted shoreward along the parallel contours in each case, and the crestline travel stays almost parallel to the reflecting surface. In Plan 1, the crestlines do not intersect the breaker region for some distance upcoast. An interesting observation in Plate 105 (Plan 3C, 45-deg weir) is the focussing of reflected wave energy by the weir section along the shoreline.

58. The circulation cells (Figure 32) set up by the incident-wave

reflected wave plus the incoming longshore current can probably be compared or identified with other coastal phenomena. Komar (1976) mentions two ways to generate circulation cells along the shoreline. One is by wave refraction, creating regions of high waves and low waves along the coast. The other is the generation of standing edge waves by the ordinary incident swell waves, which again will create regions of high waves and low waves along the shoreline as they interact with the incoming swell. Clearly, the cell development noted in this study is a third mechanism for creating high and low wave regions along the coast but is not related to edge wave phenomena. The short-crested wave field created by incident and reflected waves provides a high and low wave region along the coast which is persistent in location (necessary for cell development) since the incident and reflected waves are of the same period.

59. Observations of waves reflected off jetty structures and their effects on the shoreline noted by others have been represented in model and prototype work by Tanaka and Sato (1976) and in the prototype by Penland (1979). Tanaka and Sato noted upcoast erosion on a prototype jetty structure at Kashumro Port, Japan, which had an outer part oblique to the shore and an inner part perpendicular to the shore. In a model test of such a structure, where only waves normal to the coast were generated, a current was formed flowing shoreward along the structure, which, as it approached shore, turned upcoast then offshore. Tanaka and Sato mentioned that reflected wave energy contributed 40 to 50 percent of the alongshore energy in the upcoast direction. No tests were run with waves oblique to the shoreline which would probably cause longshore currents approaching the structure to predominate over the circulation cells caused by the reflected waves. Penland discussed the reflection off the north jetty at St. John's River, Fla., and its effect on an adjacent upcoast inlet. The reflection-generated upcoast-directed currents aided in the inlet's migrating upcoast. In this case, the natural longshore current is interrupted by the upcoast inlet so the reflected wave energy predominates in creating an upcoast current.

Preliminary Testing

60. The concept for the beach response tests was to inject a tracer material onto the concrete bed of the model in the region upcoast of the jetties and let the wave-generated littoral currents bring the tracer to the jetty system. It then would be determined what percentage of the tracer entered the deposition basin. Initially, it was decided that the most important aspect of a tracer study would be to determine the plan of the shoreline upcoast of the jetty system. It was thought that a beach could be formed by feeding tracer at the upcoast end of the model and subjecting it to wave action. This proved to be impractical since the breaker zone was relatively wide on the 1:60 concrete beach slope, and the material tended to move only at the location of the strongest littoral currents. The solution to the problem was to mold a beach of tracer material to a steeper slope than that of the model, narrowing the surf zone and concentrating littoral currents. In order to choose a suitable tracer material, two-dimensional beach profile tests were conducted in a 2-ft-wide, 166-ft-long wave flume. These tests are discussed in Appendix A and resulted in the selection of glass beads with a specific gravity of 2.42 and a diameter of 0.13 mm. The glass beads were used throughout six tests at which time it was decided that operational and functional problems precluded further use of the beads, and coal with a specific gravity of 1.35 and a median diameter of 0.50 mm was selected as the final tracer. Operational problems encountered with the glass beads were concerned with quantities of material on hand and with the long response time required for the glass beads to be transported in the model. This resulted in unreasonably and unnecessarily large costs for conducting model tests since similar movement and conclusions could be reached using a coal tracer in a much shorter period of time.

Detailed Beach Response Testing

61. Initial detailed beach response tests were performed with

coal and plastic as additional quantities of glass beads had to be ordered to form a beach. These early tests with coal and plastics were run in order to develop test procedures and parameters.

Test conditions

62. The beach response tests were conducted with a constant water level set at high water (+2.5 ft mtl). Tides were not used until later in the testing program, and then comparisons with nontidal tests of similar conditions indicated there was not a significant difference in the results. Constant high-water levels maximized material movement over the weir. A deepwater wave angle of 30 deg was used initially for both the upcoast and downcoast waves. Later in the testing, a 40-deg deepwater wave angle was used. The wave period was maintained at 10 sec for the prototype (1 sec for the model) for all testing. Deepwater wave height was either 5 ft (0.05 ft for the model) or 10 ft (0.10 ft for the model). Three different initial slopes for the molded beach were used and are noted on the plates showing test results. During the tests the shoreline planform was periodically measured from a reference line and when an equilibrium planform for the upcoast wave was reached near the weir jetty, the test was stopped and a downcoast wave was run. The equilibrium planform was determined by repeated measurements of the beach planform at 1-ft increments (model feet) from a shoreward reference line at half-hour intervals of the test and determining the rate of change at each location for each time interval. When the rate of change was small or began oscillating plus or minus, a near-equilibrium planform was assumed. In some tests the material moving over the weir was periodically removed and measured, but in other tests it was permitted to accumulate in order to note patterns of deposition. The 19 tests conducted are reviewed in the following paragraphs and Table 3 summarizes the testing. Fillet areas and deposition volume given in Table 3 are presented in model dimensions and should not be extrapolated to prototype conditions for direct use in design or planning purposes but are only to be used for relative comparisons.

Test 1 (Plan 1)

63. Plate 33 shows test conditions and the resulting planform for

the 0.5 mm coal. The fillet formed by the upcoast wave was small, extending 400 ft (4 ft for the model) upcoast from the jetty before receding behind the original shoreline for the next 700 ft. Also, the fillet would not build out to the shoreward end of the weir section. The relatively large storm wave (10 ft) was assumed to be the cause of the limited amount of accretion. Plate 34 is a photograph of the region after the upcoast wave. Interesting to note is the accumulation of material in the shoreward end of the deposition basin behind the shoreward edge of the weir and also the significant amount of material in the seaward portion of the basin. Plate 35 shows the study area after the downcoast wave had been run. Seventy-one percent of the fillet was eroded by the downcoast wave (see Table 3 for details of testing). During the test, feeding of the beach was by demand; that is, a uniform beach was maintained at the initial waterline at the upcoast end of the beach.

Test 2 (Plan 1)

64. The upcoast wave was reduced to 5 ft from the previous test. A much larger fillet was obtained (five times larger in area, see Plate 36) even though the upcoast wave was run 1 hr less. The downcoast wave removed all the fillet except for a small area adjacent to the jetty.

Test 3 (Plan 1)

65. Plastic was used for the same wave conditions as test 2. Since only a limited supply was available, a smaller beach was prepared for testing than was previously used (Plate 37). This resulted in increased time to build the beach to a near-equilibrium planform since the fillet development was begun from a more shoreward position. The 5-ft wave again provided a large fillet (Plate 38) and the downcoast wave removed 90 percent of this fillet. The large accretionary region located along the upcoast beach after running the downcoast wave was a model effect due to the limits of coverage of the shoreline by the downcoast wave (i.e., it was in the diffraction zone of the downcoast wave generator). This is true for all other tests for which the downcoast wave generator was used. Plate 39 shows the fillet after it has been eroded at the end of the test and shows accumulation in the deposition basin shoreward of the weir.

Test 4 (Plan 1)

66. This was the first test with the 0.13-mm glass beads which had been selected on the basis of the two-dimensional wave flume testing. The initial beach slope was 1:13 and a 5-ft upcoast wave was run for 50 hr (model). The beachline was measured every 2 hr to determine when a nearly "equilibrium" planform was obtained. Plates 40-42 show the resulting planforms after the upcoast and downcoast waves. Gradual erosion occurred in the region 600 to 1400 ft upcoast of the jetty while the upcoast wave was run. Just upcoast of the eroding area there was an accumulation of sediment offshore (see top of Plate 42) accompanied by a rip current at that location. It was thought that perhaps the feeding rate was too high causing an accumulation at this location which in turn aided in generating a rip current and thus short-circuiting the littoral movement. Table 3 shows that the fillet area of 4.78 ft^2 is only about one-half that of Test 2, run with coal, although the bead test was run 12 times longer. Of the 2.051 ft^3 of material fed, only 0.118 ft^3 deposited in the basin. Therefore the next test was designed to lower the feeding rate to reduce the possibility of "clogging" the littoral drift.

Test 5 (Plan 1)

67. Test conditions were similar to those for test 4 except that the feed rate was reduced. After 60 hr (model) of upcoast waves the fillet size of 4.90 ft^2 was only slightly larger than the one of test 4 and deposition into the basin was slightly less-- 0.095 ft^3 . Results are shown in Plates 43-45. As discussed earlier, an interesting phenomenon was noted during this test which was thought to contribute to understanding sediment movement upcoast of the jetty. Waves were observed being reflected off the outer leg of the upcoast jetty. These reflected waves became noticeable as they shoaled on the sediment accumulation as seen in Plate 46 (looking upcoast from the jetty). Their initial contact with the shoreline began at this location and stretched upcoast. The interaction of incident and reflected waves in this area aided in the offshore transport of sediment.

Test 6 (Plan 1)

68. In order to increase littoral transport and direct the wave

reflected off the outer leg of the weir jetty farther upcoast, the deepwater wave angle with the coast was increased from 30 to 40 deg. The upcoast wave was run for 60 hr (model) and a slightly smaller fillet (3.77 ft^2) was formed. Material volume deposited in the basin was slightly increased over test 5 (Table 3). Plates 47 and 48 show the results. Also Table 3 shows that 1.121 ft^3 was fed upcoast but only 0.107 ft^3 deposited in the basin, a somewhat similar proportion as for the previous tests with glass beads. As seen in Plate 48 there is still a similar pattern of sediment accumulation offshore and erosion just upcoast of the fillet. It appeared that reflected waves were still inhibiting longshore transport and creating offshore movement.

Test 7 (Plan 1)

69. It was postulated that perhaps a larger wave would increase the littoral transport along the coast by increasing turbulence and alongshore wave thrust at the 1:100 scale and thereby overcome effects of waves reflecting off the structure. Plates 49-52 show results for this test which was run for the upcoast wave only for 16 hr (model). This test had close to the same wave energy input as test 6 since the 10-ft wave duration was about one-fourth as great. A fillet of 2.60 ft^2 was formed, smaller than the previous test by about 30 percent; however, the deposition basin captured almost double the amount of sediment. Plate 50 shows that two distinct zones in the deposition basin were filling. The shoreward portion of the basin was filling in the same manner as in previous tests, but the oceanward portion was filling due to suspended sediment coming over the oceanward end of the weir. Plate 51 shows also a significant amount of sediment was moving oceanward along the outer portion of the upcoast jetty. Plate 52 (looking upcoast) shows a cusplike beachline created by the interaction of incident and reflected waves as discussed in a previous section.

Test 8 (Plan 1)

70. In test 7, the molded beach did not extend far enough oceanward to reach the point of initial breaking for the larger wave used in that test. In order to extend the seaward toe of the beach to that location with the limited supply of bead sediment, the beach slope was

reduced from 1:13 to 1:27. The initial high-water line was maintained at the same location as for the previous tests. This test was run for 60 hr and Plates 53-56 show test results. Plate 54 shows the testing after 16 hr (which can be compared with test 7, which also was run for 16 hr). Comparison of Plates 50 and 54 shows that there was more offshore movement along the jetty. At the end of the test, the fillet against the jetty was smaller than that of the previous test by about one-third. However, the shoreline trend is similar (compare Plates 49 and 53) as there was still erosion in the region just upcoast of the fillet. Plate 56 shows the movement of sediment offshore along the jetty. The path of the sediment is initially along the ocean side of the weir, then there is a gradual lateral transfer (in the upcoast direction) of some sediment. This region had a complex circulation due to the short-crested wave field caused by waves reflected off the outer leg of the jetty plus a circulation induced by the longshore currents being deflected first offshore along the weir section, then tending to be recirculated back upcoast. There also was an oceanward component of movement of the sediment in a direction parallel to the outer leg of the jetty caused by the velocities created in the short-crested wave field superimposed on the deflected longshore currents and also aided by the offshore slope of the beach. Plate 56 also shows a region of no offshore movement where the model bottom was clear of sediment. Shoreward of this region was the point of maximum shoreline recession. Upcoast of this area there was offshore transport of sediment due to a net bottom current in the wave field (also noted in the two-dimensional flume tests in Appendix A). It appeared that a very slow return circulation eddy was cancelling this offshore movement in the area of erosion and changing the character of the approaching wave so that the breaker was closer to the shore at this location. Also at this location the longshore current tended to deviate from the shoreline and move offshore (Plate 19), which might aid in keeping the shoreline more recessed than the region upcoast.

Test 9 (Plan 1)

71. In order to determine the influence of the waves reflected

off the upcoast jetty on the movement of the bead sediment, wave absorber was placed along the upcoast jetty to significantly reduce wave reflection. The test was run for 20 hr and erosion just upcoast of the fillet still occurred but at a slower rate. Plates 57 and 58 show the results. Table 3 indicates a larger fillet (by a factor of two) for this test relative to the previous test, though as in earlier tests, erosion of the fillet area continued. Deposition in the basin was occurring at a faster rate than in test 8, indicating that significant reduction of the reflected wave permitted better transport to the weir. At this point in the testing program it became obvious that due to time and cost limitations, coal would be a more satisfactory tracer material. In the preliminary tests (for a small accretionary-type wave), a full fillet was built upcoast with coal without the erosional tendencies noted in the glass bead tests. Another key factor in using coal was the reduction in testing time. Bead tests required a run time on the order of 70 model hours, while coal tests could be completed in about 8 model hours. The primary fault with the bead appeared to be its lack of response to the longshore currents parallel to the coast. Onshore-offshore movement was correctly simulated in the model for the given test condition when compared with what would be expected from a similar prototype condition. The tendency for more offshore movement with the bead than the coal as seen in the flume tests should not have deterred the formation of a fillet near the weir. As seen by Shepard (1950) in a study of a pocket beach in California responding to a change in wave direction, at a time of high waves the beach would grow oceanward at the downdrift end of the pocket yet maintain a storm profile. It would seem reasonable to expect the beads to respond in a similar manner.

72. The threshold velocity (Komar and Miller 1973) of the beads due to a 1-sec wave of 0.1 ft height in 0.1 ft of water was 0.40 fps and that of the coal was 0.28 fps. For incipient motion of a particle on a fixed smooth bed due to unidirectional flow (Novak and Nalluri 1974) calculations show the incipient velocity for the bead was 0.37 fps and that of coal was 0.25 fps. For the smaller waves used in this study the incipient velocity of the bead was close to that of the longshore current

being generated and the coal was able to move more readily alongshore.

73. An examination of previous mathematical modeling of fillet evolution indicates good results have been obtained without simulating onshore-offshore transport, thus indicating that the longshore transport mechanism dominates the onshore-offshore two-dimensional transport in the formation of fillets. If this is the case, the higher incipient velocities required for the bead must be the main factor preventing formation of a fully accretionary fillet by permitting the shoreline circulation cells generated by the reflected waves to control the longshore movement of the relatively heavier bead; that is, longshore movement is reduced which permits accumulations upcoast in the presence of circulation cells which deflect material offshore.

Test 10 (Plan 1)

74. The 0.5-mm coal was molded to a 1:27 slope, as in bead tests 8 and 9, and the 5.0-ft upcoast wave was run for 7 hr. Every hour the deposition in the basin was removed and measured volumetrically. After 4 hr the rate of deposition in the basin reached a constant level. Deposition during hour 4 was 0.495 ft^3 and deposition during hour 5 was 0.484 ft^3 . Simultaneously with the volumetric measurements, the rate of shoreline change also was being examined hourly. After 5 hr there were no significant changes in the fillet planform near the weir. During hour 6 an increased feed rate was tried but only resulted in upbeach accumulations that slowed transport into the basin. The fillet region showed no significant change during the last 2 hr. Therefore it was decided that a 7-hr test was of sufficient duration to develop an equilibrium fillet near the weir (in the range of 1000 ft upcoast of the weir). This test (Plate 59) can be compared with test 6 (Plate 47), a bead test similar in wave parameters but different in beach slope and duration. When shorelines after the upcoast waves are compared, it can be seen that there was no erosion region along the upcoast shoreline as there was for bead test 6 due to the increased rate of longshore movement of coal over that of the beads. Also it is of interest to compare this test with test 3 (Plate 37) in which plastic beads were used. The accumulation near the jetty for upcoast waves was similar, and farther

upcoast, the plastic beach receded more due to the initial shoreline being located farther landward.

75. Because of the fairly rapid movement of the coal, a 1-hr (model) downcoast wave duration was selected. It was anticipated that the time interval would provide some indication of fillet shape variation among the various jetty plans for a downcoast wave. Plates 60 and 61 show photographs after the upcoast and downcoast waves, respectively. Table 3 shows that the fillet contained 12.00 ft^2 of surface area after the upcoast wave and 5.77 ft^2 after the downcoast wave, a reduction of 52 percent during the 1-hr (model) downcoast wave exposure.

76. As shown in Plates 59 and 60, the fillet never reached the weir but stabilized at a point about 80 ft (0.8 ft model) landward of the weir section. This location was reached after 1 hr into the test and remained constant for the remainder of the upcoast wave. Plate 60 indicates the manner in which the basin filled. The sediment moved over the weir and to the shoreward corner of the basin, settling adjacent to the jetty. As this region filled enough to emerge above the water level, it was pushed shoreward along the inside face of the jetty by refracting waves.

Test 11 (Plan 2)

77. The Plan 2 jetty system (with the upcoast jetty making an angle of 60 deg with the shoreline) was tested in the same manner as the Plan 1 system of test 10. Results are shown in Plates 62-64. The upcoast fillet had a surface area of 9.61 ft^2 after the upcoast wave and was totally removed back upcoast by 1 hr of the downcoast wave. Also, a lesser amount of material was deposited in the basin (Table 3) than in test 10. This was probably due to increased movement of material offshore (see Plate 63) as a result of incident wave-reflected wave interaction at the shoreline. Sediment transport over the weir occurred at the shoreward edge as in test 10.

Test 12 (Plan 3)

78. The Plan 3 jetty system, with the inner weir section of the jetty making an angle of 30 deg with the shoreline, was tested for the same conditions as tests 10 and 11 (i.e., Plans 1 and 2). Plates 65-67

show the results after upcoast and downcoast waves. The fillet stabilized shoreward of the edge of the weir as in the previous tests and sediment transport was confined to the shoreward portion of the weir. Once again there was offshore movement of some sediment upcoast of the weir due to the interaction of incident and reflected waves (Plates 66 and 67). Table 3 indicates that 2.520 ft^3 of material was deposited in the basin--less than that of test 10 (Plan 1) but more than that of test 11 (Plan 2). The upcoast fillet size was 6.25 ft^2 , less than Plan 1 or Plan 2 fillets by a considerable amount. Therefore, it appears that offshore movement upcoast of the weir is greater for Plan 3 than for Plan 1 and Plan 2. The downcoast wave completely removed the accumulated fillet (Plate 67).

Test 13 (Plan 3)

79. This test was designed to investigate the effect of a 5.0-ft tide on the sediment movement. Therefore, when compared with previous testing, this test had a variable water surface and tidal currents. The test was run for six tidal cycles for the upcoast wave (equalling about 7.5 model hours) and one tidal cycle for downcoast waves (equalling about 1.25 model hours). Therefore, the test duration was nearly the same as for the no-tide testing. The fillet size accumulated during the upcoast wave was narrower but longer (compare Plates 65 and 68) and contained 15.35 ft^2 . This is significantly larger than the no-tide fillet of test 12, and was due to its longer extent upcoast which may, in turn, be due to having an average lower water level during the test. Deposition in the basin was reduced by 19 percent. Also, comparison of Plates 66 and 69 shows that there is a slight increase in deposition seaward of the fillet upcoast of the weir. This probably is due to the times when the water level was below the weir crest and longshore currents were deflected along the offshore jetty. In addition, the lower water levels permit greater wave reflection off the weir which interacted with the incident wave, producing increased offshore transport. The downcoast wave did not cut back the shoreline near the jetty as far (the fillet was reduced in size by 53 percent) as the no-tide test (compare Plates 67 and 70), probably due to the varying water level and

possibly due to the effects of the ebb jet (exiting the channel) on the downcoast wave. This jet would refract the wave crest, thus reducing its angle with the shoreline.

Test 14 (Plan 3)

80. To examine effects of a storm wave on the movement of sediment near the jetty, the Plan 3 configuration was subjected to an increased upcoast wave height of 10.0 ft for the same duration (7.0 hr) as used in previous tests. Other test conditions remained the same as in tests 10, 11, and 12. It had been noted in the hydraulic testing that strong currents along the upcoast side of the jetty existed for high wave conditions. Plates 71 and 72 indicate that there was only a small fillet (1.15 ft^2) built against the jetty and a slight erosion of the original shoreline upcoast of the accumulation. Farther upcoast of the region of erosion there was a buildup of the beachline which indicated the region adjacent to the jetty was not being underfed, but that sediment was leaving the beachline before it could accumulate against the jetty by moving along the weir and oceanward along the upcoast side of the jetty. Plate 73 shows the accumulations oceanward of the weir. Plate 73 also shows that the major accumulation of sediment transported over the weir occurs in the oceanward portion of the deposition basin. The lobe of sediment extending oceanward directly offshore of the weir section, as seen in Plate 73, was observed to be created primarily by wave energy reflected off the weir section. Material that moved into the region of the bend of the jetty was carried there by the littoral current along the jetty. The total amount of material in this region was 1.708 ft^3 and the total amount deposited in the basin was 7.736 ft^3 . Therefore, 18 percent of the total amount of sediment moving to the weir region bypassed the weir section for this no-tide test. The downcoast wave removed the small fillet plus an additional quantity of shoreline as seen in Plate 74.

Test 15 (Plan 3)

81. The previous test was repeated with tidal conditions similar to test 13 and Plates 75-79 show the results. The fillet for this test (Plate 75) was somewhat similar in shape and twice as large (2.08 ft^2)

as that for the no-tide condition (test 14), but it was small in magnitude with respect to the smaller wave conditions for Plan 3. The total amount received by the deposition basin (3.707 ft^3) was just over one-half that captured by the basin for the no-tide test 14 (see Table 3). There also was an increase of sediment bypassing the weir. Of the total amount reaching the weir, 26 percent bypassed the weir as compared with 18 percent for the no-tide condition. Also it was noted during the testing that with the addition of tidal currents, the distribution of sediment entering the deposition basin was along the entire length of weir. With the no-tide condition and the 10.0-ft wave, sediment passed over the oceanward portion of the weir. The downcoast wave removed the small fillet (Plate 77). Test 15 was extended by running a 10-ft wave for 7 hr with no tide. No feeding of the beach was performed due to the buildup of the upcoast beach during testing with the tide (see Plate 75 and compare shoreline with Plate 71 for a no-tide condition). Plate 78 shows the model after the 7 additional hours. No dredging of the basin was performed as it filled. Interesting to note was the formation of a bar separating the basin and the navigation channel. The total volume in the basin was 7.703 ft^3 . The total amount of sediment oceanward of the weir and along the upcoast jetty was 5.454 ft^3 . Therefore, for this high-energy condition and high feed rate (due to upcoast beach storage), 41 percent of the sediment moving into the weir region moved offshore and 59 percent moved into the basin. Also, movement of sediment into the channel can be seen in the top of Plate 78. Plate 79 shows the coal sediment with water drained from the model. Undulations in the sediment bed due to the reflected wave field can be seen. The test was continued for 7 more hours (test conditions similar to previous 7 hr) with the upcoast beach the sole provider of sediment. Since the beach had been eroded significantly, transport was reduced and the basin captured 4.211 ft^3 with 0.960 ft^3 moving offshore in front of the weir. Thus 19 percent of the total material moving toward the weir moved offshore.

Test 16 (Plan 3A)

82. A groin was placed upcoast of the weir as shown in Figure 14.

The groin, with crest uniformly set to +7.0 ft msl, extended out to the same depth as the shoreward end of the weir. The purpose of this test was to examine sediment movement around an auxiliary structure intended to aid in maximizing fillet storage. One question to be answered would be whether sediment from upcoast might be deflected offshore away from the weir; thus conditions of impermeability and high crest elevation were selected to maximize this possibility. Plates 80-83 show test results. Plate 81 is after 7 hr, the usual test interval, and Plate 82 is after 8 hr of the test. The 1-hr extension of the test was necessary due to the longer duration required to stabilize a uniform rate of transport into the basin since the region between the groin and weir was initially empty of sediment. The test was stopped before an equilibrium rate was reached. The longshore sediment movement was not significantly deflected offshore by the groin but bypassed the groin once a fillet had built up. The beachline in the compartment between the groin and the weir then gradually accreted up to the shoreward end of the weir. The downcoast wave then shifted the fillet in the compartment against the groin (Plate 83). The initial accumulated fillet storage upcoast of the groin was 18.25 ft^2 . Because of its location significantly farther upbeach than previous fillets, part of the fillet was outside the influence of the shoreline covered by the downcoast wave. Therefore the erosion of the total fillet was extrapolated from that part where the fillet was eroded by the downcoast wave, and it thus was determined that 79 percent of the fillet was eroded during the 1-hr duration of downcoast wave (see Table 3). The effect of the increase in beach storage for this configuration and also the initially empty compartment between the groin and the weir is reflected in the total basin accumulation of 1.139 ft^3 .

Test 17 (Plan 3B)

83. This plan involved placing a groin adjacent to the upcoast side of the weir. The groin of the previous test could not be shifted laterally downcoast since this would place the groin tip in relatively deep water and probably would not be considered a feasible plan. Therefore the weir was shifted along the line of its 30-deg trunk until it

intersected the shoreline. The groin then was constructed perpendicular to shore from this point until it extended to the contour at which the weir section was initiated in previous testing. This is possibly a better location for a weir since it is shifted farther away from the navigation channel which would aid in reducing any tendency for ebb flows to migrate into the deposition basin and exit over the weir. Plate 84 shows the beach planforms after the 5-ft 10-sec upcoast and downcoast waves. Plate 85 shows the beach at the start of the test, Plate 86 after 8 hr of upcoast waves, and Plate 87 after 1 hr of downcoast waves. The surface area of the fillet was 28.20 ft^2 after the upcoast wave and was reduced 90 percent by the downcoast wave (with an extrapolation of the eroded area due to limited beach coverage by the downcoast wave as discussed for the previous test). It was noted that sediment did not bypass the weir section but started accreting at the shoreward edge of the weir (Plate 86) and accumulated in the shoreward portion of the basin (in the corner adjacent to the jetty). Dredging of the basin was stopped at hour 4 of the test in order to let the basin fill and to note any tendency for sediment accumulation to cut off in front of the weir. The accumulation in the basin seen in Plate 86 is the major portion of the transport into the basin since 2.051 ft^3 of the total transport (2.264 ft^3) occurred between hours 4 and 8 of the test. Observations during the test indicated that waves reflected off the weir seemed to aid in keeping transport over the weir toward that portion of weir adjacent to the groin. A strong current movement into the basin was noted (even though no tide was reproduced) which would further augment sediment transport over the weir.

84. Test 17 was extended to determine shoreline response for a 10-ft, 10-sec wave. First, the fillet was reformed by running the 5-ft, 10-sec upcoast wave for 4 hr (see Plate 88 and compare with Plate 86) and the basin was allowed to fill. At this point, the 10-ft, 10-sec wave was run for 7 hr and Plates 89 and 90 show the results. The region at the weir crest gradually filled from the shoreward end of the weir to the oceanward portion as the test progressed and the basin filled. There was no tendency to form a bar from the groin tip which might have

cut off the weir. The basin contained 5.642 ft^3 at this time and 3.077 ft^3 bypassed the weir, accumulating along the upcoast side of the outer jetty trunk. Plate 91 shows the model bed after the ocean was drained. The 10-ft wave once again moved significant amounts of sediment offshore with 35 percent moving offshore and 65 percent moving into the basin. These figures show less offshore movement than the basic Plan 3 configuration, perhaps indicative of reducing offshore transport near the jetty by reduction in wave reflection effects on the upcoast region.

Test 18 (Plan 3C)

85. Plan 3C called for an examination of a 45-deg weir (see Figure 14). The outer trunk of the upcoast jetty remained the same as in previous Plan 3 testing. Plate 92 shows the resulting beach planform for the 5-ft, 10-sec upcoast and downcoast wave conditions. Wave reflections off both the outer and inner portions of the upcoast jetty appeared to minimize the fillet size seen in Plate 93. The basin was permitted to accumulate tracer throughout the test. The fillet size was 7.60 ft^2 (Table 3) and was eroded 91 percent by the downcoast wave (Plate 94). There was significant offshore movement during the upcoast wave, but no material moved past the weir for this 5-ft wave.

86. The fillet was rebuilt by running 2 additional hours of 5-ft upcoast waves. Subsequently the wave height was increased to 10 ft and run for 2 hr; Plates 95 and 96 show the results. The fillet was reduced and an erosional area occurred along the upcoast shoreline where the waves reflected off the weir provided increased energy. Plate 96 shows considerable movement of sediment along the jetty. During the 2-hr test period 2.696 ft^3 entered the basin and 2.373 cu ft bypassed the weir. Therefore, the basin captured 53 percent of the littoral drift with 47 percent bypassing.

Test 19 (Plan 3D)

87. Plan 3D was a modification of Plan 3C and consisted of placing a groin downcoast of the weir to determine its effect on material bypassing the weir (noted to be quite severe for the 10-ft wave test of Plan 3C). Initial test conditions consisted of having a fillet formed upcoast of the weir by a 5-ft wave. The 10-ft, 10-sec upcoast wave then

was run for 3 hr. Plate 97 shows the planform and Plates 98 and 99 show the model. There was still movement past the groin toward the jetty tip. During the test 2.323 ft³ deposited in the basin; 0.432 ft³ deposited in front of the weir and 0.678 ft³ bypassed the groin and settled along the ocean side of the jetty trunk. Thus, 71 percent of the sediment reached the deposition basin, an 18 percent increase from the previous test.

Comments on Test Conditions and Effects on Test Results

88. The relatively deeper water along the jetties in the model may have reduced wave effects which generate longshore currents along the jetties. In many smaller inlets, depths at the oceanward end of the jetties might be about 10 ft compared with the scaled depth of ~14 ft at the end of the jetties in the model. Therefore, one might expect stronger current action for more typical inlet bathymetries which might transport more sediment to the channel than was observed in this study.

89. The curvature of contours generally paralleling the outer ends of jetties rather than the *model contours* which paralleled the shoreline might also augment wave effects relative to that observed in the model by the concentration of wave orthogonals in the vicinity of the jetties.

90. A design concept used in this study of starting the weir section at a depth of 10 ft so as to create a large storage fillet will probably not be feasible in many projects due to the shallow depths and bars in the region of a natural inlet. The Plan 3B system probably would represent a functional weir jetty system if depths are shallow.

91. For the type of jetties investigated herein (i.e., jetties with the weir offset oceanward in order to provide an impermeable portion between the shore and the weir which in turn permits a storage fillet to be created upcoast of the weir) it has been seen that there is a strong probability that not all downdrift transport will move over the weir, but some will move offshore in the upcoast vicinity of the jetty. As wave conditions are increased, more of this sediment can be carried

offshore. The combination of the deflected longshore current and the interaction between incident and reflected waves contributes to offshore sediment transport. Most likely, the more irregular the wave field the less offshore transport will occur since the offshore circulation cells would be more diffuse and not as concentrated as those in a monochromatic wave field. However, extreme wave conditions probably would carry substantial quantities of sediment offshore due to the extreme turbulence near the jetty caused by incident waves, reflected waves, and longshore currents.

92. As shown in a number of test photos there was an offshore-onshore component of sediment movement. In the two-dimensional tests (see Appendix A), onshore-offshore movement was relatively straightforward in that criteria such as that of Dean (1973) can be applied to determine whether movement is offshore or onshore. In the three-dimensional model, other factors influenced onshore-offshore motion. In the region of the jetty, littoral currents were being deflected offshore which could carry material offshore, and there was incident wave-reflected wave interaction which influenced onshore-offshore movement. Also, further upcoast outside the influence of the jetty-created effects of onshore-offshore movement, there appeared to be onshore-offshore effects caused by the condition of the beachline. For example, it was noted during testing with coal in test 15, that during the first portion of the test, when feeding the beach at regular intervals, there was some movement in an offshore direction from the beach. In a later phase of the testing, when feeding was stopped and the beach was gradually receding, the offshore deposits moved onshore and downcoast. All tests were for a large upcoast wave angle (40 deg).

93. Reflected energy would be less for rubble weirs but still could be significant based on prototype reflection coefficients of Thornton and Calhoun (1972). It was noted in this study that if the outer leg of the jetty was inclined to the shore at some angle (60 deg for Plans 1 and 2), there was significant reflected energy impinging on the shoreline. The model reflection coefficient of 0.3 is comparable to that of prototype structures. For structures with outer legs

perpendicular to shore (Plan 3), the reflection would not extend very far upcoast for the predominant angles of wave approach or would not exist at all due to the Mach-stem effect. It is also noted that the weir probably was not acting as a full reflecting surface for most of the testing, since the water level was higher than the weir and some wave energy was transmitted into the basin.

Discussion of Beach Response Tests

94. The first important point noted throughout the testing was the offshore movement of material near the weir jetty system. It appears that one cannot expect all the sediment moving downcoast to deposit in either the basin or the fillet, but some part will move offshore (most likely a greater percentage for larger wave conditions). This type of offshore movement differs from that along a uniform coastline in which a beach profile is adjusting to various wave conditions. The offshore movement discussed here is related to the presence of a jetty, and the offshore movement occurs due to an oceanward deflection of the wave-generated longshore current by the jetty system even with the presence of a weir (which might be conceptually expected to entirely capture this current). Also, the interaction of the longshore current with the short-crested wave field, created by incident waves and waves reflected off the upcoast jetty, is important in creating circulation cells which can remove sediment from the beach as seen in preceding discussions.

95. Distinguishing differences can be seen among the plans due to reflected wave phenomena because of the various jetty orientations. The extent that these differences among structural configurations can be extrapolated from model to prototype conditions is a difficult question. The model provides a relatively uniform environment of monochromatic waves and smooth slopes in contrast to the broader spectrum of waves and varying bathymetry of the prototype. However prototype conditions similar to the model can occur part of the time as evidenced by the reflected wave pattern seen in Figure 22 of Masonboro Inlet.

96. Whether the model tracer material correctly simulates the movement of sand is another problem of concern. It appears evident that the coal tracer responds to all the existing forces--longshore currents, short-crested wave circulation currents, reflected wave energy, and tidal currents. Since these forces dominate in the region of the jetty system, the coal is most likely responding as a tracer in an excellent manner; i.e., the coal is moving in directions in which prototype materials would move. Also, it appears that the coal, which has a tendency to provide an accretionary beach in two-dimensional testing, would probably respond well to an accretionary beach situation such as the creation of a fillet upcoast of the jetty. Perhaps then, the accretionary planforms could be considered representative of a prototype situation. Situations where erosion dominates along the shoreline are more difficult to evaluate, especially due to the nature of testing in which the beach is placed on a concrete bed. Erosion can occur to just the limit of the coal beach depth. Perhaps in nature erosion would continue to greater depths which in turn would affect erosion of the beach planform. Also, offshore bars would form in nature which would protect the beach somewhat from further erosion, but these bars do not always form on the underlying concrete model bed. It appears that the best approach to take with the beach planform data is to make relative comparisons among the plans.

97. It has been suggested that the optimal weir jetty system should not capture the entire amount of longshore drift approaching the weir but that it should only capture the net drift. This would permit the wave energy from the downcoast direction to remove some sediment which had been stored in the upcoast fillet by the upcoast wave energy. Thus, in evaluating the beach planform tests, one criterion for comparison would be relative amounts of upcoast storage of the stabilized fillet and the amount of removal of the fillet by the downcoast wave. It should be recognized that test conditions were limited, with only one upcoast and one downcoast wave condition.

98. Table 3 shows the necessary data to make a comparison in fillet size (in terms of surface area) accumulated during upcoast wave

conditions and the amount eroded during downcoast waves. Tests 10, 11, 12, and 18 should be compared as far as the basic weir orientations are concerned. The Plan 1 jetty with a 90-deg weir has the largest fillet (test 10), followed by the 60-deg weir (test 11), the 45-deg weir (test 18), and the 30-deg weir (test 12). Fillet size is thus reduced as weir angle decreases. Figure 39 shows a plot of these fillets and it

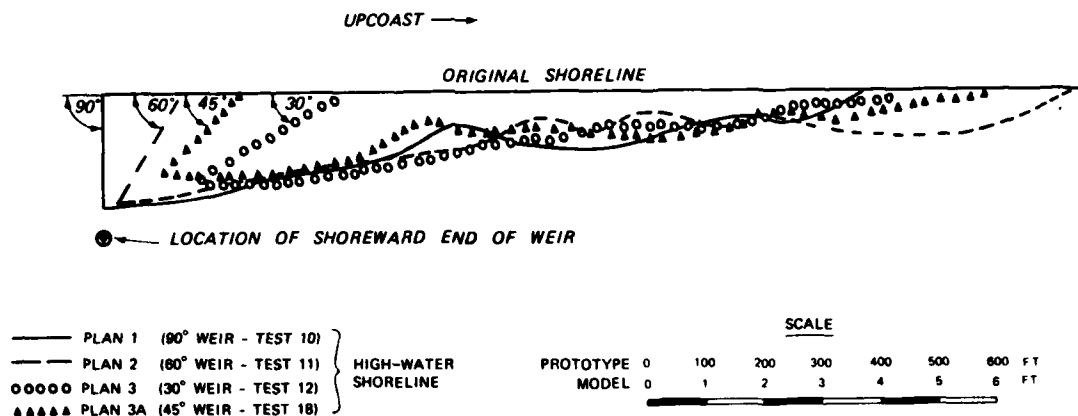


Figure 39. Fillet development for 5-ft, 10-sec 40-deg upcoast wave can be seen that they are fairly similar, with small undulations occurring at different locations for each separate condition. These plots were made using the shoreward end of the weir as a reference point. As the weir angle decreases, more surface area of the fillet is removed relative to the larger angles, accounting for most of the reduction in fillet surface area as weir angle decreases. Examining the fillets upcoast of the region where weir angle affects storage, it appears that the 45-deg weir has the smallest surface area in the midsection of the fillets, probably due to the focussing of reflected wave energy just upcoast of this region which aided in removal of sediment from the shoreline. Also from Figure 39, it is seen that the fillet approached closest to the weir for the 90-deg orientation, followed by the 60-, 30-, and 45-deg orientations, respectively. Reflected wave energy into this region appeared to control the location of the meeting of the

fillet's shoreline and the jetty, since small circulation cells were usually set up adjacent to the jetty.

99. The downcoast wave removed varying amounts of sediment from the four basic configurations (tests 10, 11, 12, and 18) as seen in Table 3. Plans 1, 2, 3, and 3C removed 52, 100, 100, and 91 percent of the fillet, respectively. These percentages correspond to losses of 6.18, 9.61, 6.25, and 6.95 ft^2 from each respective fillet. The orientation with an outer leg perpendicular to shore certainly showed an advantage over the Plan 1 dogleg orientation with respect to removing sediment from the fillet toward the upcoast beach.

100. During testing, measurements of the volume of sediment entering the basin were usually made on an hourly basis for the tests with coal and every 4 hr when using glass beads. Figures 40 and 41 show the accumulative deposition in the basin versus time for tests 4-19. Discussing only the "basic" tests (10, 11, 12, and 18) at this time, Figure 40 shows that test 10 (90-deg weir), test 18 (45-deg weir), test 12 (30-deg weir) and test 11 (60-deg weir) had decreasing total deposition of 2.907 ft^3 , 2.523 ft^2 , 2.520 ft^3 , and 2.283 ft^3 , respectively. It should be noted that the feeding of sediment was increased over that of other tests for test 10 during the last 2 hr, which caused an increase in basin deposition during hour 6 of the test but then resulted in a decrease during hour 7. If the curve of test 10 were extrapolated from hour 5 to hour 7, about the same cumulative total is reached, so the accelerated feeding did not affect the total accumulation at hour 7. If the test had run longer there may have been significant changes. Tests 11, 12, and 18, plus the first 5 hr of test 10, all had a uniform feed rate of $0.494 \text{ ft}^3/\text{hr}$ and all tests should prove to be directly comparable. Assuming that an area change of 1 ft^2 of fillet represents a volume change of 1 yd^3 (27 ft^3) of sediment (rule of thumb, Shore Protection Manual (CERC 1977) though not directly applicable to model values but used for the sake of providing relative comparisons), and adding the fillet volume and basin volume, the following volumes are determined, ranked by magnitude: Plan 1, 6.147 ft^3 ; Plan 2, 4.860 ft^3 ; Plan 3C, 4.575 ft^3 ; and Plan 3, 4.208 ft^3 . The reason for the difference

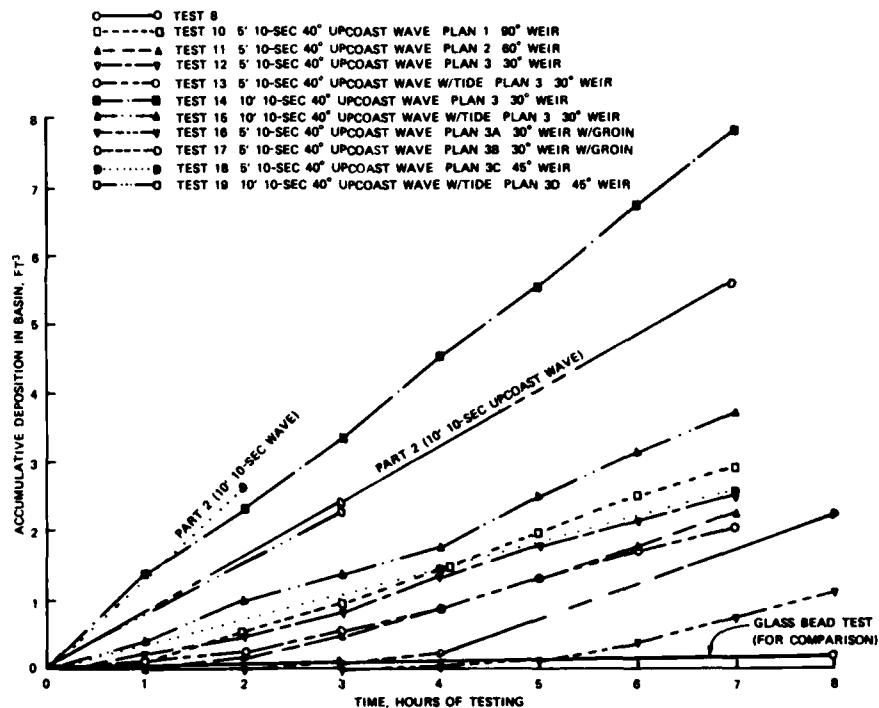


Figure 40. Accumulative deposition in basin, coal beach response tests

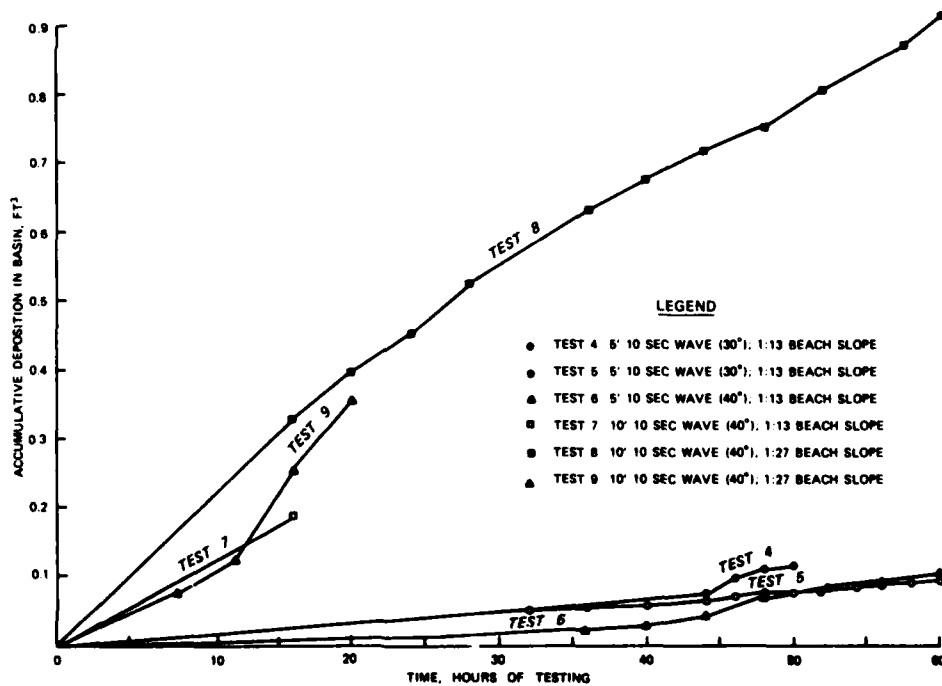


Figure 41. Accumulative deposition in basin, glass bead beach response tests

among these totals is the increased offshore movement as the fillet-basin total decreases and as the angle of the weir decreases. This is evident from the photographs of Figures 34 and 36-38 shown previously.

101. Figure 42, taken from preliminary testing of glass beads, with a 10-ft, 10-sec 30-deg upcoast wave, generally typifies sediment movement patterns for the Plan 1 beach response tests. When a large wave was run (10 ft), there were usually two zones of movement over the weir. Seaward, at the location of the initial breaker, there was transport of suspended sediment over the weir straight across into the deposition basin. Shoreward, there was movement of sediment over the landward edge of the weir. This sediment was pushed into the lee of the inner rubble-mound portion of the jetty toward the shore by refracting waves coming over the weir and by wave energy which had entered between the seaward tips of the jetties and diffracted into the deposition basin. For the smaller waves (5 ft), which broke near the shoreline, only the second portion of the above description holds true. It was difficult to make direct comparisons of the accumulative patterns of deposition in the basin since in many tests, dredging of the deposition basin was performed. Plates 34 and 39 show the full test's deposition of the Plan 1 system for coal and plastic sediments, respectively. In each case the sediment was moved to the shoreward end of the deposition basin.

102. Plate 63 shows movement over the weir for Plan 2. The sediment moved over the weir and behind the shoreward portion of the jetty. The photograph shows the deposition for only the last 1 hr of the test since dredging of the basin was performed during the test. The basin was not cut into the model bed for Plan 2, so the deposition is spread over a broader area than if the basin had been installed. Plate 66 shows the last hour's deposition for Plan 3, with sediment accumulating in the lee of the shoreward portion of the jetty. Plate 81 shows the last hour's deposition for Plan 3A, and Plate 86 shows deposition for Plan 3B for the last 4 hr of testing. Plate 93 shows the entire test's basin deposition for Plan 3C. The shoreline has built across the basin to the other side. For the tests discussed in this paragraph only the 5-ft, 10-sec wave was reproduced.



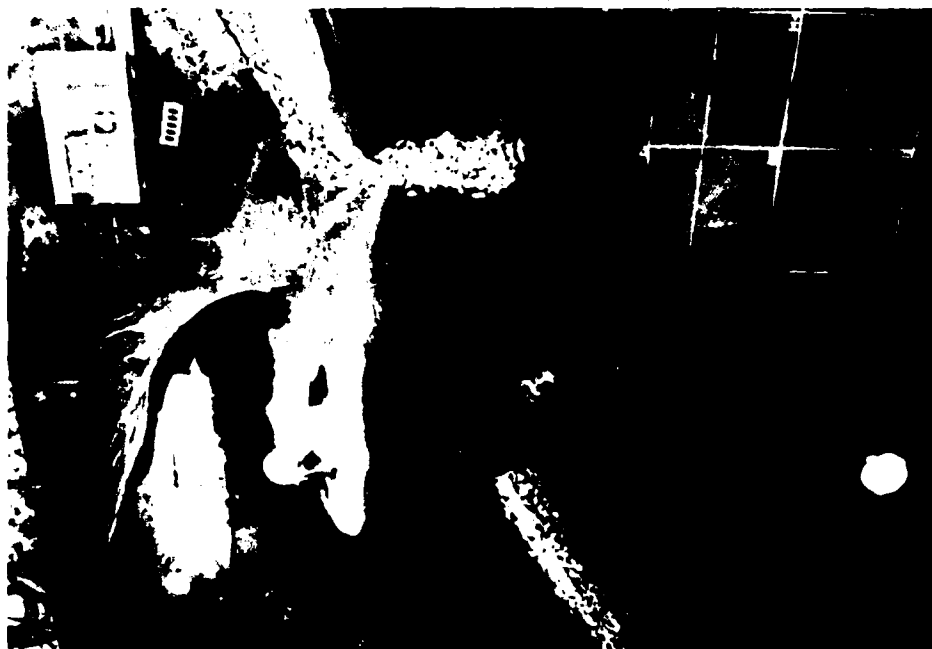
Figure 42. Typical sediment movement over weir section

103. Sediment movement over the weir for the 10-ft, 10-sec wave with Plan 3 (Plate 73) indicated movement of sediment over the entire width of the weir due to the accumulation of sediment along the entire seaward side of the weir; accumulation is in the outer one-third of the basin. Plan 3C's response (Plate 96) is similar to that of Plan 3. The response of Plans 3B and 3D, which have groins adjacent to the weir, was to promote basin filling straight across the basin, parallel to the shoreline for the 10-ft wave condition and is shown in Figure 43. The shoreward spit development in Figure 43a was due to the earlier portions of the test when the 5-ft upcoast wave and 10-ft downcoast waves were run.

104. From the above discussion it was seen that for initial conditions, that is, for a newly dredged basin, and for wave conditions where the breaker is close to shore, sediment moved over the shoreward edge of the weir and deposited in the lee of the shoreward portion of the jetty, and a spit developed across the shoreward portion of the basin. However, for larger waves, suspended sediment would be transported over the more seaward portion of the weir, and for some tests where sediment had accumulated to shallow depths in front of the weir (Plates 78 and 96) sediment movement over the entire weir length took place. Other tests, like that shown in Figure 43b, show that certain conditions might produce spit development across the basin which could short-circuit the use of a portion of the deposition basin for larger wave conditions.

Other tests with coal

105. The Plan 3 system also was subjected to testing with tides and with larger waves. It was desired to see whether any significant differences were noted when the regularly scaled tide was run with sediment beach and feed conditions similar to the no-tide testing. As discussed previously, test 13 provided a fillet similar to the no-tide test (test 12), but of much longer extent alongshore due to the varying water level. Total volume deposited in the basin for test 13 was reduced from the test 12 value by 0.469 ft^3 (or 19 percent); however Figure 40 shows that the slopes of the two test curves are similar, indicating that each



a. Plan 3B



b. Plan 3D

Figure 43. Effects of 10-ft wave on basin filling for Plans 3B and 3D

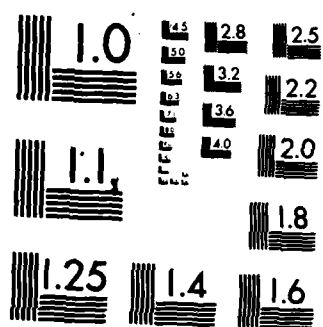
UNCLASSIFIED

MAR 83 WES/TR/HL-83-5

F/G 13/2

2/4

NL



MICROCOPY RESOLUTION TEST CHART
NATIONAL BUREAU OF STANDARDS-1963-A

test had reached a similar rate of deposition. Therefore, for the 5-ft, 10-sec wave condition, results between the tide and no-tide testing were not significantly different.

106. Test 14 (no-tide) and test 15 (tidal) were conducted in a similar manner to tests 12 and 13 except a 10-ft, 10-sec wave was reproduced. Although the fillets were not significantly different, more deposition in the basin and more movement offshore past the weir was measured for the no tide test due to the constant high water level. However, the percentage of sediment moving past the weir was higher for the tide test--24 percent compared with 18 percent for the no-tide condition of test 14.

107. Tests 16, 17, and 19 were designed to examine the possibilities of preventing some of the problems such as small fillet development or sediment bypassing the weir section. Neither of the groins upcoast of the weir (tests 16 and 17) appeared to adversely affect transport to the weir and did provide increased fillet storage. Also, when a 10-ft, 10-sec wave was added as a continuation to test 17, no tendency for sediment to cut off the weir was noted. The groin downcoast of the weir aided in reducing the amount of material bypassing the weir and moving toward the jetty tip.

Time scale

108. It might be of interest to determine an estimate or range of the model prototype time scale for sediment transport. The 5-ft, 10-sec test data were used and a $0.494 \text{ ft}^3/\text{hr}$ feed rate was experimentally found to be the maximum capacity for this wave. This also was about the average rate that was depositing in the basin once a near-equilibrium fillet was obtained. Using the Shore Protection Manual (CERC 1977) equation

$$Q = (7.5 \times 10^3) P_{ls}$$

where

Q = longshore transport rate (yd^3/yr)

P_{ls} = longshore energy flux factor ($\text{ft-lb/sec/linear ft of beach}$)

with $P_{\ell s}$ determined from the expression (CERC 1977)

$$P_{\ell s} = 32.1 H_b^{5/2} \sin 2\alpha_b$$

where

H_b = breaker height in ft (use 5 ft)

α_b = breaker angle (use 10 deg)

From the above $P_{\ell s} = 613 \text{ ft-lb/sec/ft}$ and $Q = 4,597,500 \text{ yd}^3/\text{yr} = 0.146 \text{ yd}^3/\text{sec}$. As mentioned earlier, 0.494 ft^3 was depositing in the basin hourly. This represents about $18,300 \text{ yd}^3$ in prototype units. Dividing $18,300 \text{ yd}^3$ by $0.146 \text{ yd}^3/\text{sec}$ equals $125,342 \text{ sec} = 34.8 \text{ hr}$. Therefore, 1 hour in the model represents 34.8 hr prototype. However, this prototype estimate of sand transport used is usually considered near a maximum especially at higher energy levels (as the calculated $P_{\ell s}$ is). Some prototype measurements show transport rates can be two orders of magnitude less than those calculated. For the sake of this illustration, a range from that rate calculated to one order of magnitude less will be assumed. Therefore, one hour in the model can represent 34.8 to 348 hours in the prototype or one model hour can represent 1.45 to 14.5 days.

109. The manner in which the model sediment is moving can be examined by use of Inman and Bagnold's (1963) equation:

$$I_{\ell} = (\rho_s - \rho) g a' S_{\ell}$$

where

I_{ℓ} = immersed weight transport rate (lb/sec)

ρ_s = sediment density ($\text{lb-sec}^2/\text{ft}^4$)

ρ = water density ($\text{lb-sec}^2/\text{ft}^4$)

g = acceleration due to gravity (ft/sec^2)

a' = correction factor for pore space (equal to 0.62 for coal)

S_{ℓ} = volume transport rate (ft^3/sec)

and Komar and Inman's (1970) equation:

$$I_{\ell} = K P_{\ell}$$

where

K = a dimensionless constant

I_λ = as defined above

P_λ = as defined above

Calculating P_λ for the 5-ft, 10-sec and 10-ft, 10-sec, 40-deg deepwater angle wave conditions scaled down to model dimensions and determining I_λ from Inman and Bagnold's equation, values of K were determined for Komar and Inman's equation. For the 5-ft wave, $K = 0.31$ and for the 10-ft wave $K = 0.18$. Model values of K in past studies have been in this range, while the value of K for field data has been ~ 0.77 . Considering K an efficiency factor, it is seen that the model is not as efficient as the prototype in moving sediment, possibly due to reduced turbulence in the model. This is illustrated by the observation that the model transport is almost all bed load for the 5-ft, 10-sec wave condition, with little or no suspended sediment. Also, the lack of sediment for transport became a problem for the larger 10-ft wave. The sediment wedge extended out to near the depth of breaking for the 10-ft wave, but the thin veneer near the tip of the beach wedge quickly eroded so that the absence of sediment at the seaward edge of the breaker zone reduced transport for a given wave energy. This is reflected in the calculation of a $K = 0.18$ for the 10-ft wave.

110. A final comment on time scale would be to conclude that a time scale is not critical to evaluation of results of this study since the movable-bed portion was examining an "equilibrium" shoreline upcoast of the weir. However, it might be of interest to determine the time to obtain "equilibrium" fillets. It probably would be very difficult to extrapolate such information from the present study, especially since the model was not fully a movable-bed type. Consequently, it may not be possible to obtain meaningful results on the time required to develop equilibrium fillets from this information.

PART VI: OBSERVATIONS AND CONCLUSIONS

111. The present study has permitted a number of observations which hopefully will contribute to weir jetty design. Major objectives of the study were to determine optimum jetty and weir orientation, weir elevation, and weir length with respect to impounding the net longshore transport while providing safe navigation in the channel and dredging operations in the deposition basin.

Hydraulic Testing

Flow over the weir

112. Results of the hydraulic studies indicate the following:

- a. High Keulegan K (Plan I) and low Keulegan K (Plan IA) inlets were tested. High K inlets have maximum ebb and flood currents near midtide elevation and low K inlets have maximum ebb and flood currents near low- and high-water elevations, respectively. As a result (considering a weir at mtl), high K inlets have less flood flow and greater ebb flow over a weir than low K inlets. For low K inlets there is very little, if any, ebb flow over an mtl weir. For high K inlets, flood flow predominates over ebb flow for an mtl weir. Therefore mtl can be considered a reasonable elevation for a weir section since it appears desirable to minimize ebb flow over the weir due to the possibility of aiding migration of the navigation channel toward the weir and thus through the deposition basin. Although low-water weirs were not tested in this study, another model study (Seabergh and Sager 1980) in which dual low water weirs were examined revealed that for an inlet with a moderate tide range (~ 4.0 ft) and $K = 0.9$, continued ebb flow was maintained over the low-water weir which tended to disperse the ebb flow over the entire region between the jetties. This aided currents in flowing along the inner walls of the weir and jetty rather than concentrating the ebb flow in the navigation channel. While a low-water weir has been used successfully at Perdido Pass, Fla., without scouring along the weir or jetty trunk, the tide range is small and wave activity low.
- b. The reduction in weir length from 600 to 300 ft did not change the unit flow over the weir.

- c. For tests without waves, flood tidal flow was uniformly distributed over the length of the weir.
- d. As flow area between the oceanward end of the jetties is reduced relative to the minimum cross-sectional area at the inlet gorge, ebb and flood velocities over the weir are increased, flood durations are increased, and ebb durations decreased.
- e. In general, a lower Keulegan K inlet will have greater flood q (unit discharge) over the weir and smaller ebb q than a higher K inlet.
- f. The ratio of flood flow volume over the weir to the tidal prism varied from 0.5 to 4.7 percent, with the maximum ratio for a low K inlet.

Surface current
flow pattern photographs

113. Conclusions and observations derived from the surface current photographs indicated the following:

a. Tide only--all plans.

- (1) Plan 1 showed a slight tendency for early ebb and flood flows to deflect to the inside region of the upcoast jetty.
- (2) Plan 1A ebb and flood flows were well aligned with the navigation channel. The phase shift in the time of maximum currents from the Plan 1 condition accounted for the improvement relative to Plan 1 inlet which had the same jetty alignment as Plan 1A.
- (3) Plan 2 showed slightly improved alignment of flood and ebb currents in the channel relative to Plan 1.
- (4) Plan 3 showed better alignment of flood currents in the entrance channel than Plan 1 or 2, but during the early ebb flow there was a diversion of currents over the seaward end of the weir for Plan 3, since the weir was closer to the channel than for Plan 1 or 2.
- (5) Tidal currents are better guided by having the outer leg of the weir jetty parallel to the downcoast jetty; however, the oceanward end of the weir should be placed as far from the channel as possible to reduce the tendency for ebb currents to move across the deposition basin.

b. Tide plus waves from upcoast--Plan 1.

- (1) Plan 1 flood tide flow at the jetty entrance was pushed to the downcoast side of the channel by large upcoast waves.

- (2) Strong oceanward currents were generated along the upcoast side of the weir jetty and along the face of the weir even though considerable overtopping of the weir occurred during early flood flows.
- (3) Currents along the outer leg of the weir jetty decrease during late flood flow when flow over the weir is strongest.
- (4) Ebb flow in the navigation channel concentrated on the side adjacent to the weir jetty as it moved oceanward (Photo 24).
- (5) Strong currents moved oceanward along the upcoast side of the weir jetty during ebb tidal conditions.
- (6) Strong eddylike circulations existed in the deposition basin during most of the tidal cycle, thus being conducive to sedimentation in the basin.

c. Tide plus waves from downcoast--Plan 1.

- (1) Upcoast moving longshore currents began about 700 to 900 ft upcoast of the shoreward end of the weir for the 10-ft, 10-sec waves.
- (2) Strong eddy circulations existed in the deposition basin.
- (3) Flow over the weir was very slight.
- (4) Flood flow in the entrance channel was confined to the upcoast side of the channel and ebb flow was confined to the downcoast side of the entrance channel.

d. Tide plus waves from upcoast--Plan 2. Comments for this plan are similar to those for Plan 1 upcoast waves, except that currents along the upcoast side of the oceanward section of the weir jetty were slightly increased.

e. Tide plus waves from downcoast--Plan 2. Same as for Plan 1 except that the upcoast movement of the longshore current began very close to the weir jetty.

f. Tide plus waves from upcoast--Plan 3.

- (1) This plan showed the best ebb and flood flow surface current patterns in the entrance channel, being the least affected by waves and showing a lesser tendency for flow into the deposition basin. Tests with waves also corrected the minor deficiency seen in tide tests without waves in which there was ebb flow over the weir.
- (2) There was less wave protection in the basin due to the greater exposure to waves because of the 30-deg weir angle.

- g. Tide plus waves from downcoast--Plan 3. The longshore current moved upcoast from near the weir, although velocities initially were very low near the weir.
- h. Summary. Waves significantly affect flow patterns in the vicinity of the weir jetty. Longshore currents generated by upcoast waves are split between flowing over the weir and flowing oceanward along the upcoast jetty. At lower falling tide stages, the entire current may be directed oceanward along the jetty. In the region of the jetty entrance, ebb and flood currents are shifted by the effect of the waves. For upcoast waves, ebb flows are confined to the upcoast side of the channel and flood flows to the downcoast side of the channel. The more acute the angle of the weir with the shore, the greater the exposure of the deposition basin to waves. Thus the ranking of plans from less to greater upcoast wave exposure would be: Plans 1, 2, and 3. However, a qualitative evaluation of the amount of wave activity in the deposition basin by downcoast waves would reverse, i.e., Plans 3, 2, 1, since Plans 1 and 2 let greater downcoast wave energy through the entrance channel to the deposition basin. The Plan 3 deposition basin is in the diffraction zone of the waves entering between the jetties. Flow patterns over the basin also were significantly affected by waves.

Dye streak velocity measurements

114. Results from the dye streak velocity measurements indicated:

- a. These measurements supported observations from the surface current photographs that as the tide elevation falls and the breaker zone moves seaward, there is increased current flow along the upcoast face of the jetty and weir. Plan 3 had higher, more concentrated currents in this region along the outer portion of the jetty due to its geometry.
- b. As the weir angle was reduced from 90 deg, there was an increase in seaward-flowing velocities at the oceanside base of the weir section.

Beach Response Tests

115. Results from the beach response tests indicated the following:

- a. Not all sediment entering the vicinity of a weir jetty system from upcoast moved over the weir into the

deposition basin or was stored in a fillet upcoast of the weir. Some sediment moved offshore due to two mechanisms. First, longshore currents for the larger wave conditions were deflected offshore along the ocean side of the jetty, moving sediments with them. Second, reflected waves from the upcoast jetty interacted with incident waves forming a short-crested wave field upcoast of the weir jetty. The interaction of this wave field and the shoreline created circulation cells with rip currents which carried sediment offshore just upcoast of the weir section.

- b. The fillet storage with upcoast waves for the various weir angles was ranked as follows, from greatest to least: 90, 60, 45, and 30 deg. Since shapes of fillets were similar, if the reduction of area for smaller angles due to slicing out more of the storage area is neglected, the 45-deg weir would have the minimum surface area due to focusing of reflected waves on it for the given model wave condition.
- c. The amount of sediment moving offshore was dependent on weir angle, with the 90-deg weir (Plan 1) having the least offshore movement followed by the 60-deg weir (Plan 2), 45-deg weir (Plan 3C), and the 30-deg weir (Plan 3).
- d. Considering the basic weir jetty orientations, the percentage of fillet removal by the downcoast wave, desirable for backpassing, was greatest for Plans 2 and 3, with 100 percent removal; and Plan 1, with 52 percent removal.
- e. Testing of Plan 3 with a tide showed little difference from the usual no-tide tests with a 5-ft, 10-sec wave.
- f. The location of a groin upcoast of Plan 3 did not deter sediment movement to the weir once a fillet was created upcoast of the groin. These configurations (Plans 3A and 3B) then permitted easier natural backpassing outside the shadow of the jetties.
- g. A groin downcoast of the weir section (Plan 3D) aided in reducing the amount of sediment bypassing the weir and moving to the jetty tips, but it did not totally stop that movement.

Application to Weir Jetty Design

116. In concept, the most desirable weir jetty system would involve the following functions:

- a. The weir would be so located and designed that flow over the weir would occur predominantly on the flood tide so that sediment is carried into the deposition basin.
- b. Ebb flow would be predominantly between the jetties and not over the weir for two primary reasons. First, strong ebb flow toward and over the weir might train the navigation channel toward the weir and thus through the deposition basin. Second, if there is net flood flow over the weir, there will be net ebb flow in the navigation channel, aiding in flushing out sediments which might enter between the jetties.
- c. The weir would be elevated and positioned in such a manner that only the net longshore drift would be captured.
- d. The jetty system would be so aligned to encourage the transport of most of the sediment deposited in the fillet up beach during longshore transport reversals.

117. A discussion of the application of results of this report to weir jetty design must be considered in view of the limitations of this testing program, including simplified bathymetry and channel orientation, limited wave conditions, and limited tidal conditions. Prototype situations have complex bathymetries, variable shoreline orientation, a variety of bay channel(s) configurations, and possible large variations in wave conditions. This discussion will hopefully supplement information provided by Weggel (1981) and other jetty design guidance.

118. Important parameters which need to be defined as well as possible include gross and net longshore sediment transport rates and variations within the yearly cycle, this of course coupled with wave climatology; the local bathymetry and historical records of its variation; tide range; the type of inlet as defined by its tidal response, which can be determined by evaluation of its Keulegan K value.

119. Two series of recommendations will be presented. The first will deal with hydraulics, the second with sediment movement.

Hydraulic considerations

120. Flow over the weir and weir elevation. It is recommended that ebb flow over the weir be minimized by examination of the tidal-level, ebb-velocity relation at the inlet entrance. This can be done based on an evaluation of the Keulegan K (Keulegan 1967) and use of Figure 5. As was noted in the testing, high Keulegan K value inlets

have higher ebb flows so the elevation of a weir for this type of inlet should be kept at midtide. For low Keulegan K inlets the weir could be lower if other factors would permit this; factors such as a low wave energy environment, desire to capture all sediment in basin, and minimized velocities carrying sediment seaward along jetty. On the other hand, low K inlets can have the weir higher than midtide if required due to strong wave conditions and the desire to have more protection in the basin since maximum flood flows occur at higher water levels than at the midtide level.

121. Weir location. With respect to tidal currents within the jetty system, the farther the weir is from the navigation channel, the less likely it is to capture channel ebb currents that are directed seaward. This can depend on the location of the predominant ebb channels and their orientation. Care must be taken in evaluation of ebb flow direction because once the jetty system is constructed, adjustments of channel orientation may take place due to removal of some wave effects and thus sediment movement which, for example, may have deflected the ebb channel downcoast.

122. Jetty alignment. Parallel oceanward jetty segments provided the best current patterns on both ebb and flood flows, with and without wave action; there was less tendency for tidal flows to meander toward the basin region. With respect to wave action from the downcoast direction, qualitative observations from this study indicate less wave activity in the basin region for the jetty systems with parallel outer jetties (Plan 3 in this study) than those with flared outer jetty sections (Plan 1 or 2 in this study). The flared outer sections act as wave guides in bringing downcoast waves through the main entrance channel toward the deposition basin.

123. Weir length. Primary transport over the weir exists at its intersection with the shoreline. If wave climate is mild, the weir length should only be as long as necessary to prevent a chance of closure, something which has not yet been noted to occur in existing weir jetty systems. The length to prevent closure would need to be evaluated based on wave conditions, beach slope, orientation of the

structure, etc. If the wave climate is highly variable, the weir should probably extend further oceanward so as to include a large percentage of the breaker zone since it was noted that there was heavy transport over the weir at the breaker location for larger wave conditions; otherwise, the sediment will move offshore along the jetty. Another factor influencing weir length will be the consideration of the amount of flow which is desired in the system. If a design objective is to obtain high ebb dominance of flow in the navigation channel, then the weir should be longer, if this would not interfere with other constraints, such as placement of a portion of the weir too close to the channel. The complete hydraulic flow situation must be considered to determine whether the additional flow provided by a wider weir will substantially augment ebb flow predominance and provide additional scouring ability in the entrance channel.

124. Jetty and weir orientation. A weir which is perpendicular to shore will normally have an outer section flared channelward (Plan 1 system) to provide a niche for the deposition basin away from the channel. This combination is probably the least likely system to permit sediment movement along the upcoast side of the jetty system toward the jetty tip and thus the navigation channel. This assumes that depths are fairly deep at the jetty tip; otherwise, if depths are shallow and the breaker zone is close to the jetty tip, then sediment may move along the breaker line to the jetty tip. Jetties with angled weir sections and parallel outer trunks tend to concentrate the longshore currents along the structure and might have more sediment transport along the upcoast face of the structure toward the entrance channel.

Sediment movement considerations

125. Location of shoreward end of weir. The shifting of the start point of the weir seaward from the initial shoreline permits greater fillet development (and thus storage for sediment in a reversing longshore drift environment) and may aid in placement of the deposition basin in a more recessed location, which otherwise might not be possible due to land acquisition constraints. The location of the basin somewhat recessed is appropriate due to the tendency for the sediment moving over the weir

for moderate wave conditions to follow the shoreline. If the weir is initiated at the original shoreline, sediment will tend to move around the existing inlet shoulder toward the navigation channel. With a portion of the deposition basin recessed shoreward of the weir, the sediment tends to wrap around the section of jetty landward of the weir by waves refracting over the accreted sediment. If transport is predominantly unidirectional, the location of the shoreward end of the weir could probably be maintained at the existing shoreline since all material will eventually move onto the basin, but the deposition basin should still be recessed landward of the weir section to prevent movement of sediment around the inlet shoulder. If the starting point of the weir section is to be located near the existing shoreline for reasons such as to move it away from the navigation channel, the use of a groin upcoast of the weir section (such as Plan 3B) may be desired to provide sediment storage for a reversing littoral climate, but if the wave climate is severe, the groin might aid in jetting some sediment offshore.

126. Reflected wave effects. The previously discussed model study noted effects on sediment transport along the beachline upcoast of the jetty system due to the interaction of waves reflected off the jetty structure and the incident waves. The orientation of the jetty structure and weir section caused varying effects. It is difficult to evaluate these effects on jetty design due to the qualitative nature of these tests in the model and the lack of knowledge as to how often conditions would be conducive to creating the phenomenon and how strong these effects might be in prototype situations. Refraction-reflection patterns (see Plates 102 to 105) could be developed for a given site condition to aid in evaluating these effects. The closer spacing of circulation cells for the 30-deg and 45-deg angled weirs created slightly more offshore sediment movement than that of the 60-deg and 90-deg weirs, even though velocities in the short-crested wave field were greater in the latter pair than in the former pair. The pulling of sediment offshore in this region may not necessarily be detrimental if littoral reversal occurs often enough, so that there is useful storage offshore and upcoast of the weir section, and assuming the sediment can move back onshore and

upcoast. If the longshore transport is predominantly unidirectional, storing sediment in this region may not be desirable as it may tend to move further offshore along the jetty and move toward and into the navigation channel at the jetty tip. Therefore, a larger angled weir might be desirable at a unidirectional longshore transport site.

REFERENCES

- Bowen, A. J. 1969. "Rip Currents, I Theoretical Investigations," J. Geophys. Res., 74, pp 5467-5478.
- Dalrymple, R. A., and Lanau, G. A. 1976. "Beach Cusps Formed by Intersecting Waves," Geological Society of America Bulletin, Vol 87, pp 57-60.
- Dean, R. G. 1971. "Coastal Inlet Mechanics and Design Course," Class notes, May 1971, U. S. Army Coastal Engineering Research Center, Fort Belvoir, Va.
- _____. 1973. "Heuristic Models of Sand Transport in the Surf Zone," Proc. Conf. on Engrg Dynamics in the Surf Zone, Sidney, Australia.
- Durham, D. L., Greer, H. C., III, and Whalin, R. W. 1975. "Automated Control Data Acquisition and Analysis for Hydraulic Models of Tidal Inlets," Proceedings, Army Numerical Analysis Conference.
- Fuchs, Robert A. 1952. "On the Theory of Short-Crested Oscillatory Waves," Gravity Waves, U. S. Department of Commerce, National Bureau of Standards Circular 521, pp 187-200.
- Hsu, J. R. C. 1975. "Sediment Transport By Short-Crested Waves," Proc. 2nd Australian Conference on Coastal Engineering, pp 223-228.
- Inman, D. L., and Bagnold, R. A. 1963. "The Sea," M. N. Hill, ed., Interscience Publishers.
- Iwagaki, Y., and Noda, E. 1962. "Laboratory Study of Scale Effects in Two-Dimensional Beach Processes," Chapter 14, 8th Conference on Coastal Engr., pp 194-210.
- Johnson, J. W. 1949. "Scale Effects in Hydraulic Models Involving Wave Motion," Trans. Amer. Geophys. Union, 30, pp 517-525.
- Keulegan, G. H. 1967. "Tidal Flow In Entrances; Water-Level Fluctuations of Basin in Communication with Seas," Technical Bulletin No. 14, Jul 1967, Committee on Tidal Hydraulics, U. S. Army Corps of Engineers, Vicksburg, Miss.
- Komar, P. D., and Inman, D. L. 1970. "Longshore Sand Transport on Beaches," J. Geophys. Res., 75, No. 30, pp 5914-27.
- Komar, P. D., and Miller, M. C. 1973. "The Threshold of Sediment Movement under Oscillatory Water Waves," Journal of Sedimentary Petrology, Vol 43, No. 4, pp 1101-1110.
- Komar, P. O. 1976. Beach Processes and Sedimentation, Prentice-Hall Inc., Englewood Cliffs, N. J. pp 175-176.
- Mason, C. 1977. "Functional Design of Tidal Entrance Structures for Effective Navigation and Channel Stability," Seventeenth Congress of the International Association for Hydraulic Research, Vol 4, Baden-Baden, Federal Republic of Germany.

- Nayak, I. V. 1970. "Equilibrium Profiles of Model Beaches," Hyd. Engr. Lab. Rept. HEL2-25, University of California, Berkley.
- Novak, P., and Nalluri, C. 1974. "Correlation of Sediment Incipient Motion and Deposition in Pipes and Open Channels with Fixed Smooth Beds," Hydrotransport 3, Third International Conference on the Hydraulic Transport of Solids in Pipes, pp E4-45 to E4-56.
- O'Brien, M. P. 1969. "Equilibrium Flow Areas of Inlets on Sandy Coasts," Journal, Waterways and Harbors Division, American Society of Civil Engineers, Vol 95, No. WW1, Feb, pp 43-52.
- O'Brien, M. P., and Dean, R.G. 1972. "Hydraulics and Sedimentary Stability of Coastal Inlets," Proceedings, Thirteenth Coastal Engineering Conference, American Society of Civil Engineers, New York, pp 761-780.
- Parker, N. E. 1979. "Weir Jetties--Their Continuing Evolution"; Journal of the American Shore and Beach Preservation Association, Vol 47, No. 4, Oct 1971, pp 15-19.
- Penland, S. 1979. "Influence of a Jetty System on Tidal Inlet Stability and Morphology: Fort George Inlet, Florida," Coastal Structures 79, Alexandria, Va., pp 665-689.
- Rouse, H. 1937. "Nomogram for the Setting Velocity of Spheres," Division of Geology and Geography Exhibit D of the Report of the Commission on Sedimentation, 1936-37, National Research Council, Washington, D. C. pp 57-64.
- Seabergh, W. C., and Sager, R. A. 1980. "Supplementary Tests of Masonboro Inlet Fixed-Bed Model," General Investigation of Tidal Inlets, Report 11, U. S. Army Engineer Waterways Experiment Station, CE, Vicksburg, Miss., and U. S. Army Coastal Engineering Research Center, CE, Fort Belvoir, Va.
- Shepard, F. P. 1950. "Beach Cycles in Southern California," U. S. Army Corps of Engineers, Beach Erosion Board Tech. Memo No. 20.
- Silvester, R. 1975. "Sediment Transmission Across Entrances by Natural Means," Proc. 16th Int. Assoc. Hyd. Res. Congress I, pp 145-156.
- _____. 1977. "The Role of Wave Reflection in Coastal Processes," Coastal Sediments '77, Fifth Symposium of the Waterway, Port, Coastal, and Ocean Division of ASCE, pp 639-654.
- Sunamura, T., and Horikawa, K. 1974. "Two-Dimensional Beach Transformation Due to Waves," Proc. 14th Conf. Coastal Engr.
- Tanaka, N., and Sato, Shoji. 1976. "Topographic Change Resulting from Construction of a Harbor on a Sandy Beach: Kashima Port," Proc. 15th Conf. Coastal Engr, pp 1824-1843.
- Thornton, E. B., and Calhoun, R. J. 1972. "Spectral Resolution of Breakwater Reflected Waves," Journal of Waterways, Harbors, and Coastal Engineering Division, WW4, pp 443-460.

U. S. Army Coastal Engineering Research Center. 1977. Shore Protection Manual, Fort Belvoir, Va.

Weggel, J. R. 1981. "Weir Sand Bypassing Systems," Special Report No. 8, April 1981. U. S. Army Coastal Engineering Research Center, CE, Fort Belvoir, Va.

Wiegel, R. L. 1964. Oceanographical Engineering, Prentice-Hall, Englewood Cliffs, N. J., p 56.

Table 1
Hydraulic Test Parameters for Plans 1 and 1A

Plan	Jetty Opening Width, ft	Area Between Jetty Tips ft ²	Ratio of Area Between Jetty Tips and Gorge*	Keulegan K	Weir Width ft	Tidal Prism ft ³ × 10 ⁹	Velocity Adjustment Factor	Adjusted Maximum Velocities, fps**	
								Flood	Ebb
1	1200	29,925	1.48	1.75	610	1.225	1.00	3.0	0.9
1	1200	29,925	1.48	1.75	300	1.225	1.00	3.4	0.7
1	800	20,800	1.03	1.50	610	1.222	1.00	3.3	1.1
1	800	20,800	1.03	1.50	300	1.222	1.00	2.5	1.0
1	600	15,600	0.77	1.30	610	1.157	1.06	4.7	2.8
1	600	15,600	0.77	1.30	300	1.157	1.06	4.4	2.1
1A	1200	29,925	1.48	0.52	610	1.592	0.77	2.8	0.5
1A	800	20,800	1.03	0.35	610	1.533	0.80	4.1	0.6
1A	800	20,800	1.03	0.35	300	1.533	0.80	4.7	0.5
1A	600	15,600	0.77	0.28	610	1.464	0.83	4.9	1.2
1A	600	15,600	0.77	0.28	300	1.464	0.83	5.1	1.4

* Gorge area = 20,167 ft².

** See paragraph 28.

Table 2
Flow Over the Plan I and 1A Weirs

Plan	Jetty Opening Width ft	Ratio of Area Between Jetty Tips and Gorge	Keulegan K	Weir Width ft	Adjusted Peak Unit Discharge ft ³ /sec/ft		Adjusted Flow Volume Over Weir, ft ³ × 10 ⁶		Ratio of Flow Volume Over Weir to Flood Volume	Ratio of Flood Flow Over Weir to Tidal Prism
					Flood	Ebb	Flood	Ebb		
1	1200	1.48	1.75	600	6.2	2.2	21.9	5.9	0.27	0.018
1	1200	1.48	1.75	300	6.8	1.7	11.9	2.6	0.22	0.010
1	800	1.03	1.50	600	5.6	2.2	19.7	7.1	0.36	0.016
1	800	1.03	1.50	300	4.3	2.3	5.6	4.4	0.79	0.005
1	600	0.77	1.30	600	8.9	4.9	36.2	16.0	0.44	0.030
1	600	0.77	1.30	300	7.9	3.3	11.9	8.3	0.70	0.010
1A	1200	1.48	0.52	600	6.1	0.4	38.0	0.8	0.02	0.031
1A	800	1.03	0.35	600	8.8	0.7	49.1	0.8	0.02	0.040
1A	800	1.03	0.35	300	9.2	0.4	23.5	0.2	0.01	0.019
1A	600	0.77	0.28	600	9.8	0.8	56.9	0.7	0.01	0.047
1A	600	0.77	0.28	300	10.1	0.8	28.5	0.4	0.01	0.023

Table 3
Beach Response Test Data

Test No.	Plan	Tracer Material	Slope of Tracer Beach	Upcoast Wave			Downcoast Wave		
				Angle deg	Height* ft	Duration of Wave hr	Angle deg	Height* ft	Duration of Wave hr
1	1	Coal	1:13	30	10.0	6	30	5.0	3.0
2	1	Coal	1:13	30	5.0	5	30	5.0	2.5
3	1	Plastic	1:7	30	5.0	11	30	5.0	5.0
4	1	Glass beads	1:13	30	5.0	50	30	5.0	22.0
5	1	Glass beads	1:13	30	5.0	60	30	5.0	22.0
6	1	Glass beads	1:13	40	5.0	60	--	--	--
7	1	Glass beads	1:13	40	10.0	16	--	--	--
8	1	Glass beads	1:27	40	10.0	60	--	--	--
9	1	Glass beads	1:27	40	10.0	20	--	--	--
10	1	Coal	1:27	40	5.0	7	30	5.0	1.0
11	2	Coal	1:27	40	5.0	7	30	5.0	1.0
12	3	Coal	1:27	40	5.0	7	30	5.0	1.0
13**	3	Coal	1:27	40	5.0	7	30	5.0	1.0
14	3	Coal	1:27	40	10.0	7	30	5.0	1.0
15**	3	Coal	1:27	40	10.0	7	30	5.0	1.0
16	3A	Coal	1:27	40	5.0	8	30	5.0	1.0
17	3B	Coal	1:27	40	5.0	8	30	5.0	1.0
18	3C	Coal	1:27	40	5.0	7	30	5.0	1.0
19	3D	Coal	1:27	40	10.0	3	--	--	--

Continued

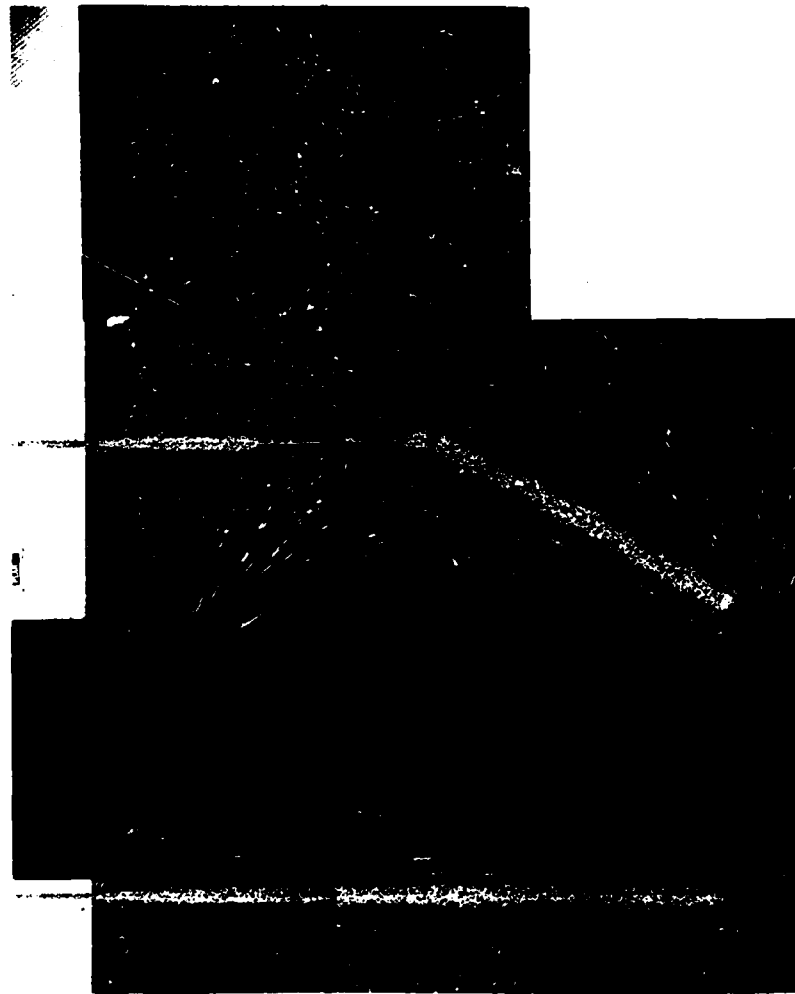
Note: M = model dimensions.

* Wave period = 10 sec.

** Test with tide reproduced.

Table 3 (Concluded)

Test No.	Plan	Tracer Material	Surface Area of Fillet After			Total Amount		Percent of Original Fillet Lost	Total Amount		Total Amount Fed to Beach ft3 (M)
			Upcoast Wave ft2 (M)	Percent of Test 10 Fillet Area	Downcoast Wave ft2 (M)	Total Amount Lost from Fillet ft2 (M)	Total Amount Deposited in Basin ft3 (M)				
1	1	Coal	1.70	14	0.55	1.20	71	--	--	7.711	
2	1	Coal	8.44	70	-0.41	8.85	105	--	--	4.244	
3	1	Plastic	33.40	278	3.35	30.05	90	--	--	5.642	
4	1	Glass Beads	4.78	40	2.28	2.53	53	0.118	0.118	2.051	
5	1	Glass Beads	4.90	41	4.39	0.51	10	0.095	0.095	1.058	
6	1	Glass Beads	3.77	31	--	--	--	--	0.107	1.121	
7	1	Glass Beads	2.60	22	--	--	--	--	0.210	0.332	
8	1	Glass Beads	0.80	6	--	--	--	--	0.918	3.364	
9	1	Glass Beads	1.65	14	--	--	--	--	0.354	1.425	
10	1	Coal	12.00	100	5.77	6.18	52	2.907	2.907	8.719	
11	2	Coal	9.61	80	0.00	9.61	100	2.283	2.283	3.590	
12	3	Coal	6.25	52	0.00	6.25	100	2.520	2.520	3.590	
13	3	Coal	15.35	128	7.20	8.15	53	2.051	2.051	3.590	
14	3	Coal	1.15	10	-0.35	1.50	130	7.736	7.736	12.822	
15	3	Coal	2.08	17	-0.10	2.18	105	3.707	3.707	12.309	
16	3A	Coal	18.25	152	3.80	14.45	79	1.139	1.139	4.103	
17	3B	Coal	28.20	235	2.70	25.50	90	2.264	2.264	3.077	
18	3C	Coal	7.60	63	0.65	6.95	91	2.523	2.523	3.590	
19	3D	Coal	2.50	21	--	--	--	--	--	--	



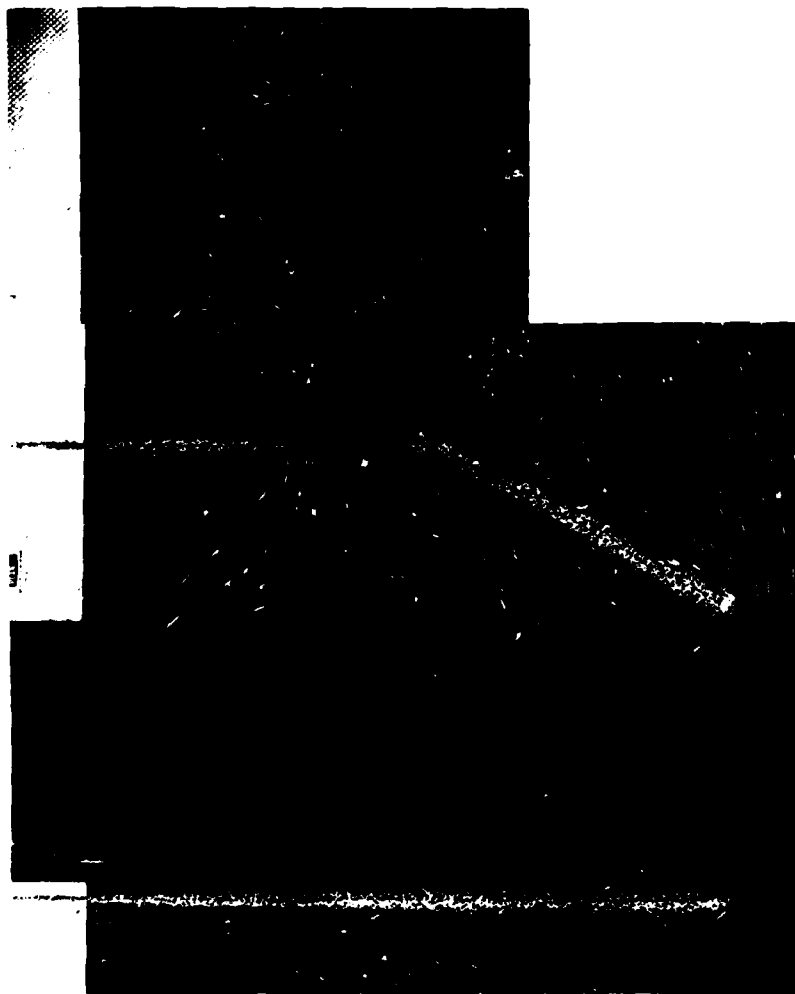
VELOCITY SCALES
 0 50 100 FPS
 PROTOTYPE [|||||]

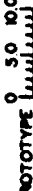
SURFACE CURRENTS
PLAN I
 FLOOD FLOW 0.2 OF CYCLE

SCALES
 200 0 200 400 600 FT
 PROTOTYPE [|||||]
 2.0 0 2.0 4.0 6.0 FT
 MODEL [|||||]

NOTE: 5 FT TIDAL RANGE



PHOTO 1



VELOCITY SCALES
 0 50 100 FPS
 PROTOTYPE 

SURFACE CURRENTS
PLAN 1

FLOOD FLOW 0.4 OF CYCLE

SCALES
 200 0 200 400 800 FT
 PROTOTYPE 
 2.0 0 2.0 4.0 8.0 FT
 MODEL 

NOTE 5 FT TIDAL RANGE

PHOTO 2



VELOCITY SCALES
 0 50 100 FPS
 PROTOTYPE 1:100

SURFACE CURRENTS
PLAN I

EBB FLOW 0.6 OF CYCLE

SCALES
 200 0 200 400 600 FT
 PROTOTYPE 1:100
 MODEL 20 0 20 40 60 FT

NOTE 5 FT TIDAL RANGE

PHOTO 3

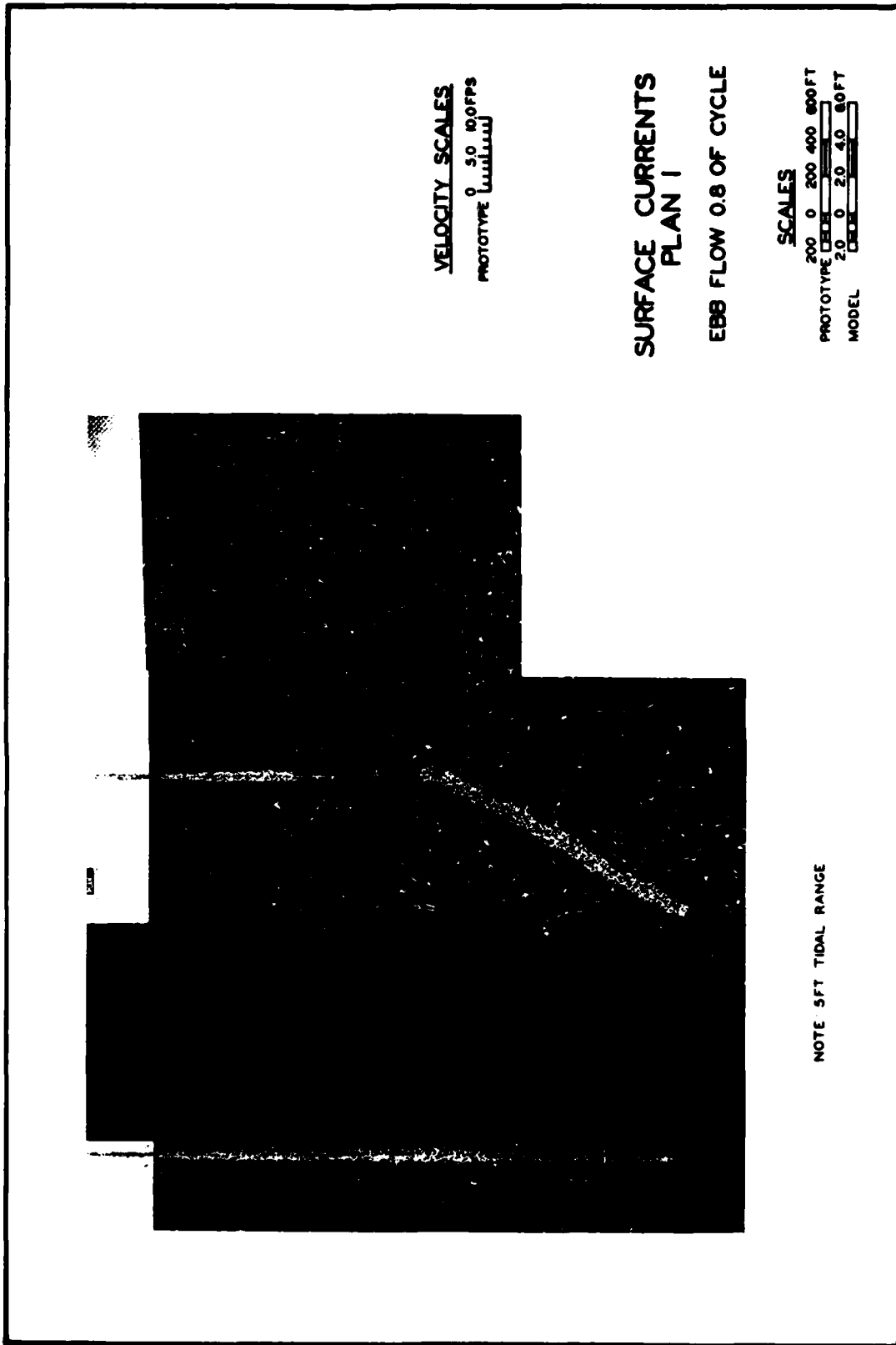


PHOTO 4

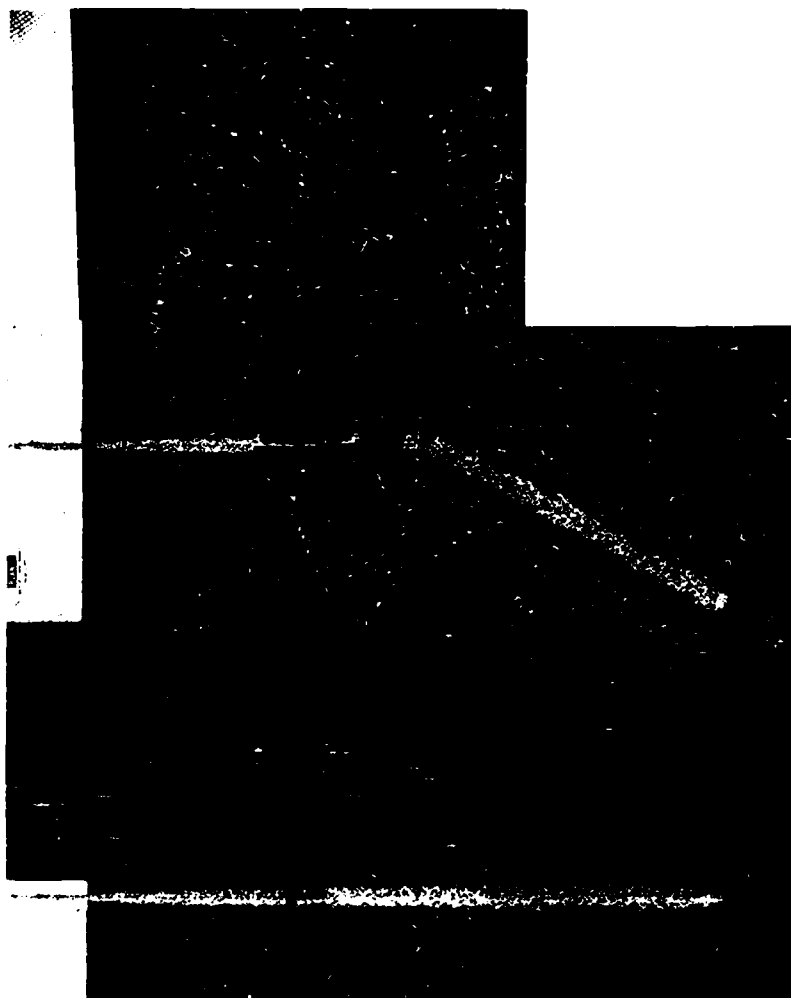
VELOCITY SCALES
 0 50 100 FPS
 PROTOTYPE (mm/min)

SURFACE CURRENTS
PLAN 1

EBB FLOW 0.8 OF CYCLE

SCALES
 200 0 200 400 600 FT
 PROTOTYPE (mm/min)
 20 0 20 40 60 FT
 MODEL

NOTE: 5 FT TIDAL RANGE



VELOCITY SCALES
0 50 100 FPS
PROTOTYPE [|||||]

**SURFACE CURRENTS
PLAN I**

EBB FLOW 0.0 OF CYCLE

SCALES
200 0 200 400 800 FT
PROTOTYPE [|||||]
20 0 20 40 80 FT
MODEL [|||||]

NOTE 5 FT TIDAL RANGE

PHOTO 5

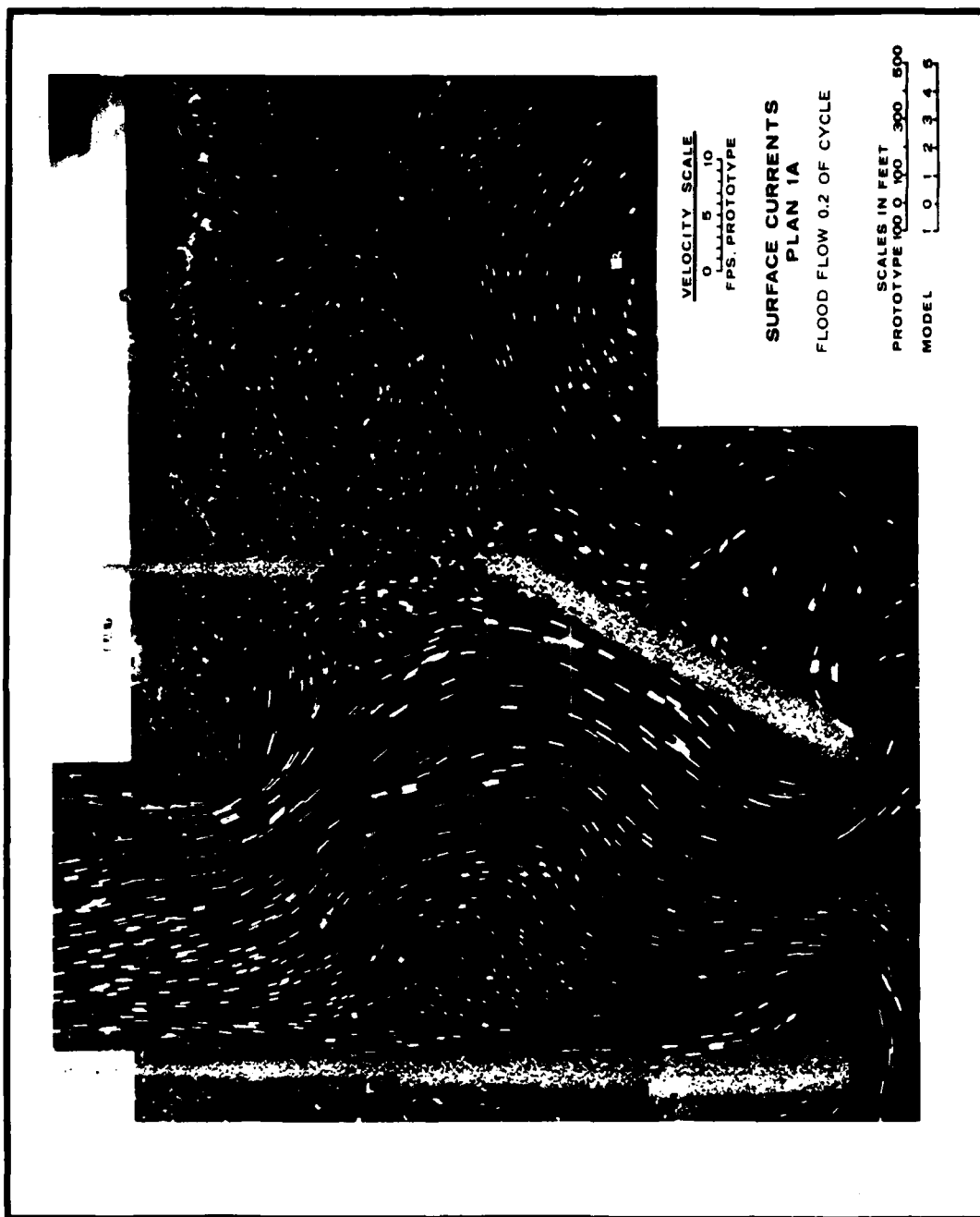


PHOTO 6

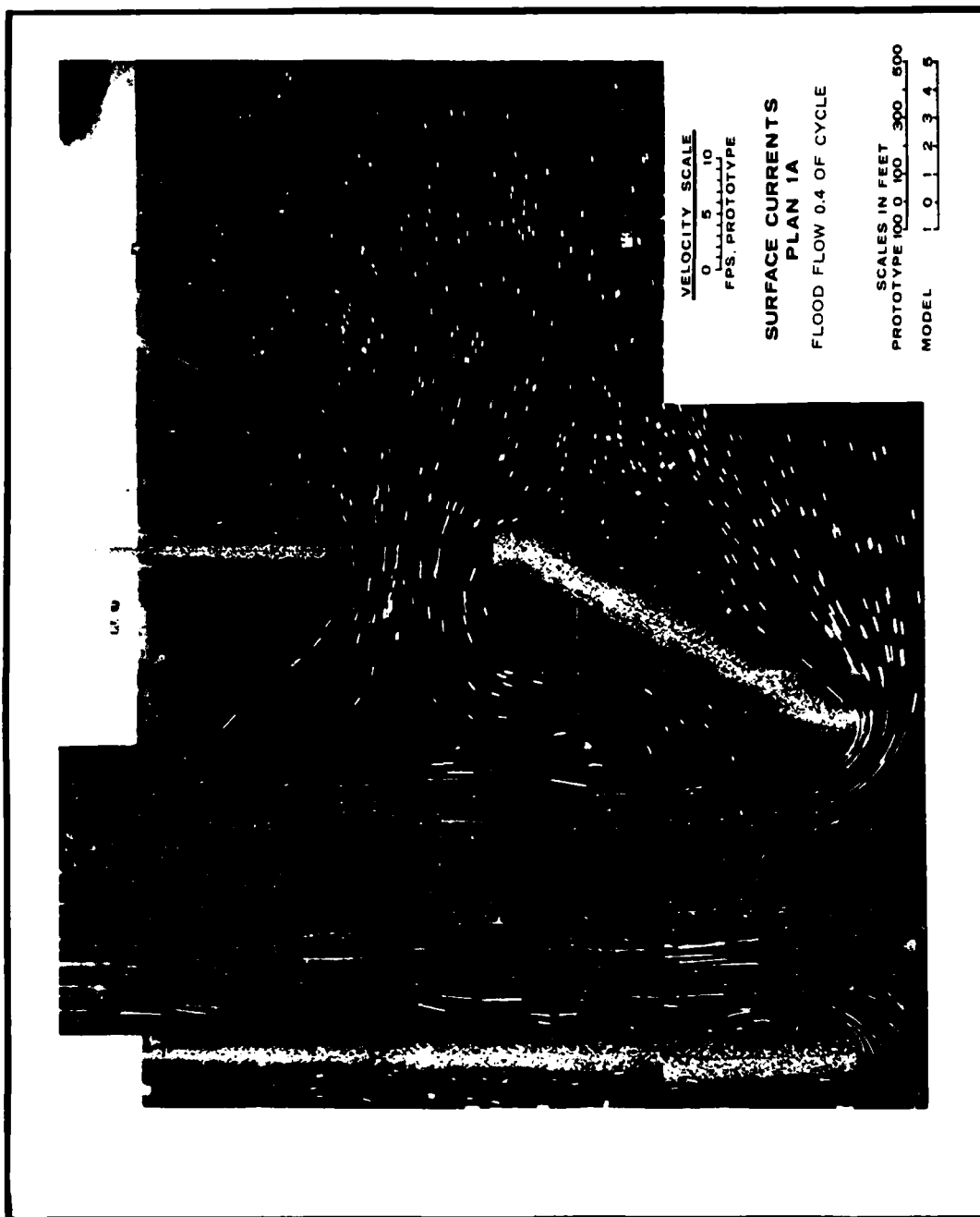


PHOTO 7

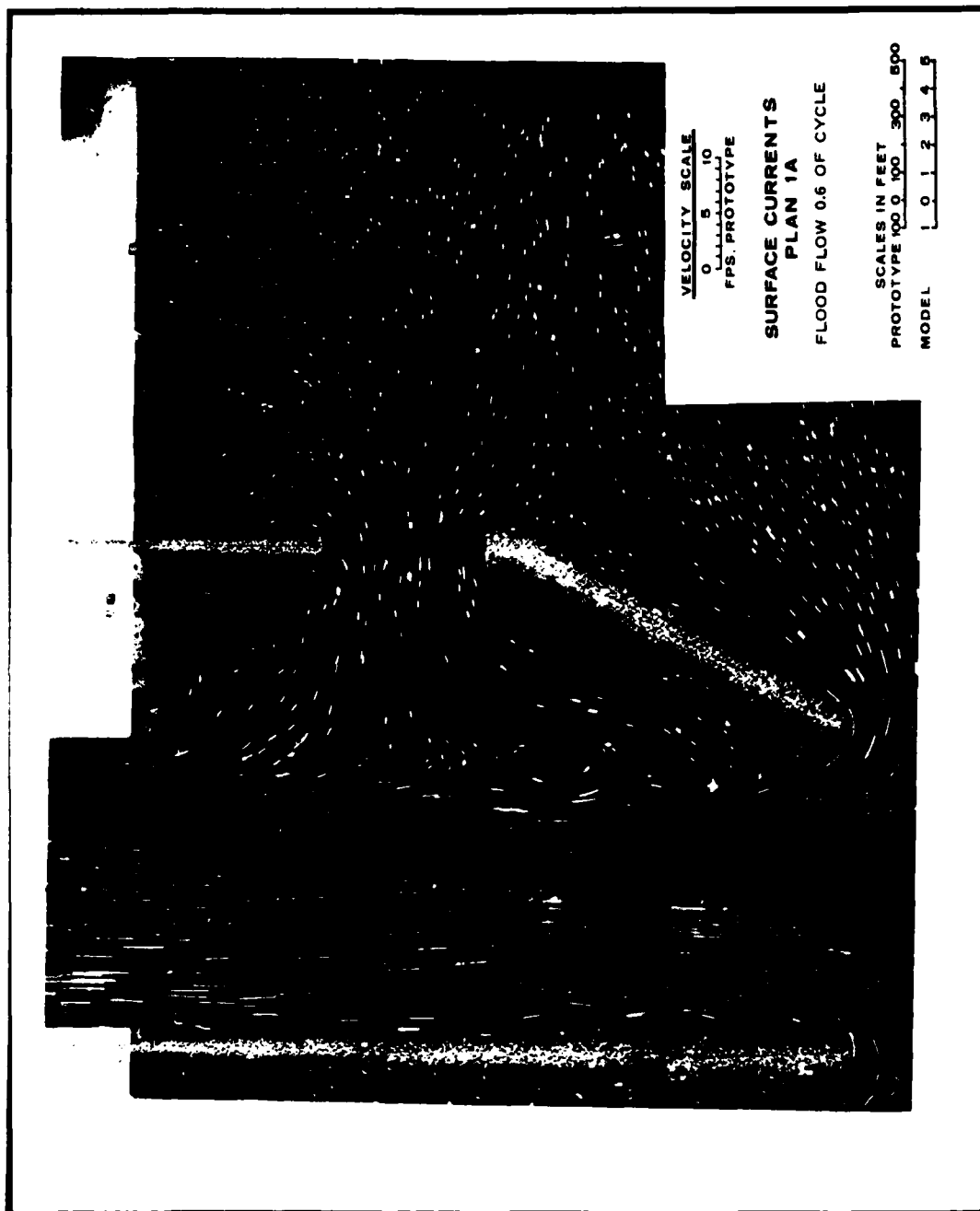


PHOTO 8

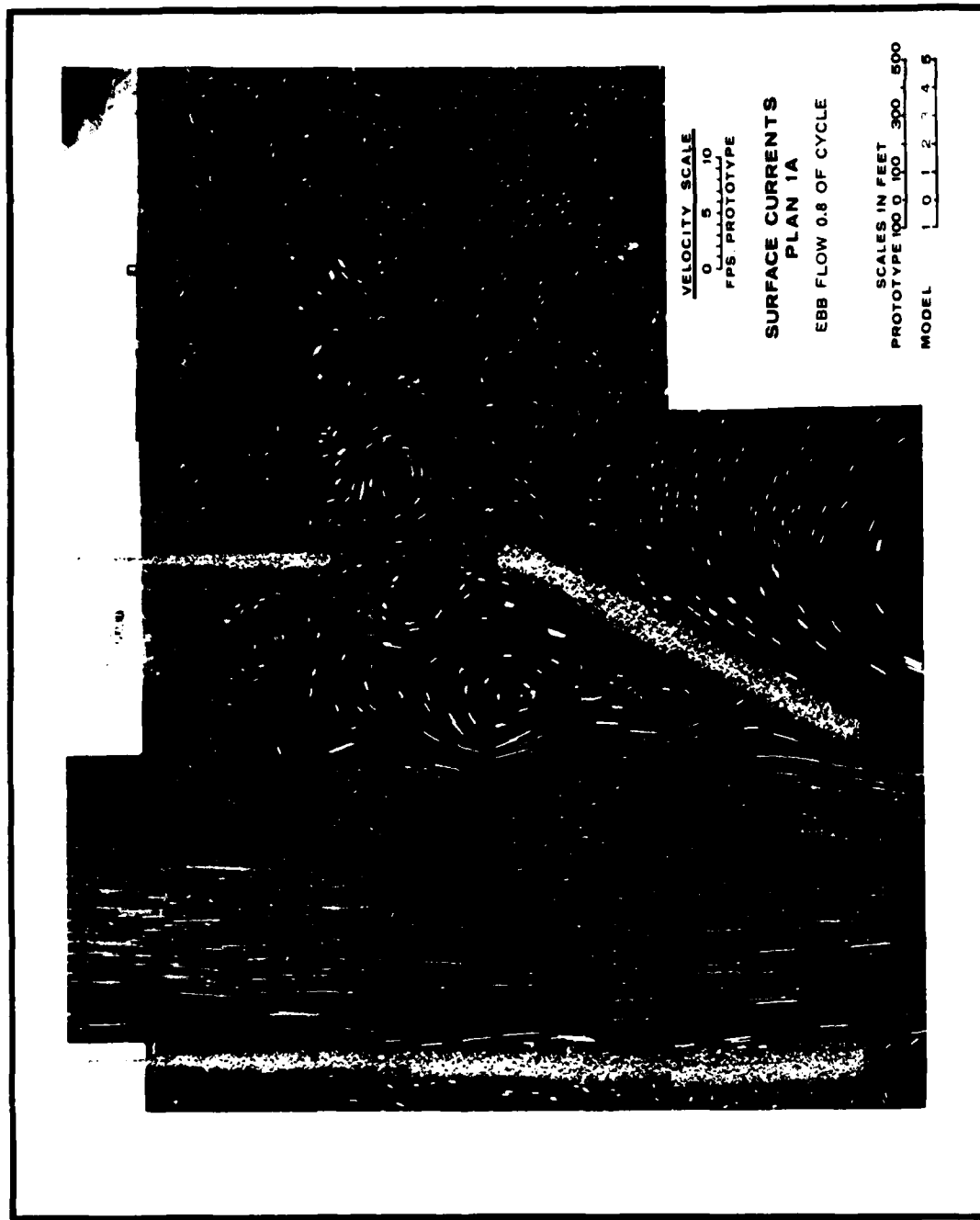


PHOTO 9

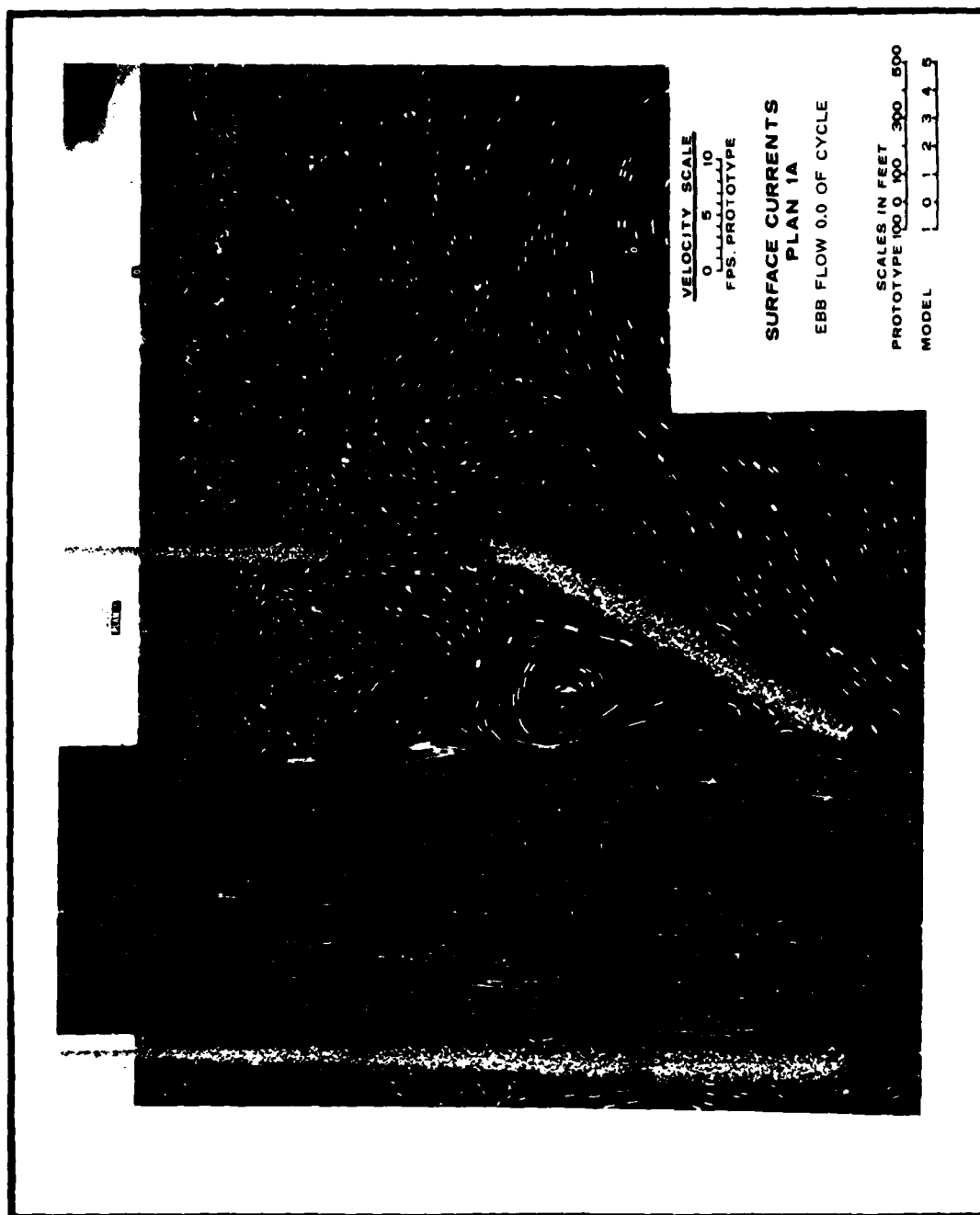
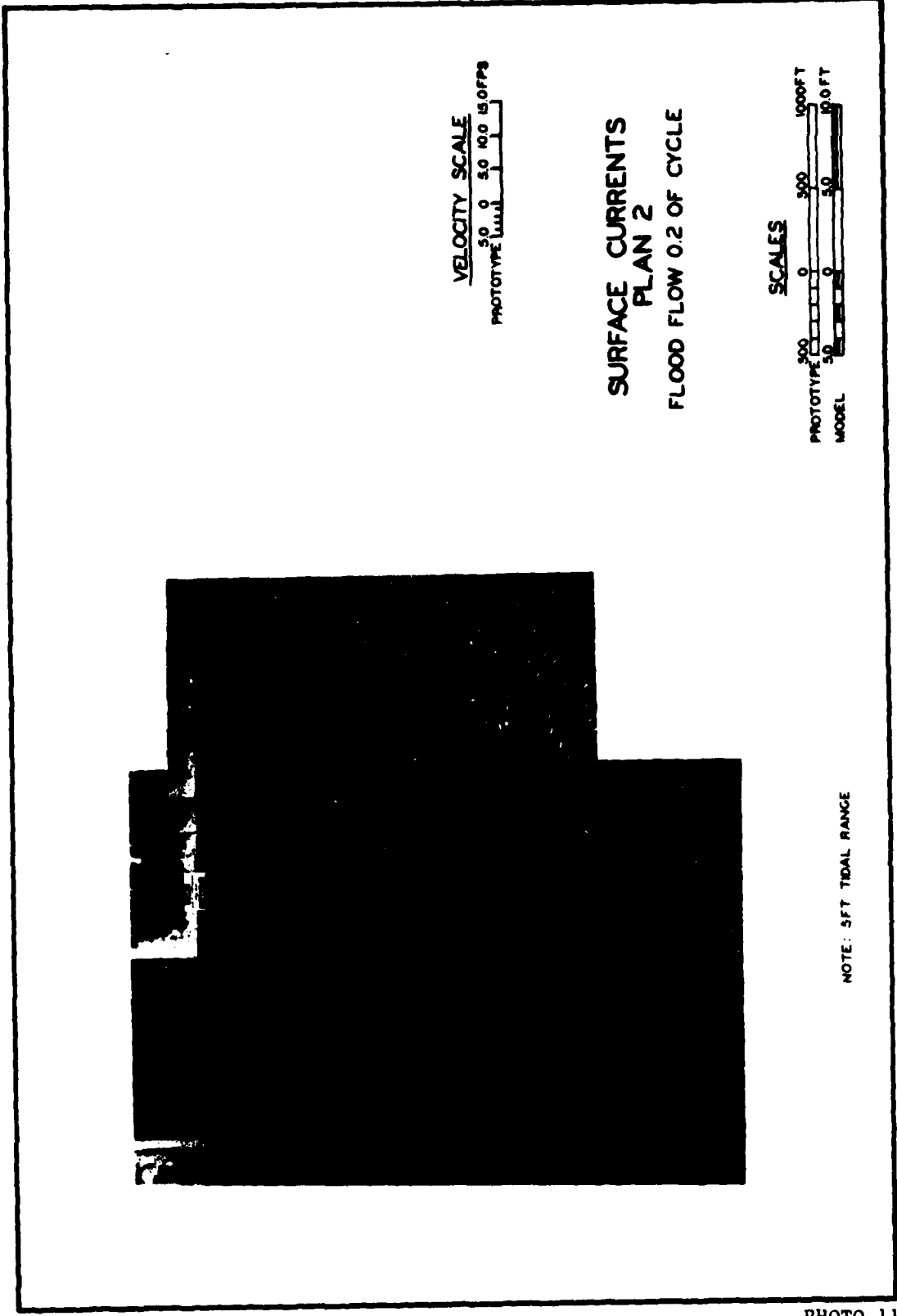


PHOTO 10



VELOCITY SCALE
5.0 0 5.0 10.0 15.0 FPS
PROTOTYPE

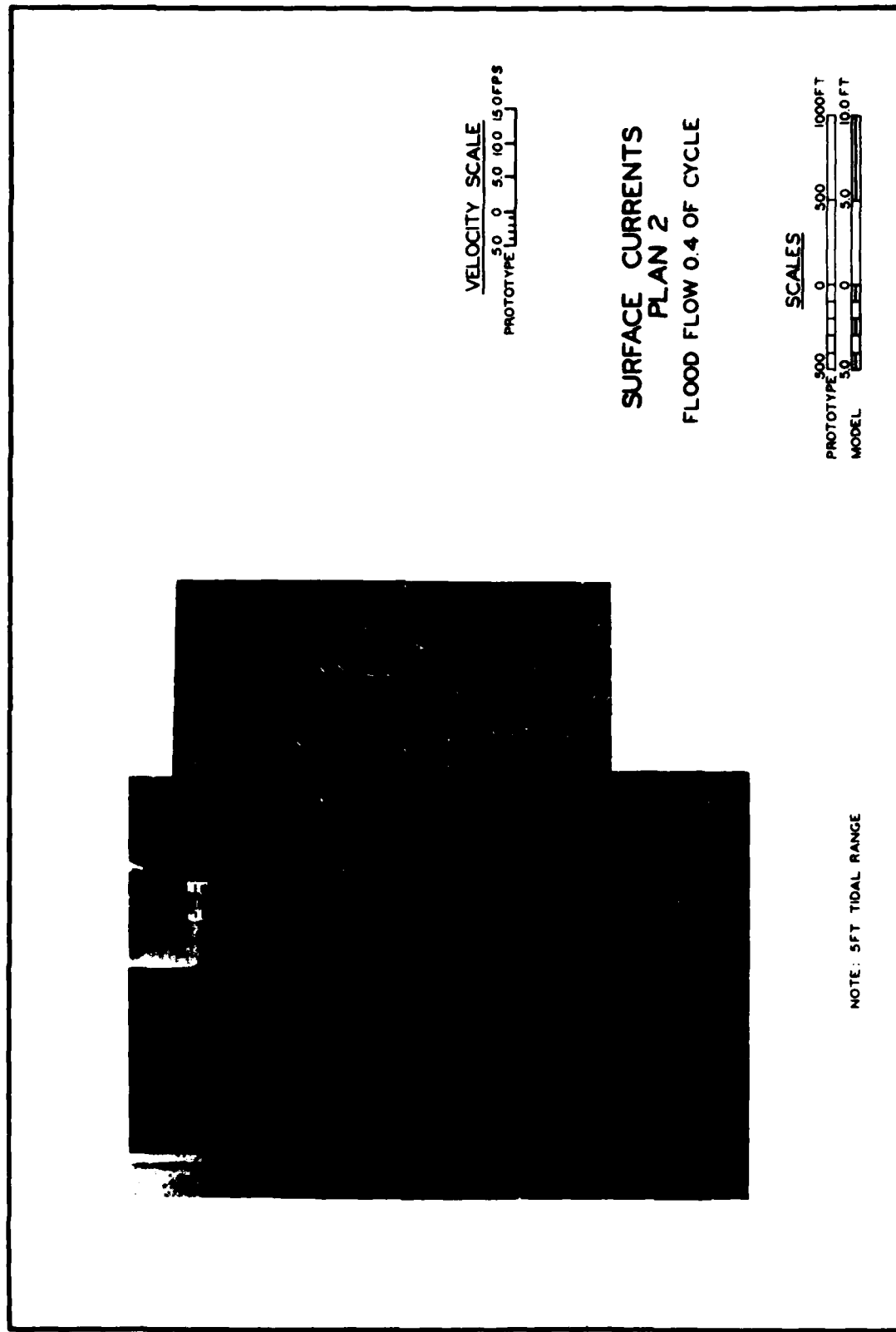
SURFACE CURRENTS
PLAN 2
FLOOD FLOW 0.2 OF CYCLE

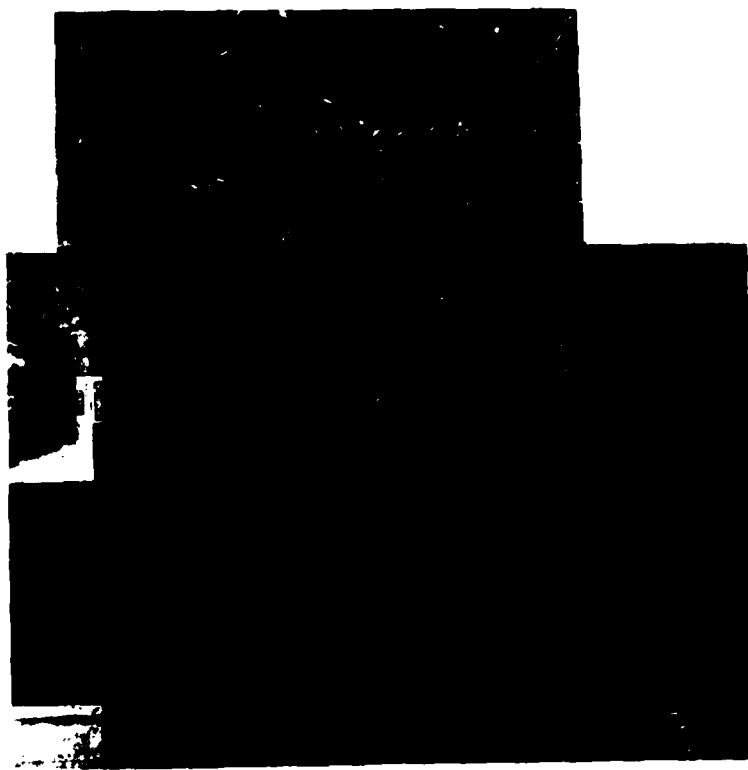
SCALES
300 0 500 1000 FT
PROTOTYPE
50 0 50 100 FT
MODEL

NOTE: 5 FT TIDAL RANGE

PHOTO 11

PHOTO 12



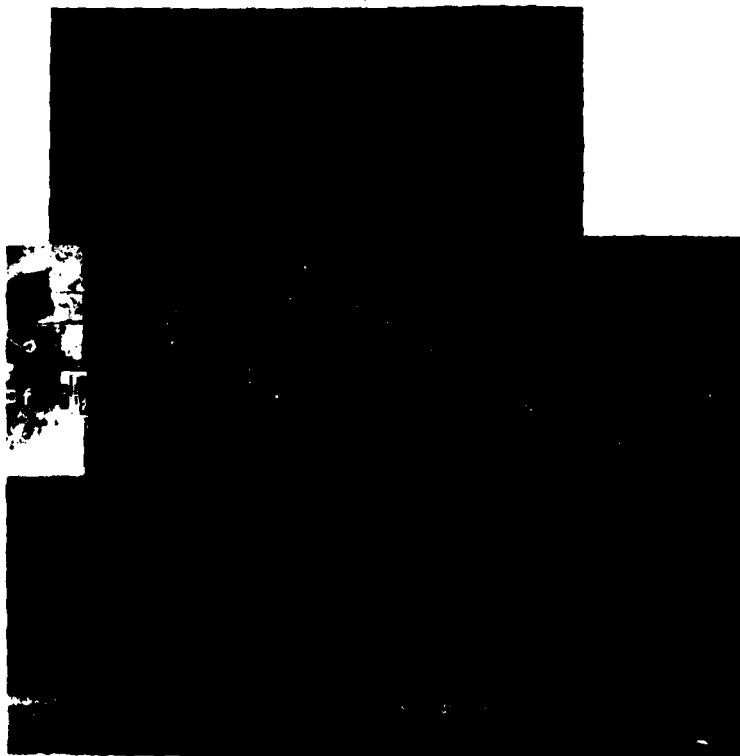


VELOCITY SCALE
50 0 50 100 150 FPS
PROTOTYPE

SURFACE CURRENTS
PLAN 2
EBB FLOW 0.6 OF CYCLE

SCALES
500 0 500 1000 FT
PROTOTYPE
50 0 50 100 FT
MODEL

NOTE: 5 FT TIDAL RANGE



VELOCITY SCALE
5.0 0 5.0 10.0 15.0 FPS
PROTOTYPE

SURFACE CURRENTS
PLAN 2
EBB FLOW 0.8 OF CYCLE

SCALES
300 0 500 1000 FT
PROTOTYPE
50 0 50 100 FT
MODEL

NOTE: 5 FT TIDAL RANGE

PHOTO 14



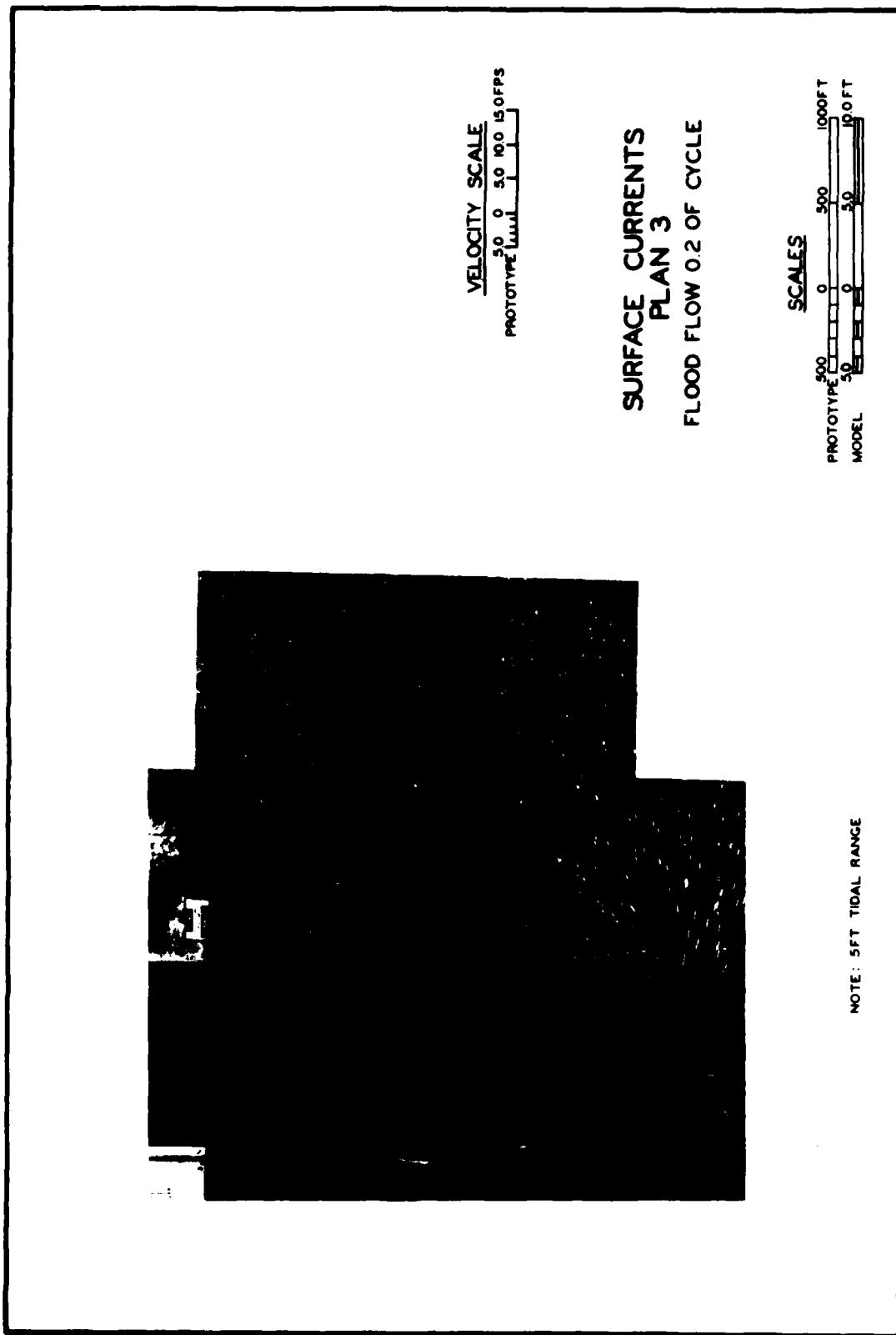
VELOCITY SCALE
50 0 50 100 150 FPS
PROTOTYPE

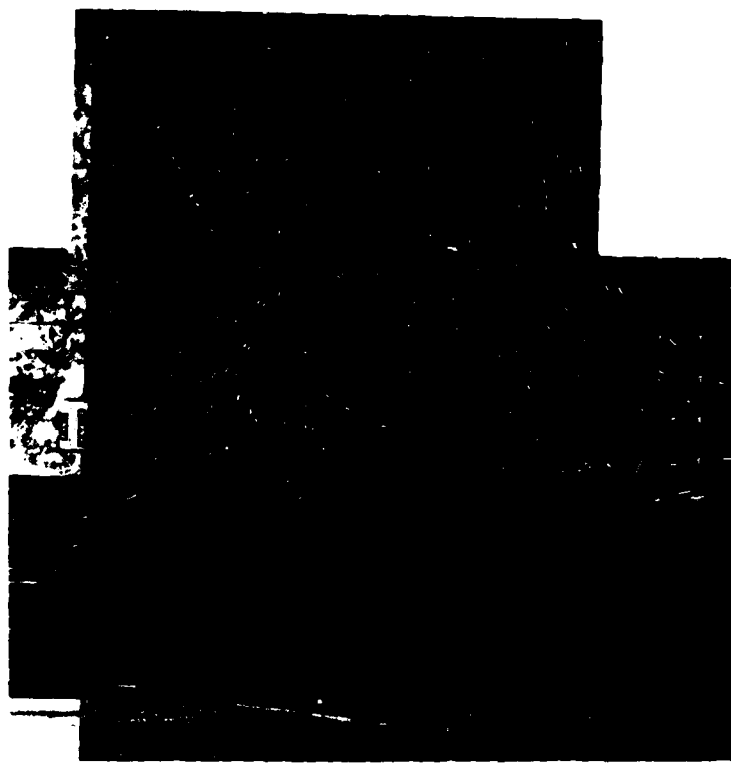
SURFACE CURRENTS
PLAN 2
EBB FLOW 0.0 OF CYCLE

SCALES
500 0 500 1000 FT
PROTOTYPE
50 0 50 100 FT
MODEL

NOTE: 5 FT TIDAL RANGE

PHOTO 16





VELOCITY SCALE
5.0 0 5.0 10.0 15.0 FPS
PROTOTYPE

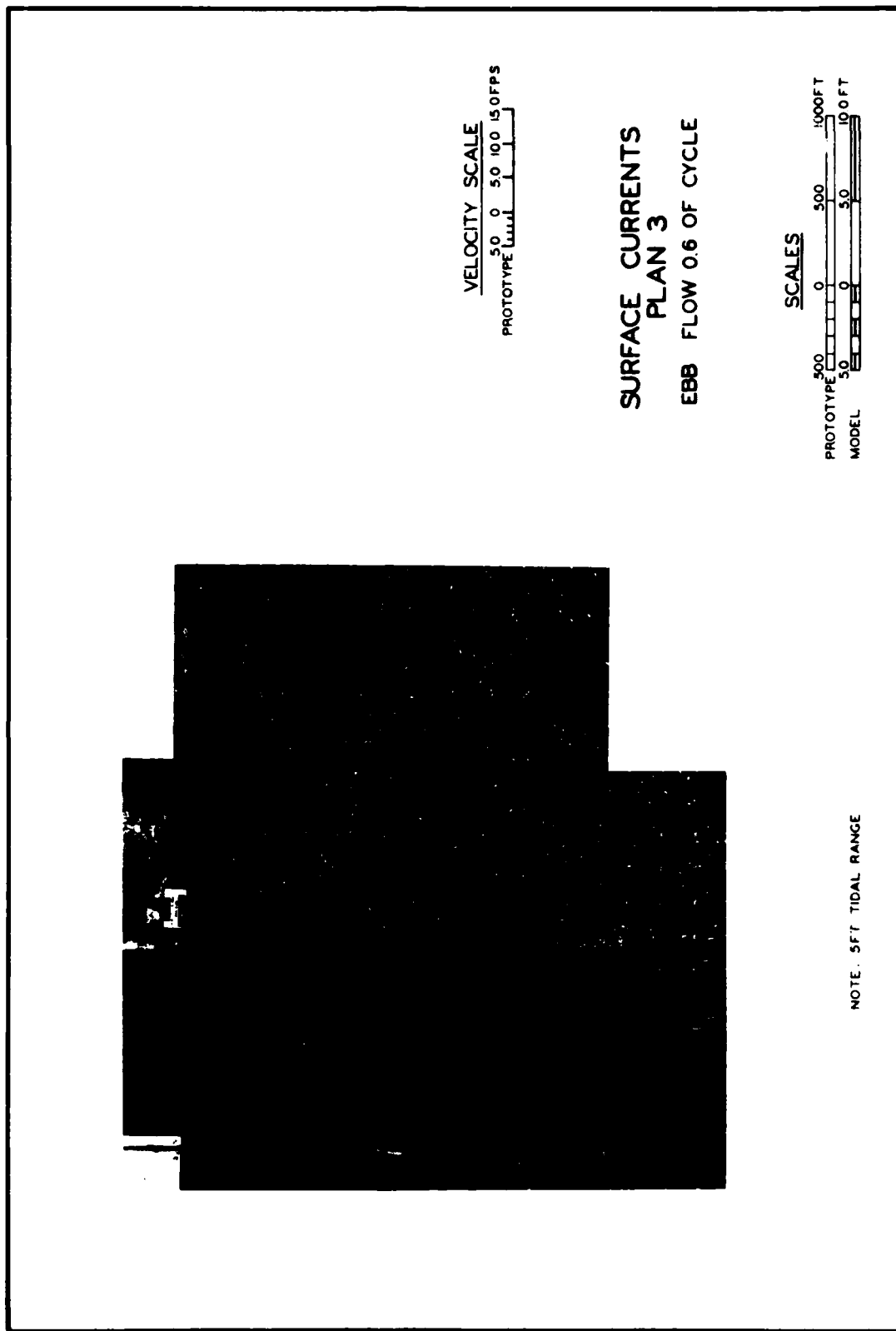
SURFACE CURRENTS
PLAN 3
FLOOD FLOW 0.4 OF CYCLE

SCALES
500 0 500 1000 FT
PROTOTYPE
50 0 50 100 FT
MODEL

NOTE: 5 FT TIDAL RANGE

PHOTO 17

PHOTO 18

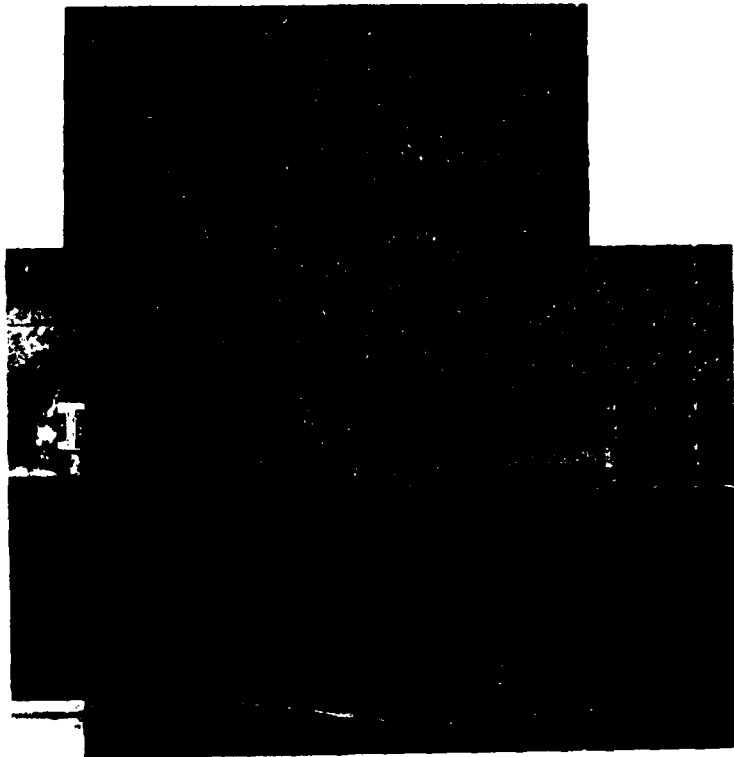


VELOCITY SCALE
5.0 0 5.0 10.0 15.0 FPS
PROTOTYPE

SURFACE CURRENTS
PLAN 3
EBB FLOW 0.6 OF CYCLE

SCALES
500 0 500 1000 FT
PROTOTYPE
50 0 50 100 FT
MODEL

NOTE. 5 FT TIDAL RANGE



VELOCITY SCALE
50 0 50 100 150 FPS
PROTOTYPE

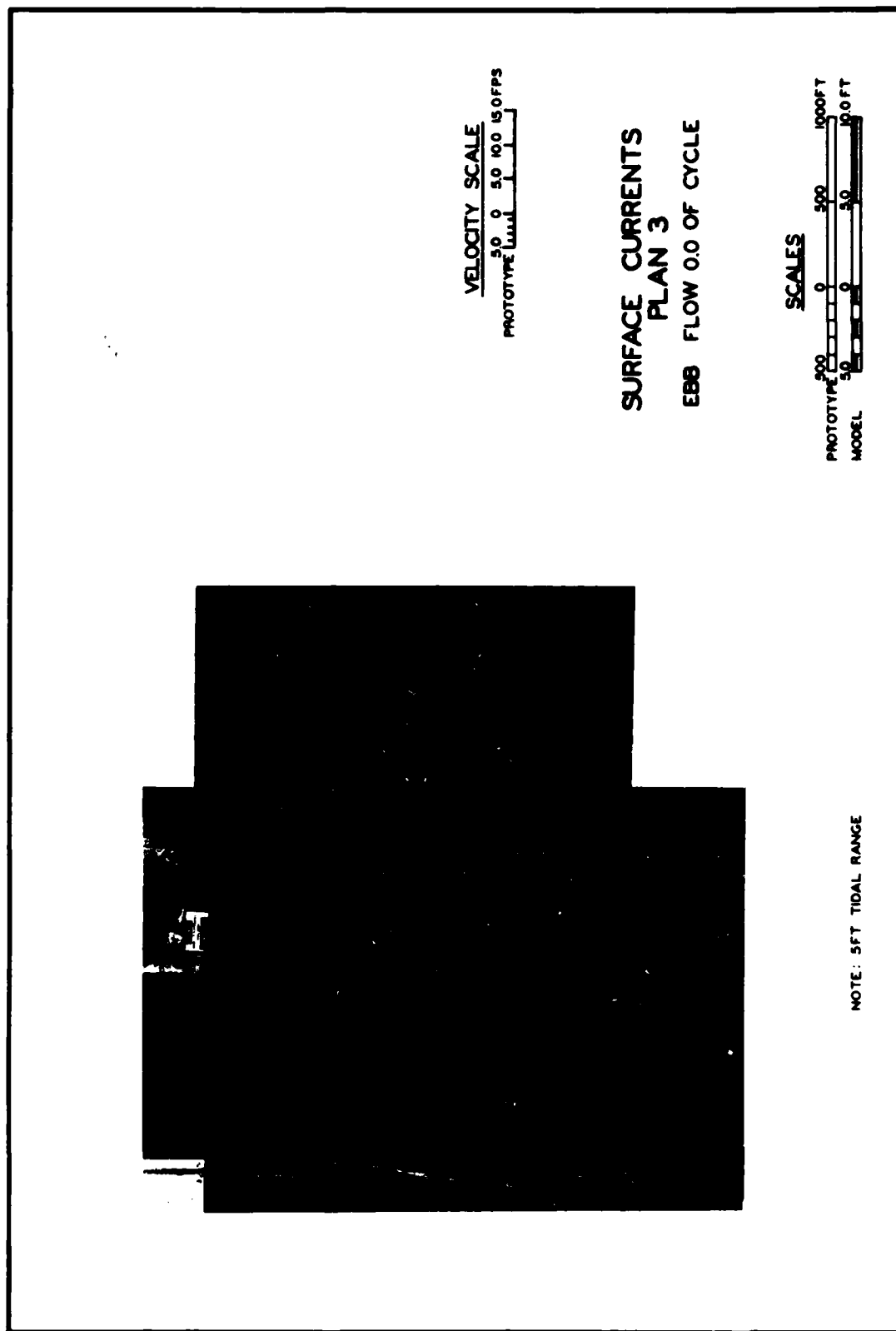
SURFACE CURRENTS
PLAN 3
EBB FLOW 0.8 OF CYCLE

SCALES
500 0 500 1000 FT
PROTOTYPE
50 0 50 100 FT
MODEL

NOTE: 5 FT TIDAL RANGE

PHOTO 19

PHOTO 20



VELOCITY SCALE
50 0 50 100 150 FPS
PROTOTYPE

SURFACE CURRENTS
PLAN 3
EBB FLOW 0.0 OF CYCLE



SCALES
500 0 500 1000 FT
PROTOTYPE
50 0 50 100 FT
MODEL

NOTE: 5 FT TIDAL RANGE



VELOCITY SCALES
 0 50 MOFPS
 PROTOTYPE (uuuuuu)

SURFACE CURRENTS
PLAN 1
 FLOOD FLOW 0.2 OF CYCLE
 DEEPWATER WAVE HEIGHT 10 FT. 10 SEC PERIOD
 DEEPWATER WAVE DIRECTION 30° UP COAST

SCALES
 200 0 200 400 800 FT
 PROTOTYPE (DEE) 
 20 0 20 40 80 FT
 MODEL (DEE) 

NOTE 5 FT TIDAL RANGE

PHOTO 21

PHOTO 22



VELOCITY SCALES
 PROTOTYPE 0 50 100 FPS
 MODEL 0 2.0 4.0 6.0

SURFACE CURRENTS
PLAN 1
 FLOOD FLOW 0.4 OF CYCLE
 DEEPWATER WAVE HEIGHT 10 FT, 10 SEC PERIOD
 DEEPWATER WAVE DIRECTION 30° UP-CAST

SCALES
 PROTOTYPE 0 200 400 800 FT
 MODEL 0 2.0 4.0 6.0
 NOTE 5 FT TIDAL RANGE



VELOCITY SCALES
 0 50 100 FPS
 PROTOTYPE (mm/min)


SURFACE CURRENTS
 PLAN 1
 EBB FLOW 0.6 OF CYCLE
 DEEPWATER WAVE HEIGHT 10 FT, 10 SEC PERIOD
 DEEPWATER WAVE DIRECTION 30° UP COAST

SCALES
 200 0 200 400 600 FT
 PROTOTYPE (mm/min)
 2.0 0 2.0 4.0 6.0 FT
 MODEL



NOTE 5 FT TIDAL RANGE



PHOTO 24

VELOCITY SCALES
 0 50 100 FPS
 PROTOTYPE 

SURFACE CURRENTS
 PLAN 1
 EBB FLOW 0.8 OF CYCLE
 DEEPWATER WAVE HEIGHT 10 FT, 10 SEC PERIOD
 DEEPWATER WAVE DIRECTION 30° UP COAST

SCALES
 200 0 200 400 800 FT
 PROTOTYPE 
 MODEL 

NOTE 5 FT TIDAL RANGE



VELOCITY SCALES
 PROTOTYPE 0 50 100 FPS

SURFACE CURRENTS
 PLAN 1
 EBB FLOW 0.0 OF CYCLE
 DEEPWATER WAVE HEIGHT 10 FT, 10 SEC PERIOD
 DEEPWATER WAVE DIRECTION 30° UP-CAST

SCALES
 PROTOTYPE 200 0 200 400 800 FT
 MODEL 20 0 20 40 80 FT

NOTE 5 FT TIDAL RANGE

PHOTO 25



VELOCITY SCALES

0 50 100 FPS
PROTOTYPE (mm/min)

SURFACE CURRENTS PLAN 1

FLOOD FLOW 0.2 OF CYCLE
DEEPWATER WAVE HEIGHT 10 FT. 10 SEC PERIOD
DEEPWATER WAVE DIRECTION 30° DOWNCOAST

SCALES

200	0	200	400	600 FT
PROTOTYPE (mm/min)				
20	0	20	40	60 FT
MODEL				

NOTE: 5 FT TIDAL RANGE

PHOTO 26



VELOCITY SCALES
 0 50 100 FPS
 PROTOTYPE (|||||)

SURFACE CURRENTS
PLAN 1
 FLOOD FLOW 0.4 OF CYCLE
 DEEPWATER WAVE HEIGHT 10 FT. 10 SEC PERIOD
 DEEPWATER WAVE DIRECTION 30° DOWNCOAST

SCALES
 200 0 200 400 600 FT
 PROTOTYPE (|||||)
 20 0 20 40 60 FT
 MODEL (|||||)

NOTE 5 FT TIDAL RANGE

PHOTO 27



PHOTO 28

VELOCITY SCALES
 0 50 100 FPS
 PROTOTYPE [|||||]
 MODEL [|||||]

SURFACE CURRENTS
PLAN 1

EBB FLOW 0.6 OF CYCLE
 DEEPWATER WAVE HEIGHT 10 FT, 10 SEC PERIOD
 DEEPWATER WAVE DIRECTION 30° DOWNCOAST

SCALES
 200 0 200 400 600 FT
 PROTOTYPE [|||||]
 20 0 20 40 60 FT
 MODEL [|||||]

NOTE 5 FT TIDAL RANGE



VELOCITY SCALES
 0 50 100FPS
 PROTOTYPE (|||||)

SURFACE CURRENTS
PLAN 1
 EBB FLOW 0.8 OF CYCLE
 DEEPWATER WAVE HEIGHT 10 FT, 10 SEC PERIOD
 DEEPWATER WAVE DIRECTION 30° DOWNCOAST

SCALES
 200 0 200 400 600 FT
 PROTOTYPE (|||||)
 20 0 20 40 60 FT
 MODEL (|||||)

NOTE 5 FT TIDAL RANGE



VELOCITY SCALES

0 50 100 FPS
PROTOTYPE 

SURFACE CURRENTS
PLAN 1

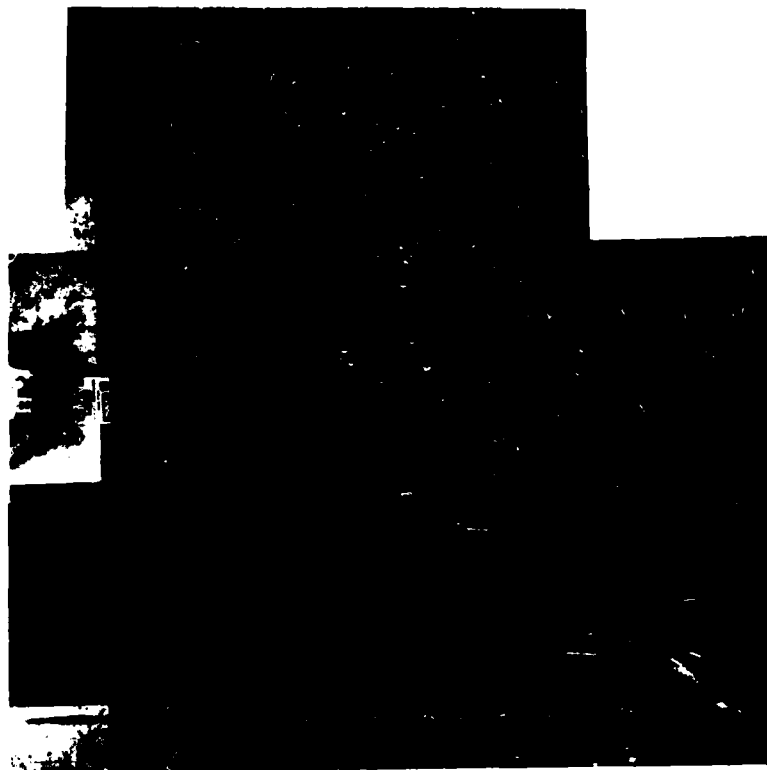
EBB FLOW 0.0 OF CYCLE
DEEPWATER WAVE HEIGHT 10 FT, 10 SEC PERIOD
DEEPWATER WAVE DIRECTION 30° DOWNCOAST

SCALES

200 0 200 400 600 FT
PROTOTYPE 
20 0 20 40 60 FT
MODEL 

NOTE: 5 FT TIDAL RANGE

PHOTO 30



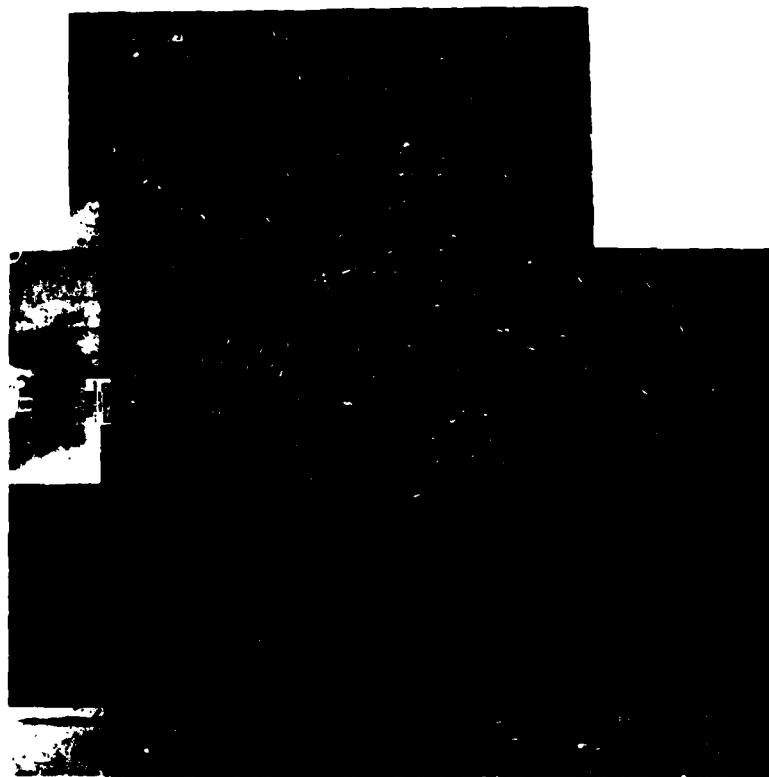
VELOCITY SCALE
 50 0 50 100 150 FPS
 PROTOTYPE MODEL

**SURFACE CURRENTS
 PLAN 2**
 FLOOD FLOW 0.2 OF CYCLE
 DEEPWATER WAVE HEIGHT 5 FT, 10 SEC PERIOD
 DEEPWATER WAVE DIRECTION 40° UP-COAST

SCALES
 500 0 500 1000 FT
 PROTOTYPE MODEL
 50 0 50 100 FT

NOTE: 5 FT TIDAL RANGE

PHOTO 32



VELOCITY SCALE
50 0 50 100 150 FPS
PROTOTYPE

SURFACE CURRENTS PLAN 2

EBB FLOW 0.4 OF CYCLE

DEEPWATER WAVE HEIGHT 5 FT, 10 SEC PERIOD

DEEPWATER WAVE DIRECTION 40° UP COAST

SCALES



NOTE: 5 FT TIDAL RANGE



VELOCITY SCALE
 50 0 50 100 150 FPS
 PROTOTYPE

**SURFACE CURRENTS
 PLAN 2**
 EBB FLOW 0.6 OF CYCLE
 DEEPWATER WAVE HEIGHT 5 FT, 10 SEC PERIOD
 DEEPWATER WAVE DIRECTION 40° UP COAST

SCALES
 500 0 500 1000 FT
 PROTOTYPE
 50 0 50 100 FT
 MODEL

NOTE 5 FT TIDAL RANGE



VELOCITY SCALE
 50 0 50 100 150 FPS
 PROTOTYPE

SURFACE CURRENTS
PLAN 2
 EBB FLOW 0.8 OF CYCLE
 DEEPWATER WAVE HEIGHT 5 FT, 10 SEC PERIOD
 DEEPWATER WAVE DIRECTION 40° UP COAST

SCALES
 500 0 500 1000 FT
 PROTOTYPE
 50 0 50 100 FT
 MODEL

NOTE: 5 FT TIDAL RANGE

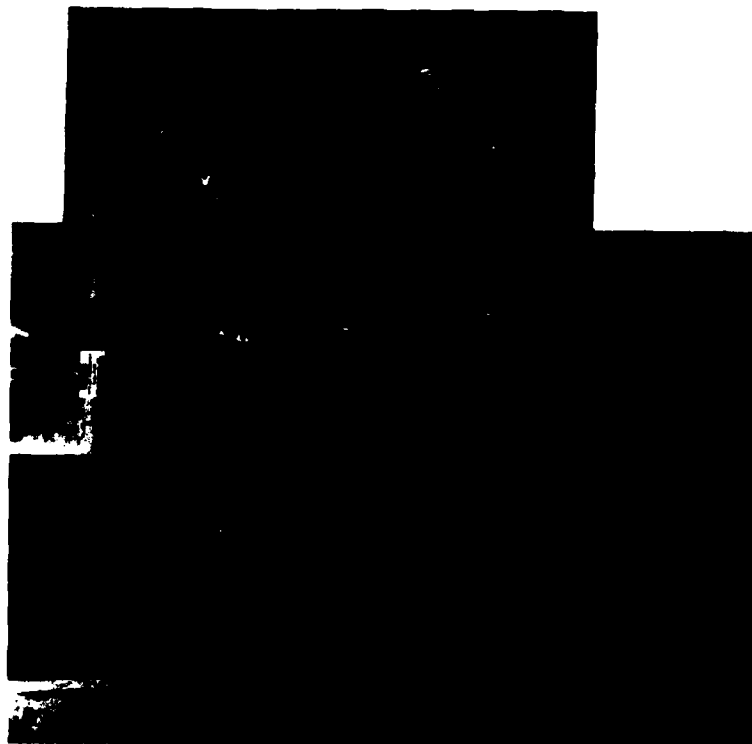


VELOCITY SCALE
 50 0 50 100 150 FPS
 PROTOTYPE

SURFACE CURRENTS
PLAN 2
 EBB FLOW 0.0 OF CYCLE
 DEEPWATER WAVE HEIGHT 5 FT, 10 SEC PERIOD
 DEEPWATER WAVE DIRECTION 40° UP COAST

SCALES
 500 0 500 1000 FT
 PROTOTYPE
 50 0 50 100 FT
 MODEL

NOTE: 5 FT TIDAL RANGE

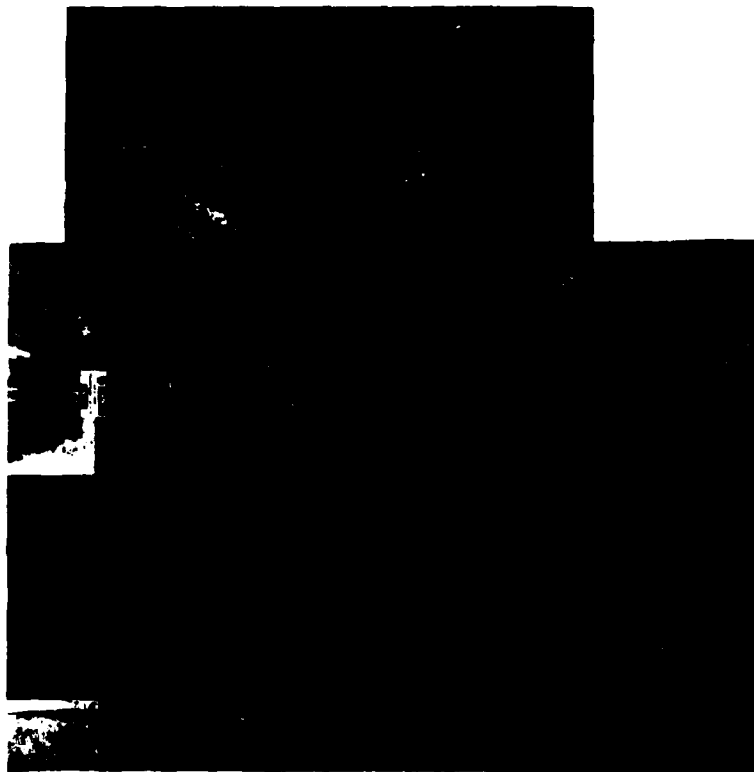


VELOCITY SCALE
 50 0 50 100 150 FPS
 PROTOTYPE

**SURFACE CURRENTS
 PLAN 2**
 FLOOD FLOW 0.2 OF CYCLE
 DEEPWATER WAVE HEIGHT 10FT, 10SEC PERIOD
 DEEPWATER WAVE DIRECTION 40° UP COAST

SCALES
 500 0 500 1000 FT
 PROTOTYPE
 50 0 50 100 FT
 MODEL

NOTE: 5FT TIDAL RANGE



VELOCITY SCALE
 50 0 50 100 150 FPS
 PROTOTYPE

**SURFACE CURRENTS
 PLAN 2**
 FLOOD FLOW 0.4 OF CYCLE
 DEEPWATER WAVE HEIGHT 10FT, 10SEC PERIOD
 DEEPWATER WAVE DIRECTION 40° UP-COAST

SCALES
 200 0 500 1000 FT
 PROTOTYPE
 50 0 50 100 FT
 MODEL

NOTE: 5 FT TIDAL RANGE



VELOCITY SCALE
 5.0 0 5.0 10.0 15.0 FPS
 PROTOTYPE

SURFACE CURRENTS PLAN 2

EBB FLOW 0.6 OF CYCLE

DEEPWATER WAVE HEIGHT 10FT, 10SEC PERIOD

DEEPWATER WAVE DIRECTION 40° UP COAST

SCALES



NOTE: 5 FT TIDAL RANGE

PHOTO 38



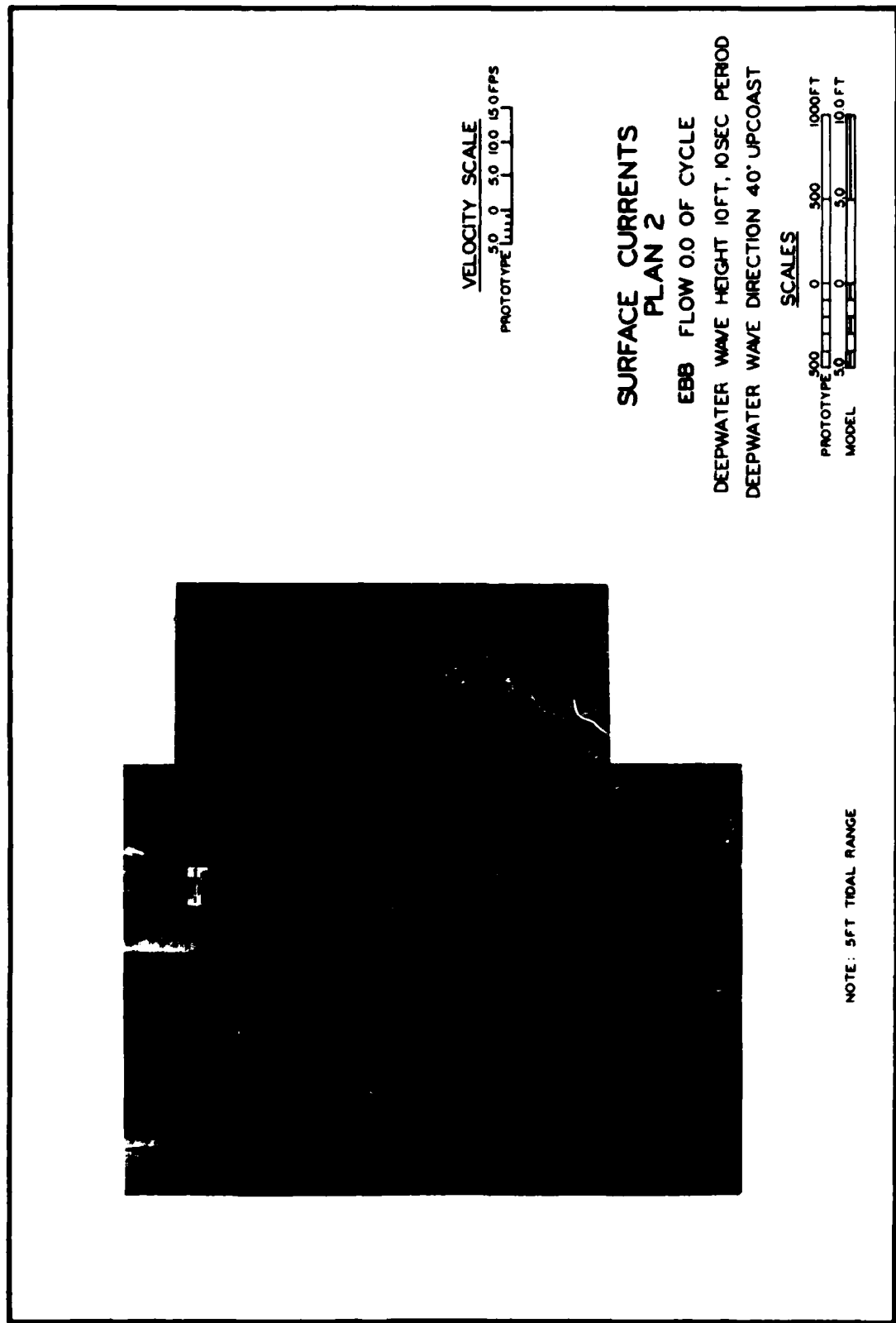
VELOCITY SCALE
50 0 50 100 150 FPS
PROTOTYPE

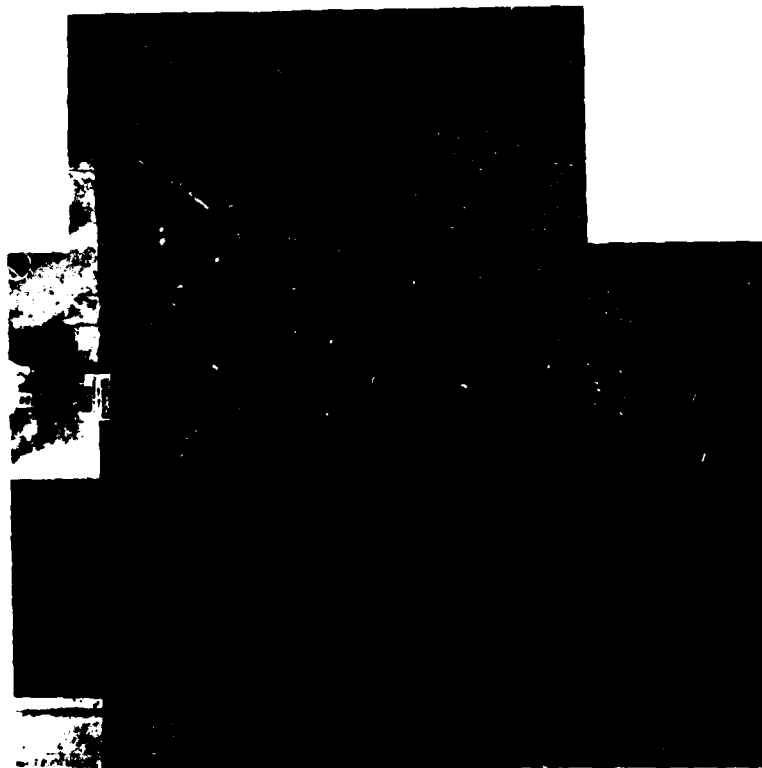
**SURFACE CURRENTS
PLAN 2**
EBB FLOW 0.8 OF CYCLE
DEEPWATER WAVE HEIGHT 10 FT, 10 SEC PERIOD
DEEPWATER WAVE DIRECTION 40° UP COAST

SCALES
500 0 500 1000 FT
PROTOTYPE
50 0 50 100 FT
MODEL

NOTE: 5 FT TIDAL RANGE

PHOTO 40





VELOCITY SCALE
 50 0 50 100 150 FPS
 PROTOTYPE

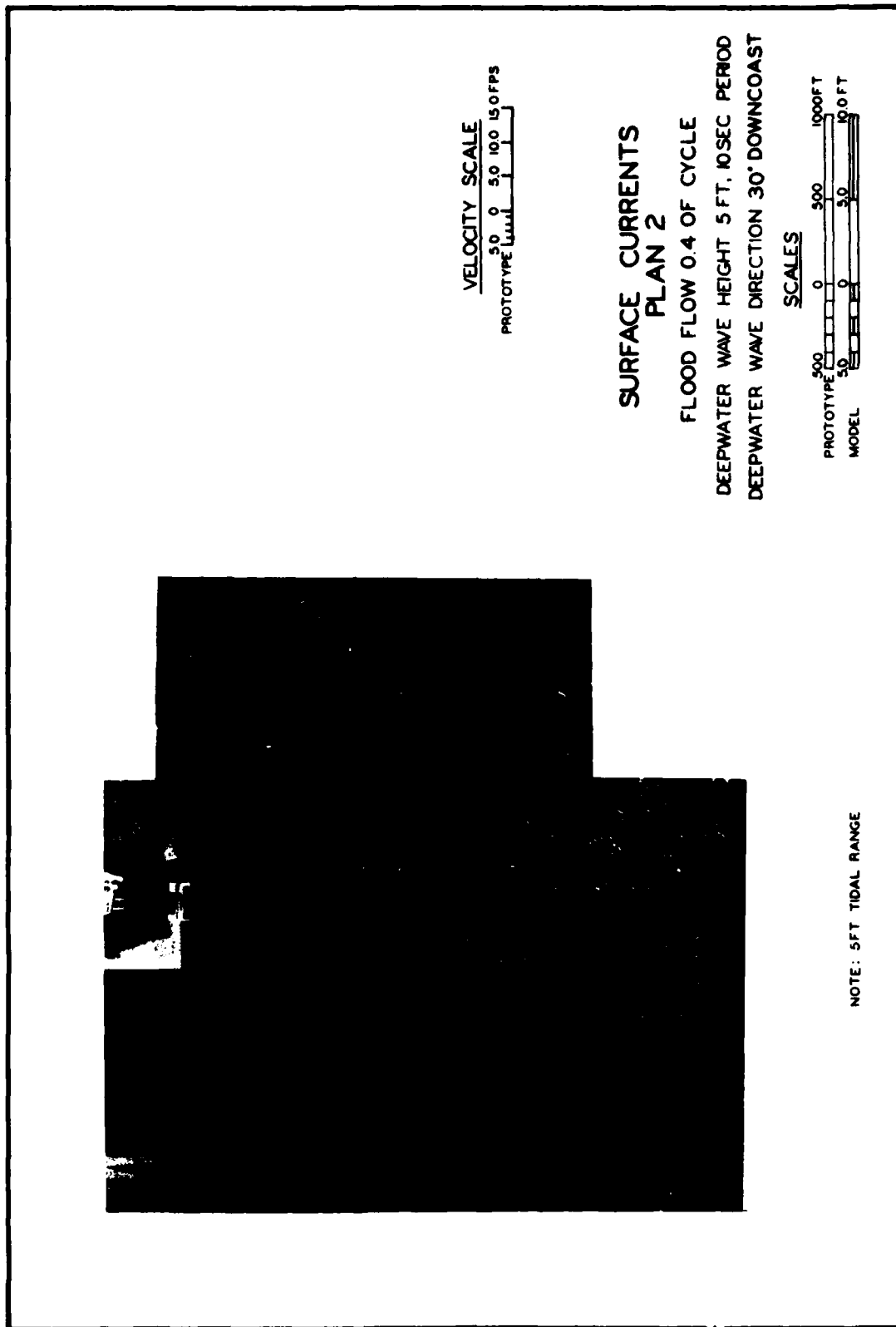
SURFACE CURRENTS PLAN 2

FLOOD FLOW 0.2 OF CYCLE
 DEEPWATER WAVE HEIGHT 5 FT, 10 SEC PERIOD
 DEEPWATER WAVE DIRECTION 30° DOWNCOAST

SCALES
 500 0 500 1000 FT
 PROTOTYPE
 50 0 50 100 FT
 MODEL

NOTE: 5 FT TIDAL RANGE

PHOTO 42





VELOCITY SCALE
 50 0 50 100 150 FPS
 PROTOTYPE

**SURFACE CURRENTS
 PLAN 2**
 EBB FLOW 0.6 OF CYCLE
 DEEPWATER WAVE HEIGHT 5 FT, 10 SEC PERIOD
 DEEPWATER WAVE DIRECTION 30° DOWNCOAST

SCALES
 PROTOTYPE 500 0 500 1000 FT
 MODEL 50 0 50 100 FT

NOTE: 5 FT TIDAL RANGE

PHOTO 44

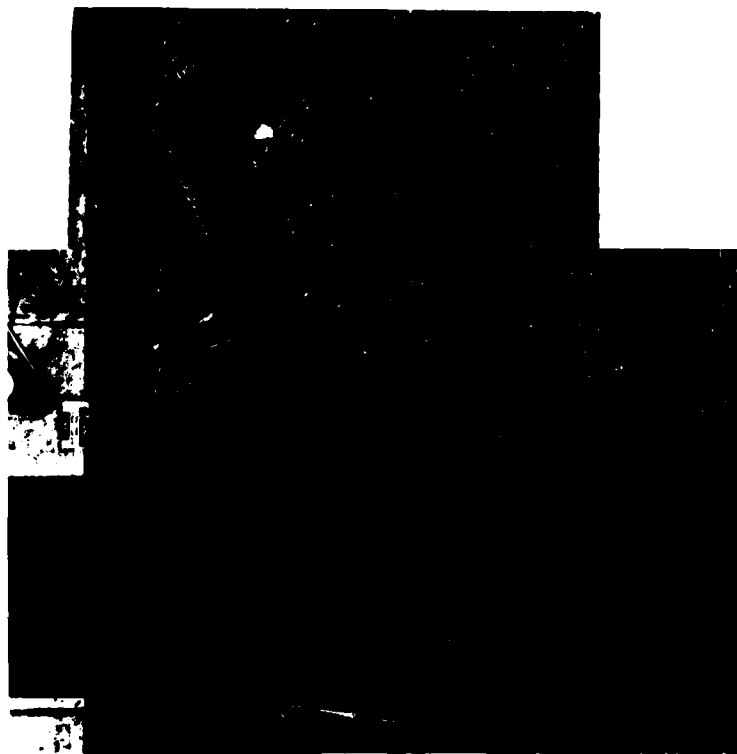


VELOCITY SCALE
50 0 50 100 150 FPS
PROTOTYPE

**SURFACE CURRENTS
PLAN 2**
FLOOD FLOW 0.8 OF CYCLE
DEEPWATER WAVE HEIGHT 5 FT, 10 SEC PERIOD
DEEPWATER WAVE DIRECTION 30° DOWNCOAST

SCALES
500 0 500 1000 FT
PROTOTYPE
50 0 50 100 FT
MODEL

NOTE: 5 FT TIDAL RANGE



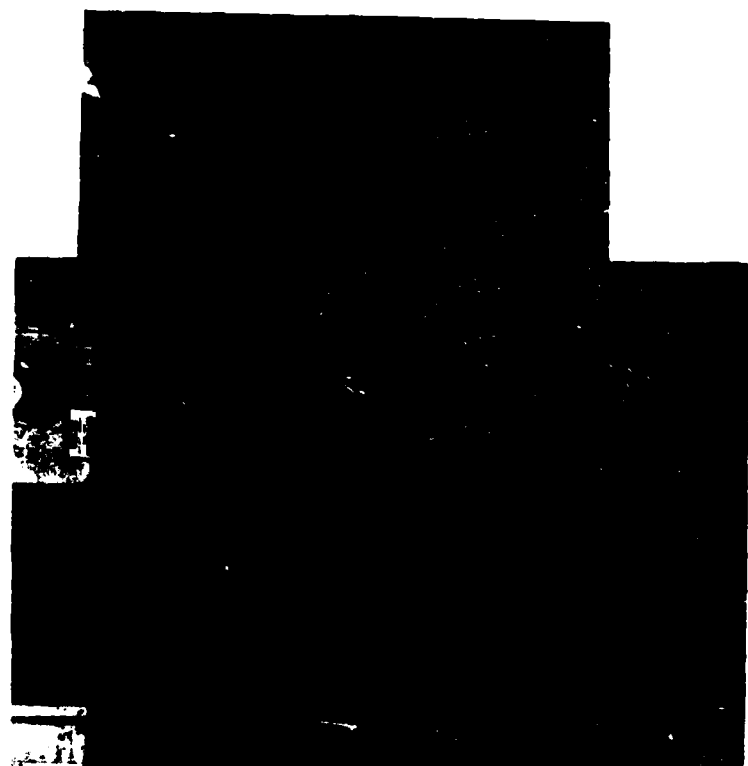
VELOCITY SCALE
50 0 50 100 150 FPS
PROTOTYPE

SURFACE CURRENTS PLAN 3

FLOOD FLOW 0.2 OF CYCLE
DEEPWATER WAVE HEIGHT 5 FT, 10 SEC PERIOD
DEEPWATER WAVE DIRECTION 40° UP COAST

SCALES
PROTOTYPE 500 0 500 1000 FT
MODEL 50 0 50 100 FT

NOTE: 5 FT TIDAL RANGE

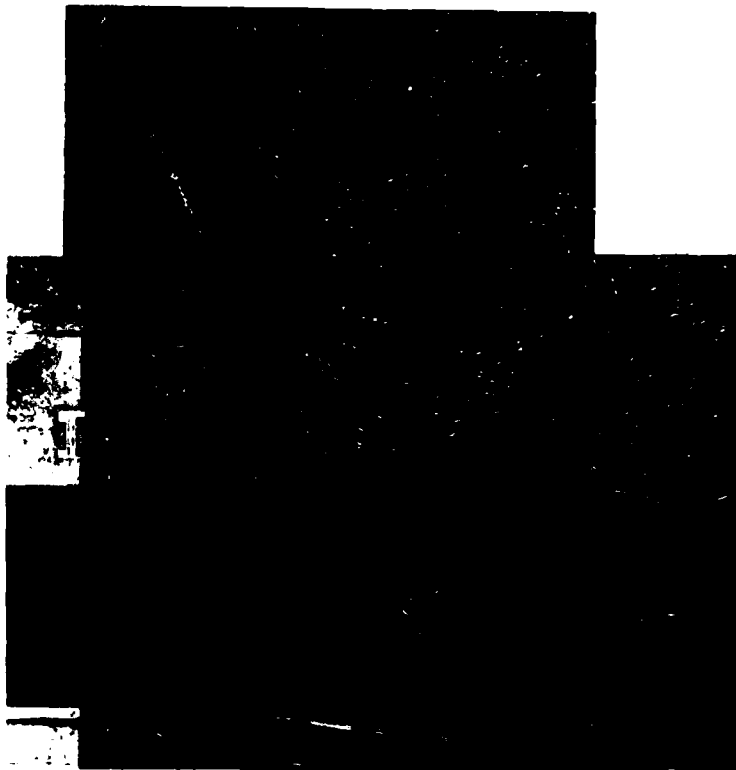


VELOCITY SCALE
50 0 50 100 150 FPS
PROTOTYPE

**SURFACE CURRENTS
PLAN 3**
FLOOD FLOW 0.4 OF CYCLE
DEEPWATER WAVE HEIGHT 5 FT, 10 SEC PERIOD
DEEPWATER WAVE DIRECTION 40° UP COAST

SCALES
500 0 500 1000 FT
PROTOTYPE
50 0 50 100 FT
MODEL

NOTE: 5 FT TIDAL RANGE



VELOCITY SCALE
 50 0 50 100 150 FPS
 PROTOTYPE

SURFACE CURRENTS PLAN 3

EBB FLOW 0.6 OF CYCLE

DEEPWATER WAVE HEIGHT 5 FT, 10 SEC PERIOD

DEEPWATER WAVE DIRECTION 40° UP COAST

SCALES

200 0 500 1000 FT
 PROTOTYPE
 50 0 50 100 FT
 MODEL

NOTE: 5 FT TIDAL RANGE



VELOCITY SCALE
5.0 0 5.0 10.0 15.0 FPS
PROTOTYPE

SURFACE CURRENTS
PLAN 3
EBB FLOW 0.8 OF CYCLE
DEEPWATER WAVE HEIGHT 5 FT, 10 SEC PERIOD
DEEPWATER WAVE DIRECTION 40° UP COAST

SCALES
500 0 500 1000 FT
PROTOTYPE
50 0 50 100 FT
MODEL

NOTE: 5 FT TIDAL RANGE



VELOCITY SCALE
 50 0 50 100 150 FPS
 PROTOTYPE

**SURFACE CURRENTS
 PLAN 3**
 EBB FLOW 0.0 OF CYCLE
 DEEPWATER WAVE HEIGHT 5 FT, 10 SEC PERIOD
 DEEPWATER WAVE DIRECTION 40° UP COAST

SCALES
 500 0 500 1000 FT
 PROTOTYPE
 50 0 50 100 FT
 MODEL

NOTE: 5 FT TIDAL RANGE

PHOTO 50

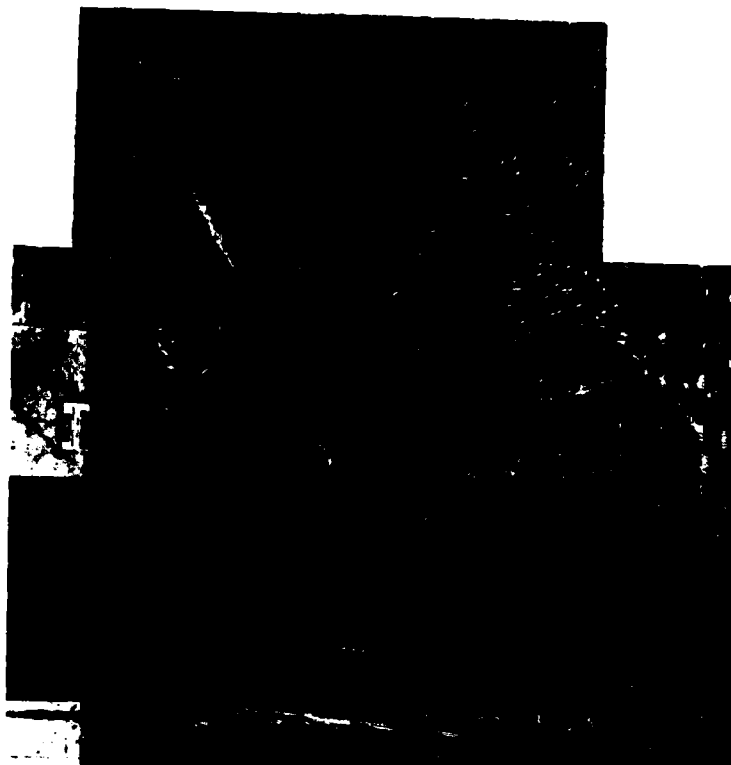


VELOCITY SCALE
50 0 50 100 150 FPS
PROTOTYPE

SURFACE CURRENTS
PLAN 3
FLOOD FLOW 0.2 OF CYCLE
DEEPWATER WAVE HEIGHT 10FT, 10SEC PERIOD
DEEPWATER WAVE DIRECTION 40° UP COAST

SCALES
PROTOTYPE 500 0 500 1000 FT
MODEL 50 0 50 100 FT

NOTE: 5 FT TIDAL RANGE

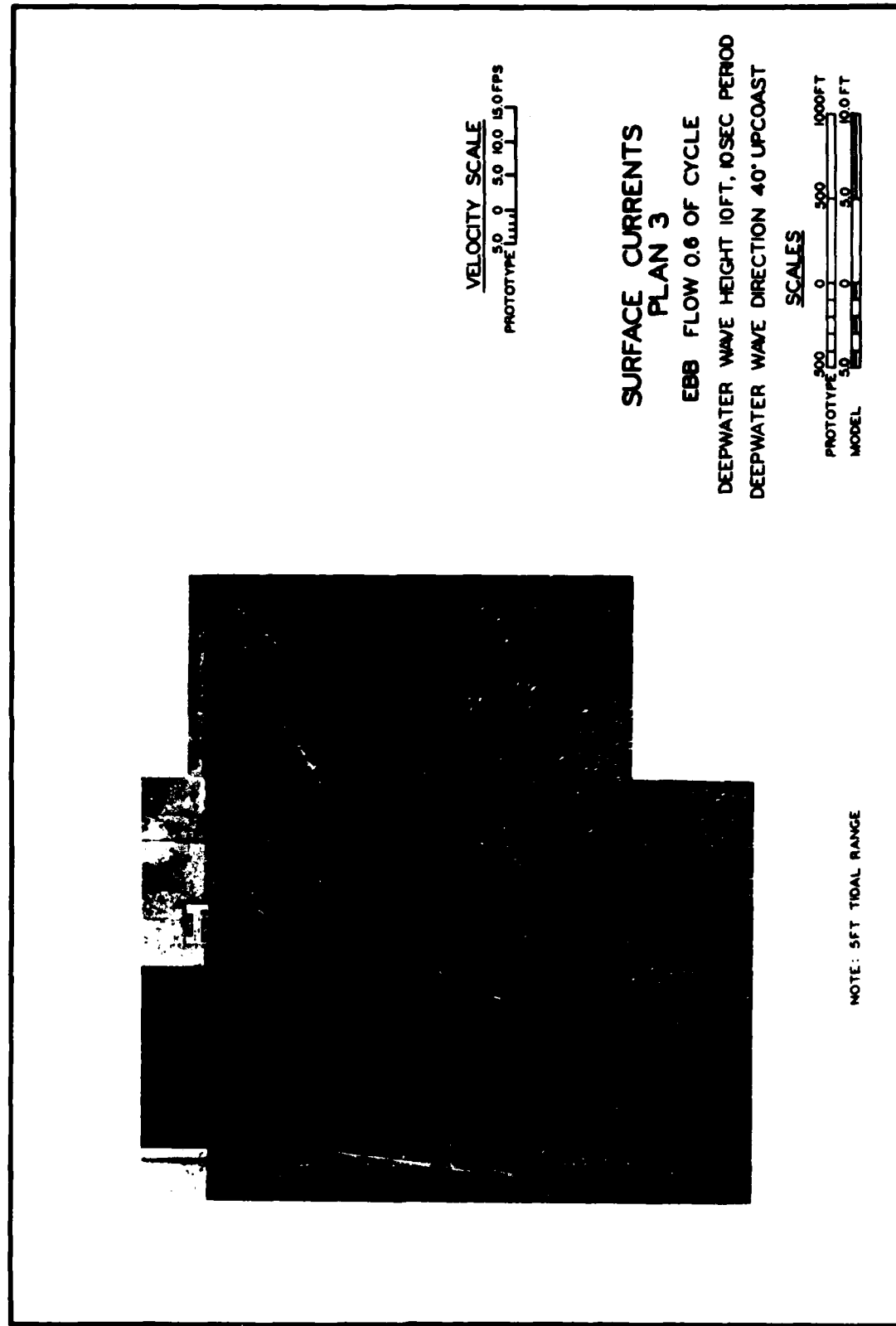


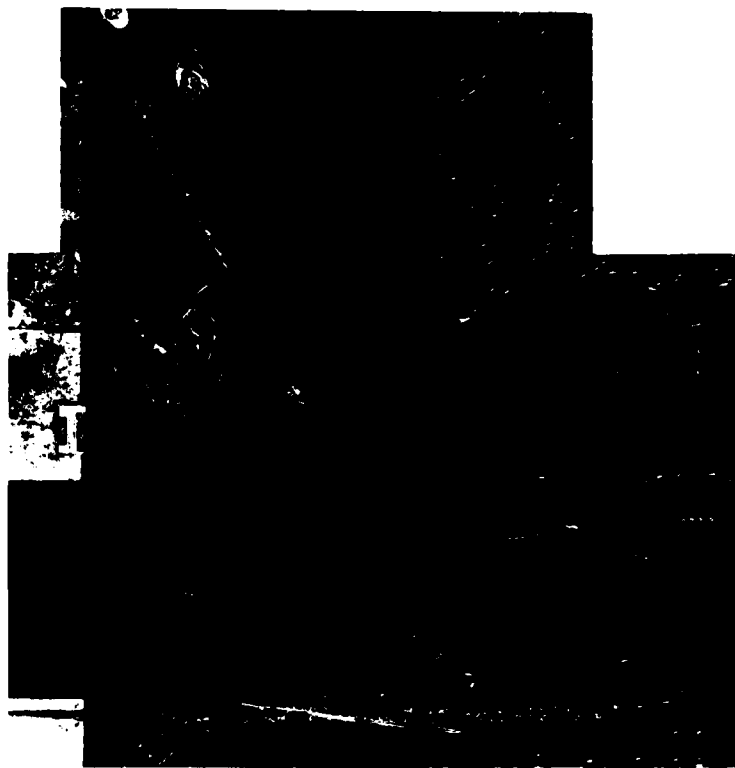
VELOCITY SCALE
 50 0 50 100 150 FPS
 PROTOTYPE 1:100

SURFACE CURRENTS
 PLAN 3
 FLOOD FLOW 0.4 OF CYCLE
 DEEPWATER WAVE HEIGHT 10 FT, 10 SEC PERIOD
 DEEPWATER WAVE DIRECTION 40° UP COAST

SCALES
 PROTOTYPE 500 0 500 1000 FT
 MODEL 50 0 50 100 FT

NOTE: 5 FT TIDAL RANGE





VELOCITY SCALE
 50 0 50 100 150 FPS
 PROTOTYPE

**SURFACE CURRENTS
 PLAN 3**
 EBB FLOW 0.8 OF CYCLE
 DEEPWATER WAVE HEIGHT 10 FT, 10 SEC PERIOD
 DEEPWATER WAVE DIRECTION 40° UP COAST

SCALES
 500 0 500 1000 FT
 PROTOTYPE
 50 0 50 100 FT
 MODEL

NOTE: 5 FT TIDAL RANGE

PHOTO 54

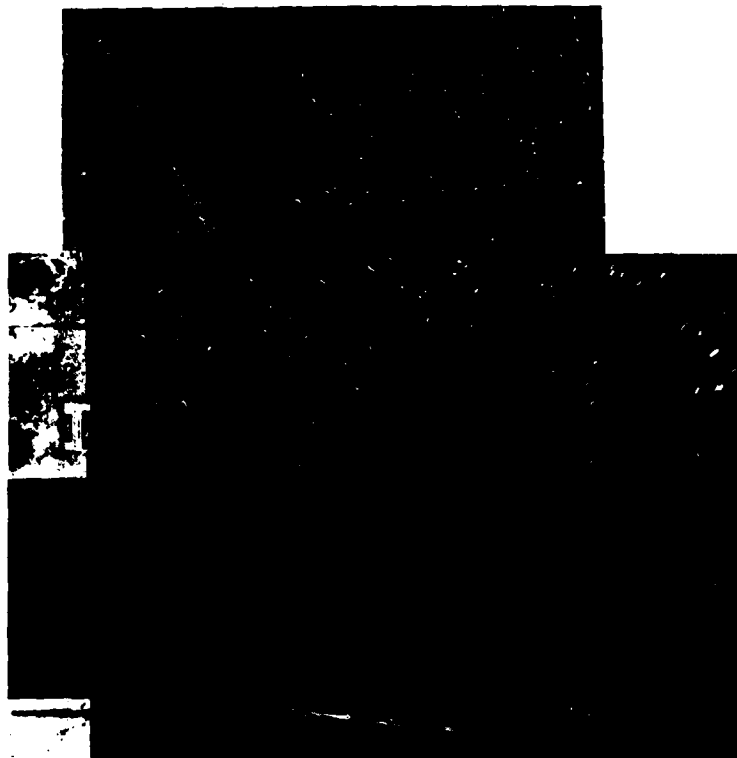


VELOCITY SCALE
5.0 0 5.0 10.0 15.0 FPS
PROTOTYPE

**SURFACE CURRENTS
PLAN 3**
EBB FLOW 0.0 OF CYCLE
DEEPWATER WAVE HEIGHT 10 FT, 10 SEC PERIOD
DEEPWATER WAVE DIRECTION 40° UP COAST

SCALES
500 0 500 1000 FT
PROTOTYPE
50 0 50 10.0 FT
MODEL

NOTE: 5 FT TIDAL RANGE



VELOCITY SCALE
50 0 50 100 150 FPS
PROTOTYPE

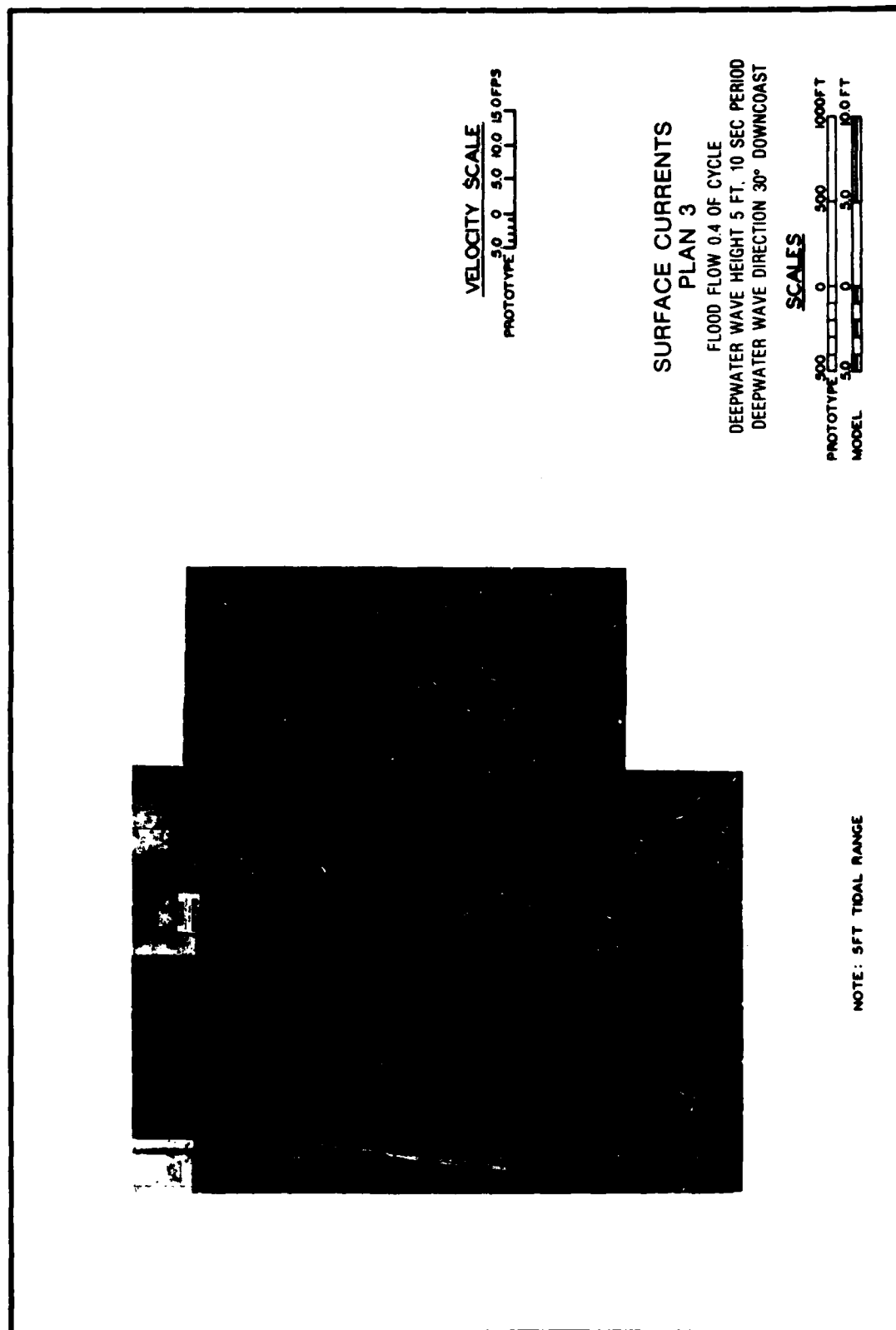
SURFACE CURRENTS
PLAN 3
FLOOD FLOW 0.2 OF CYCLE
DEEPWATER WAVE HEIGHT 5 FT, 10 SEC PERIOD
DEEPWATER WAVE DIRECTION 30° DOWNCOAST

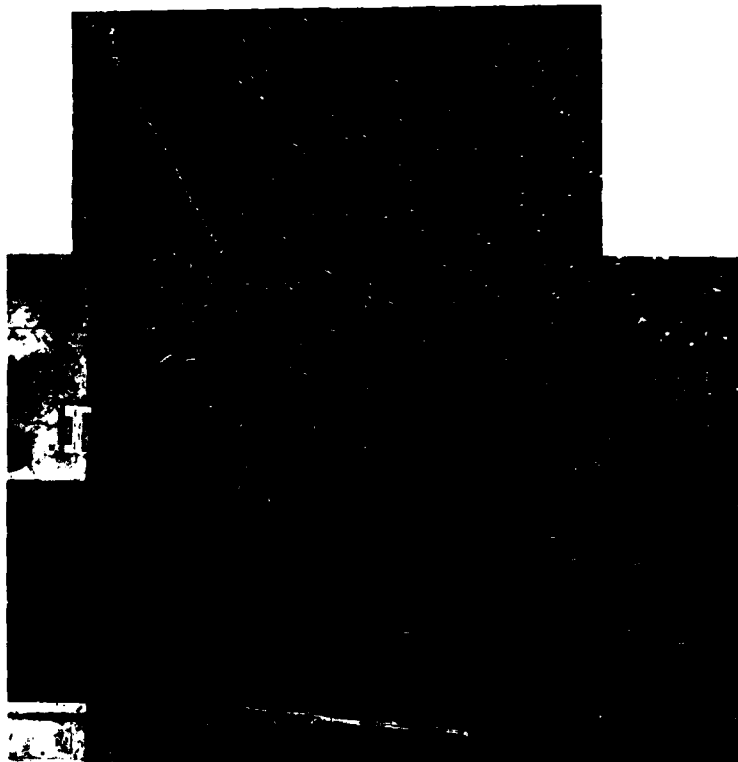
SCALES
500 0 500 1000 FT
PROTOTYPE
50 0 50 100 FT
MODEL

NOTE: 5 FT TIDAL RANGE

PHOTO 55

PHOTO 56





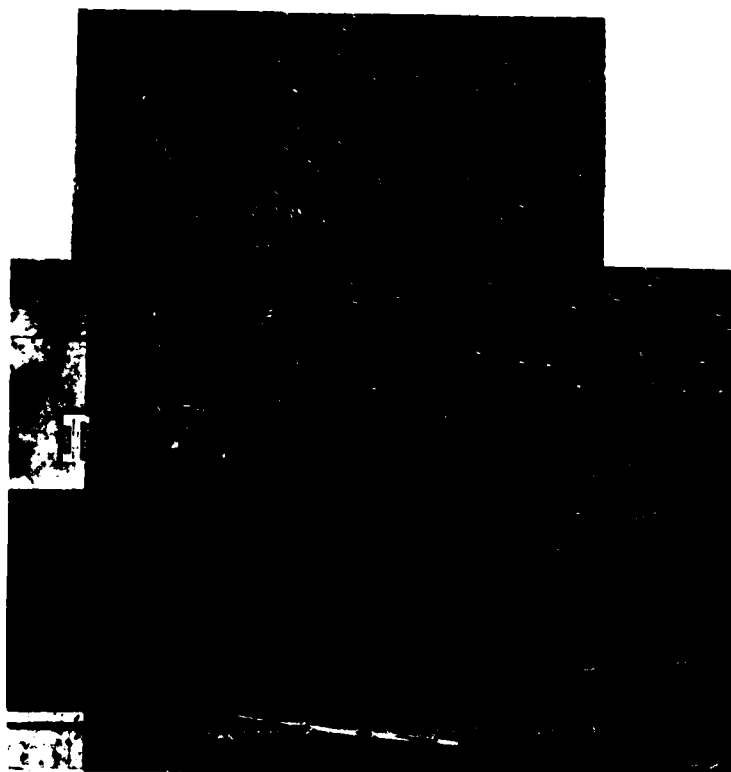
VELOCITY SCALE
 50 0 50 100 150 FPS
 PROTOTYPE

**SURFACE CURRENTS
 PLAN 3**
 EBB FLOW 0.6 OF CYCLE
 DEEPWATER WAVE HEIGHT 5 FT, 10 SEC PERIOD
 DEEPWATER WAVE DIRECTION 30° DOWNCOAST

SCALES
 PROTOTYPE 500 0 500 1000 FT
 MODEL 50 0 50 100 FT

NOTE: 5 FT TIDAL RANGE

PHOTO 58

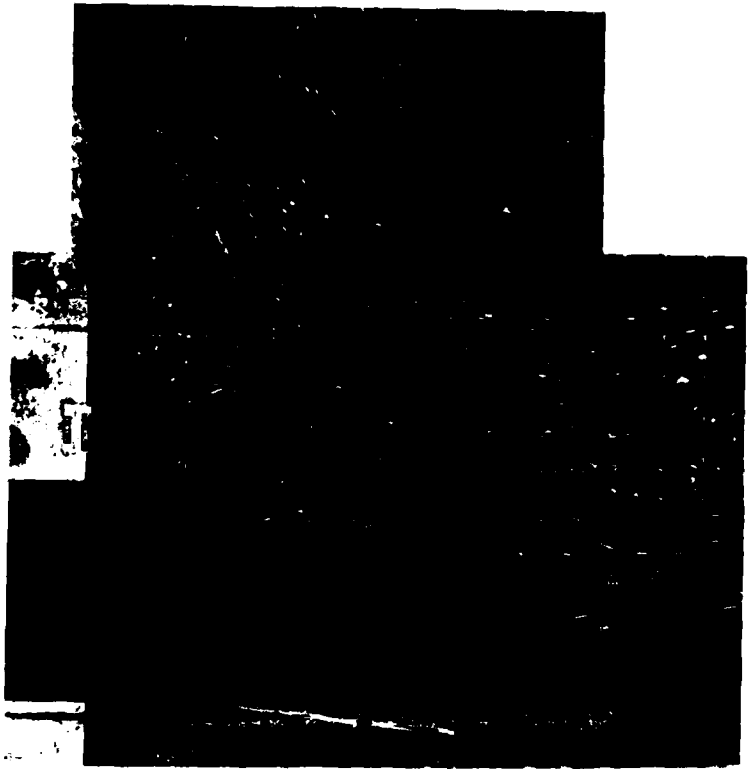


VELOCITY SCALE
5.0 0 5.0 10.0 15.0 FPS
PROTOTYPE

SURFACE CURRENTS
PLAN 3
EBB FLOW 0.8 OF CYCLE
DEEPWATER WAVE HEIGHT 5 FT, 10 SEC PERIOD
DEEPWATER WAVE DIRECTION 30° DOWNCOAST

SCALES
PROTOTYPE 200 0 500 1000 FT
MODEL 5.0 0 10.0 FT

NOTE: 5 FT TIDAL RANGE



VELOCITY SCALE
50 0 50 100 150 FPS
PROTOTYPE

SURFACE CURRENTS
PLAN 3
EBB FLOW 0.0 OF CYCLE
DEEPWATER WAVE HEIGHT 5 FT, 10 SEC PERIOD
DEEPWATER WAVE DIRECTION 30° DOWNCOAST

SCALES
500 0 500 1000 FT
PROTOTYPE
50 0 50 100 FT
MODEL

NOTE: 5 FT TIDAL RANGE

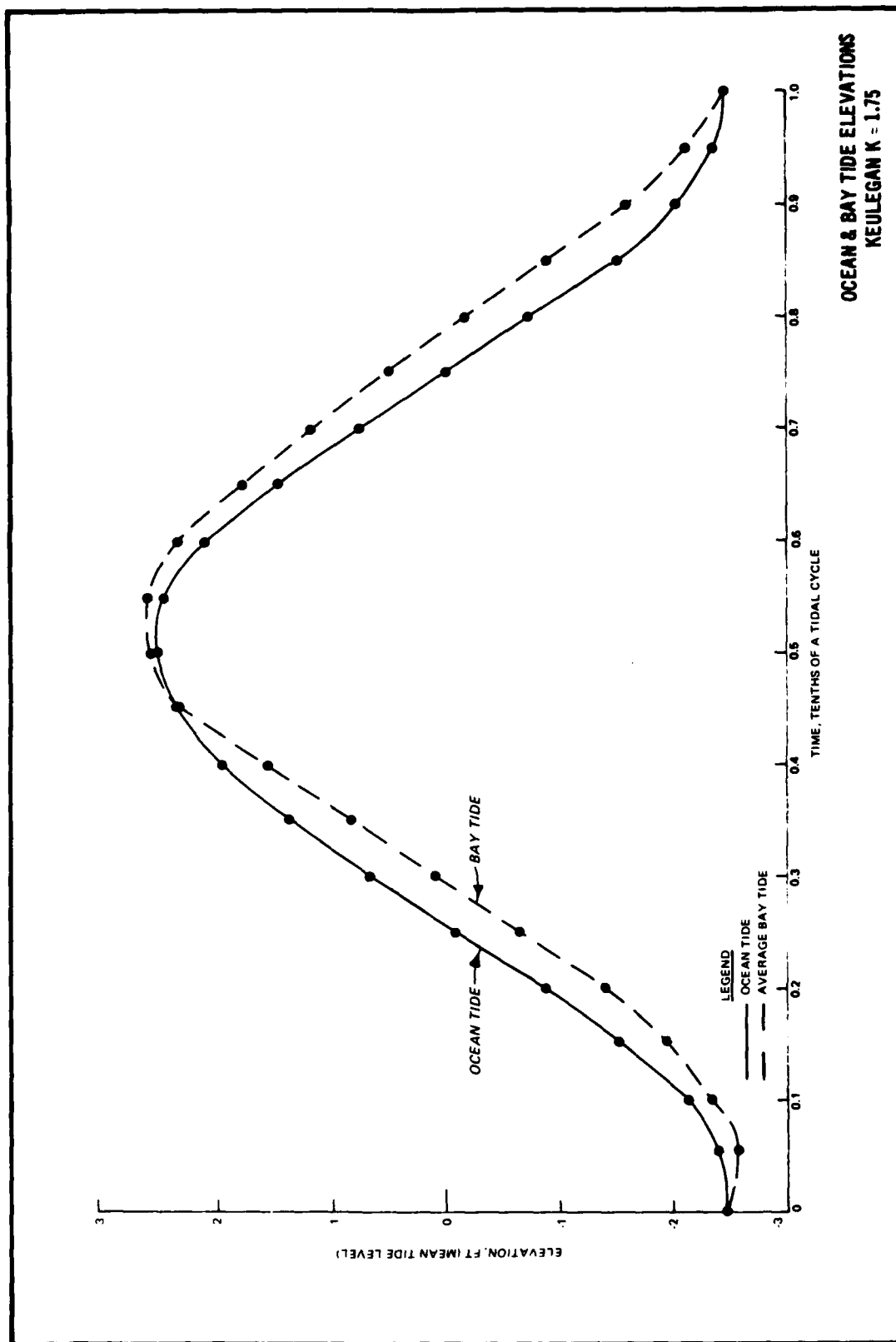


PLATE 1

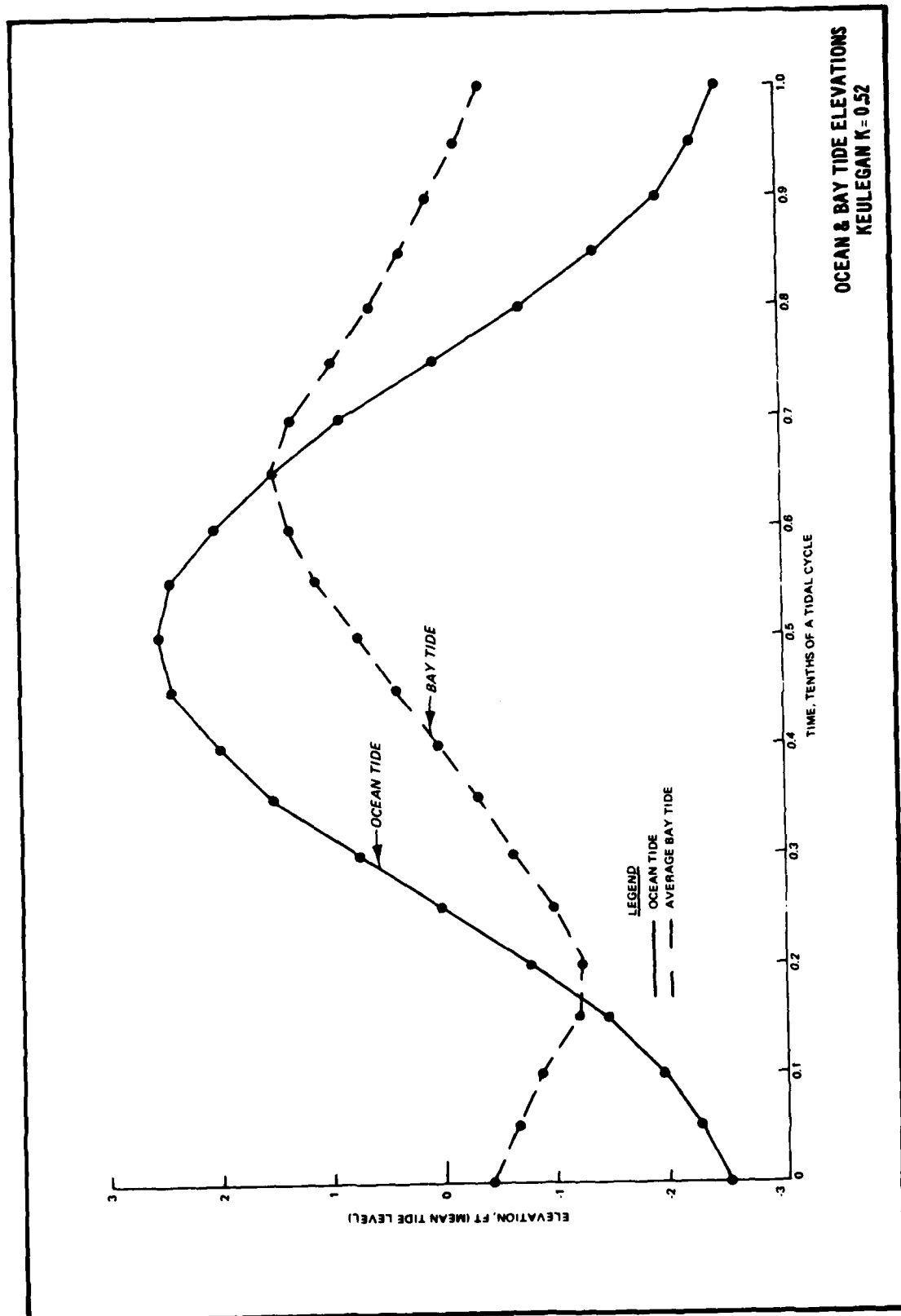
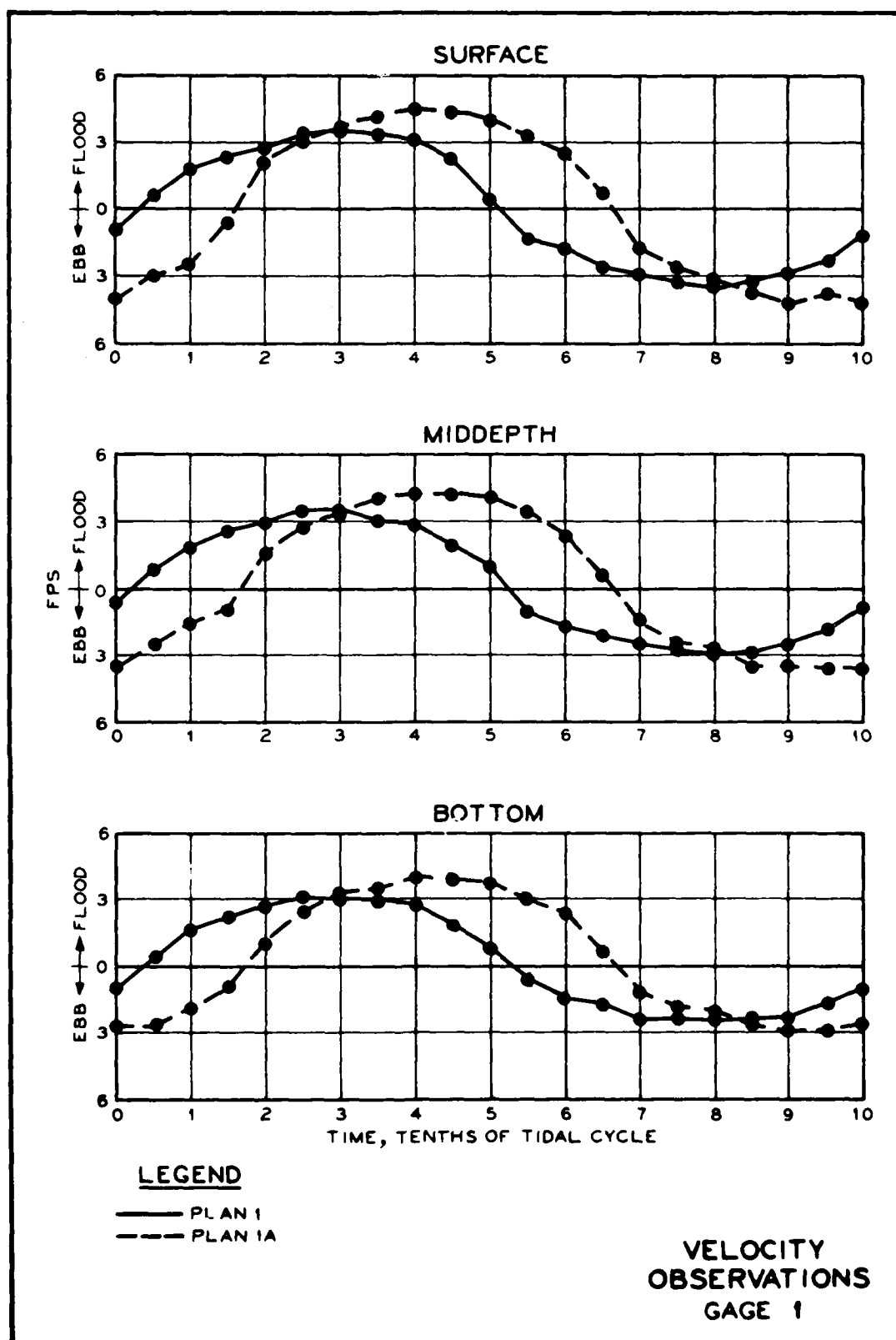


PLATE 2



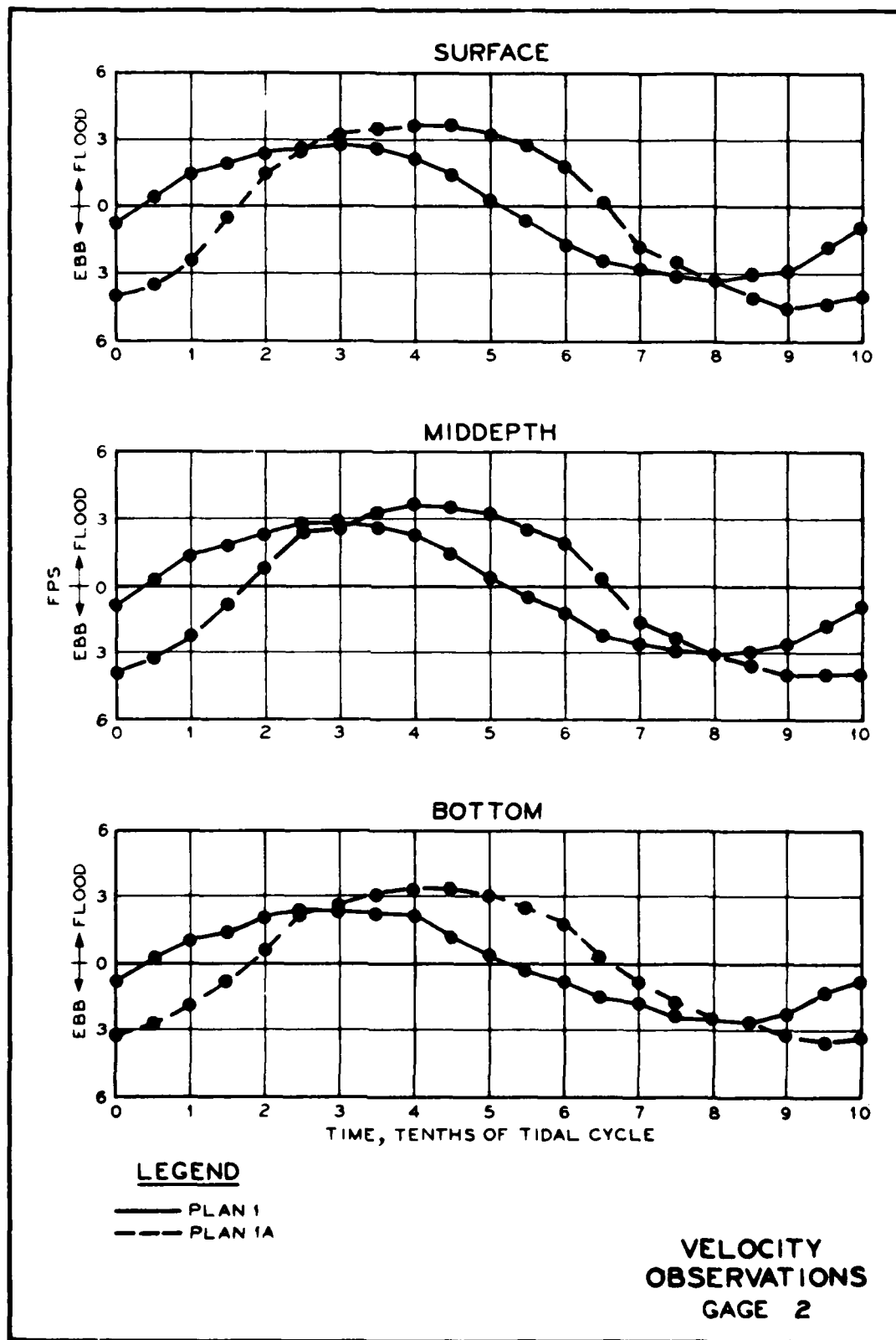
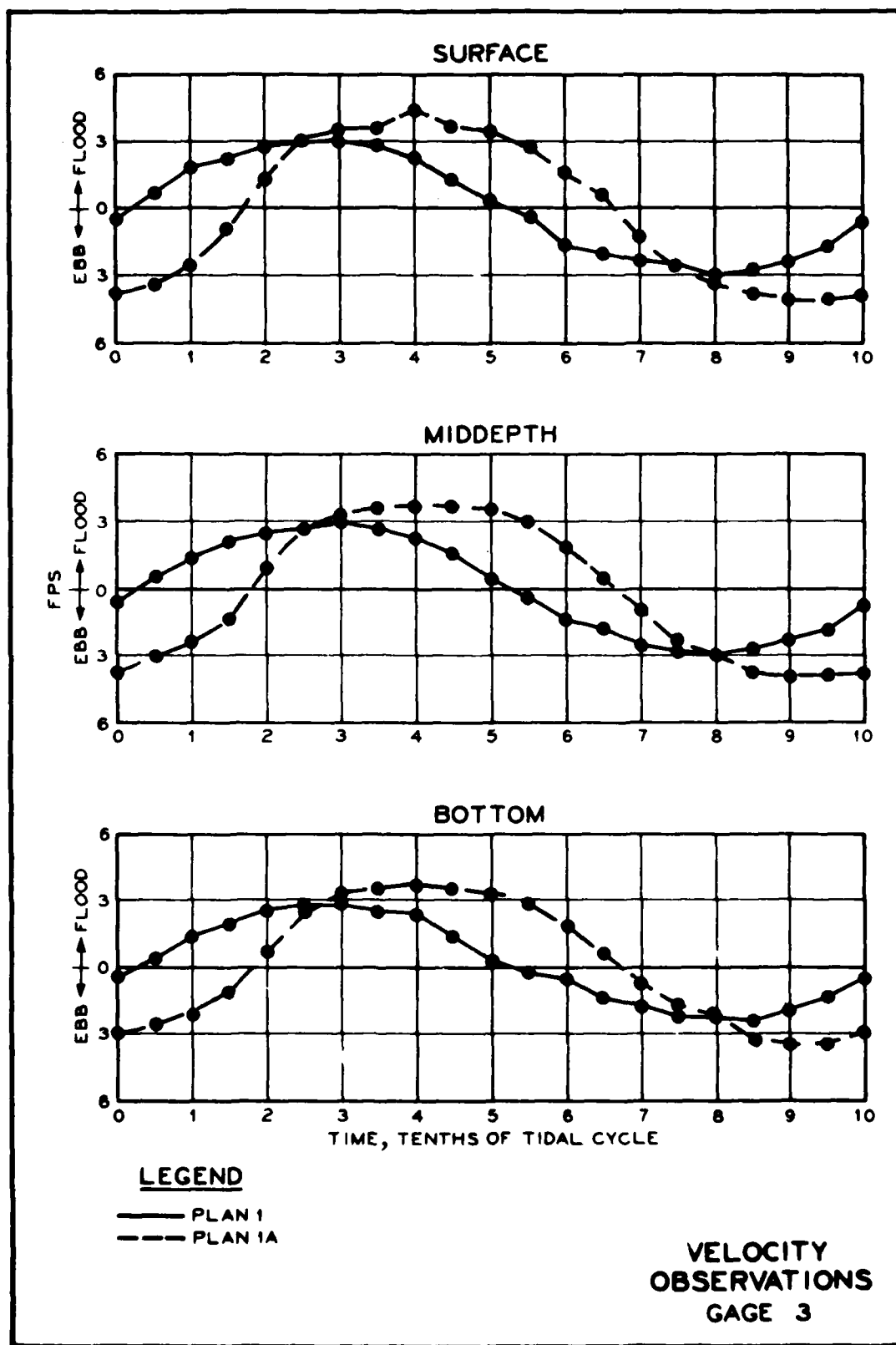
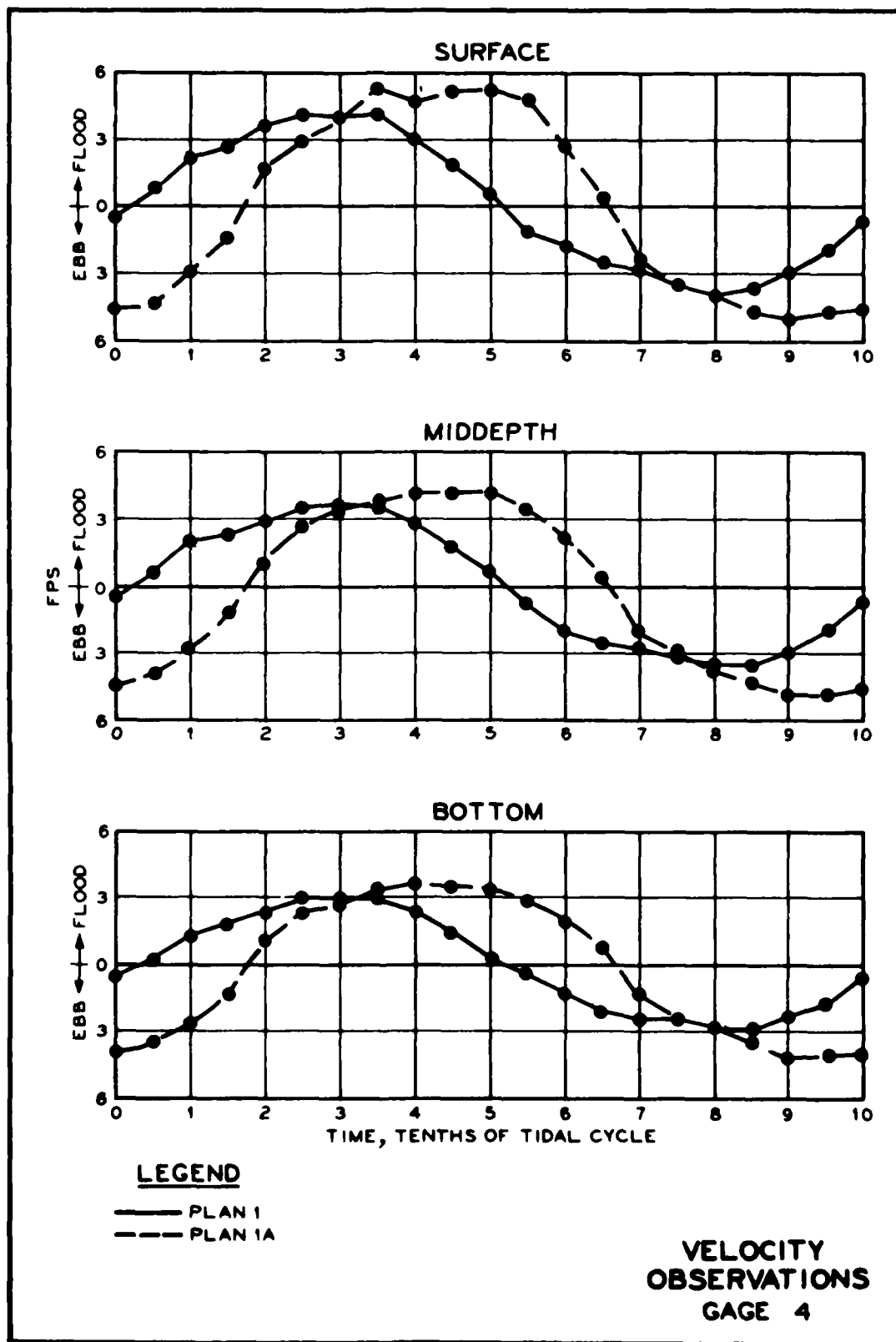
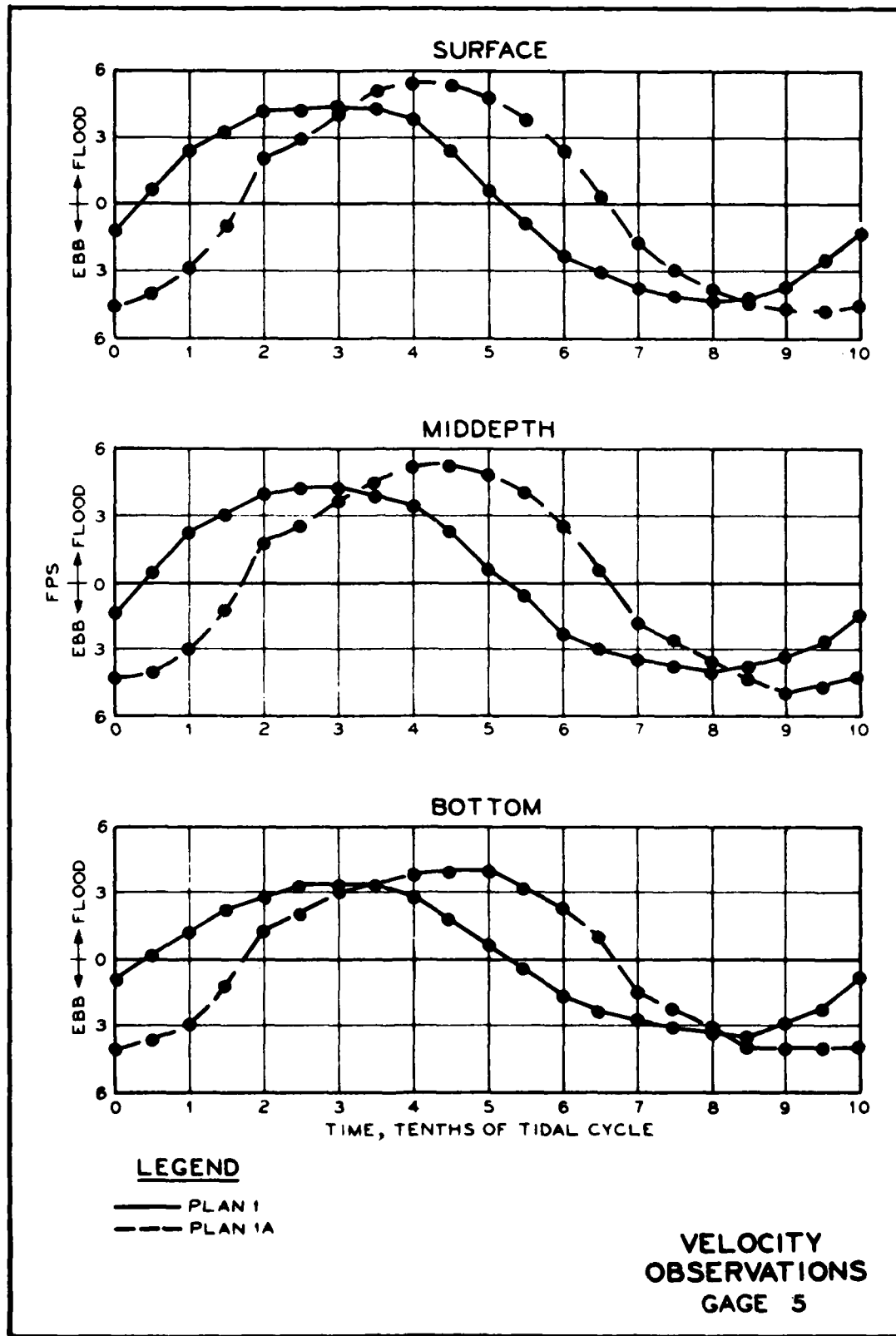


PLATE 4







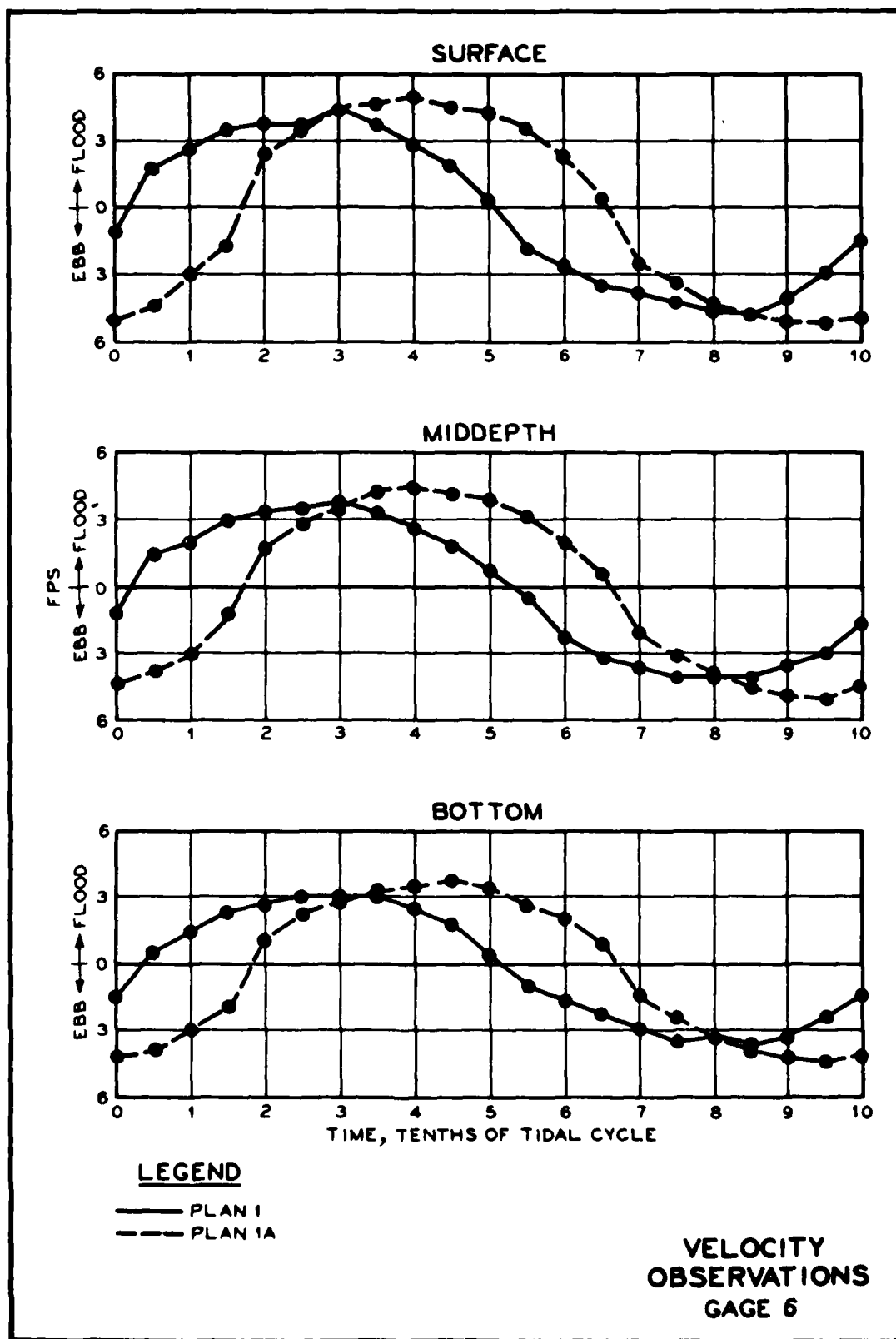
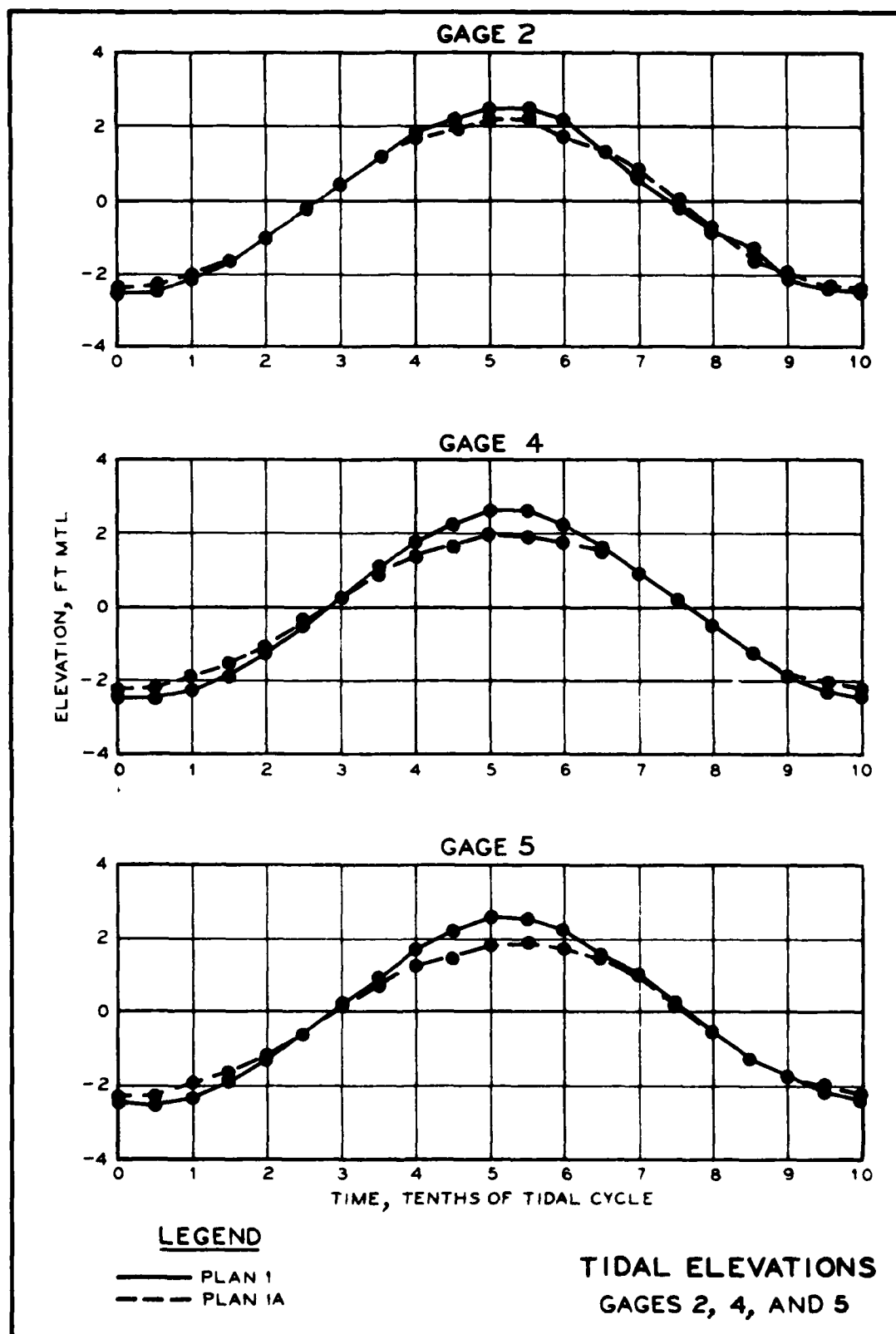
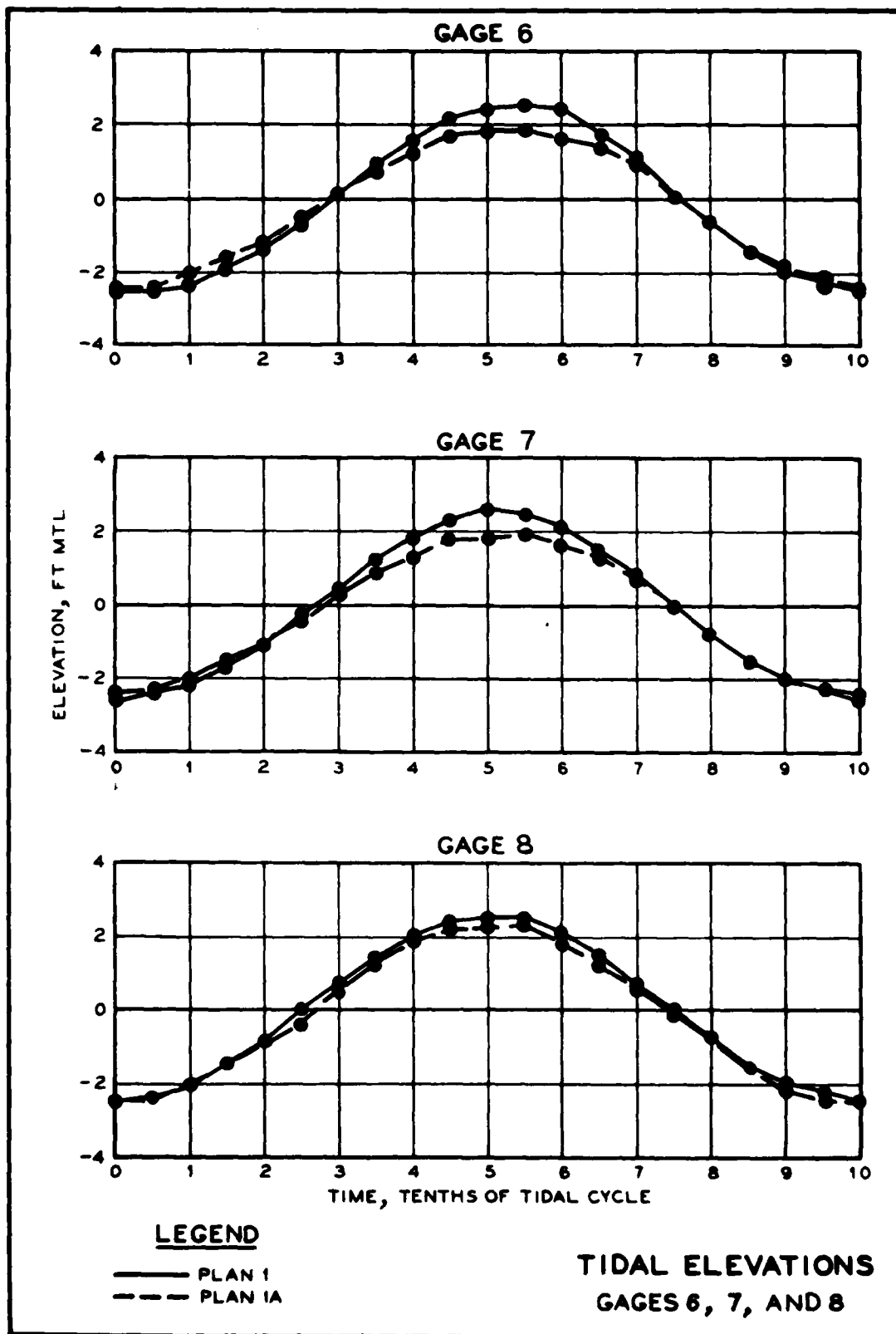


PLATE 8





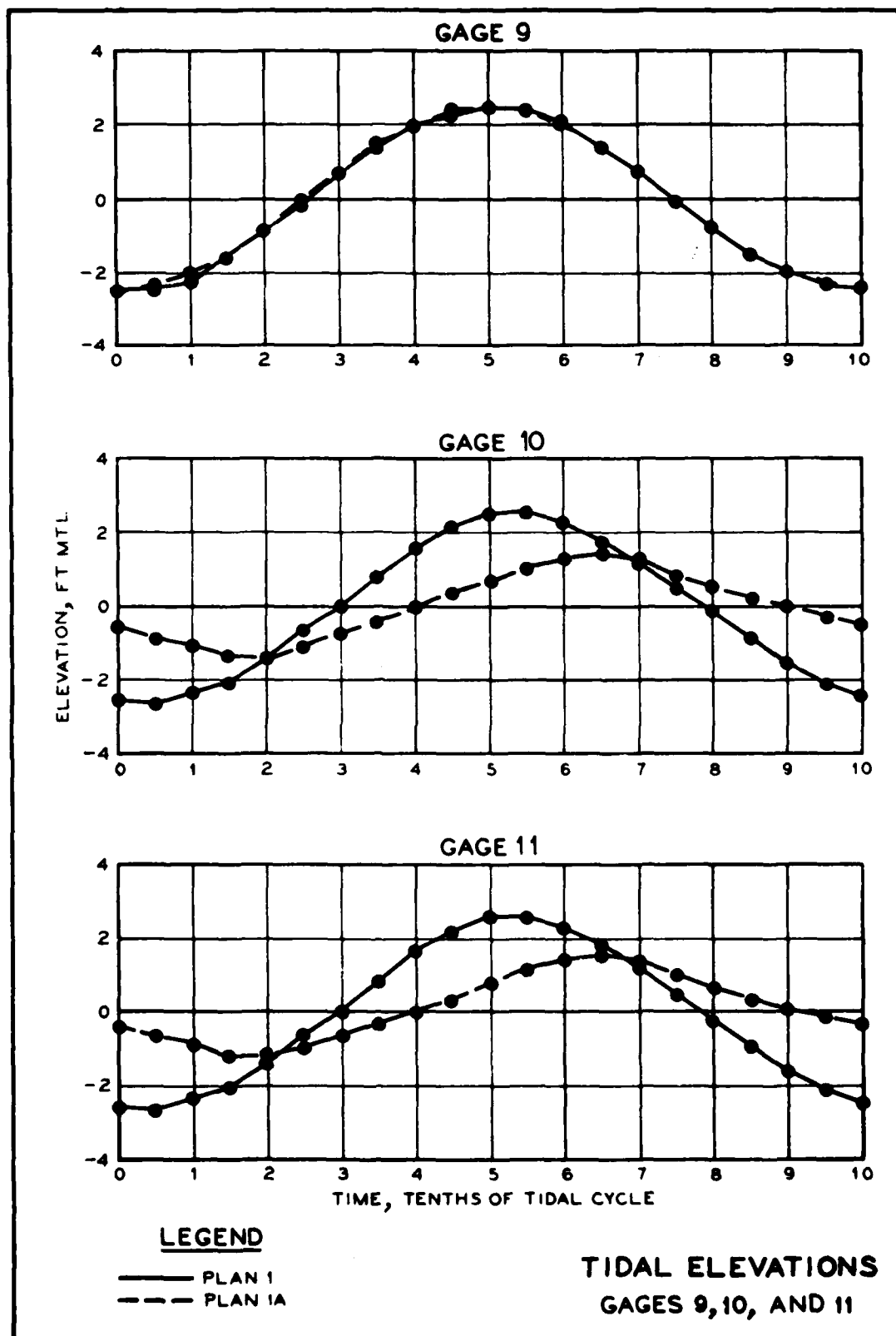
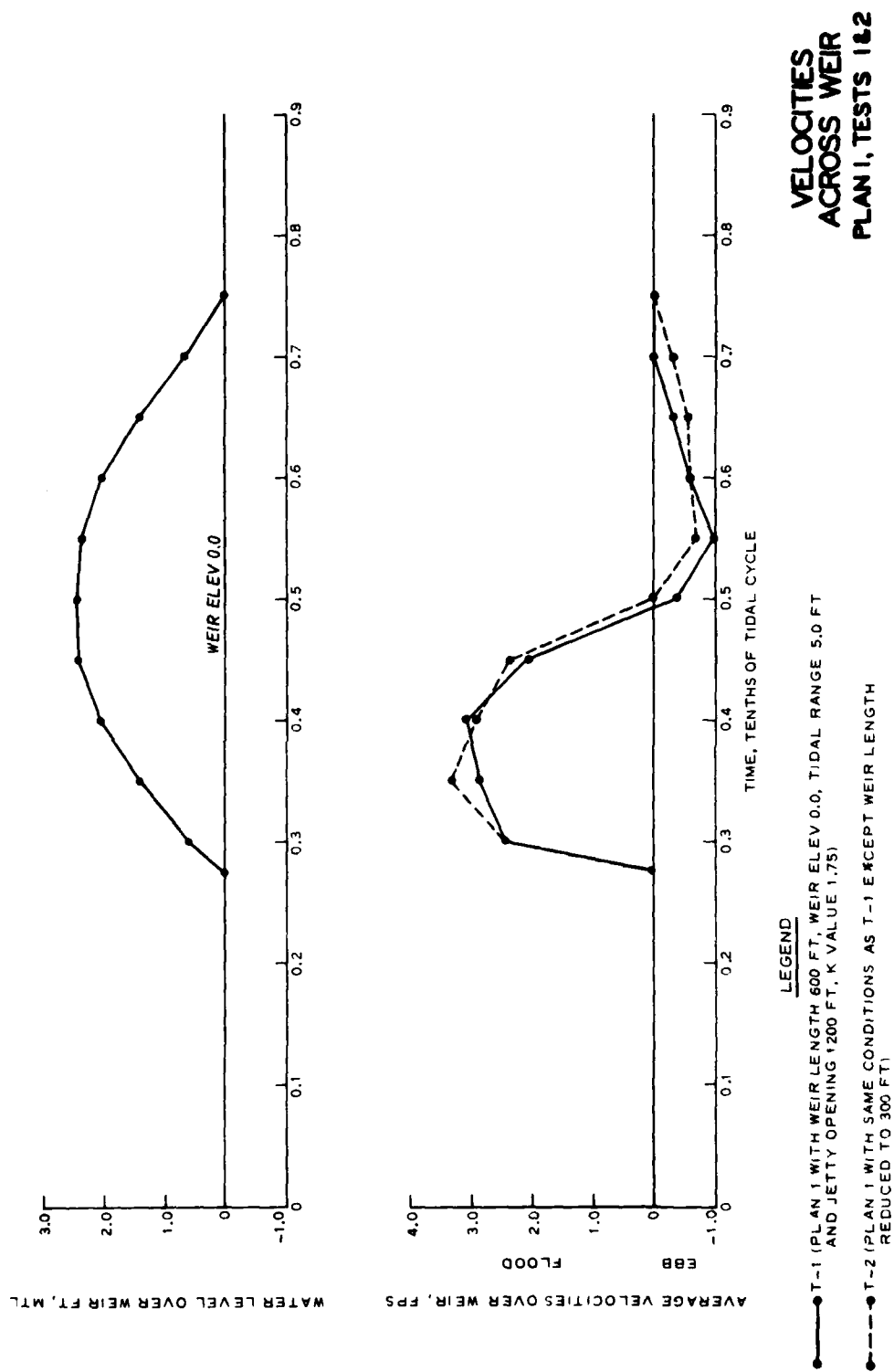


PLATE 12



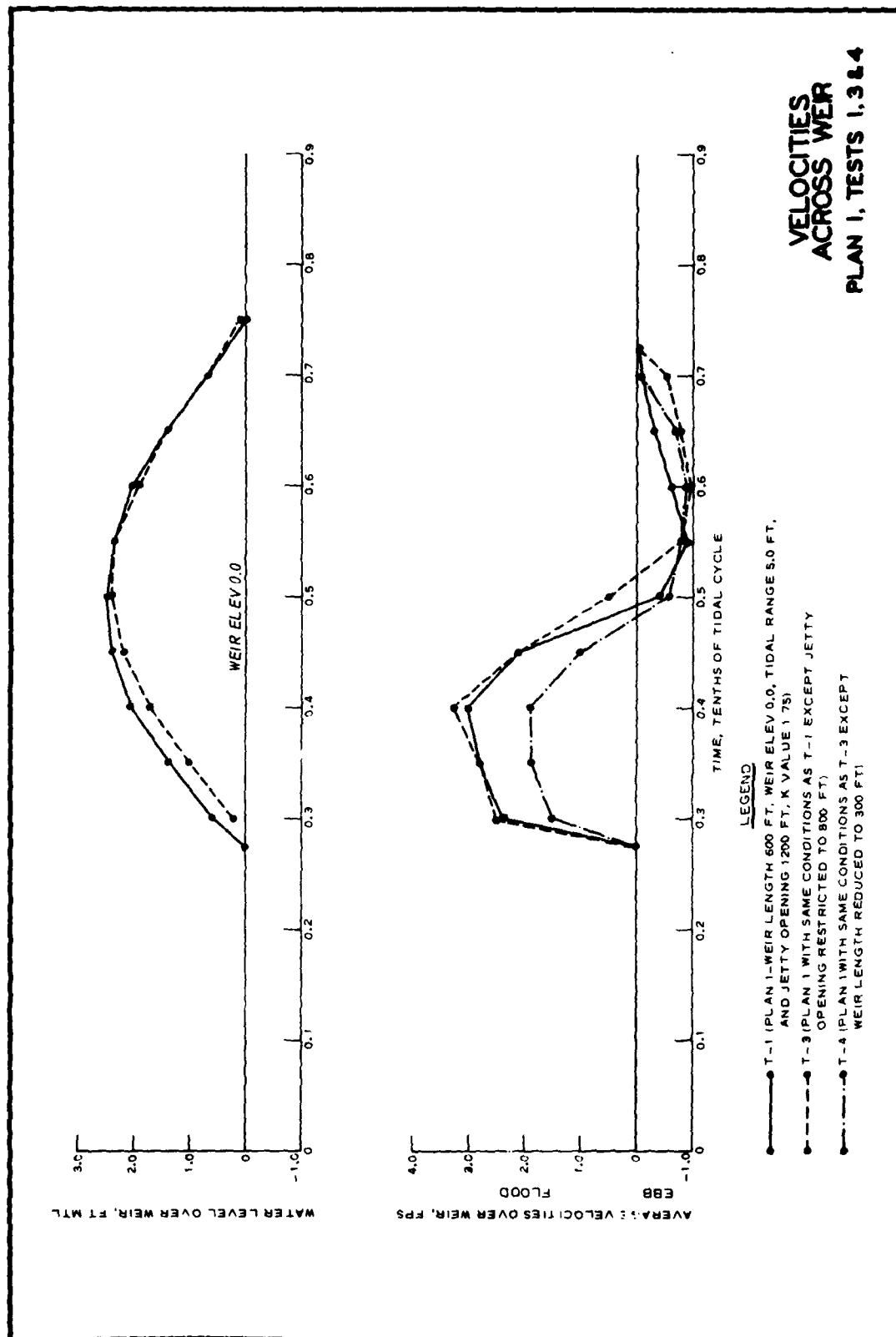
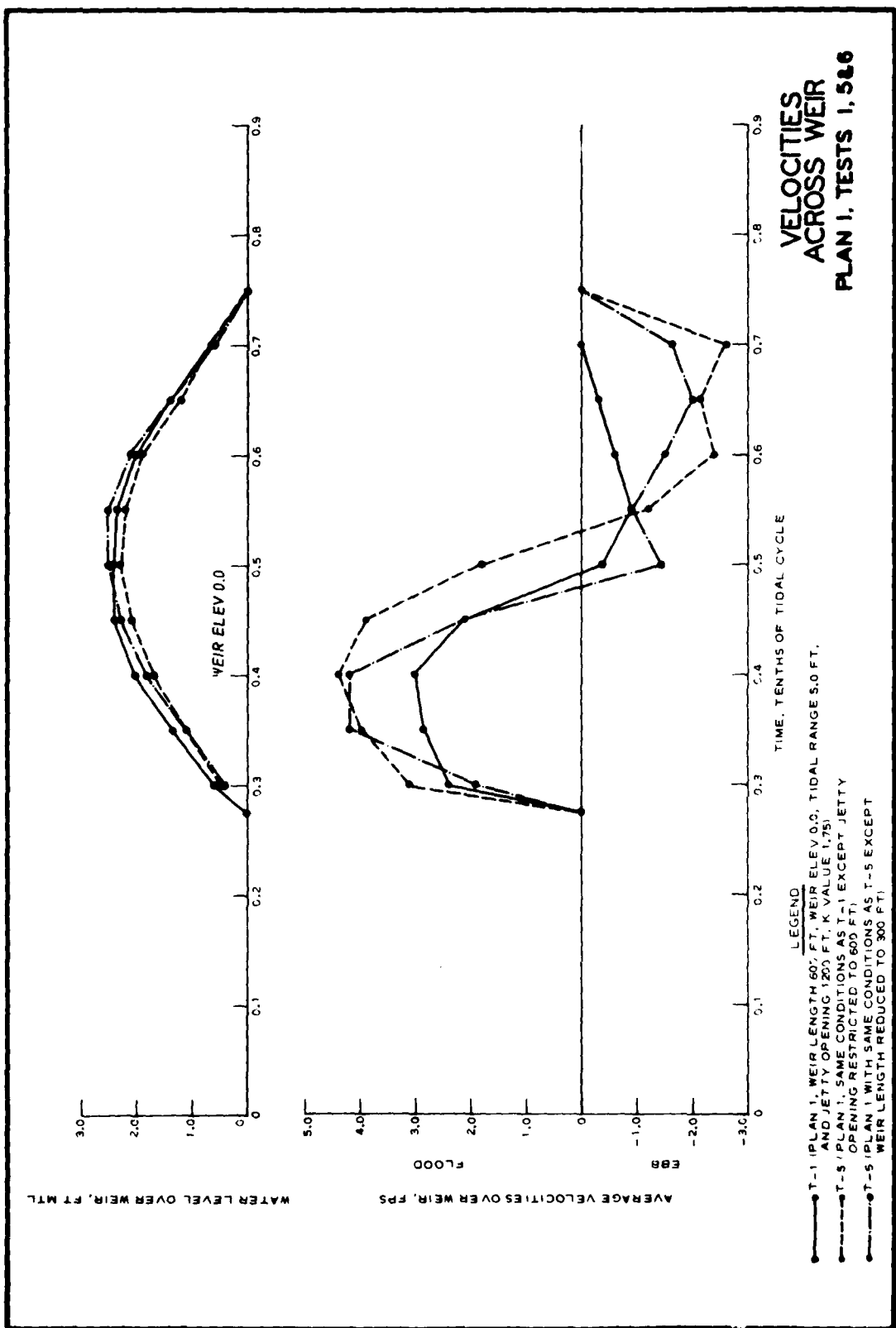
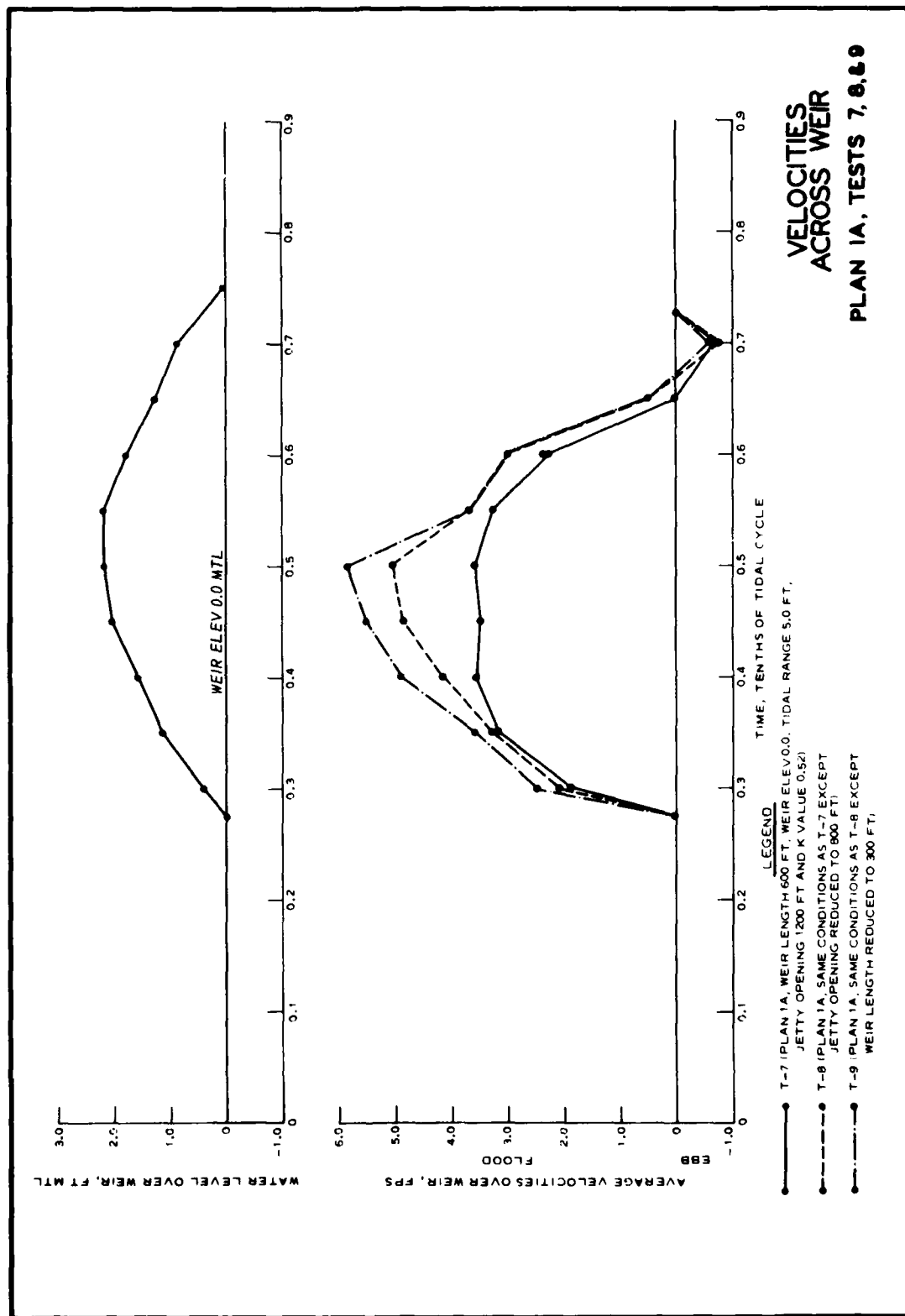


PLATE 14





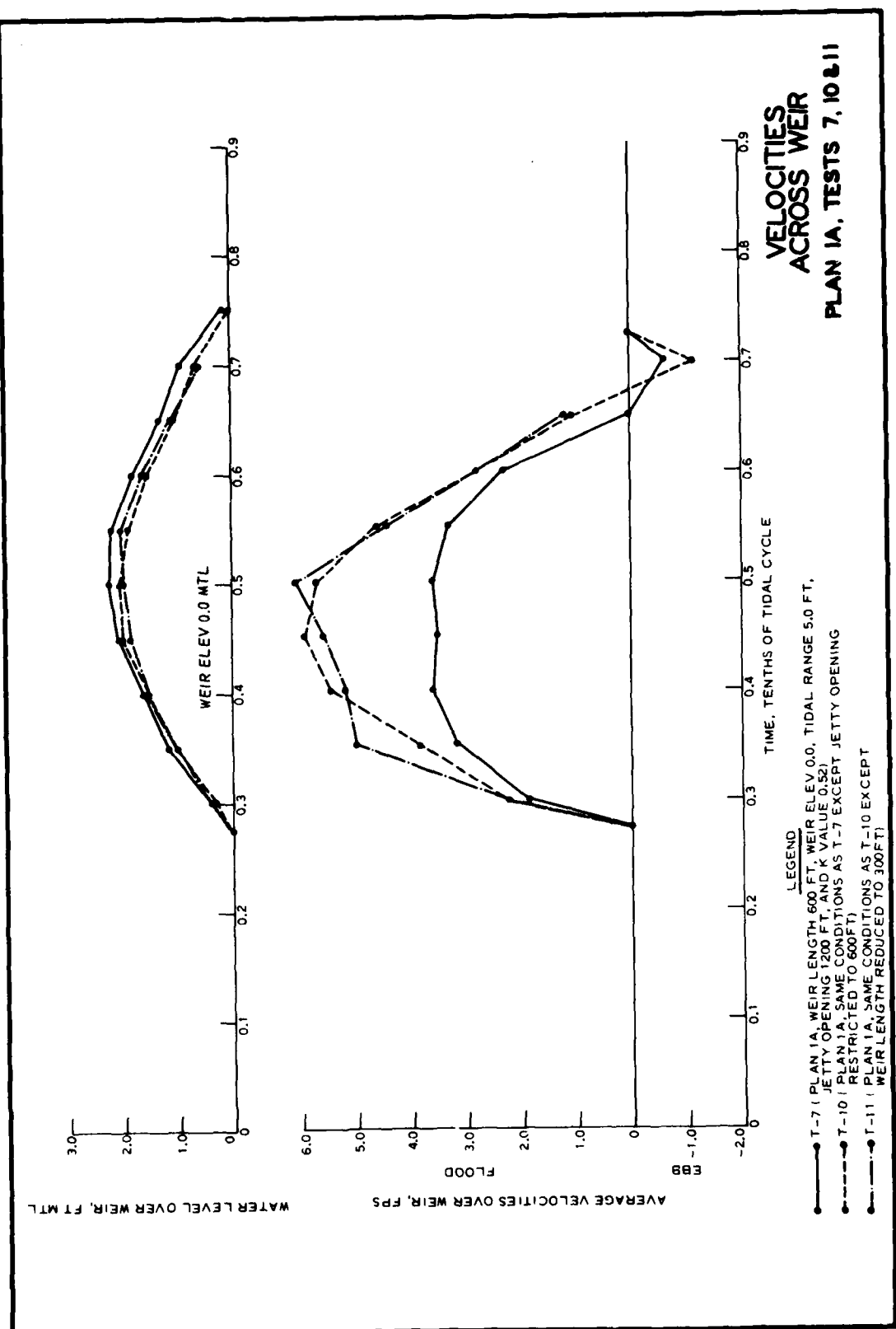
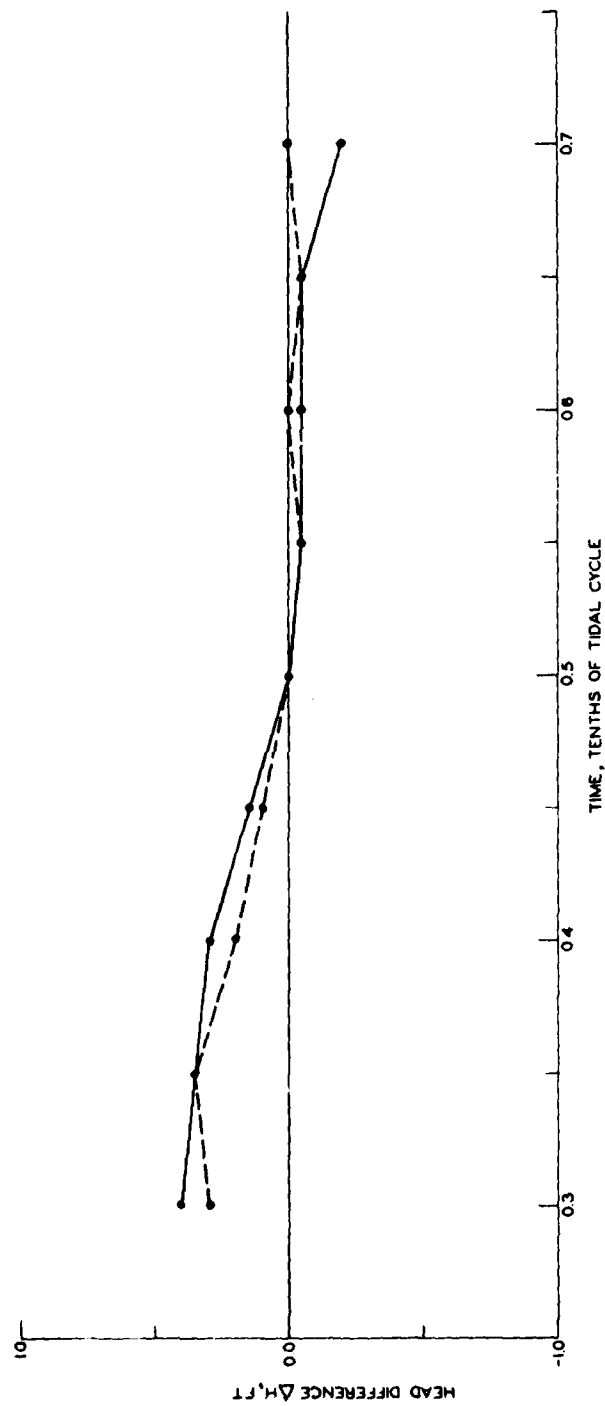


PLATE 16



LEGEND

- PLAN 1 (WEIR LENGTH 600 FT, WEIR ELEV 0.0 FT, JETTY OPENING 1200 FT, TIDAL RANGE 5 FT, K VALUE 175)
- PLAN 2 (SAME CONDITIONS AS PLAN 1)

NOTE. TIDE ELEVATIONS MEASURED 100 FT OCEANWARD AND BAYWARD OF WEIR

HEAD DIFFERENCES ACROSS WEIR PLANS 1 AND 2

AD-A129 508

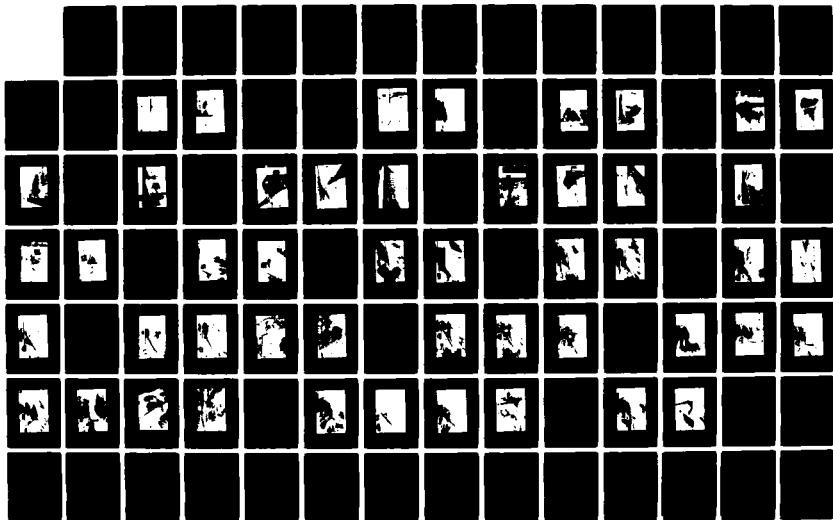
WEIR JETTY PERFORMANCE: HYDRAULIC AND SEDIMENTARY
CONSIDERATIONS(U) ARMY ENGINEER WATERWAYS EXPERIMENT
STATION VICKSBURG MS HYDRAULICS LAB W C SEABERGH
MAR 83 WES/TR/HL-83-5

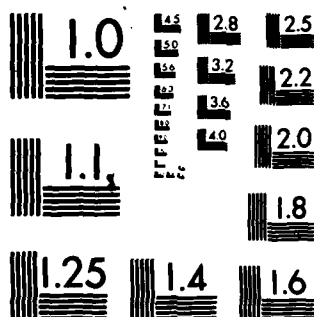
3/4

UNCLASSIFIED

F/G 13/2

NL





MICROCOPY RESOLUTION TEST CHART
NATIONAL BUREAU OF STANDARDS-1963-A

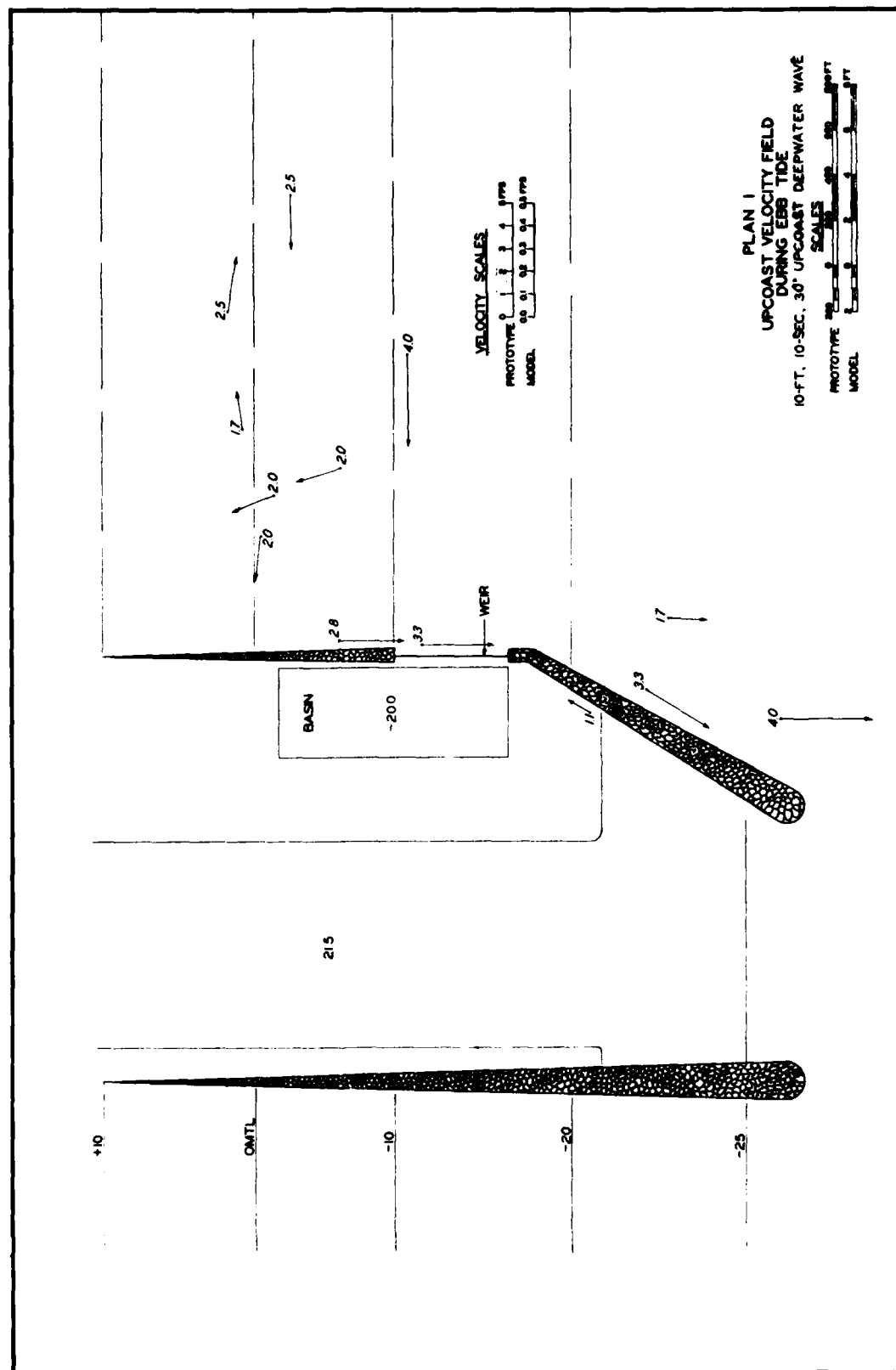


PLATE 20

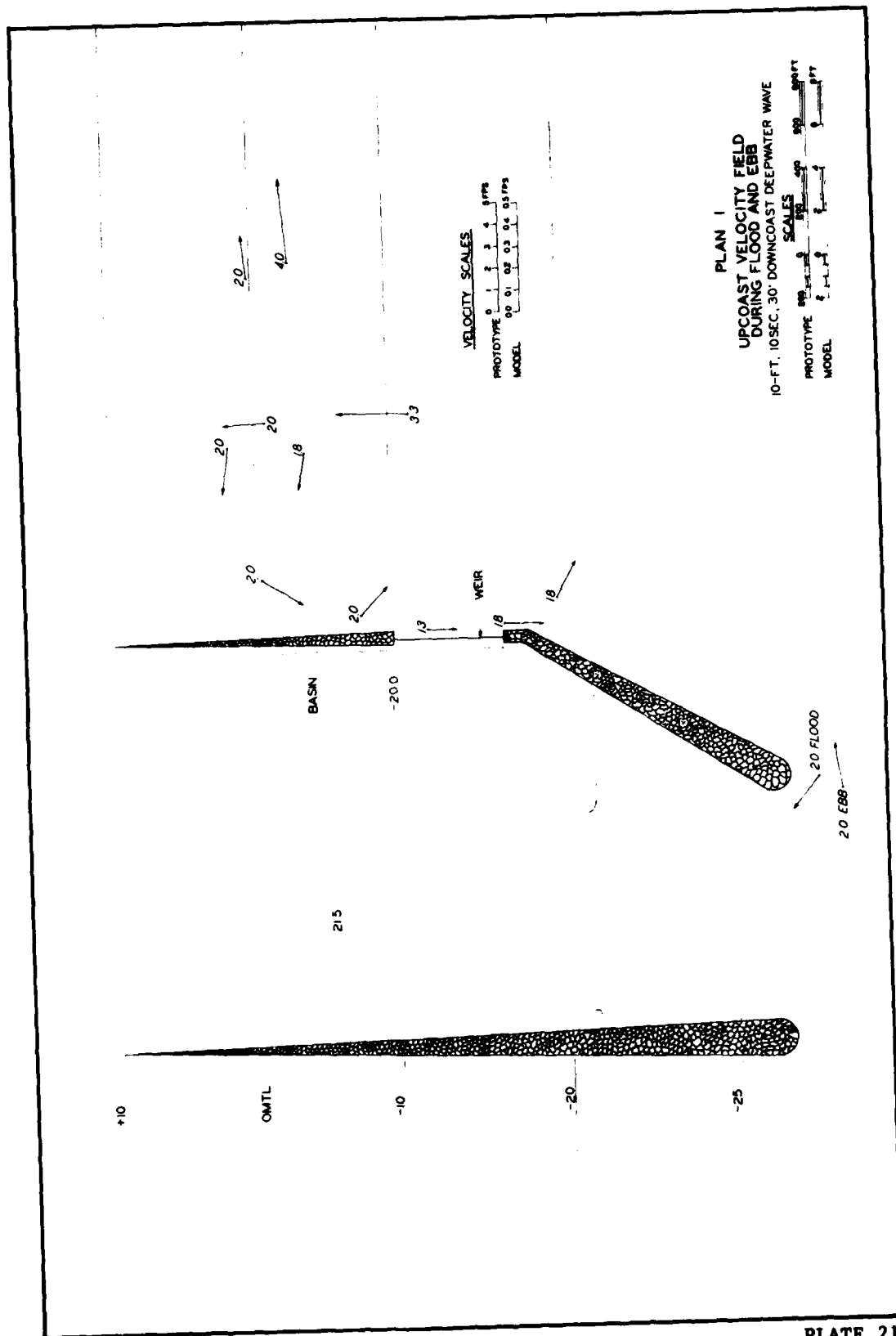
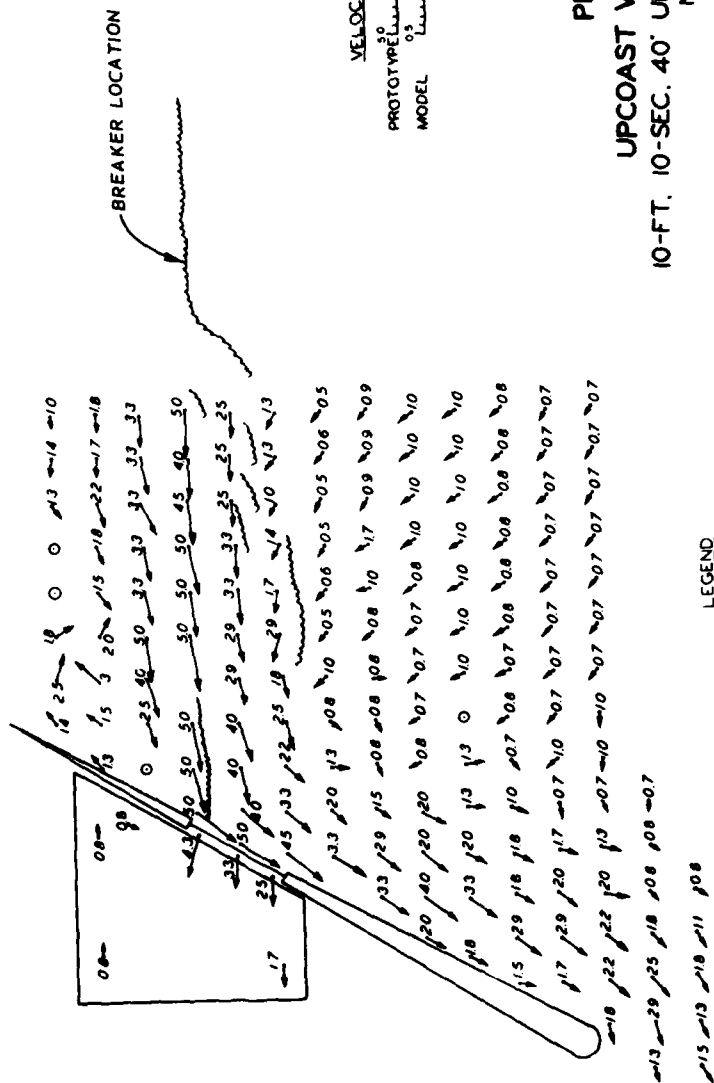
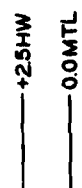


PLATE 21

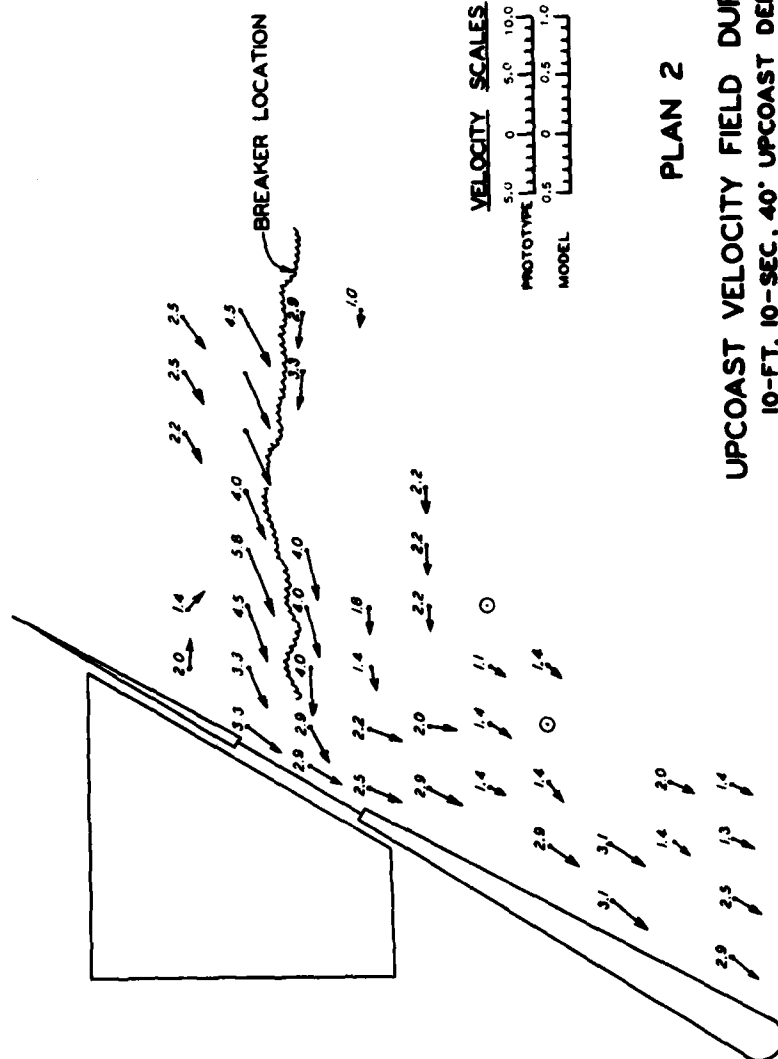




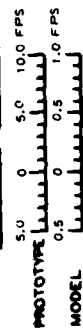


-10.0

-20.0



VELOCITY SCALES



SCALES



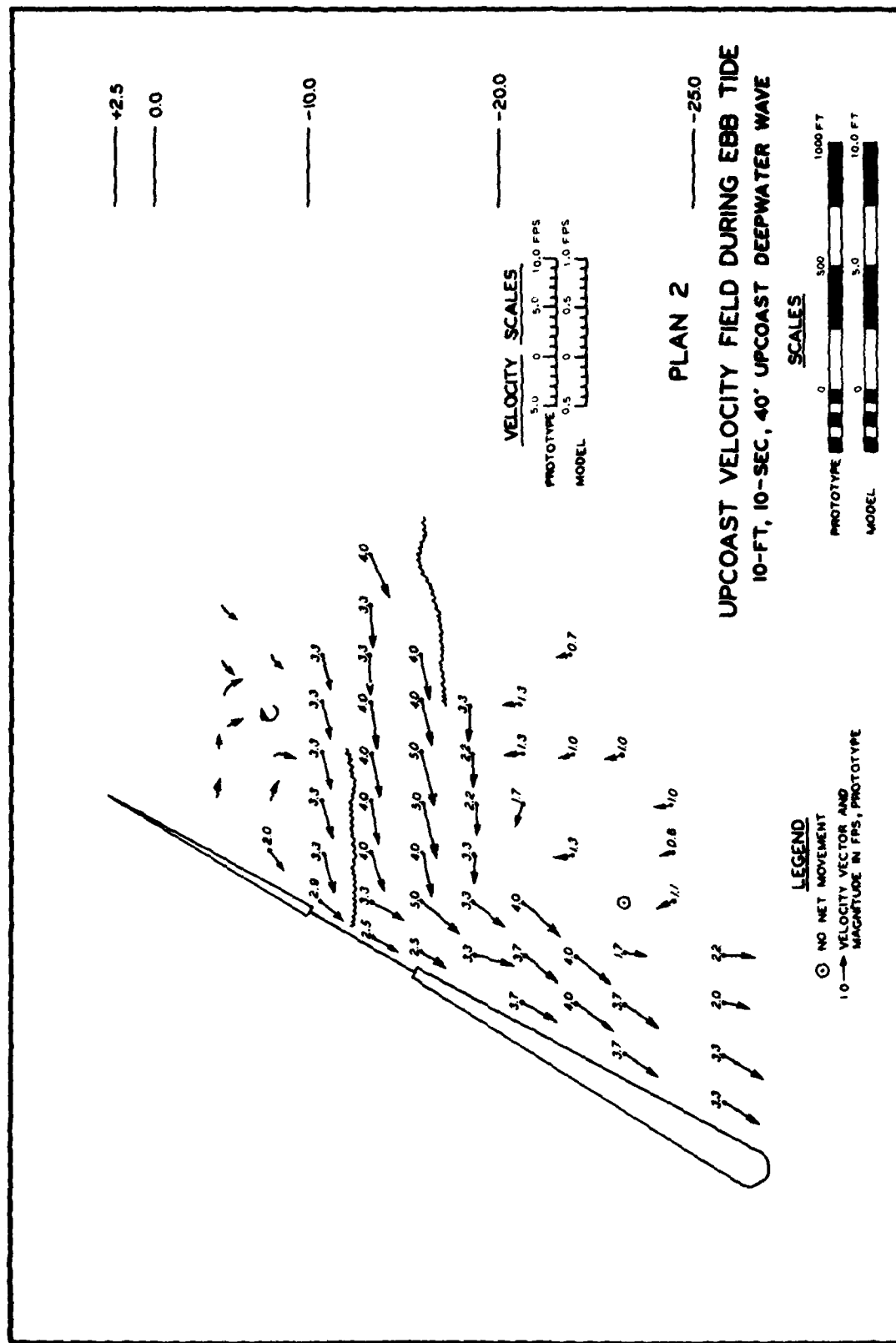
LEGEND

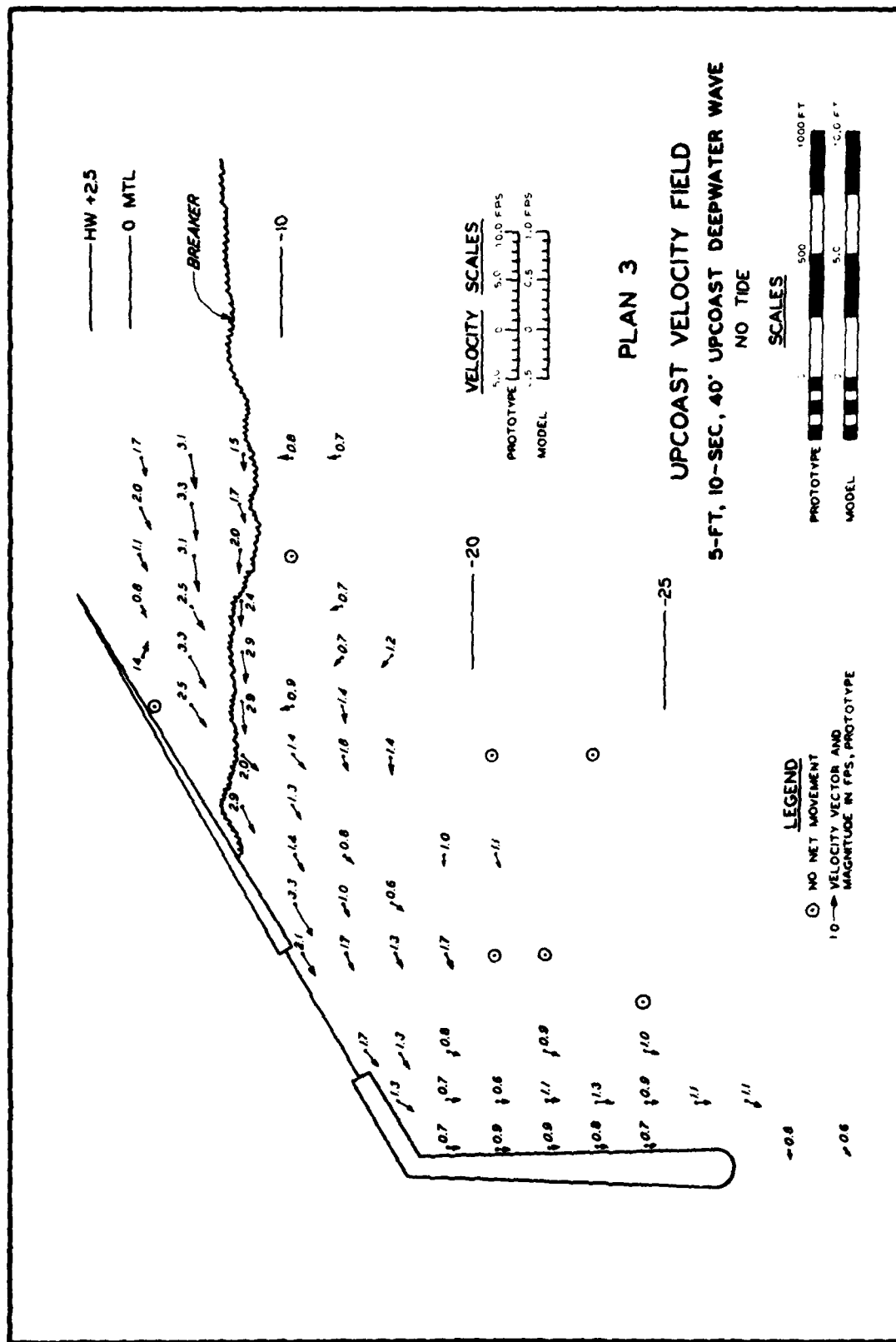
- ① NO NET MOVEMENT
10 → VELOCITY VECTOR AND
MAGNITUDE IN FPS, PROTOTYPE

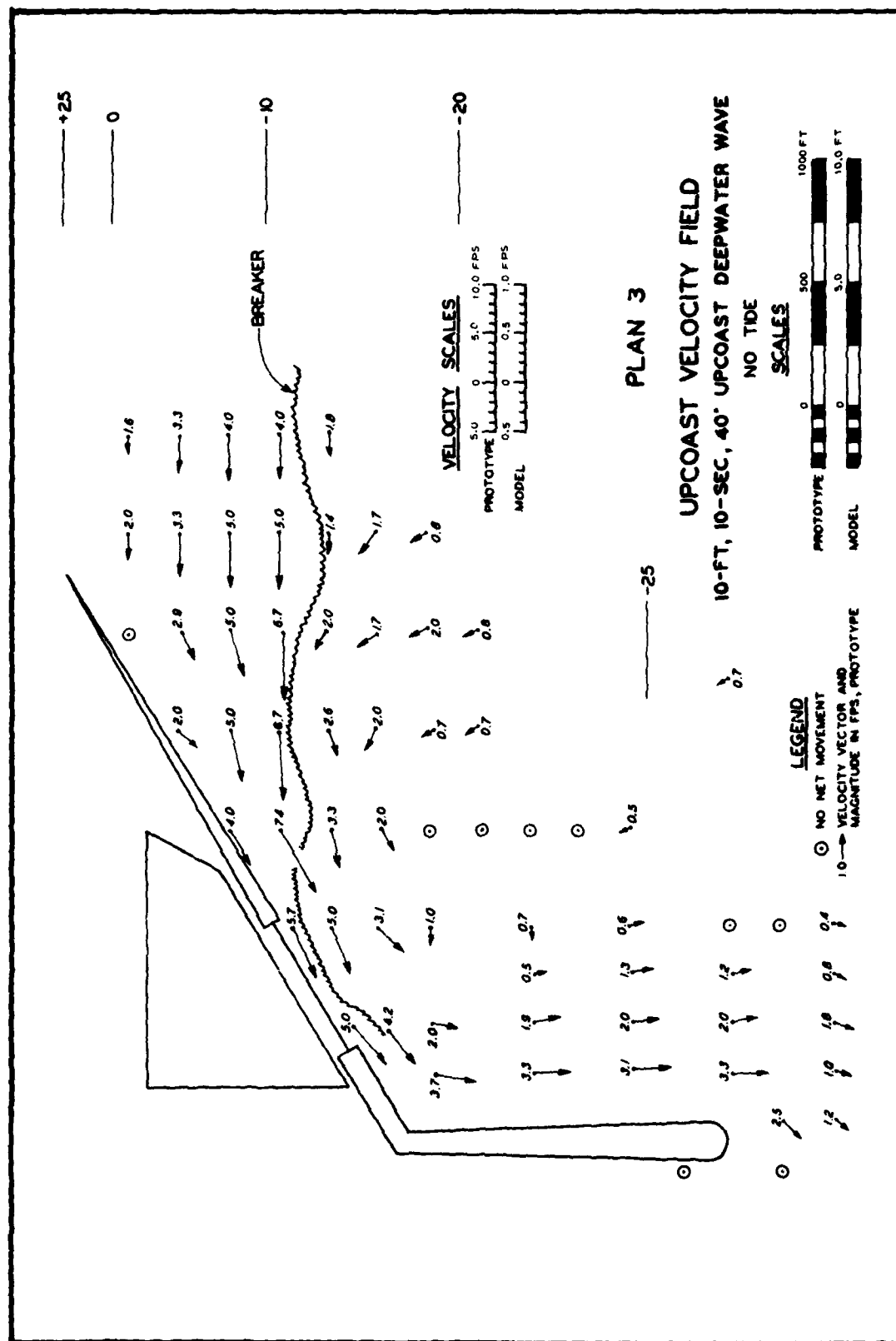
PLAN 2

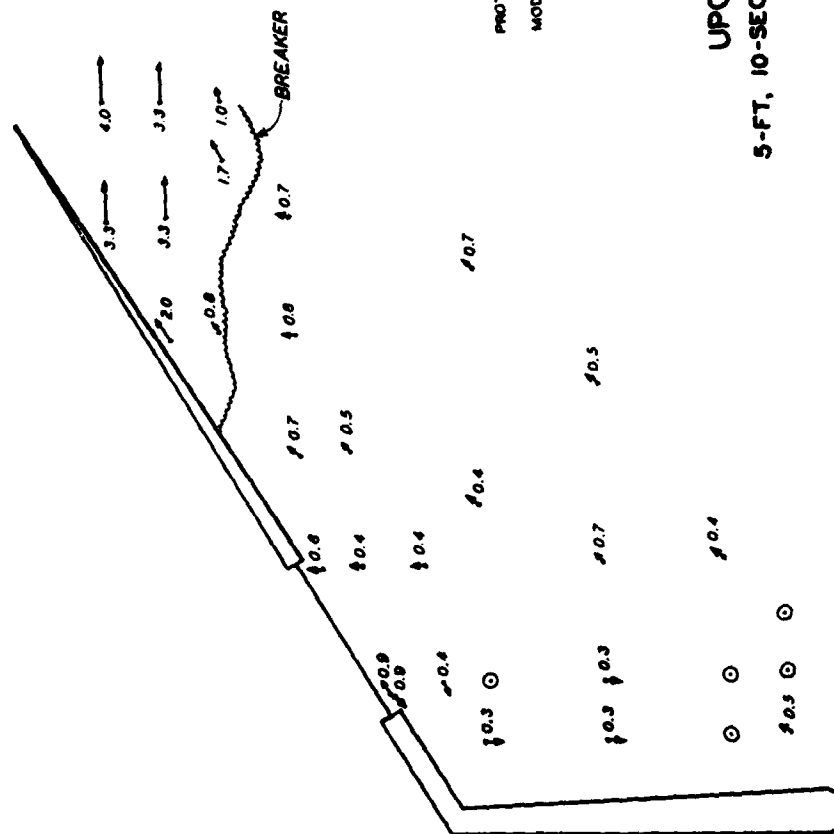
UPCOAST VELOCITY FIELD DURING FLOOD TIDE
10-FT, 10-SEC, 40' UPCOAST DEEPWATER WAVE

_____ -25.0

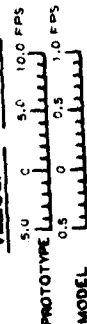








VELOCITY SCALES



PLAN 3

UPCOAST VELOCITY FIELD 5-FT, 10-SEC, 30' DOWNCOAST DEEPWATER WAVE NO TIDE

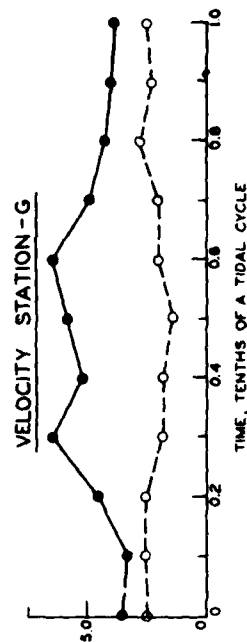
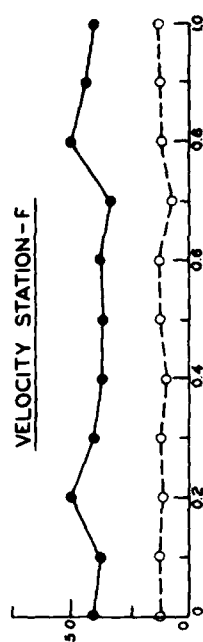
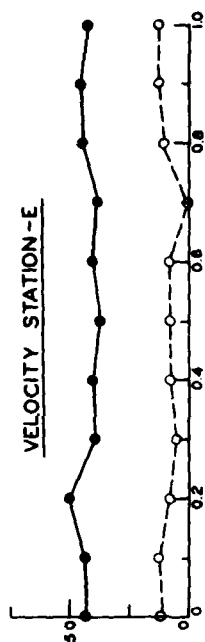
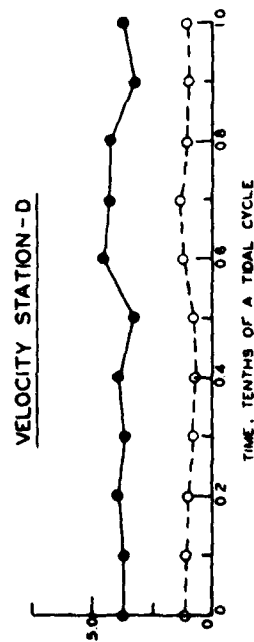
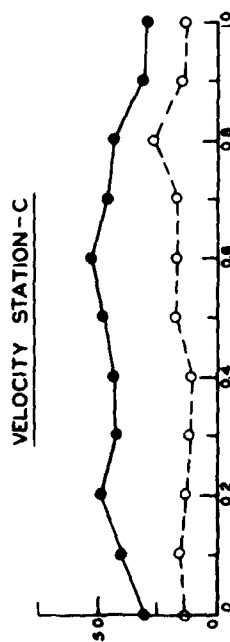
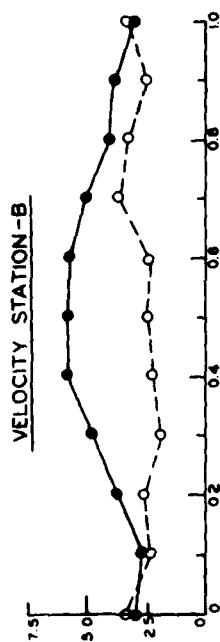
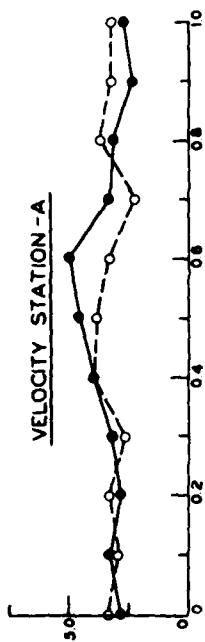
SCALES



LEGEND

- NO NET MOVEMENT
- VELOCITY VECTOR AND MAGNITUDE IN FPS, PROTOTYPE



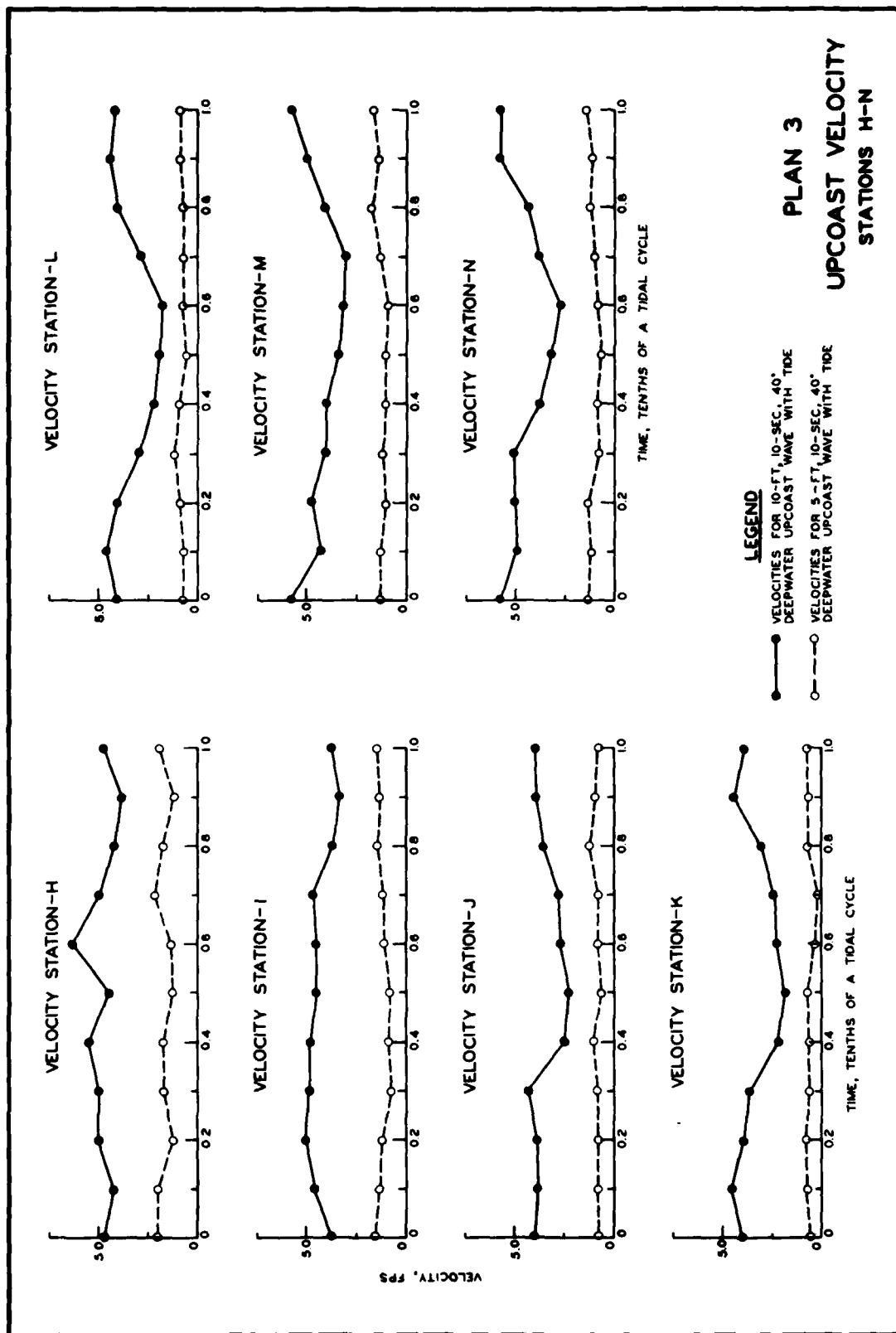


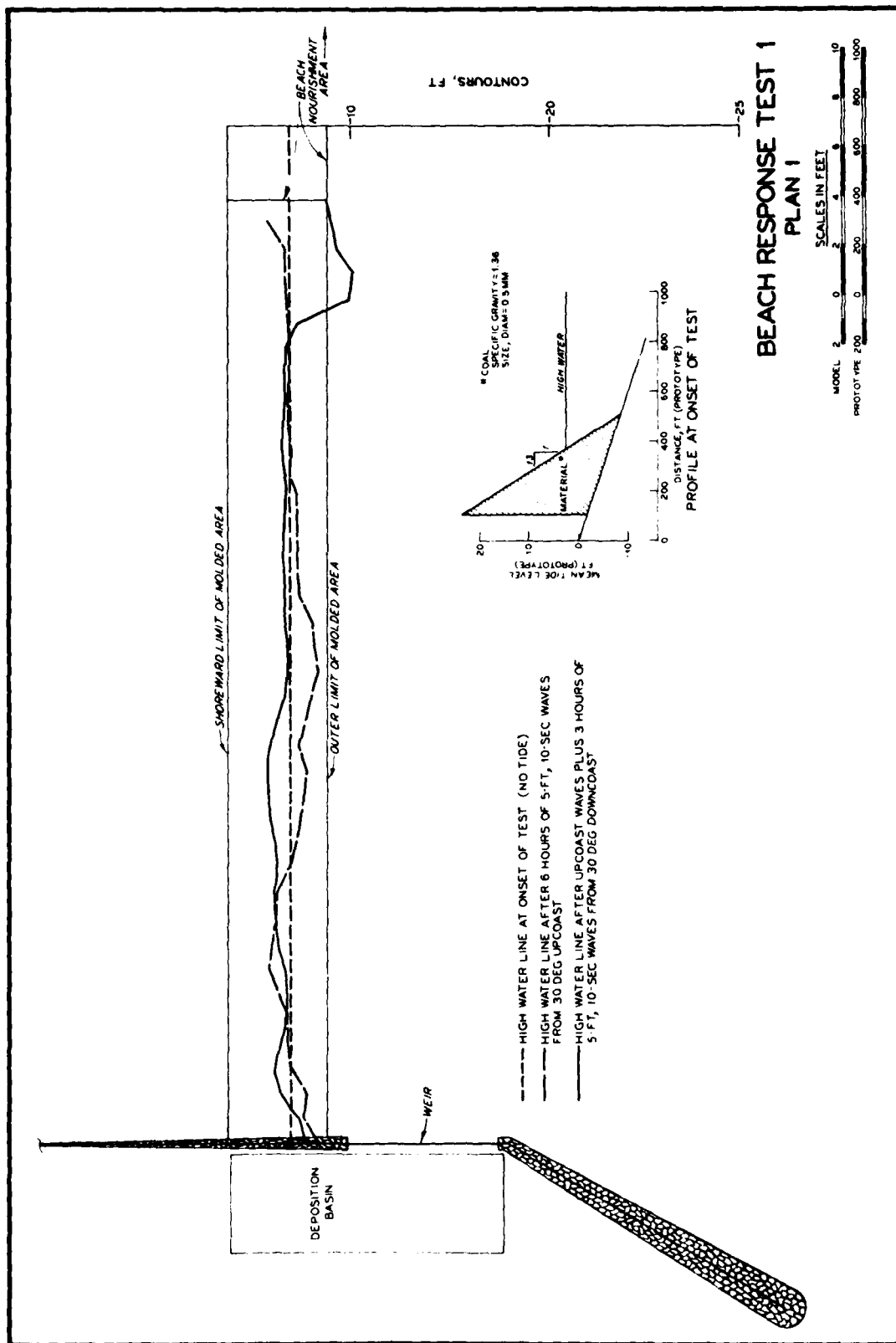
LEGEND

—●— VELOCITIES FOR 10-FT. 10-SEC. 40° DEEPWATER UPCAST WAVE WITH TIDE

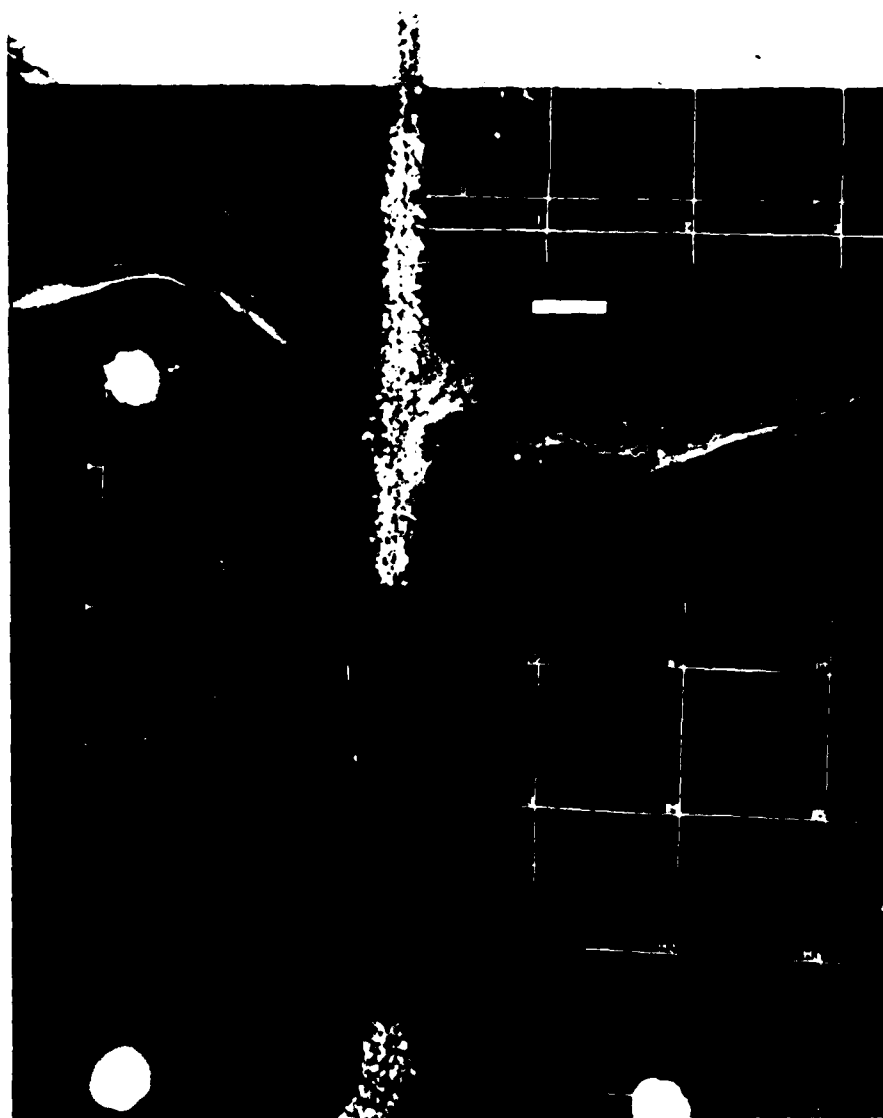
- - -○- - - VELOCITIES FOR 5-FT. 10-SEC. 40° DEEPWATER UPCAST WAVE WITH TIDE

PLAN 3
UPCAST VELOCITY
STATIONS A-G





BEACH RESPONSE TEST 1 PLAN 1



BEACH RESPONSE TEST 1
PLAN 1
HOUR 6



BEACH RESPONSE TEST 1
PLAN 1
HOUR 9

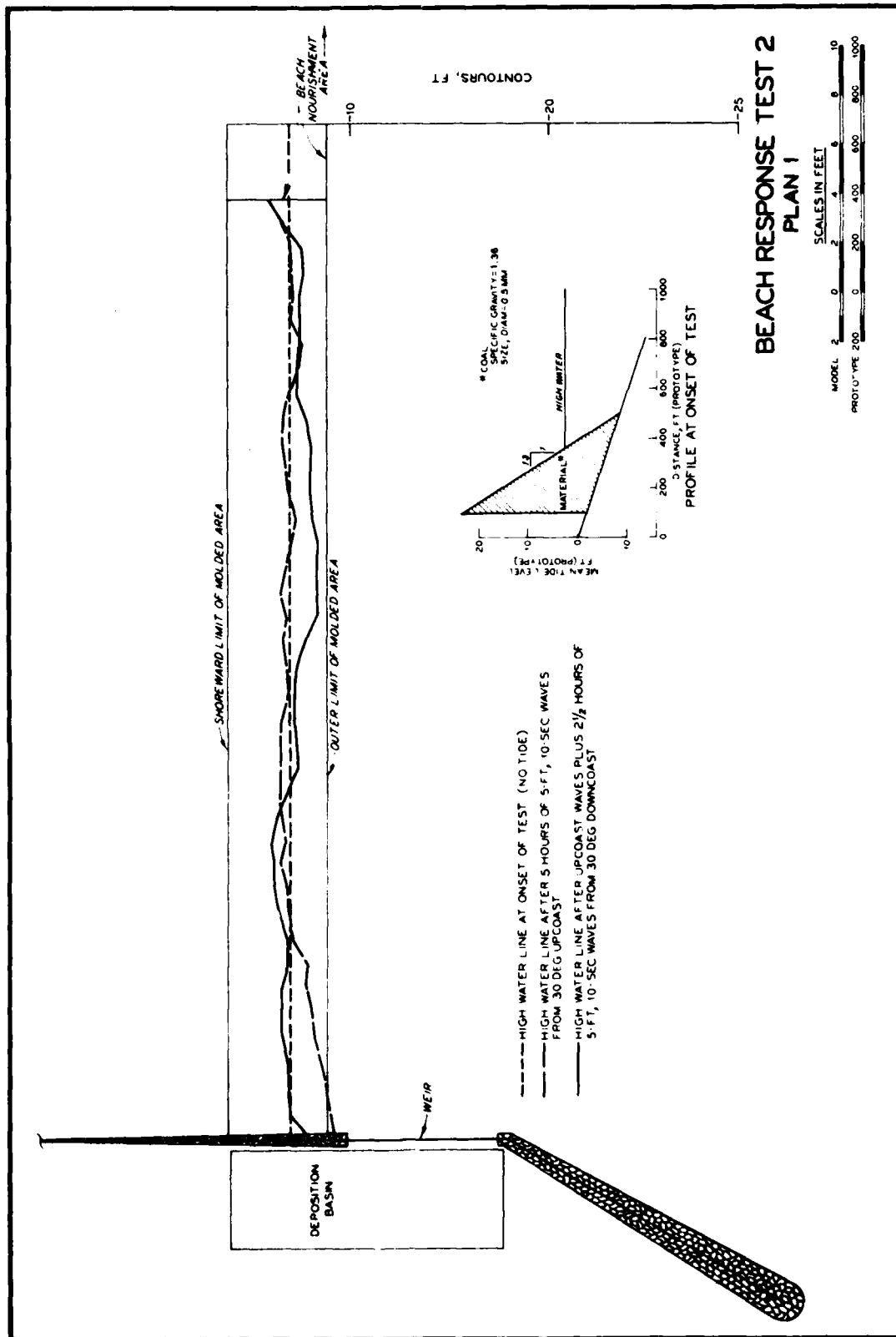
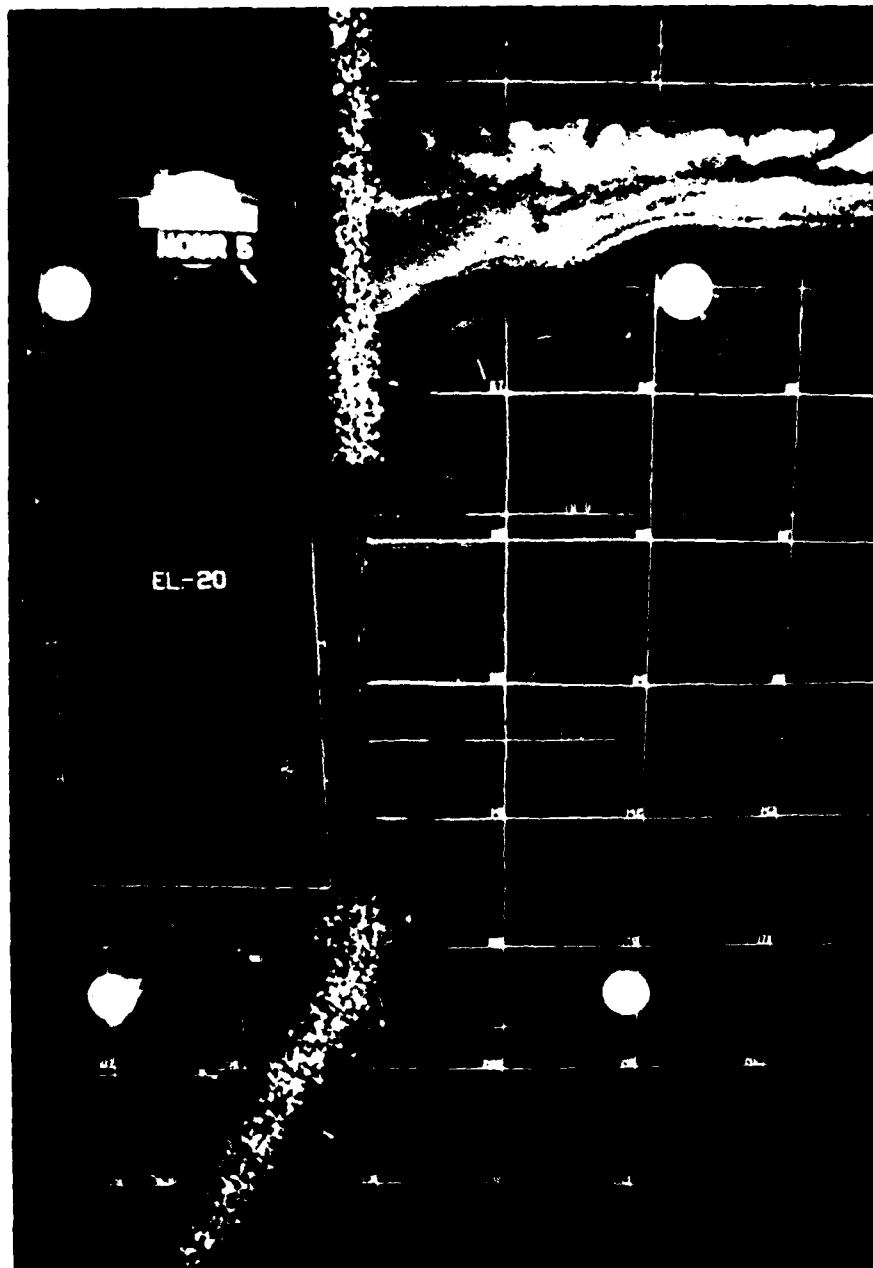
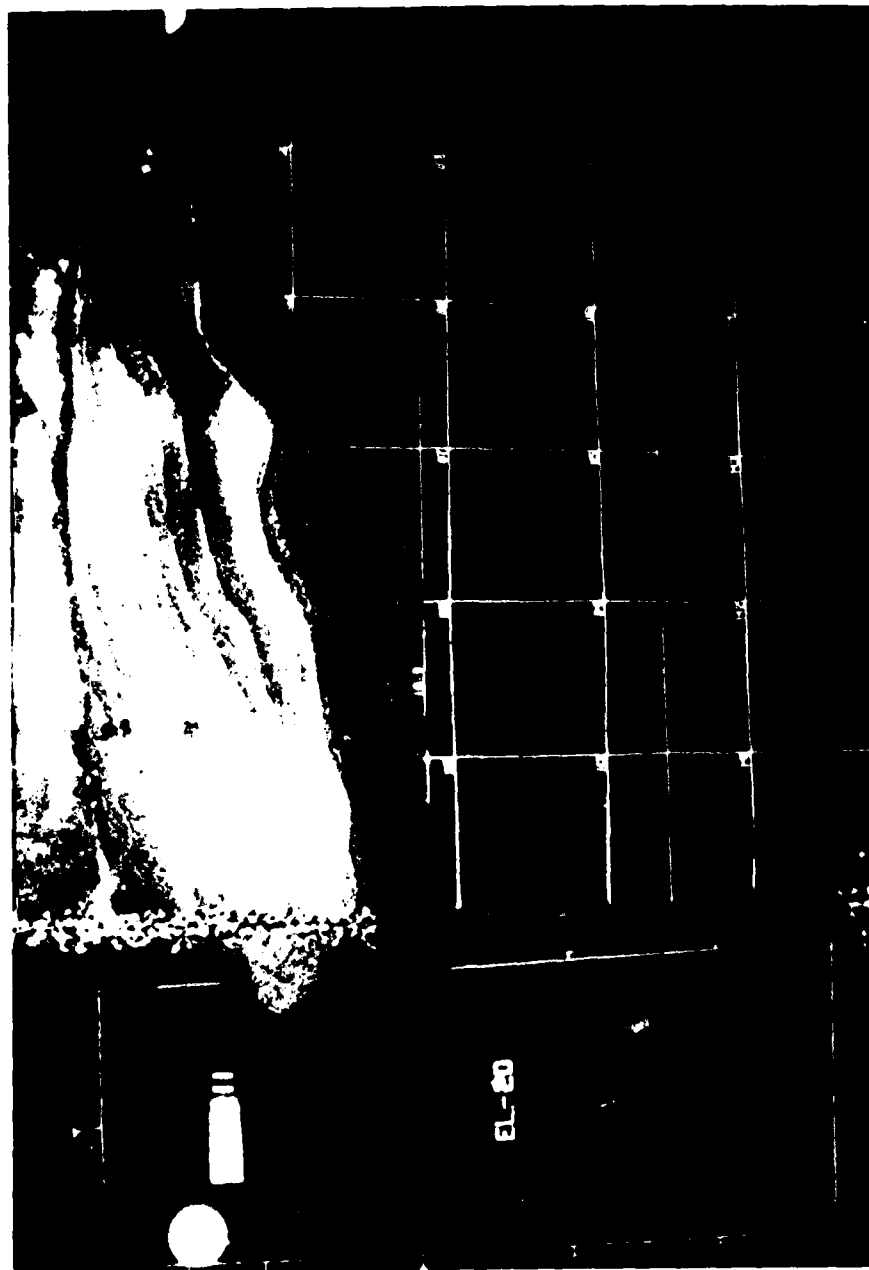


PLATE 36



BEACH RESPONSE TEST 3
PLAN 1
HOUR 5



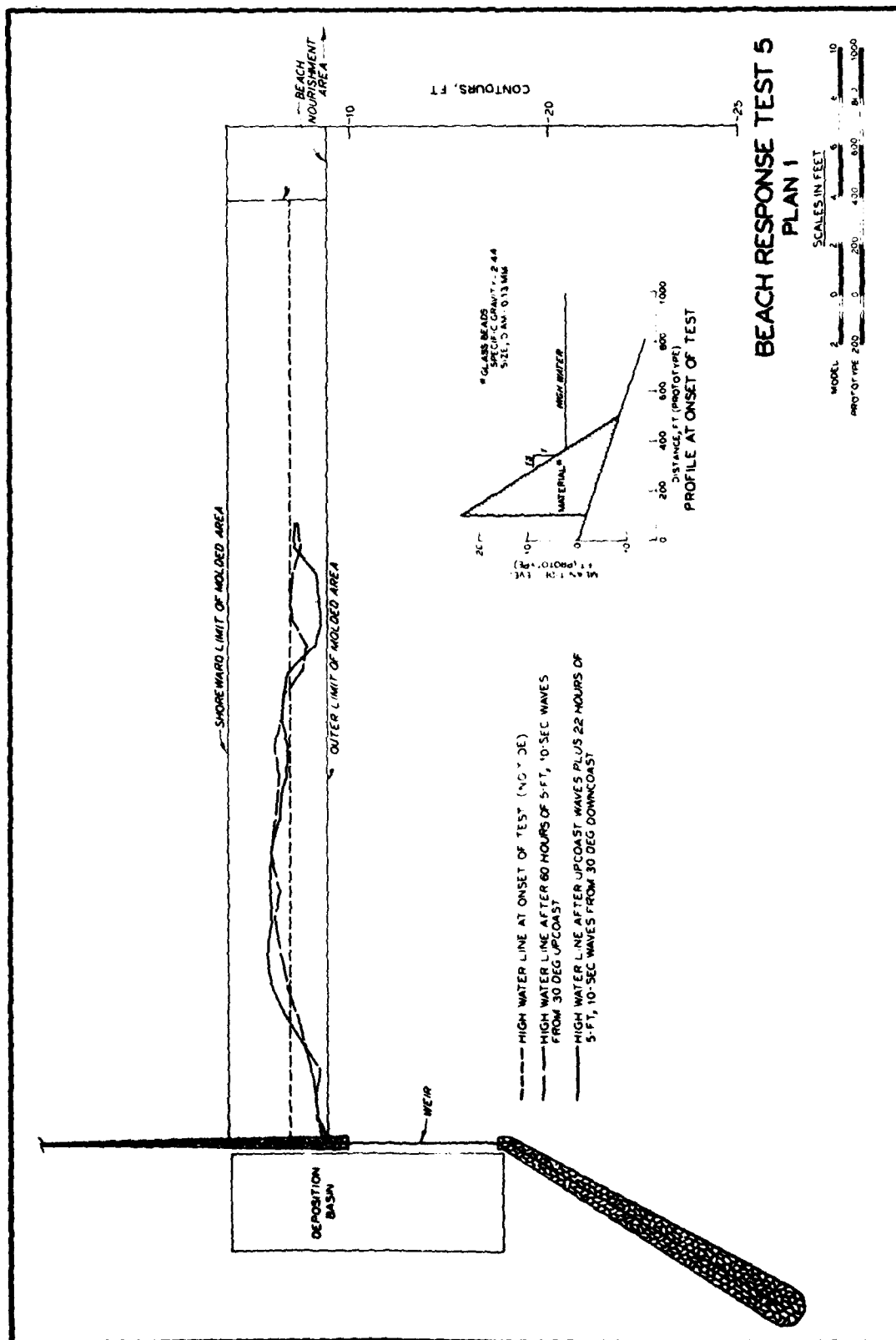
BEACH RESPONSE TEST 3
PLAN 1
HOUR 1

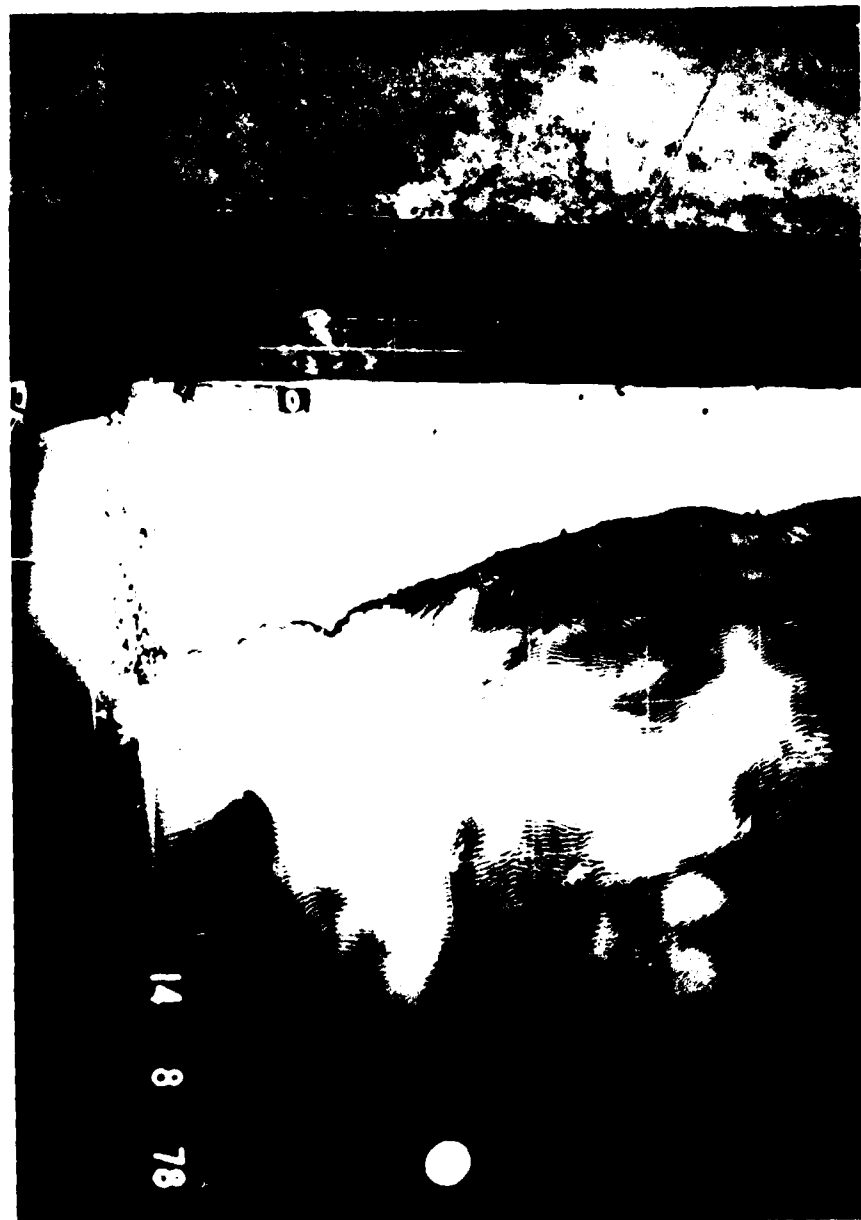


BEACH RESPONSE TEST 4
PLAN 1
HOUR 50

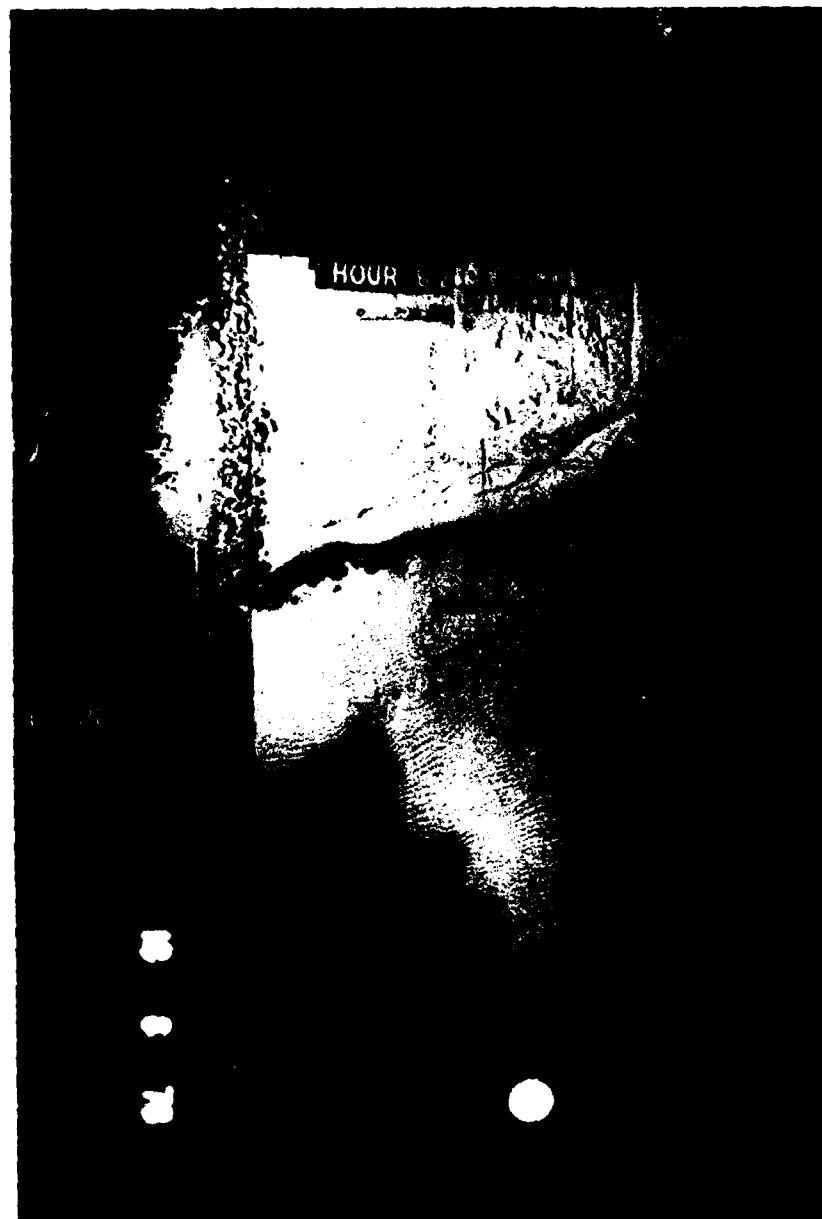


BEACH RESPONSE TEST 4
PLAN 1
HOUR 72





BEACH RESPONSE TEST 5
PLAN 1
HOUR 60



BEACH RESPONSE TEST 5
PLAN 1
HOUR 82



BEACH RESPONSE TEST 5
PLAN 1
HOUR 82

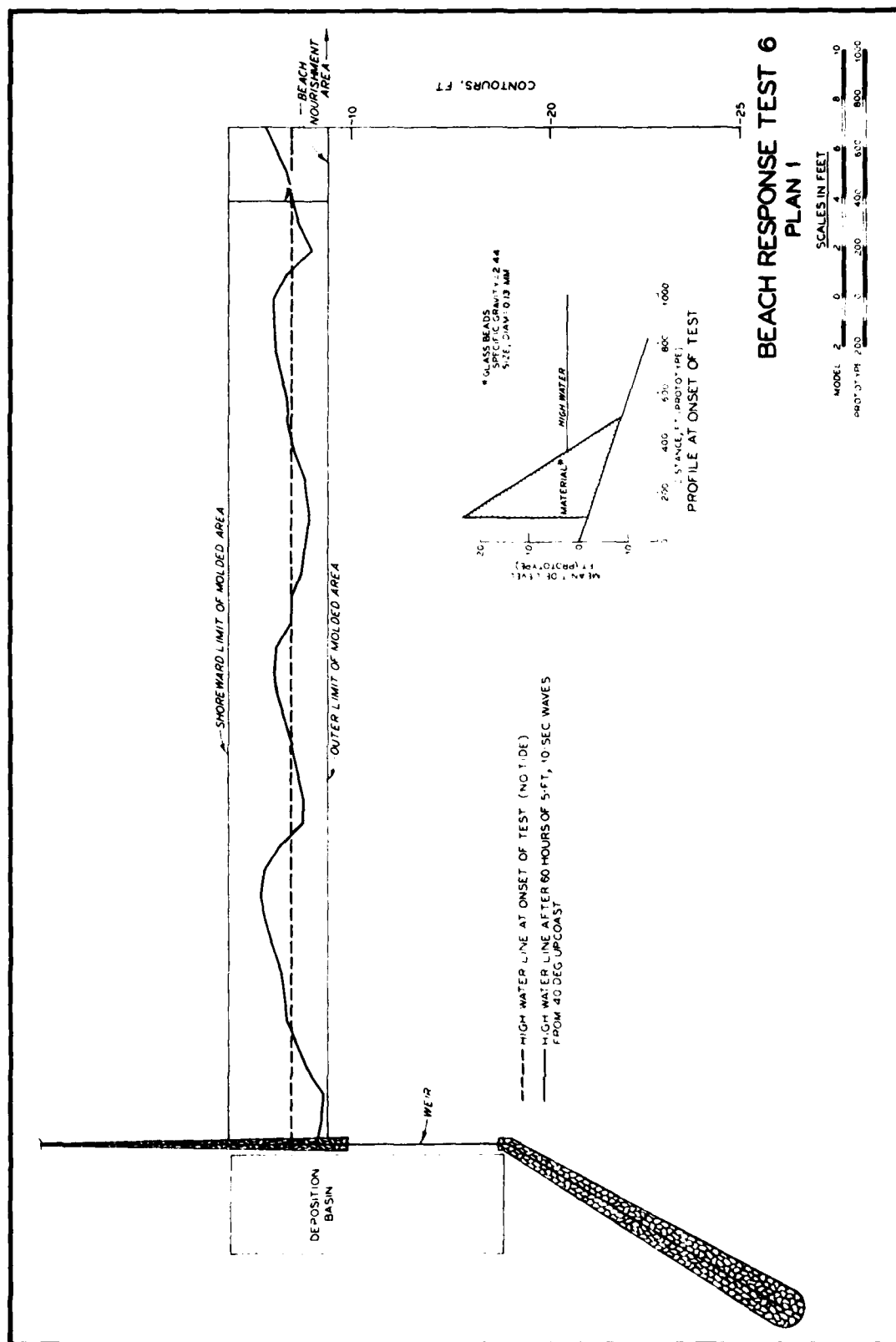
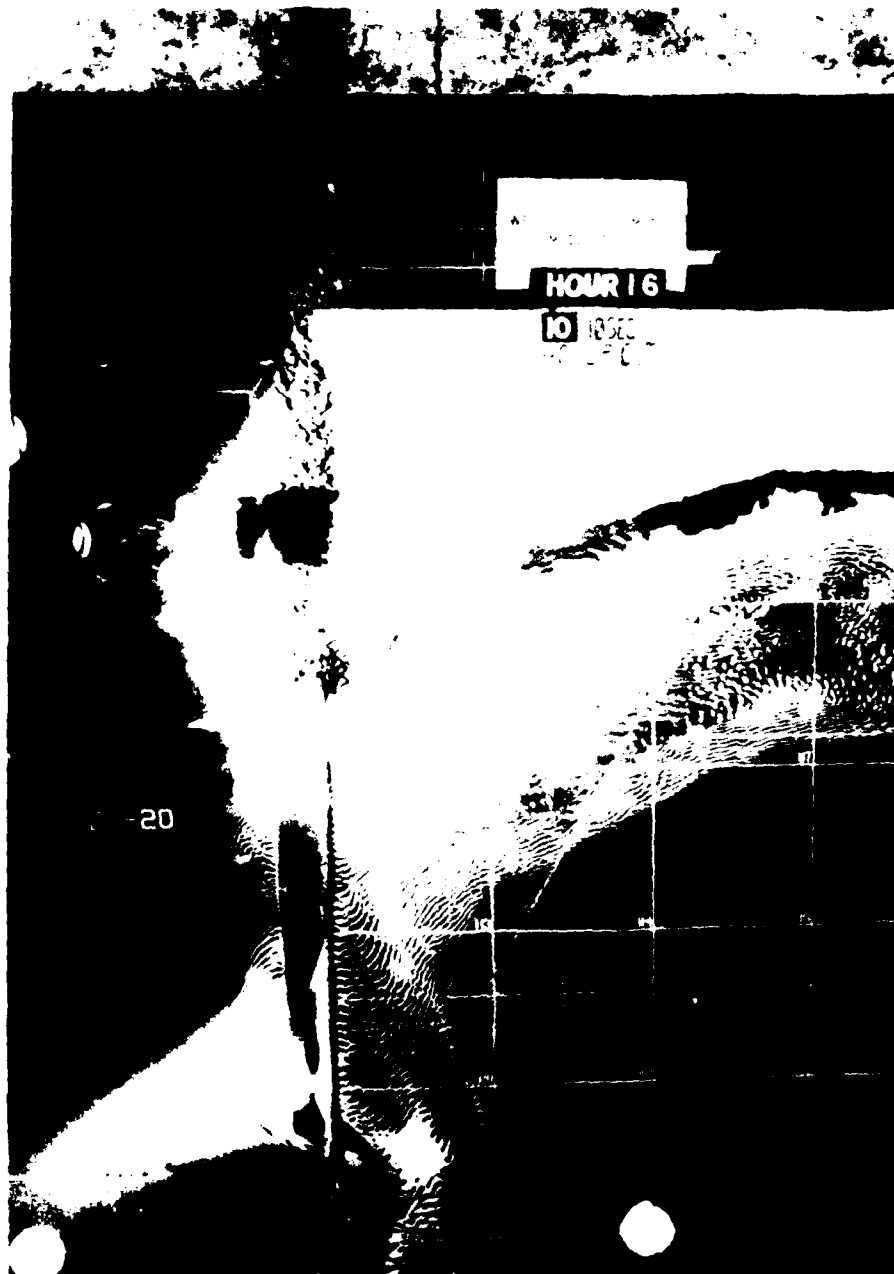


PLATE 47

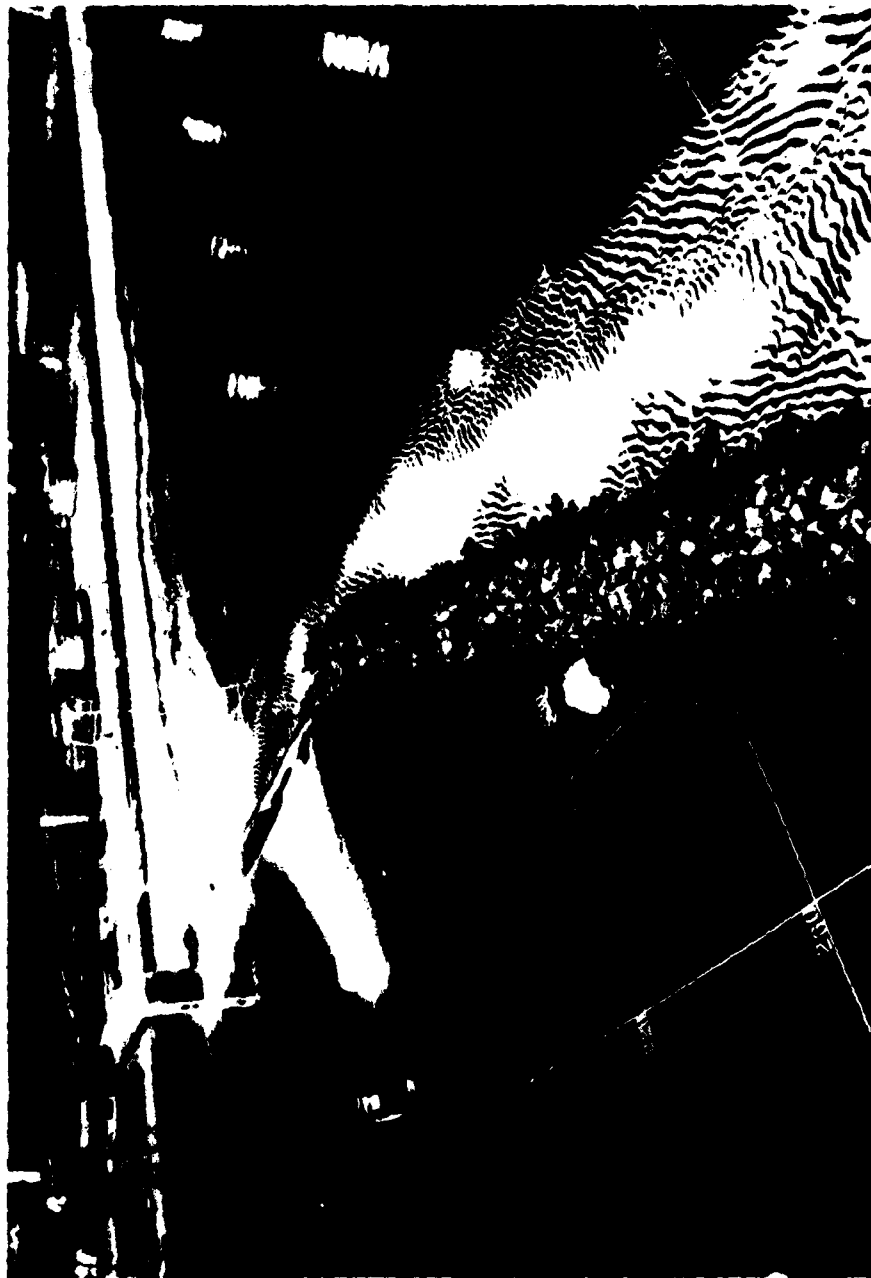


WEIR JETTY PERFORMANCE
MODEL STUDY
5 1050
40 UP 1ST
HOUR 60

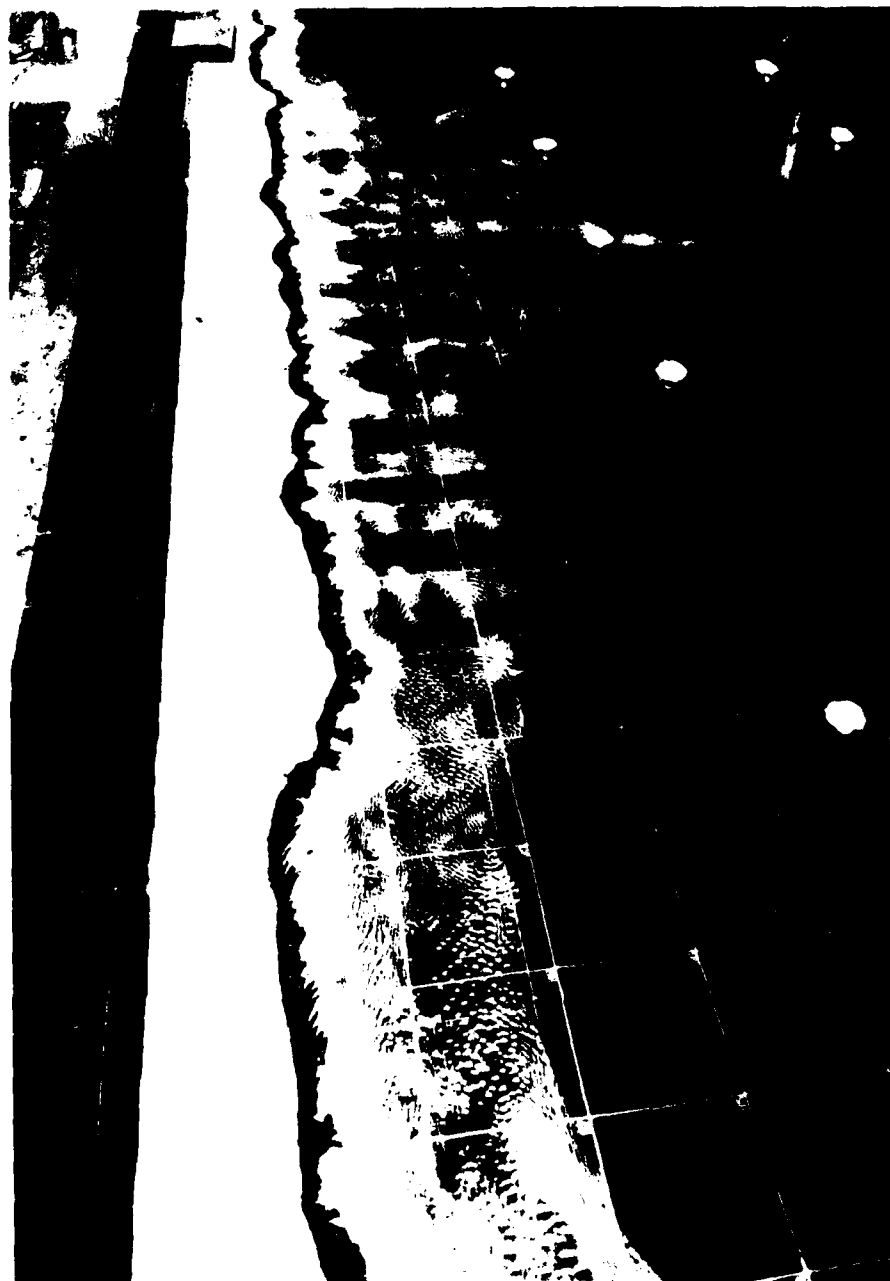
BEACH RESPONSE TEST 6
PLAN 1
HOUR 60



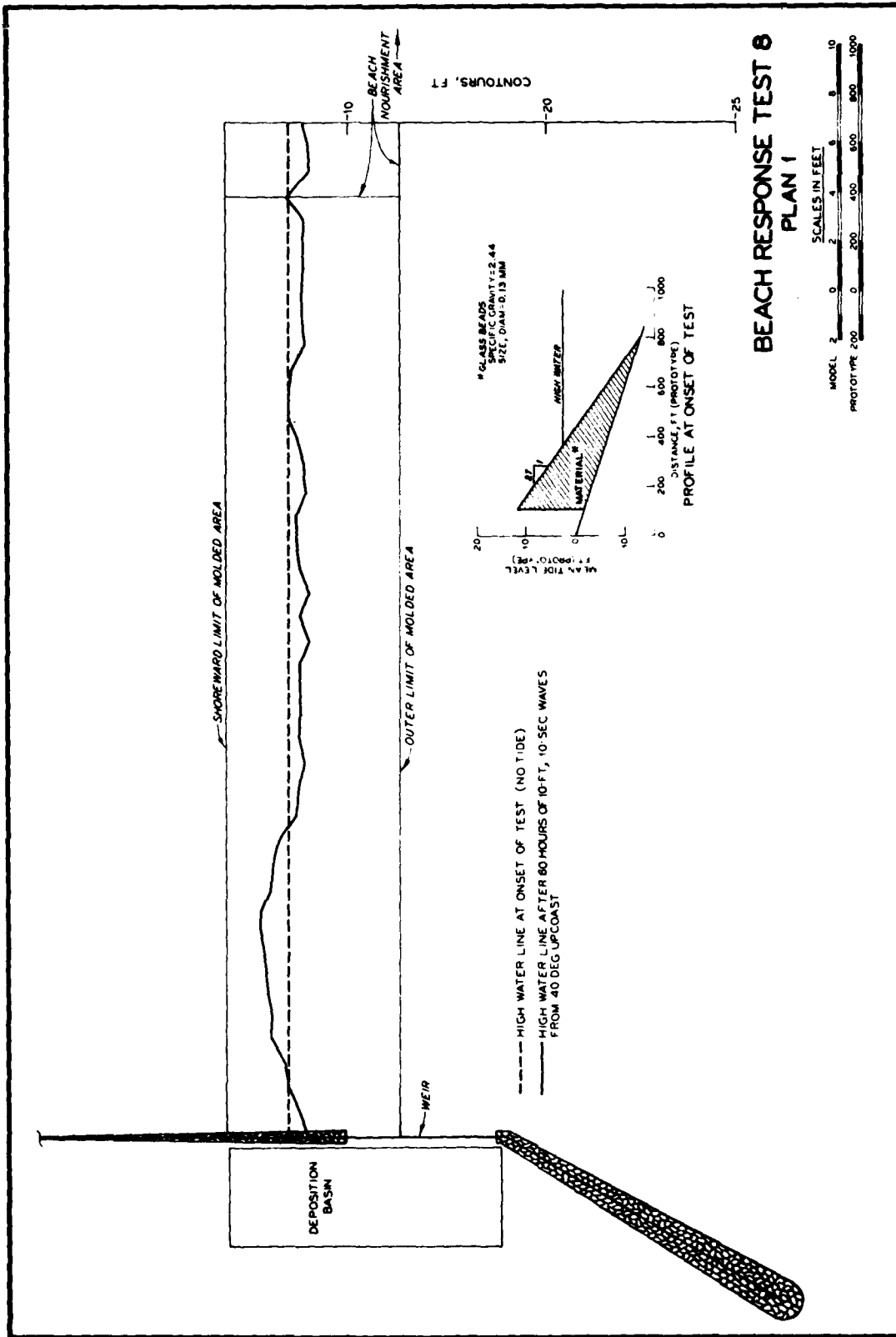
BEACH RESPONSE TEST 7
PLAN 1
HOUR 16



BEACH RESPONSE TEST 7
PLAN 1, LOOKING ALONG JETTY
HOUR 16



BEACH RESPONSE TEST 7
PLAN 1, LOOKING UP COAST
HOUR 16





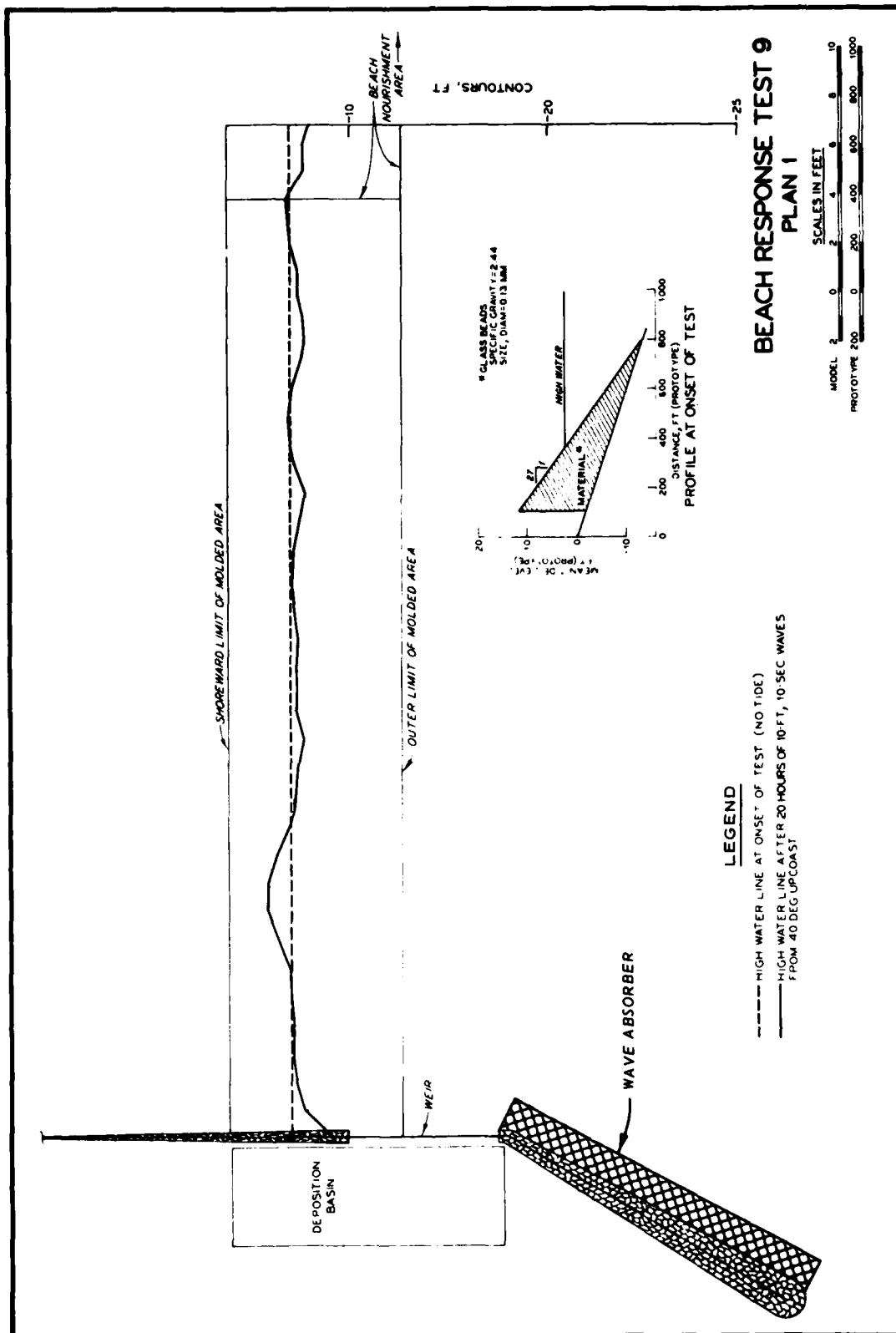
BEACH RESPONSE TEST 8
PLAN 1
HOUR 16



BEACH RESPONSE TEST 8
PLAN 1
HOUR 60

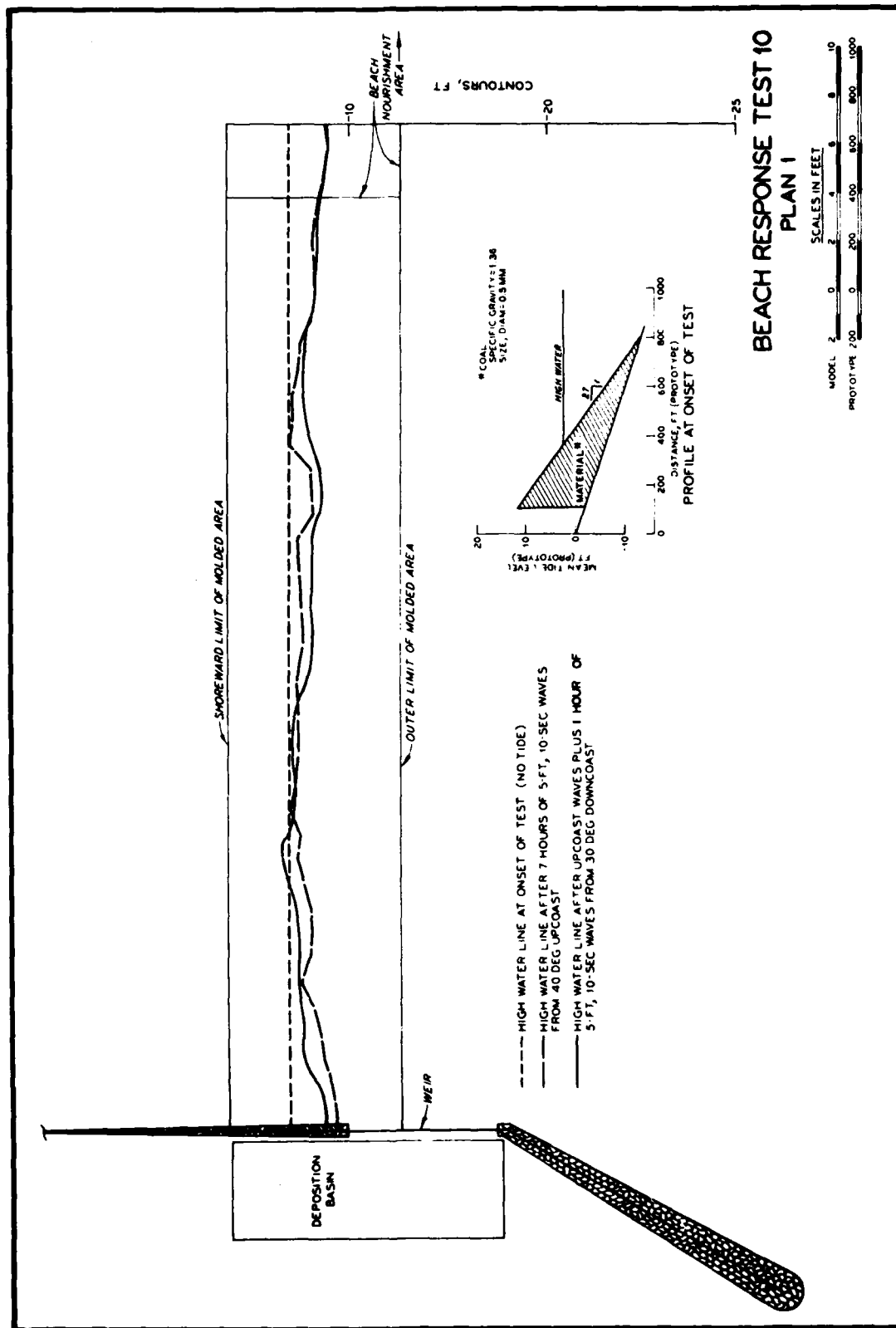


BEACH RESPONSE TEST 8
PLAN 1, LOOKING OFFSHORE
HOUR 60





BEACH RESPONSE TEST 9
PLAN 1
HOUR 20





BEACH RESPONSE TEST 10
PLAN 1
HOUR 7



BEACH RESPONSE TEST 10
PLAN 1
HOUR 8

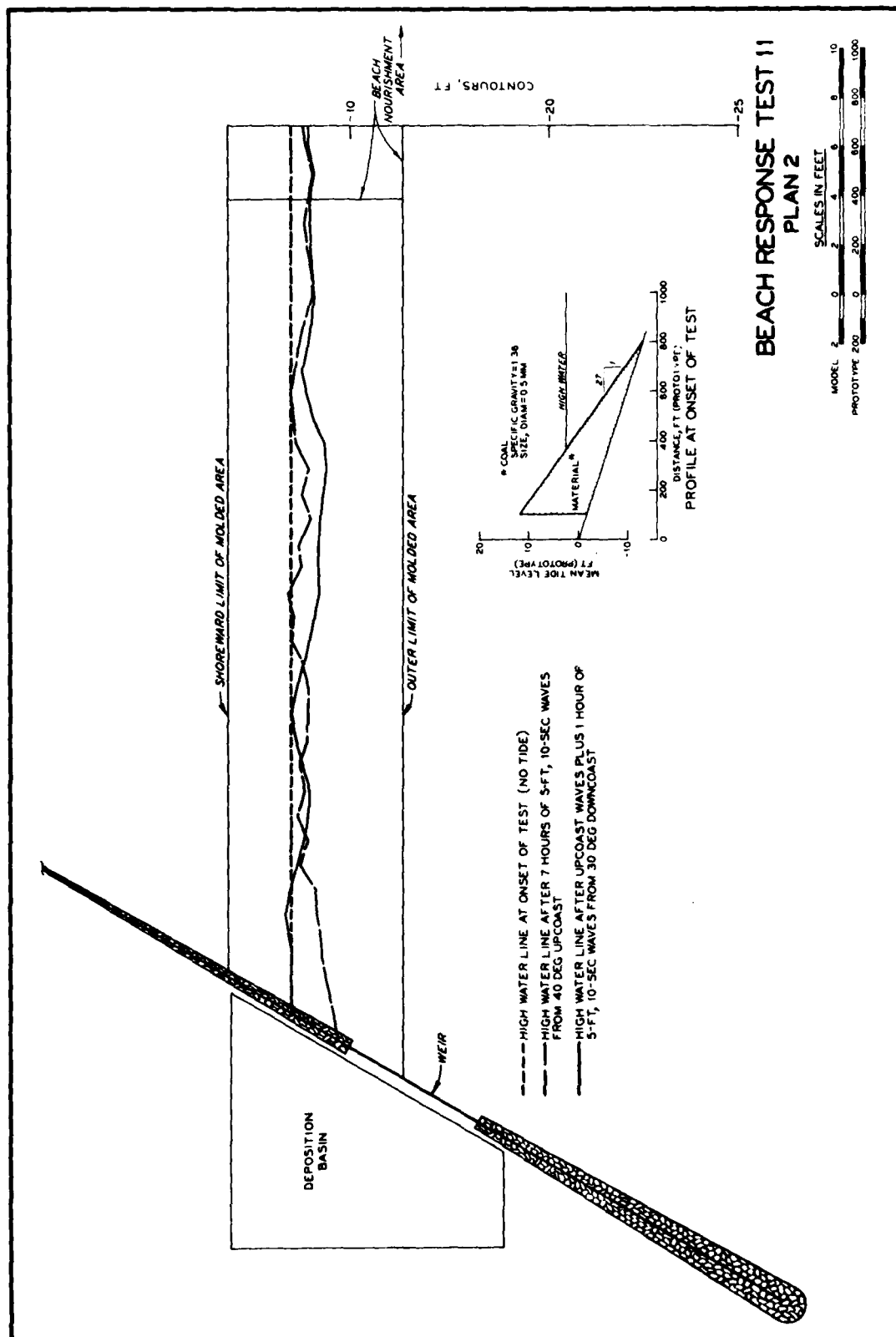


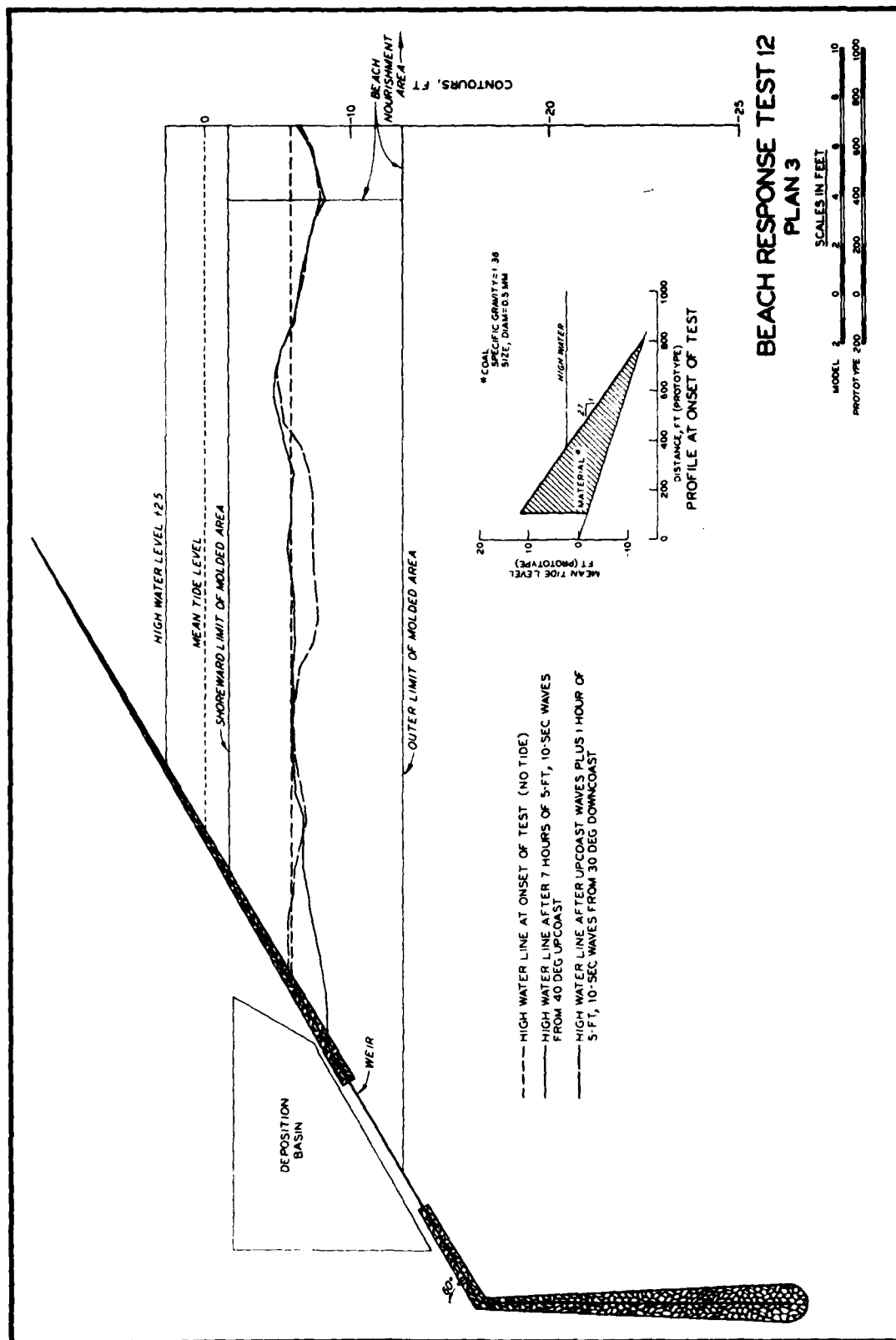
PLATE 62



BEACH RESPONSE TEST 11
PLAN 2
HOUR 7



BEACH RESPONSE TEST 11
PLAN 2
HOUR 8





BEACH RESPONSE TEST 12
PLAN 3
HOUR 7



BEACH RESPONSE TEST 12
PLAN 3
HOUR 8

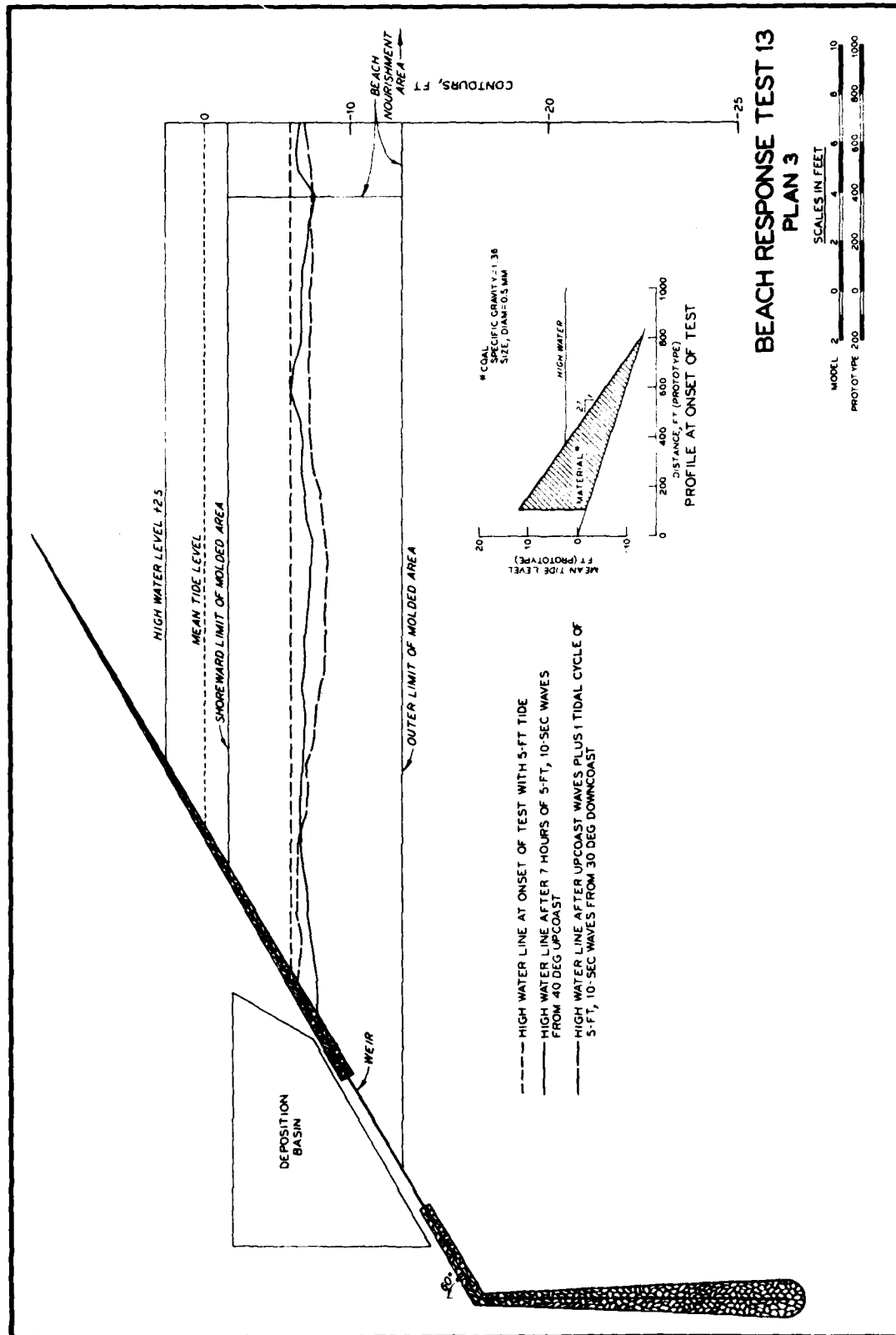


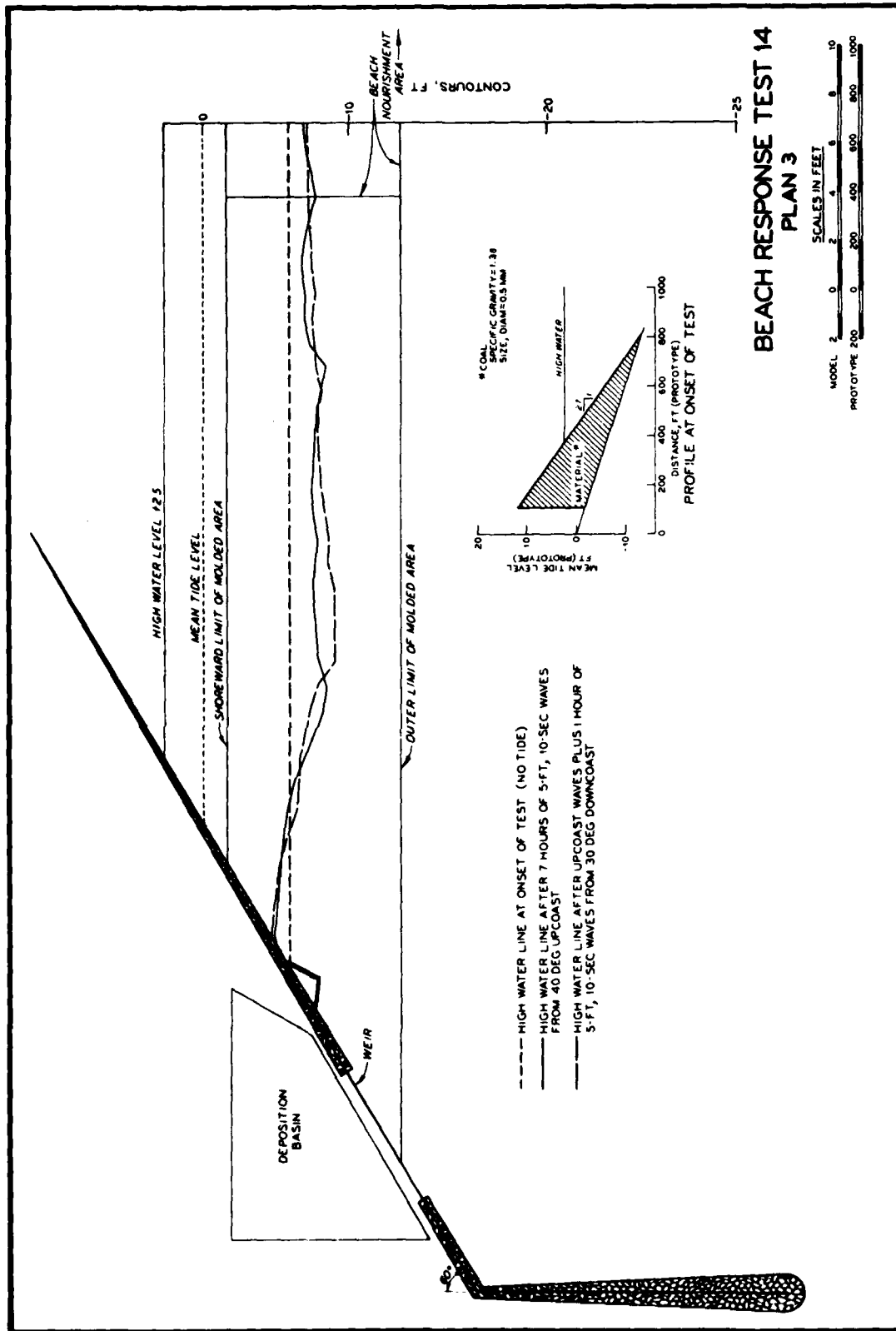
PLATE 68



BEACH RESPONSE TEST 13
PLAN 3
HOUR 7



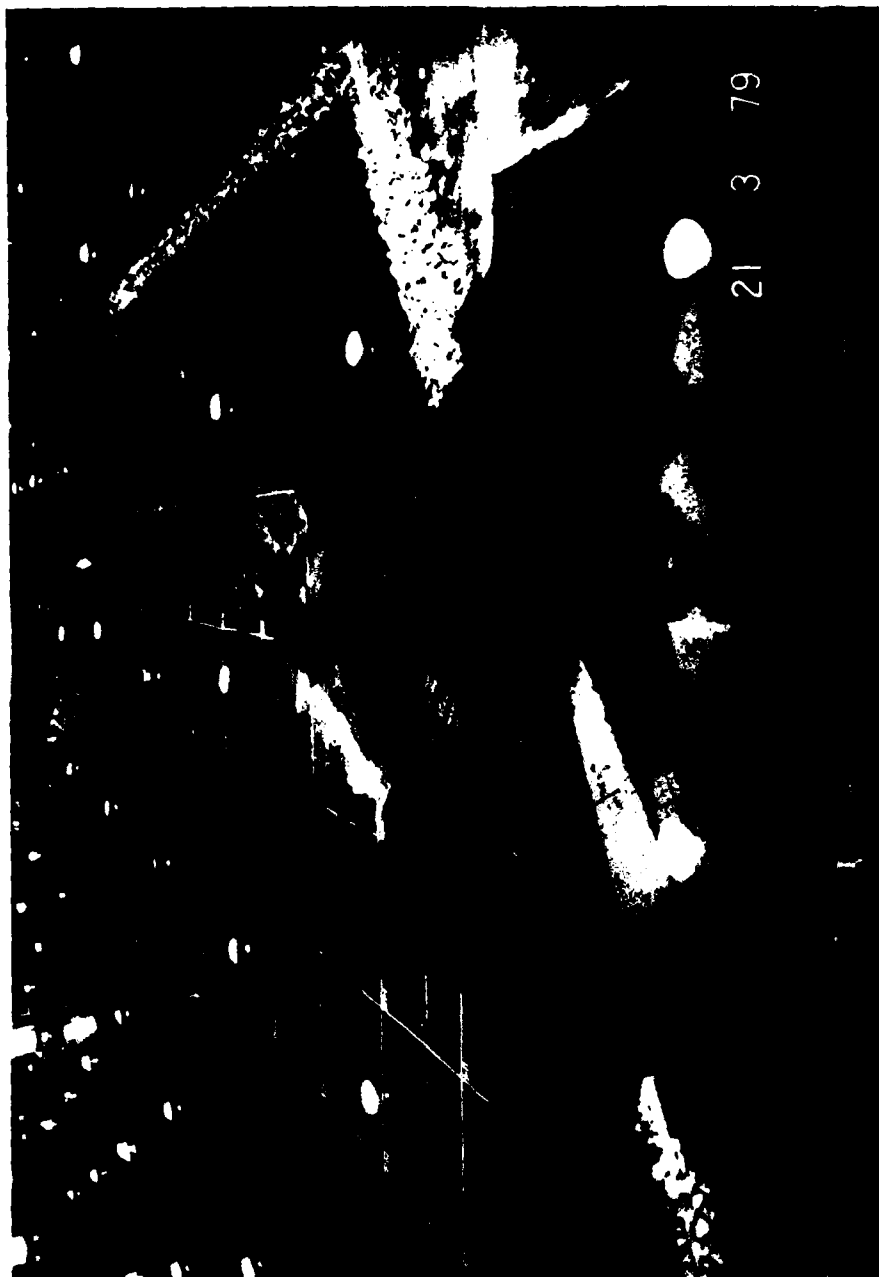
BEACH RESPONSE TEST 13
PLAN 3
HOUR 8





21 3 79

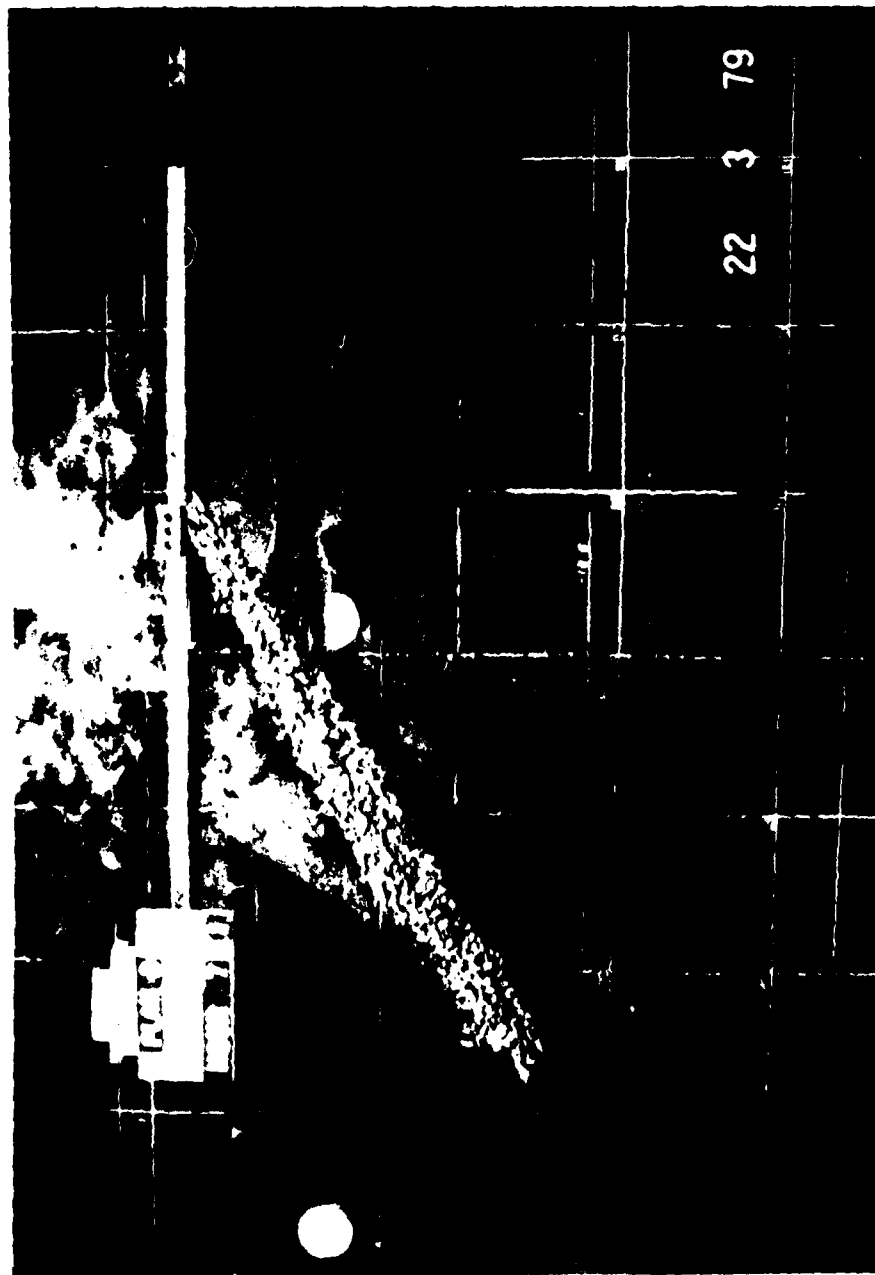
BEACH RESPONSE TEST 14
PLAN 3
HOUR 7



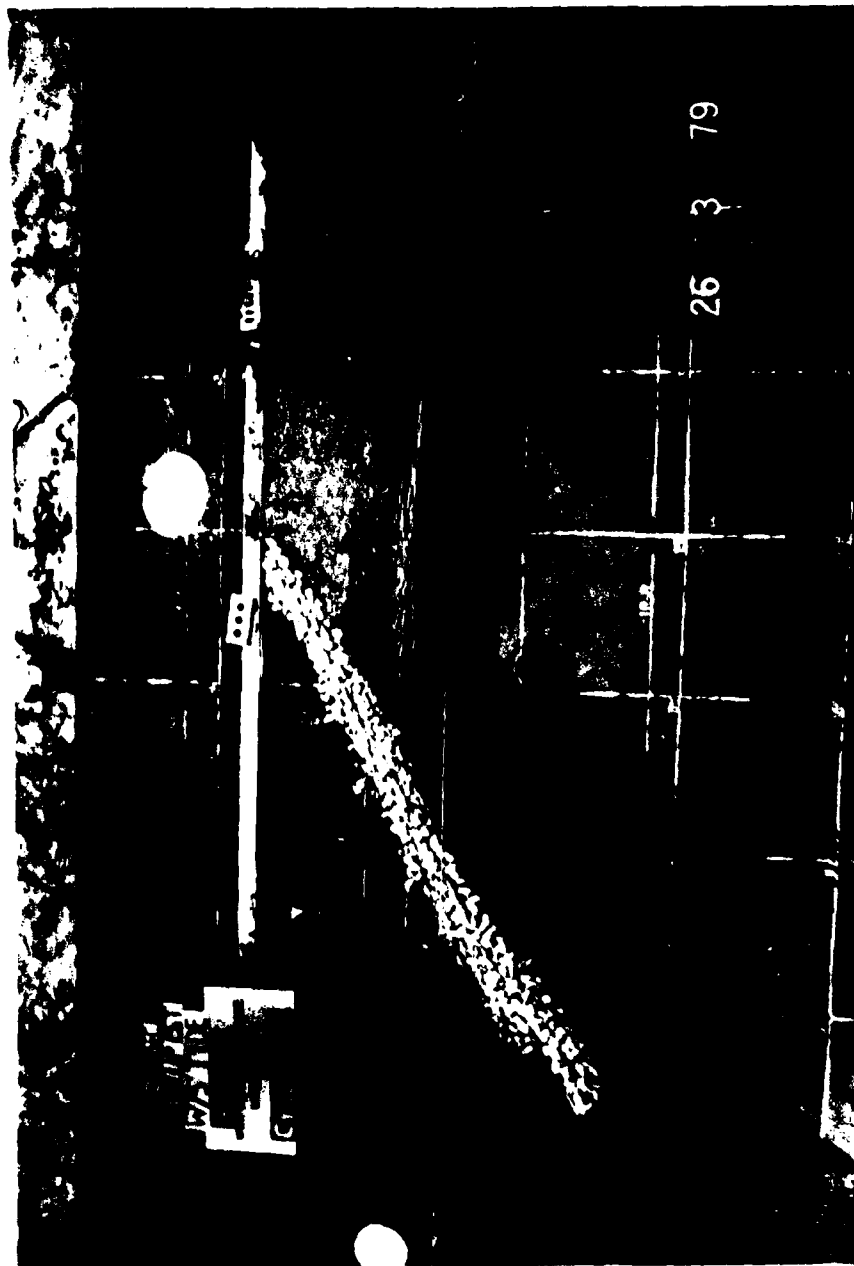
21 3 79

BEACH RESPONSE TEST 13
PLAN 3
HOUR 7, LOOKING OCEANWARD

PLATE 73



BEACH RESPONSE TEST 14
PLAN 3
HOUR 8



BEACH RESPONSE TEST 15
PLAN 3
CYCLE 6



BEACH RESPONSE TEST 15
PLAN 3
CYCLE 7



BEACH RESPONSE TEST 15
PLAN 3
CYCLE 14



BEACH RESPONSE TEST 15
PLAN 3, DRY BED
CYCLE 14





BEACH RESPONSE TEST 16
PLAN 3A
HOUR 7



BEACH RESPONSE TEST 16
PLAN 3A
HOUR 8



9 4 79

BEACH RESPONSE TEST 16
PLAN 3A
HOUR 9

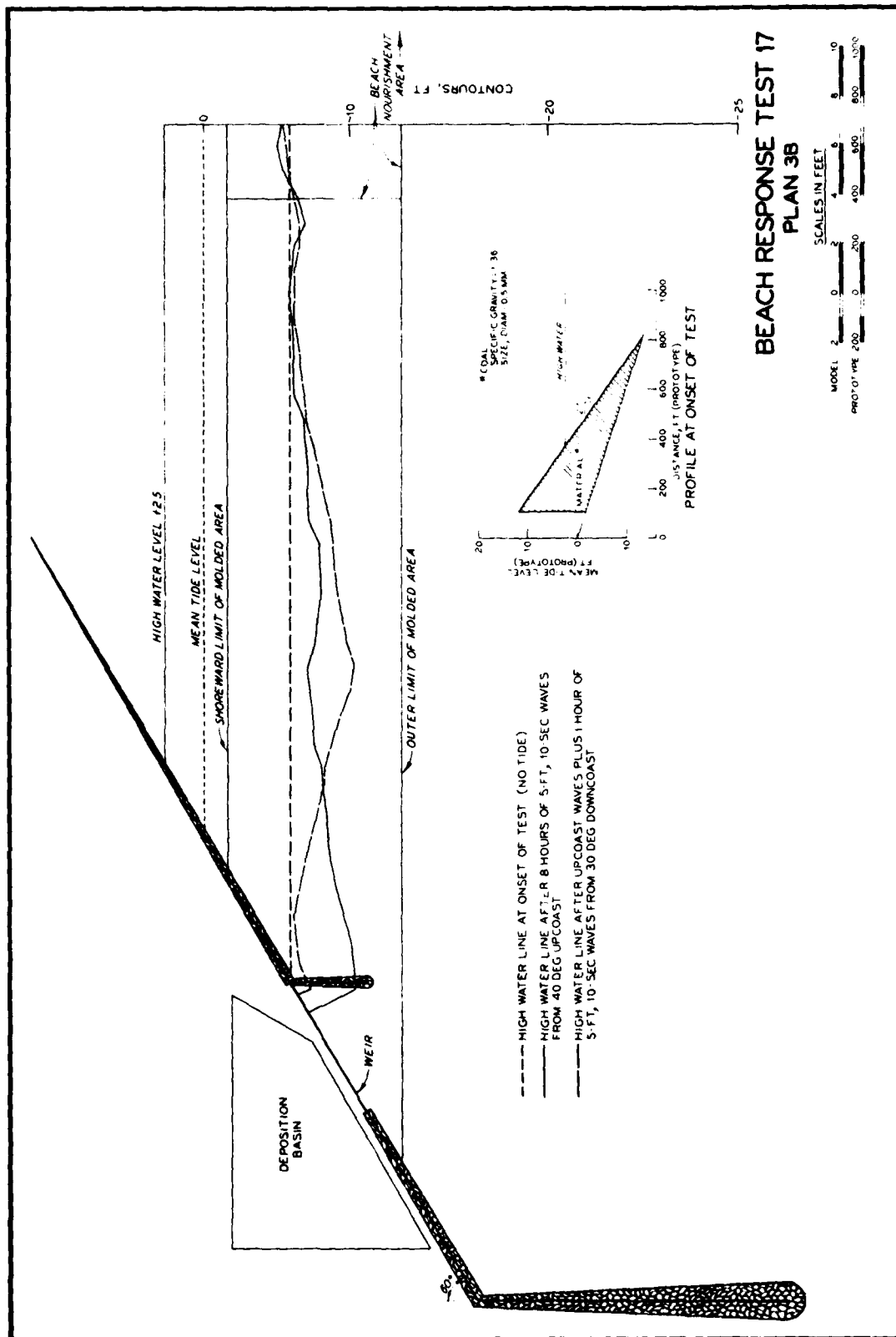
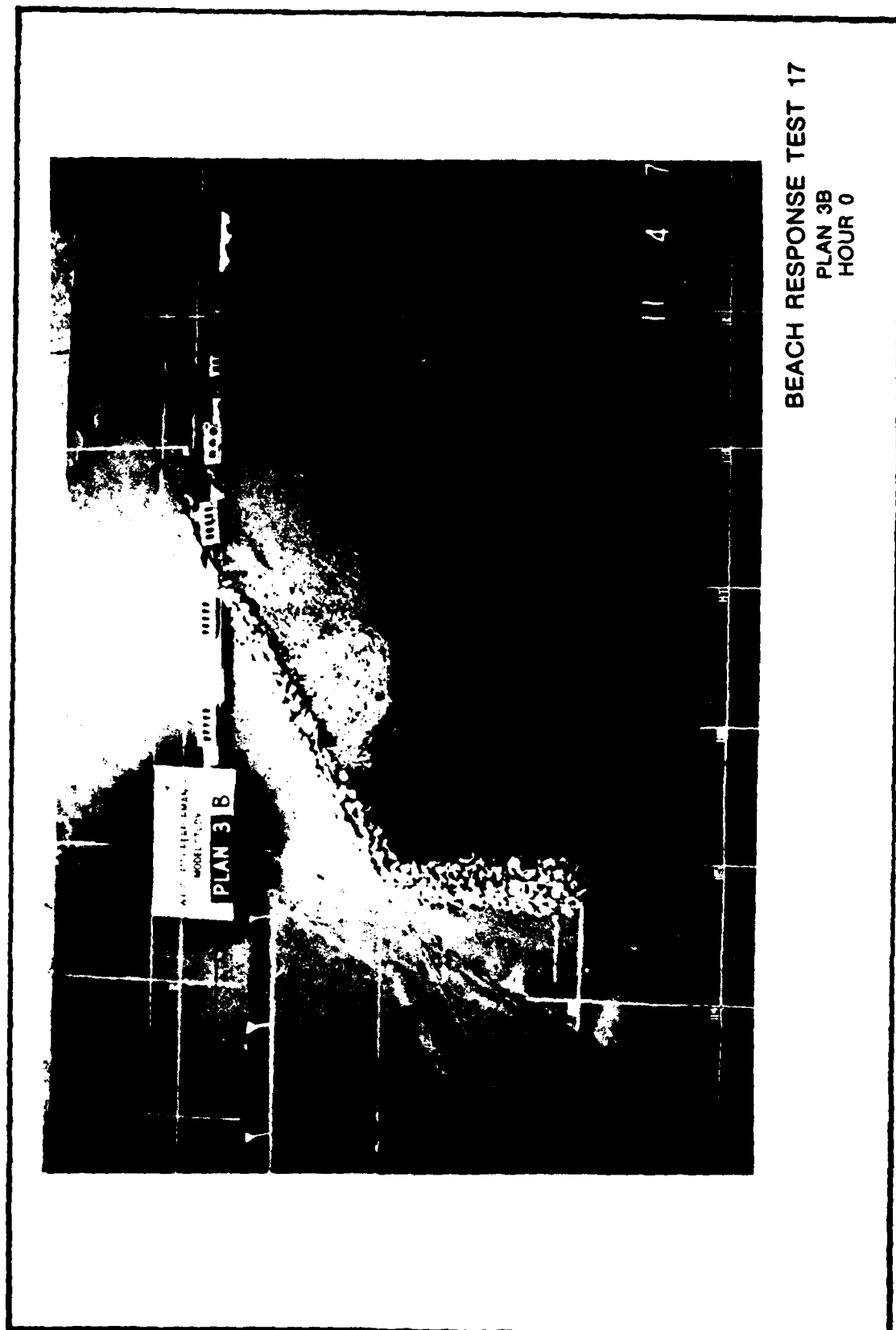
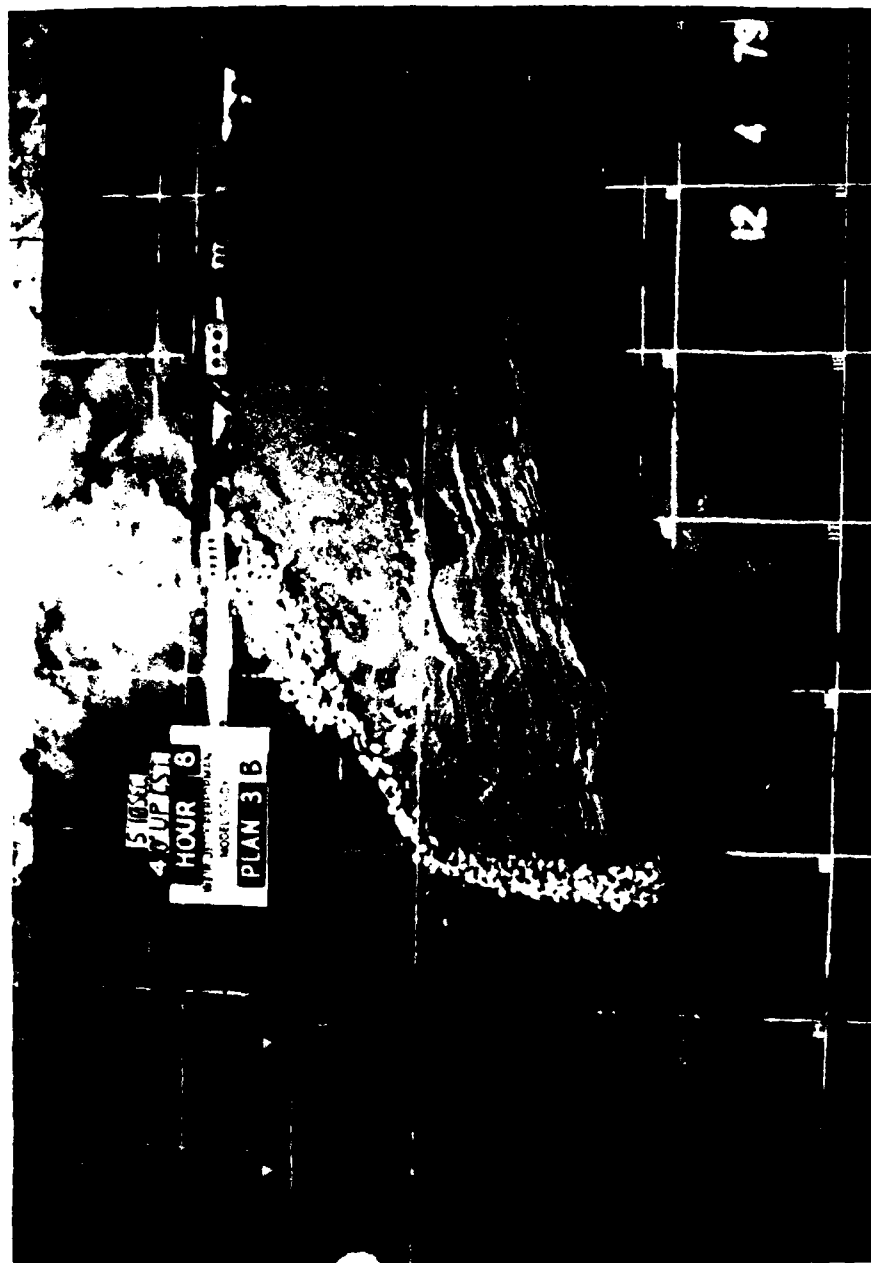


PLATE 84



BEACH RESPONSE TEST 17
PLAN 3B
HOUR 0



BEACH RESPONSE TEST 17
PLAN 3B
HOUR 8



BEACH RESPONSE TEST 17
PLAN 3B
HOUR 9



BEACH RESPONSE TEST 17
PLAN 3B
HOUR 13



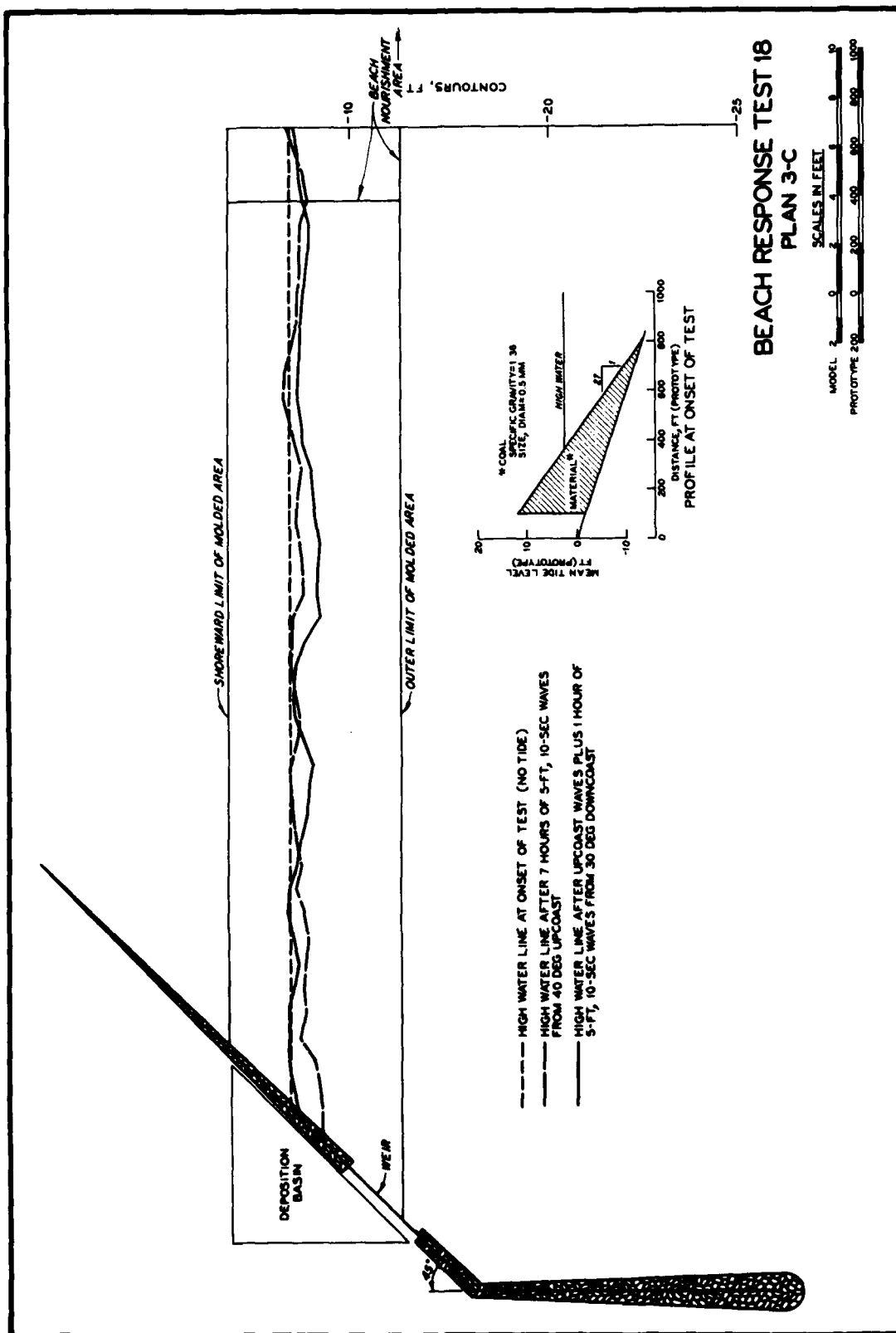
BEACH RESPONSE TEST 17
PLAN 3B
HOUR 20



BEACH RESPONSE TEST 17
PLAN 3B, DEPOSITION BASIN
HOUR 20



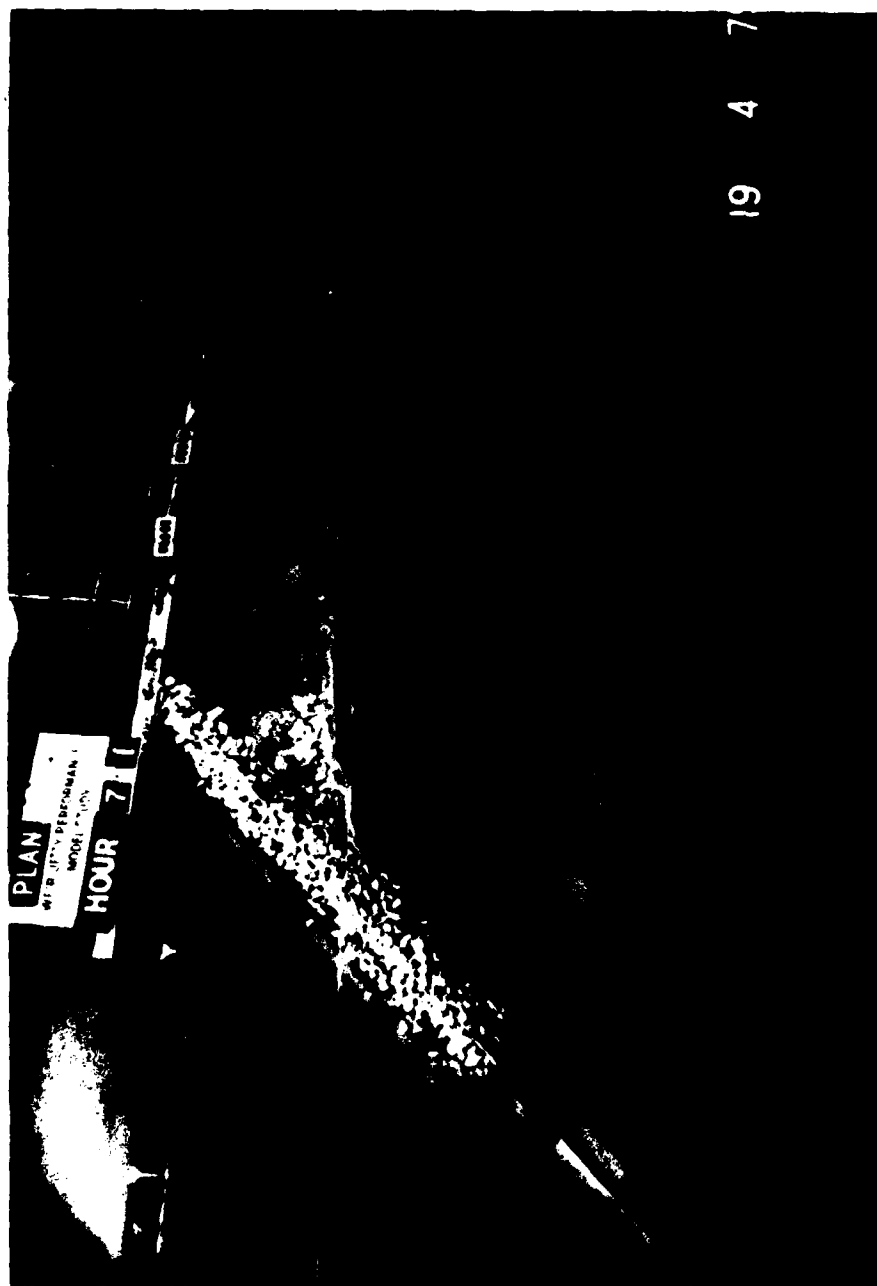
BEACH RESPONSE TEST 17
PLAN 3B, DRY BED
HOUR 20





19 4 79

BEACH RESPONSE TEST 18
PLAN 3C
HOUR 7



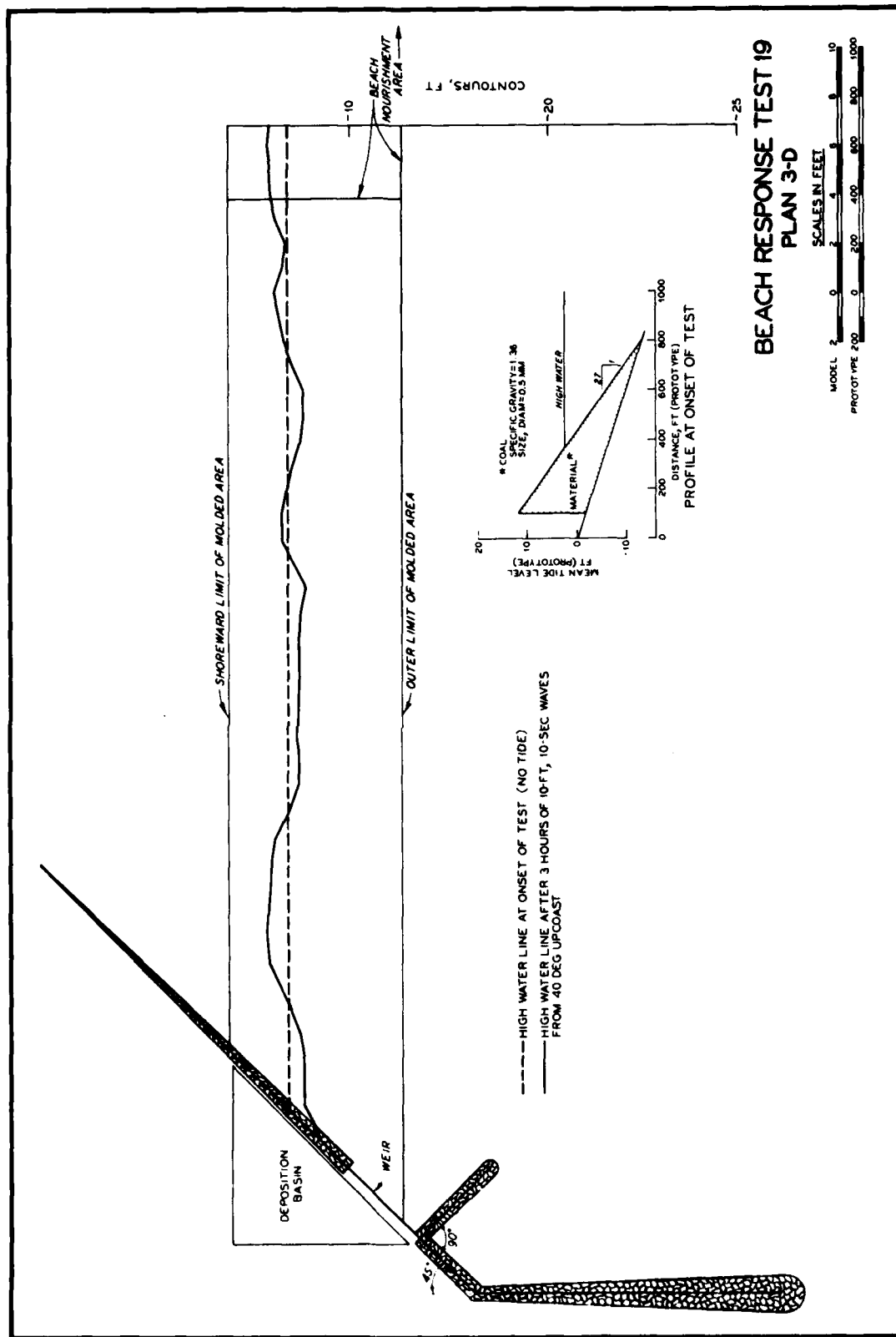
BEACH RESPONSE TEST 18
PLAN 3C
HOUR 8



BEACH RESPONSE TEST 18
PLAN 3C
HOUR 12



BEACH RESPONSE TEST 18
PLAN 3C
HOUR 12





BEACH RESPONSE TEST 19
PLAN 3D
HOUR 3



23 3 8

BEACH RESPONSE TEST 19
PLAN 3D, LOOKING OCEANWARD
HOUR 3

PLATE 99

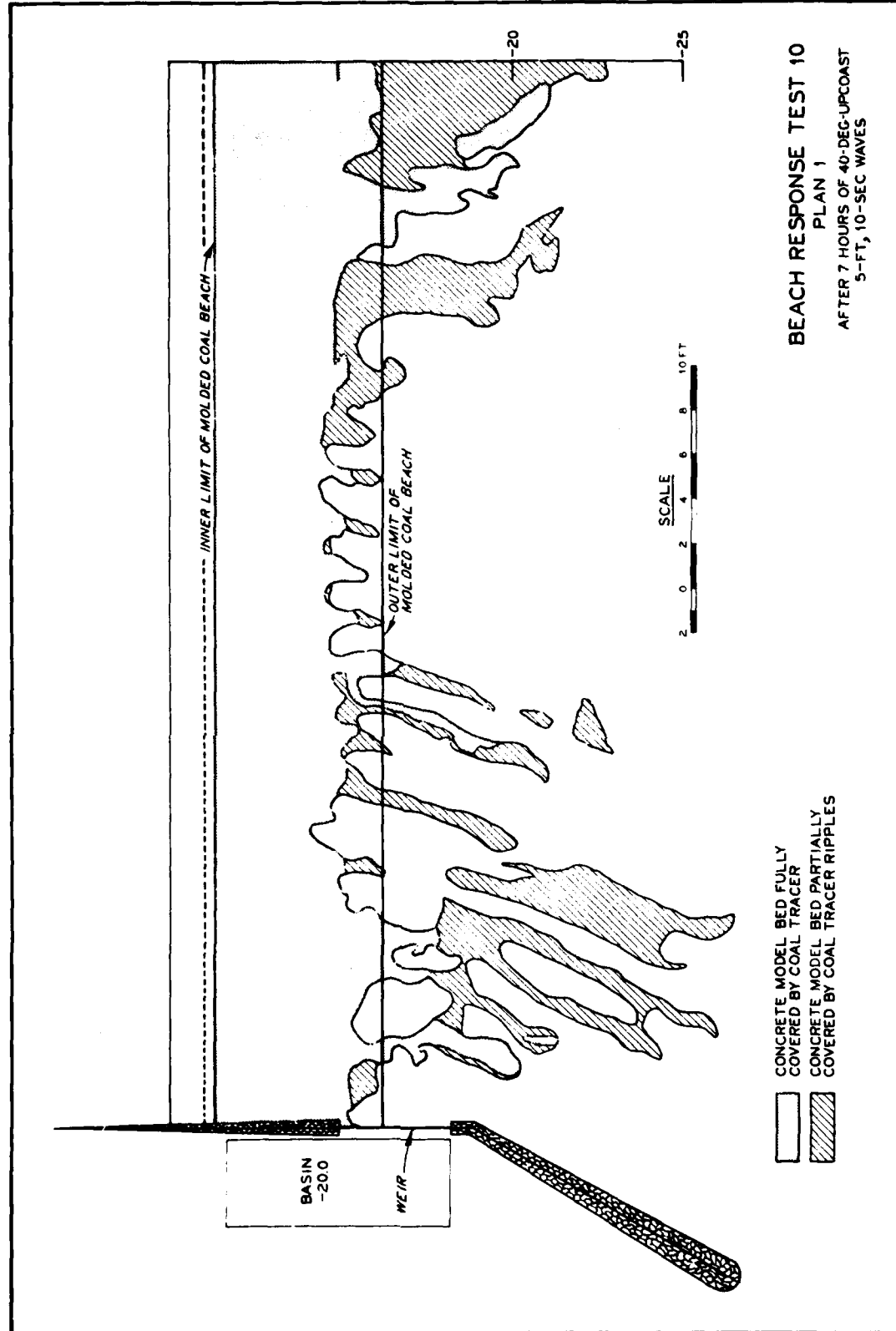
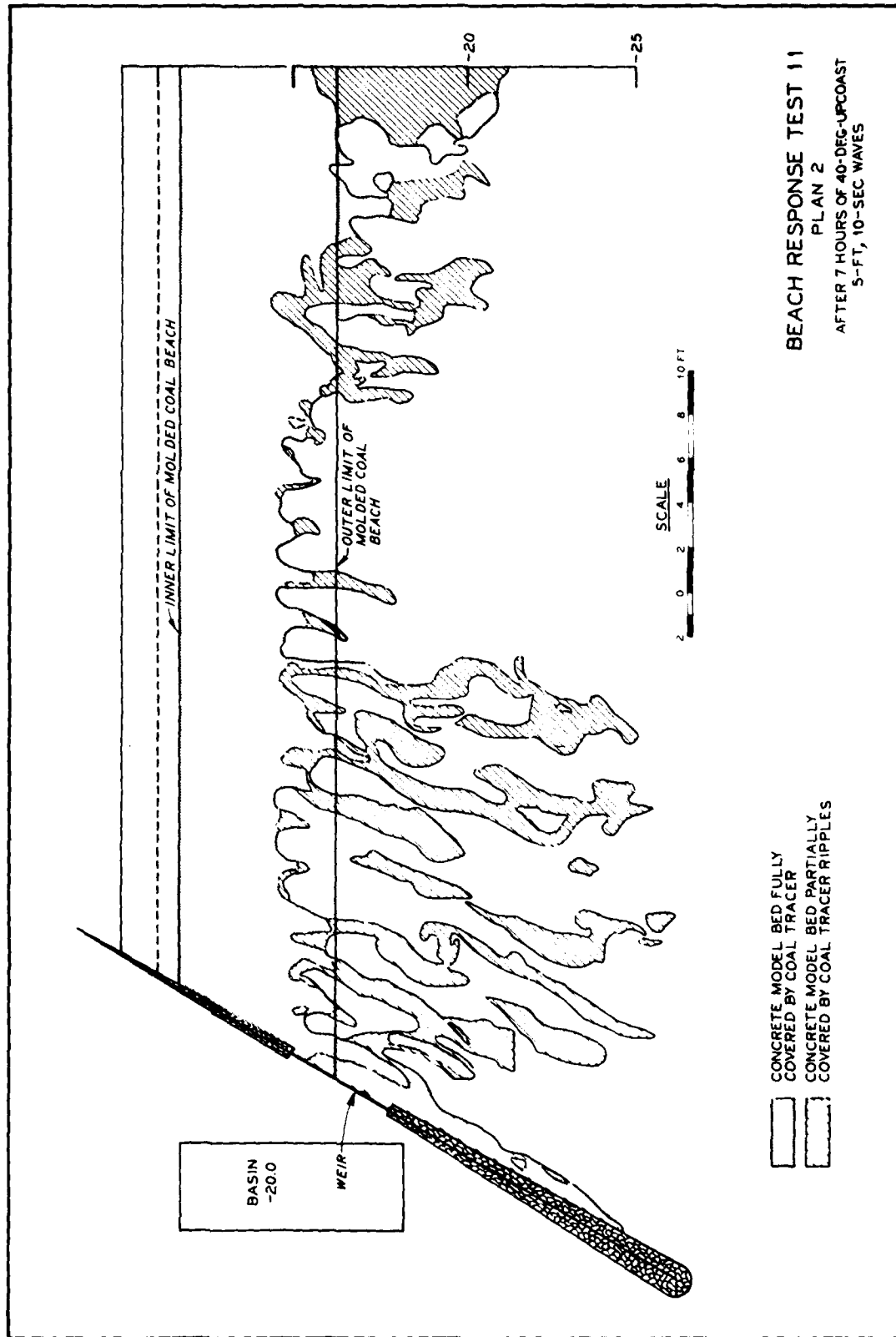


PLATE 100



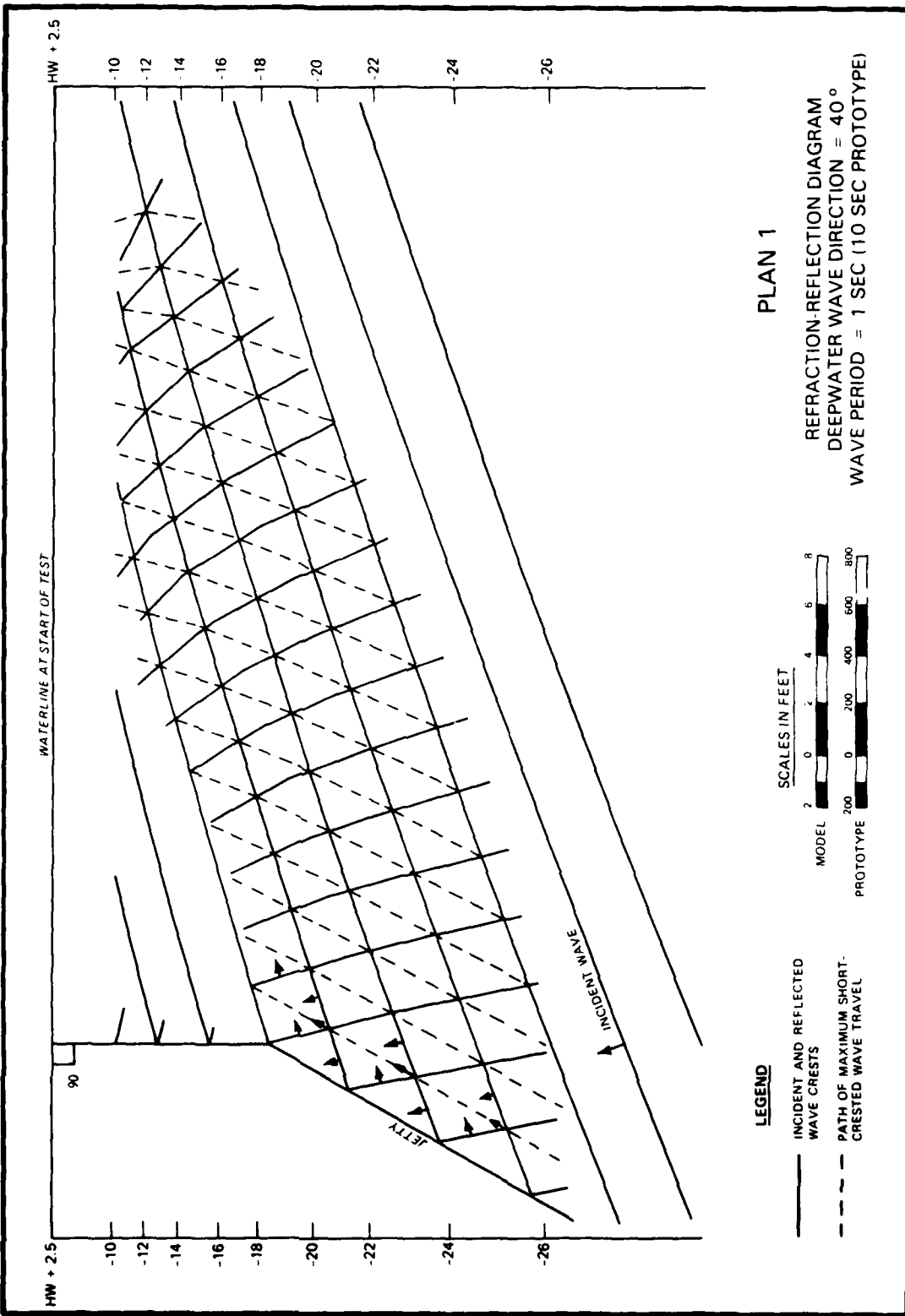
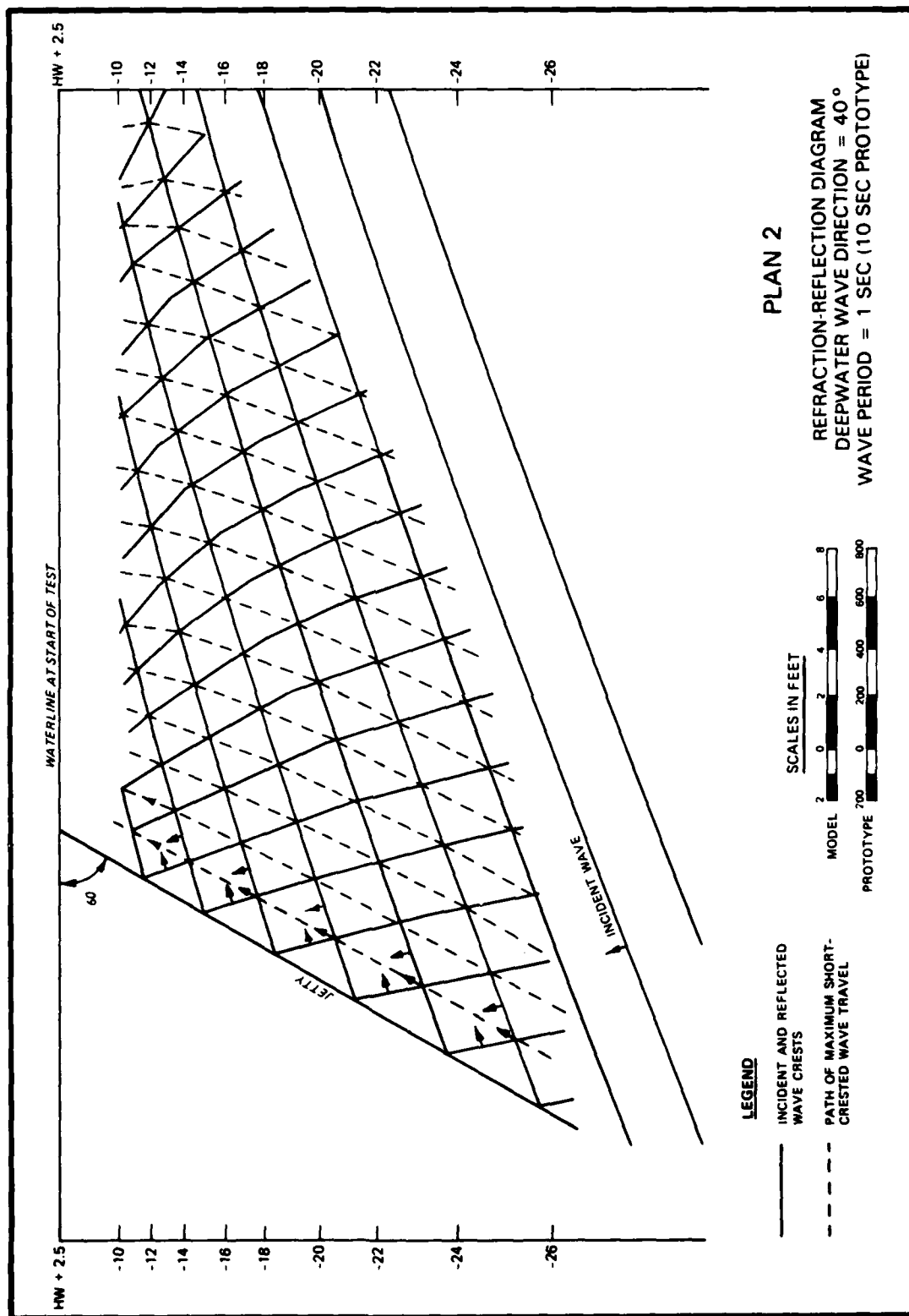
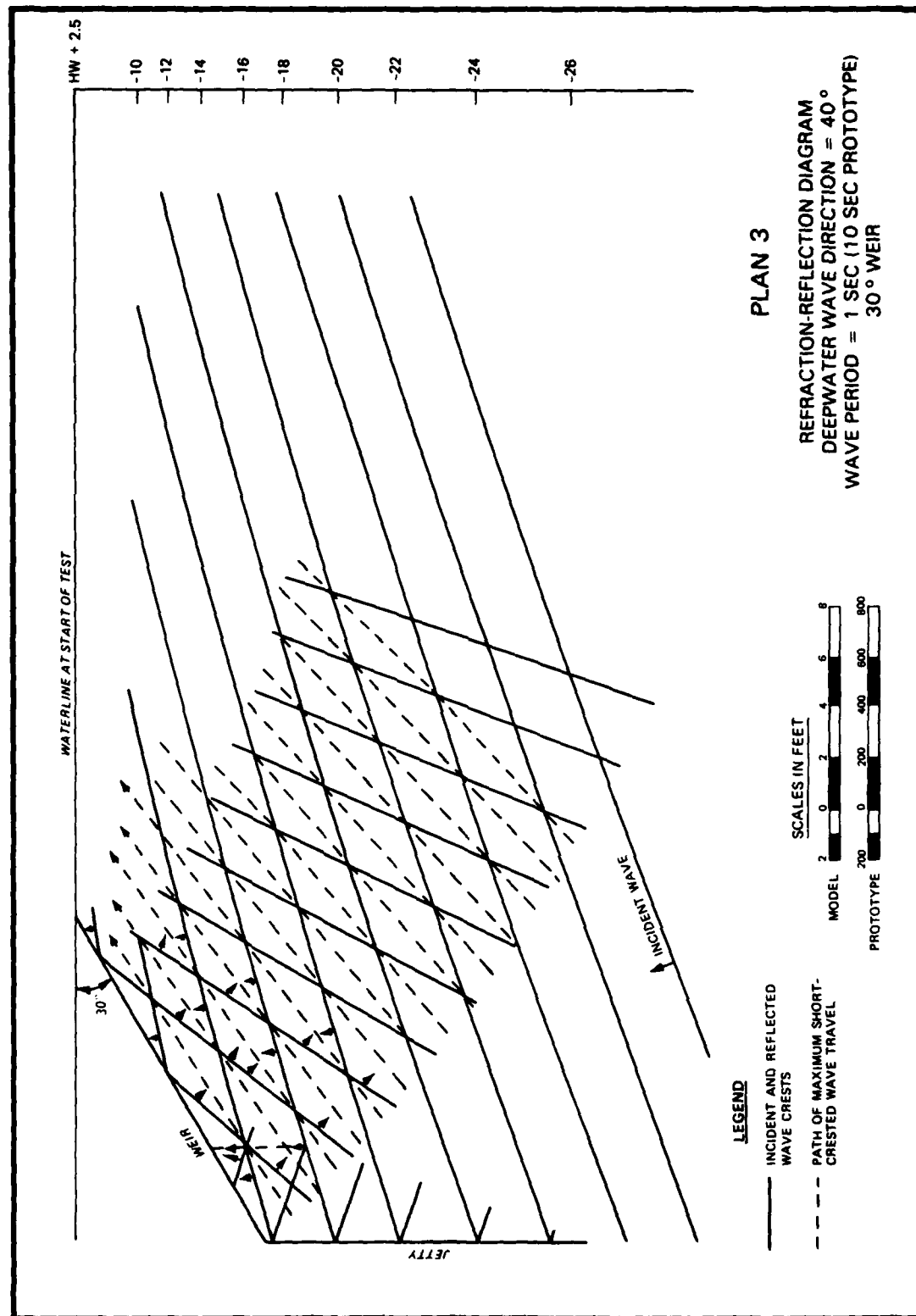
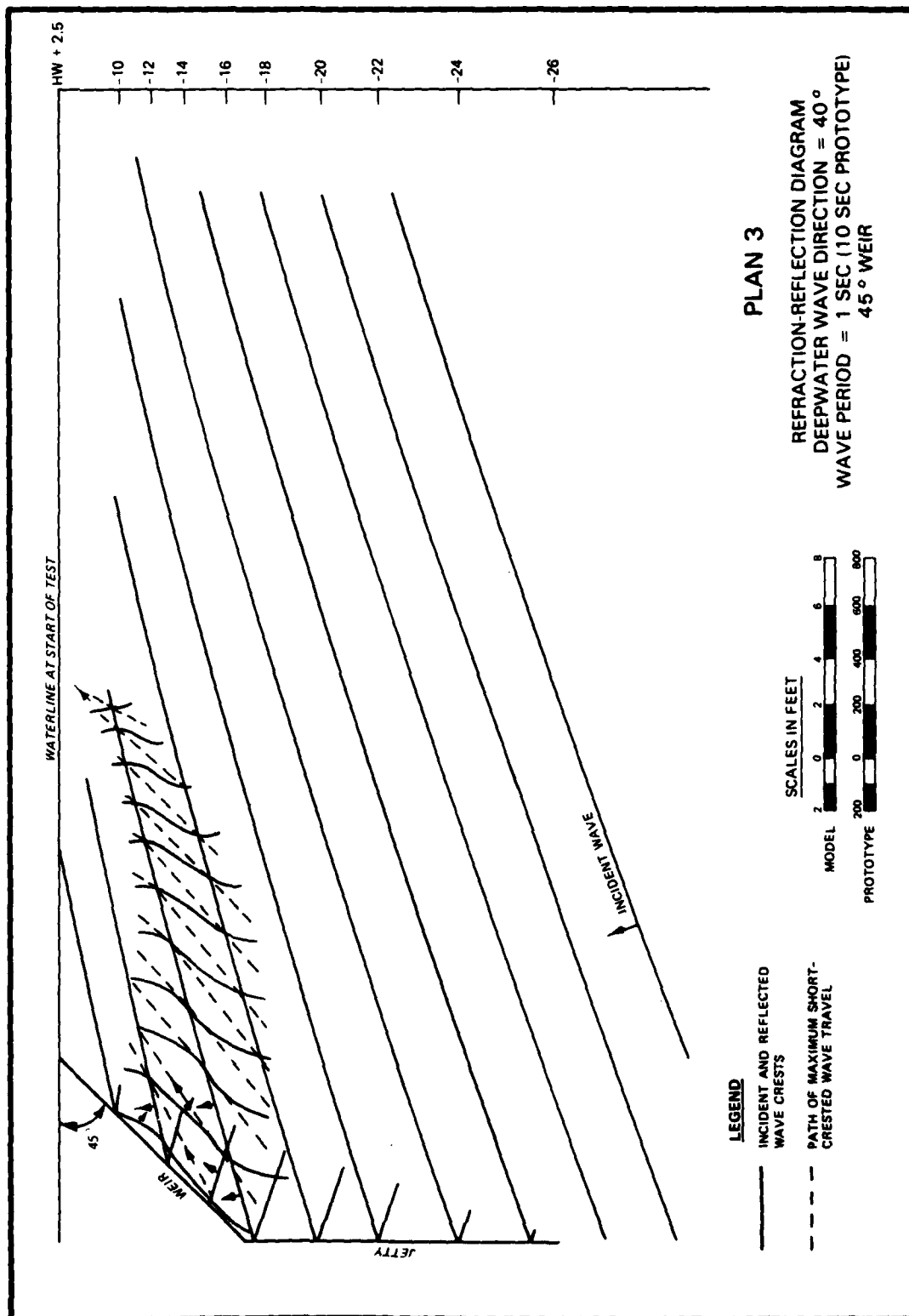


PLATE 102







APPENDIX A: TWO-DIMENSIONAL WAVE FLUME TESTS

1. The subject tests were conducted to aid in the selection of a sediment tracer for the three-dimensional weir jetty beach response testing. The sediment to be selected would be used as an overlay on the existing concrete model bed. As mentioned in the main text, the model was originally designed for hydraulic fixed-bed tests and during the testing program it was decided to examine beach response upcoast of the weir jetty. Because of time and cost limitations it was not desirable to construct a fully movable-bed model.

2. It was felt that the main criterion, in light of the constraints discussed above, would be to choose a sediment with a natural profile close to that of the molded beach profile for wave conditions that would be applied in the model. The beach slope molded in the model was a relatively flat slope (1:60) and thus representative of small particle size beaches (less than 0.3 mm) with high wave exposure (U. S. Army Coastal Engineering Research Center 1977*). This same slope was reproduced in the flume tests for the various sediments (the initial slope at the beginning of a test). Sediments chosen from those on hand at WES were: sand, $D_{50} = 0.25$ mm, specific gravity (S.G.) = 2.65; glass beads, $D_{50} = 0.13$ mm, S.G. = 2.42; glass beads, $D_{50} = 0.08$ mm, S.G. = 2.42; coal, $D_{50} = 1.0$ mm, S.G. = 1.36; coal, $D_{50} = 0.5$ mm, S.G. = 1.36; plastic (Tenite butyrate), $D_{50} = 3.0$ mm, S.G. = 1.18. The gradation curves are shown (except for plastic, which is of a uniform size) in Plates A1-A5. Plate A6 shows the angle of repose of the sediments, both wet and dry, as measured in a clear plastic box. Plate A7 shows fall velocities at standard conditions for the sediments as measured in a 4-in.-diam glass cylinder (except for the sand curve, taken from Rouse (1937)).

3. The facility used was a 2-ft-wide wave flume, 166.5 ft long, and 7.0 ft deep with details shown in Plate A8. The beach profile was

* References cited in this Appendix may be found in the References section at the end of the main text.

molded in the area of the flume where the observation windows are seen in Plate A8. The beach slope was molded from a line drawn on the side of the flume window and measurements of the profile were made from this reference line. Wave filters were installed to absorb waves reflected from the model beach to minimize interference of rereflected waves with the equilibrium profile. The test beach was molded from the -29 ft contour (from 1:100-scale three-dimensional model) to +10.0 msl, a horizontal length of approximately 50 ft. Wave conditions used were based on values considered reasonable for a 1:100 scale undistorted model. Periods used were 0.7 sec (7 sec prototype), 1.1 sec (11 sec) and 1.5 sec (15 sec). Wave heights used were 0.039 ft (3.9 ft prototype), 0.072 ft (7.2 ft), and 0.146 ft (14.6 ft). The tests were run until it appeared the profile was stabilized. It was fairly easy to determine this for the lighter weight materials, but normally there was still some minor movement continuing for glass beads and sand, due to the relatively small waves used in the study.

4. The beach profiles are presented in Plates A9-A15. In many cases a beach slope was created offshore of the original waterline. The 1-mm coal (tests 1-8) showed material transport shoreward where a new beach was built seaward of the original one. Tests 9-11 with 0.08-mm glass beads did not respond as the coal did, but maintained the original beach slope and showed offshore movement, creating bars. The mechanism for this was a uniformly rippled bottom (~1 in. in length) with eddies that suspended the beads high enough to be carried offshore by a net offshore current just above the bottom. This net movement was due to the cnoidal shape of the waveform producing higher, short duration velocities under the wave crest and longer term, slower velocities under the wave trough. Tests 12-18 with the 0.5-mm coal were somewhat similar to the larger coal except there was some offshore movement for the larger, longer period waves (tests 16-18). The plastic (tests 19-26) did not respond to the shorter period, small waves (tests 22 and 25). Otherwise, beaches were built seaward of the original waterline and then movement was onshore. The sand did not respond to the short period waves (tests 27-28) and built beaches for the larger waves (tests 29-32).

The 0.13-mm glass beads (tests 33-40) showed movement similar to that of the smaller glass beads as discussed previously.

5. In analyzing the 40 flume tests, two criteria were used to evaluate the possible model materials. First, it would be desirable to have a material which moved onshore and offshore as sand would for given prototype conditions that would be scaled in the model. Second, a material with a fairly flat slope would be desirable in order to blend in with the concrete model slope of 1:60 (which was designed and constructed before the decision was made to study beach planforms upcoast of the weir jetty).

6. Onshore-offshore movement of the beach profile has been associated with the magnitude of wave steepness (Johnson 1949), with wave steepness and fall velocity of the sediment particle (Dean 1973), with wave steepness and sediment diameter (Iwagaki and Noda 1962), and with wave steepness, sediment diameter, and specific gravity of the sediment (Nayak 1970). For each of the above-mentioned offshore-onshore movement models, a critical wave steepness can be determined, for which, if the wave steepness (height/length, H_o/L_o) is greater than that value, the movement will be offshore and if less, the movement will be onshore.

7. The model test conditions were converted to prototype values by the scaling ratios of 1:10 for period and 1:100 for wave height, and the movement predicted by the various models was determined. In the cases of the models by Dean, Iwagaki and Noda, and Nayak, two sediment sizes were assumed in order to cover a range of values. The prototype sediment sizes selected were 0.25 mm and 0.8 mm. In the application to the model of Dean, the fall velocities were determined by the curve of Rouse (1973) shown in Plate A7. The resultant movement is tabulated for each test and each model in Table A1 and compared with the observed movement in the two-dimensional flume tests. In the column of observed movement in the model there is an additional term used to describe sediment movement, other than onshore or offshore. The term "mixed" is included to represent those profiles that had some accumulation shoreward of the breaker and at the breaker line. This corresponds to the "Type II" beach of Sunamura and Horikawa (1974) and which has been

observed in previous model studies of beach profiles. Scanning Table A1 for each sediment group, it is seen that the 0.13-mm glass bead shows the greatest frequency of agreement with the prototype models, followed by the 0.08-mm glass bead, the 0.5-mm coal, the 0.25-mm sand and 1.0-mm coal and the 3.0-mm plastic. It should be noted that most of the prototype models call for offshore movement for the conditions specified and thus the materials that model offshore movement will do better in this comparison. The reason for most conditions predicting offshore movement was the desire to maintain fairly large waves at the 1:100 scale. The plastic and sand each had two tests where the material did not respond at all to the test conditions for small short-period waves.

8. Based on a slope criterion, the glass beads maintained the flattest slope, very close to that of the model bed. This was most likely due to their low angle of repose, resulting from their spherical shape. Sand was excluded from further consideration due to its lack of response to smaller waves (it was not desired to distort wave height in the three-dimensional model) and its steep beach slope for large waves. Plastic and coal were also undesirable due to their steep beach slopes (relative to the model bed). Therefore the bead was chosen as the modeling sediment based on slope criterion and the onshore-offshore movement criterion. The larger glass bead was chosen over the smaller glass bead in order to maintain a critical H/L ratio similar to prototype conditions. Based on Dean (1973):

$$\frac{H}{L}_{\text{critical}} = \frac{1.7\pi w}{gT}$$

where

H = wave height

L = wave length

w = fall velocity

T = wave period

The larger bead size had the greater fall velocity, thus the greater critical H/L ratio. Figure A1 shows that in order to maintain the

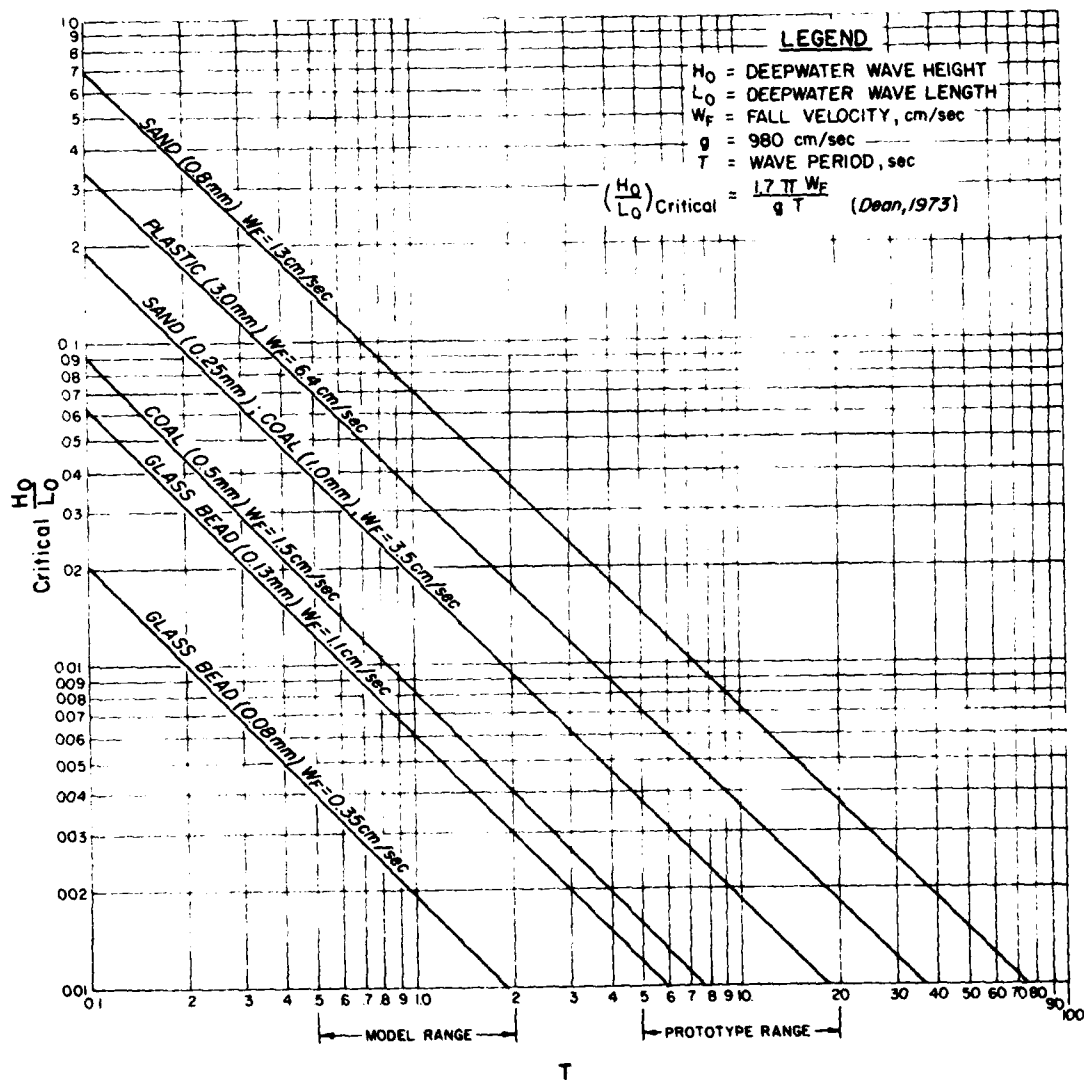


Figure A1. Critical wave steepness versus wave period

same critical H/L ratio in model and prototype for the 1:10-period scale of a 1:100 model, the 0.13-mm glass bead is closer than the 0.08-mm glass bead. Also note that the 0.5-mm coal is a close second choice in this respect.

9. The reason for the better response of the beads to the small waves than that of sand was due to the low angle of repose. The expression for longshore transport, I_1 , by Inman and Bagnold (1963) shows that

$$I_1 \propto \frac{1}{\tan \phi_f}$$

where ϕ_f is the intergranular friction coefficient which is usually assumed equivalent to the angle of repose of the sediment. Therefore the smaller the ϕ value the greater the likelihood for transport, although for the 2D flume tests this must be thought of in terms of onshore-offshore transport rather than longshore transport.

10. After initial three-dimensional testing with glass beads, it was found necessary to use coal as discussed in paragraphs 71-73 of the main text.

Test	Sediment (S.G., diam)	Wave Height H_o ft	Wave Period T sec	Wave Steepness H_o/L_o ft	Observed Sediment Movement in Model Flume*	Johnson Criterion		D of
						Direction of Movement	Agreement with Model	
1	Coal	0.036	0.7	0.016	On	On	Yes	
2	(1.37, 1.0 mm)	0.072	0.7	0.029	On	Off	No	
3		0.146	1.1	0.023	On	On	Yes	
4		0.080	1.1	0.013	On	On	Yes	
5		0.039	1.1	0.006	On	On	Yes	
6		0.153	1.5	0.013	On	On	Yes	
7		0.085	1.5	0.007	On	On	Yes	
8		0.041	1.5	0.004	On	On	Yes	
9	Glass beads	0.153	1.5	0.013	Off	On	No	
10	(2.42, 0.08 mm)	0.041	1.5	0.004	Off	On	No	
11		0.072	0.7	0.029	Off	Off	Yes	
12	Coal	0.080	1.1	0.013	Mixed	On	Yes	
13	(1.36, 0.5 mm)	0.039	1.1	0.006	On	On	Yes	
14		0.039	0.7	0.016	On	On	Yes	
15		0.072	0.7	0.029	On	Off	No	
16		0.153	1.5	0.013	Mixed	On	Yes	
17		0.085	1.5	0.007	Mixed	On	Yes	
18		0.041	1.5	0.004	Mixed	On	Yes	
19	Plastic	0.041	1.5	0.004	On	On	Yes	
20	(1.18, 3.0 mm)	0.085	1.5	0.007	On	On	Yes	
21		0.153	1.5	0.013	On	On	Yes	
22		0.039	1.1	0.016	No	On	--	
23		0.080	1.1	0.013	On	On	Yes	
24		0.146	1.1	0.023	On	On	Yes	
25		0.039	0.7	0.016	No	On	--	
26		0.072	0.7	0.029	On	Off	No	
27	Sand	0.039	0.7	0.016	No	On	--	
28	(2.65, 0.25 mm)	0.072	0.7	0.029	No	Off	--	
29		0.146	1.1	0.023	Off	On	No	
30		0.080	1.1	0.013	On	On	Yes	
31		0.153	1.5	0.013	Mixed	On	Yes	
32		0.085	1.5	0.007	On	On	Yes	
33	Glass beads	0.153	1.5	0.013	Off	On	No	
34	(2.42, 0.13 mm)	0.085	1.5	0.007	Mixed	On	Yes	
35		0.041	1.5	0.004	On	On	Yes	
36		0.146	1.1	0.023	Off	On	No	
37		0.080	1.1	0.013	Off	On	No	
38		0.039	1.1	0.006	On	On	Yes	
39		0.072	0.7	0.029	Off	Off	Yes	
40		0.039	0.7	0.016	Mixed	On	Yes	

* On = onshore movement; Off = offshore movement; Mixed = some offshore, some onshore

Table A1

Comparison of Onshore-Offshore Sediment Movement of Flume Tests with Various Prototype Criteria

Comparison Criterion		Prototype Sediment Movement Predicted by							
		Dean Criterion				Noda Criterion			
		$D_{50} = 0.25 \text{ mm}$		$D_{50} = 0.8 \text{ mm}$		$D_{50} = 0.25 \text{ mm}$		$D_{50} = 0.8 \text{ mm}$	
Direction of Movement	Agreement with Model	Direction of Movement	Agreement with Model	Direction of Movement	Agreement with Model	Direction of Movement	Agreement with Model	Direction of Movement	Agreement with Model
Off	Yes	Off	No	Off	No	Off	No	Off	No
Off	No	Off	No	Off	No	Off	No	Off	No
Off	Yes	Off	No	Off	No	Off	No	Off	No
Off	Yes	Off	No	Off	No	Off	No	Off	No
Off	Yes	Off	No	On	Yes	Off	No	On	No
Off	Yes	Off	No	Off	No	Off	No	Off	No
Off	Yes	Off	No	Off	No	Off	No	Off	No
Off	Yes	Off	No	On	Yes	Off	No	On	No
Off	No	Off	Yes	Off	Yes	Off	Yes	Off	Yes
On	No	Off	Yes	On	No	Off	Yes	On	No
Off	Yes	Off	Yes	Off	Yes	Off	Yes	Off	Yes
Off	Yes	Off	Yes	Off	Yes	Off	Yes	Off	Yes
Off	Yes	Off	No	On	Yes	Off	No	On	No
Off	Yes	Off	No	Off	No	Off	No	Off	No
Off	No	Off	No	Off	No	Off	No	Off	No
Off	Yes	Off	Yes	Off	Yes	Off	Yes	Off	Yes
Off	Yes	Off	Yes	Off	Yes	Off	Yes	Off	Yes
Off	Yes	Off	Yes	On	Yes	Off	Yes	On	No
Off	Yes	Off	No	On	Yes	Off	No	On	No
Off	Yes	Off	No	Off	No	Off	No	Off	No
Off	--	Off	--	On	--	Off	--	On	--
Off	Yes	Off	No	Off	No	Off	No	Off	No
Off	Yes	Off	No	Off	No	Off	No	Off	No
Off	--	Off	--	Off	--	Off	--	Off	--
Off	No	Off	No	Off	No	Off	No	Off	No
Off	--	Off	--	Off	--	Off	--	Off	--
Off	--	Off	--	Off	--	Off	--	Off	--
Off	No	Off	Yes	Off	Yes	Off	Yes	Off	Yes
Off	Yes	Off	No	Off	No	Off	No	Off	No
Off	Yes	Off	Yes	Off	Yes	Off	Yes	Off	Yes
Off	Yes	Off	No	Off	No	Off	No	Off	No
Off	No	Off	Yes	Off	Yes	Off	Yes	Off	Yes
Off	Yes	Off	Yes	Off	Yes	Off	Yes	Off	Yes
Off	Yes	Off	No	On	Yes	Off	No	On	No
Off	No	Off	Yes	Off	Yes	Off	Yes	Off	Yes
Off	No	Off	Yes	Off	Yes	Off	Yes	Off	Yes
Off	Yes	Off	No	On	Yes	Off	No	On	No
Off	Yes	Off	Yes	Off	Yes	Off	Yes	Off	Yes
Off	Yes	Off	Yes	Off	Yes	Off	Yes	Off	Yes

fshore, some onshore.

2

with Various Prototype Criteria

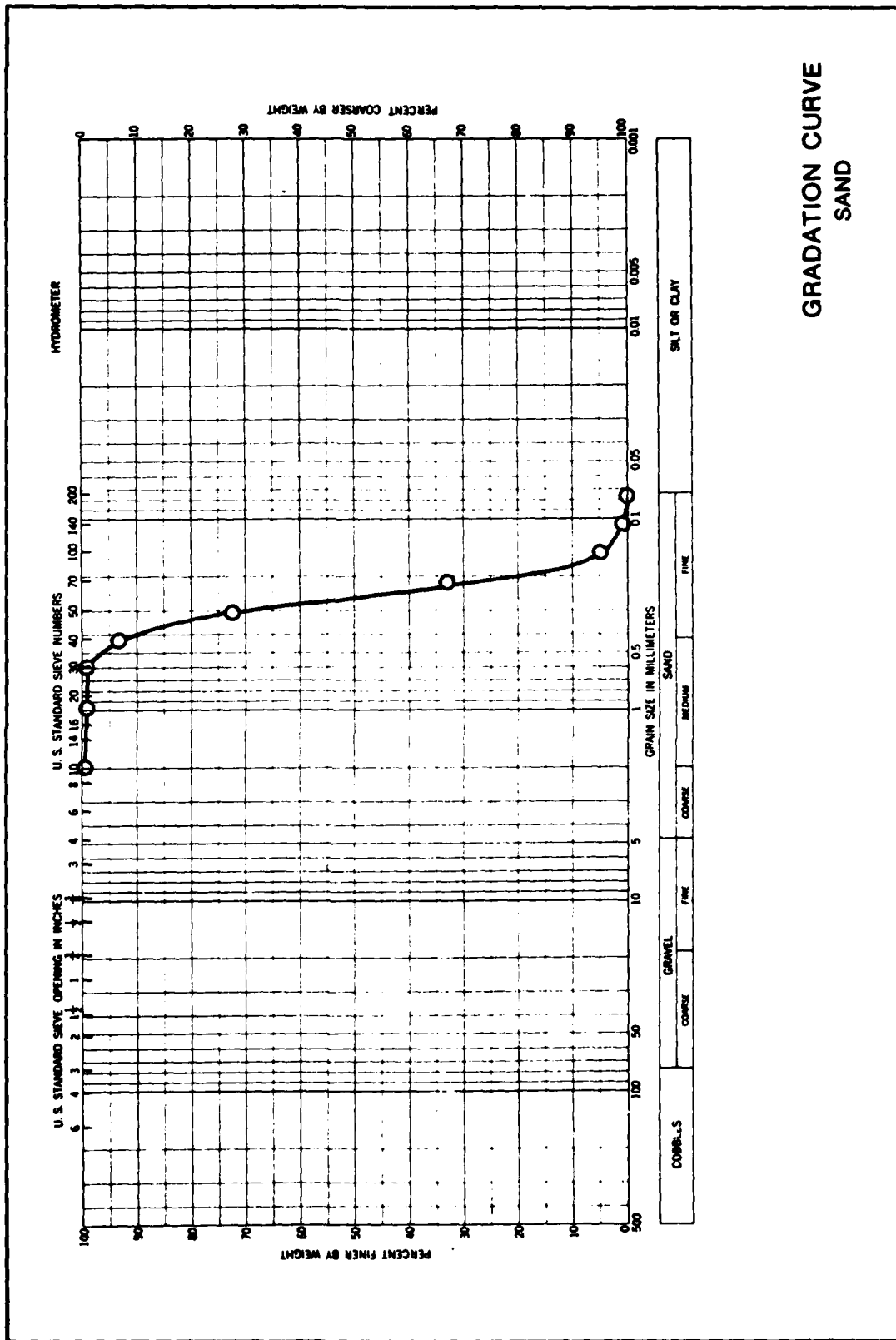
type Sediment Movement Predicted by

t el	Noda Criterion				Nayak Criterion			
	$D_{50} = 0.25 \text{ mm}$		$D_{50} = 0.8 \text{ mm}$		$D_{50} = 0.25 \text{ mm}$		$D_{50} = 0.8 \text{ mm}$	
	Direction of Movement	Agreement with Model	Direction of Movement	Agreement with Model	Direction of Movement	Agreement with Model	Direction of Movement	Agreement with Model
	Off	No	Off	No	Off	No	Off	No
	Off	No	Off	No	Off	No	Off	No
	Off	No	Off	No	Off	No	Off	No
	Off	No	Off	No	Off	No	Off	No
	Off	No	On	Yes	Off	No	Off	No
	Off	No	Off	No	Off	No	Off	No
	Off	No	Off	No	Off	No	Off	No
	Off	No	On	Yes	Off	No	Off	No
	Off	Yes	Off	Yes	Off	Yes	Off	Yes
	Off	Yes	On	No	Off	Yes	Off	Yes
	Off	Yes	Off	Yes	Off	Yes	Off	Yes
	Off	Yes	Off	Yes	Off	Yes	Off	Yes
	Off	No	On	Yes	Off	No	Off	No
	Off	No	Off	No	Off	No	Off	No
	Off	No	Off	No	Off	No	Off	No
	Off	No	Off	No	Off	No	Off	No
	Off	Yes	Off	Yes	Off	Yes	Off	Yes
	Off	Yes	Off	Yes	Off	Yes	Off	Yes
	Off	Yes	On	Yes	Off	Yes	Off	Yes
	Off	No	On	Yes	Off	No	Off	No
	Off	No	Off	No	Off	No	Off	No
	Off	No	Off	No	Off	No	Off	No
	Off	--	On	--	Off	--	Off	--
	Off	No	Off	No	Off	No	Off	No
	Off	No	Off	No	Off	No	Off	No
	Off	--	Off	--	Off	--	Off	--
	Off	No	Off	No	Off	No	Off	No
	Off	--	Off	--	Off	--	Off	--
	Off	--	Off	--	Off	--	Off	--
	Off	Yes	Off	Yes	Off	Yes	Off	Yes
	Off	No	Off	No	Off	No	Off	No
	Off	Yes	Off	Yes	Off	Yes	Off	Yes
	Off	No	Off	No	Off	No	Off	No
	Off	Yes	Off	Yes	Off	Yes	Off	Yes
	Off	Yes	Off	Yes	Off	Yes	Off	Yes
	Off	No	On	Yes	Off	No	Off	No
	Off	Yes	Off	Yes	Off	Yes	Off	Yes
	Off	No	On	Yes	Off	No	Off	No
	Off	Yes	Off	Yes	Off	Yes	Off	Yes
	Off	Yes	Off	Yes	Off	Yes	Off	Yes

2

1

3



**GRADATION CURVE
SAND**

AD-A129 508

WEIR JETTY PERFORMANCE: HYDRAULIC AND SEDIMENTARY
CONSIDERATIONS(U) ARMY ENGINEER WATERWAYS EXPERIMENT
STATION VICKSBURG MS HYDRAULICS LAB W C SEABERGH

4/4

UNCLASSIFIED

MAR 83 WES/TR/HL-83-5

F/G 13/2

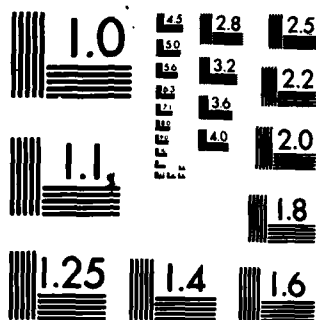
NL

END

DATE

FILED

DTIC



MICROCOPY RESOLUTION TEST CHART
NATIONAL BUREAU OF STANDARDS-1963-A

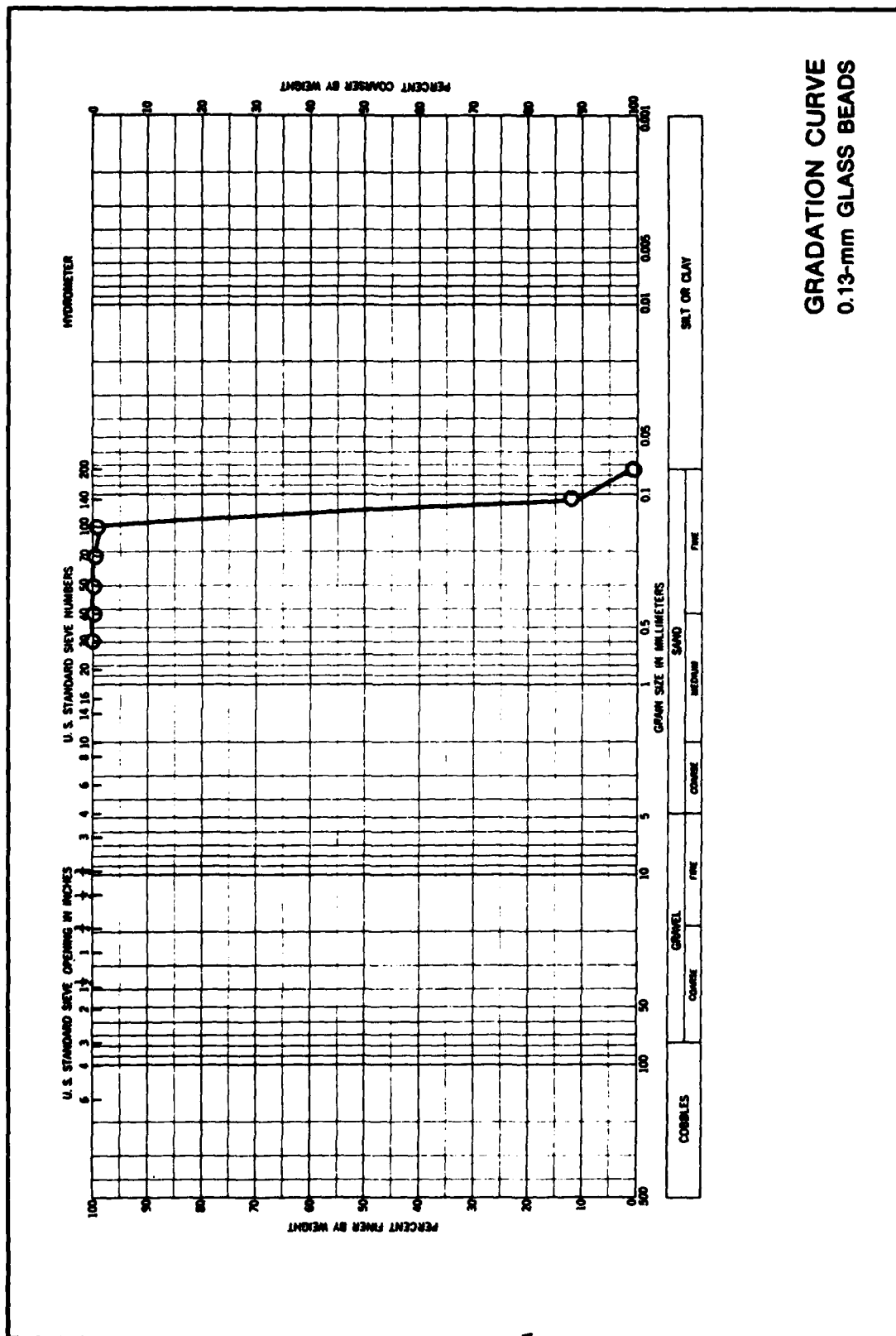
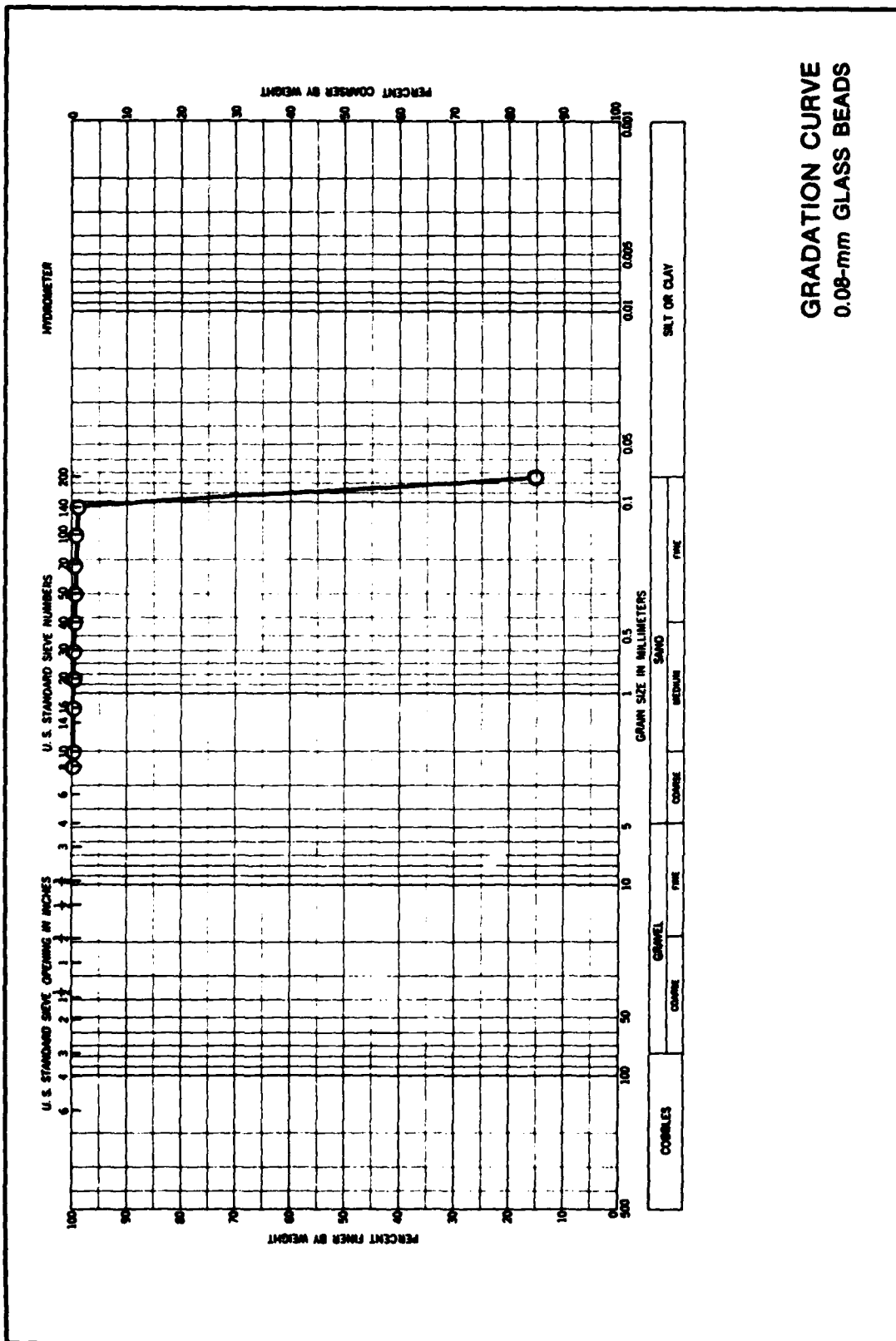


PLATE A2



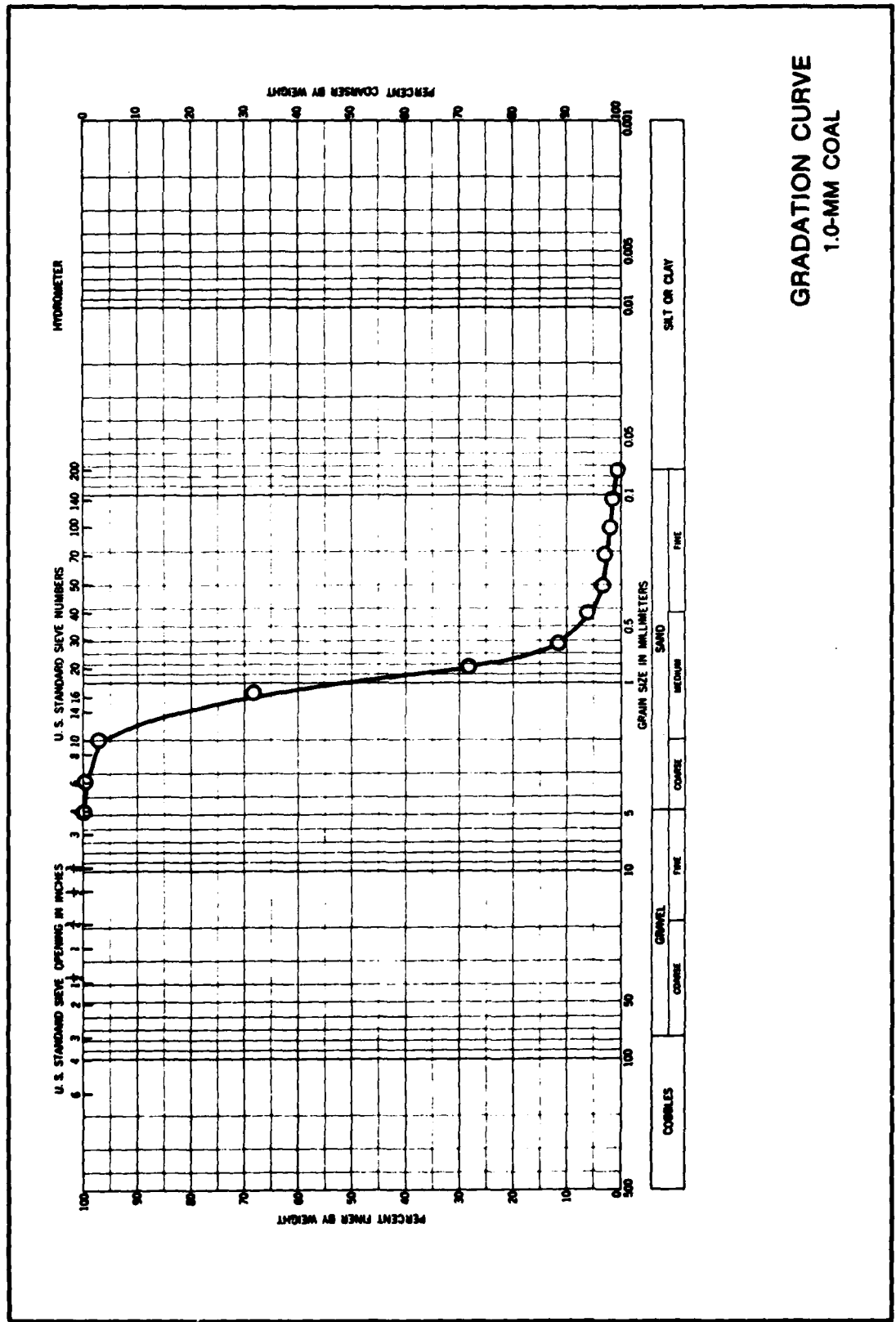
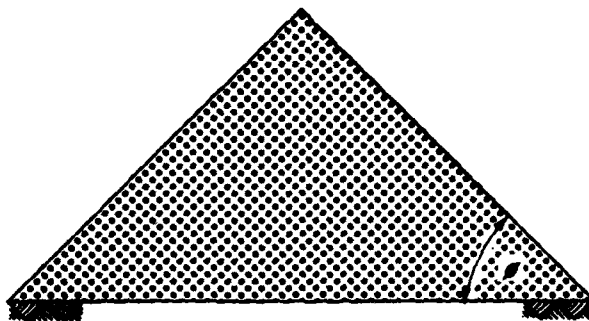


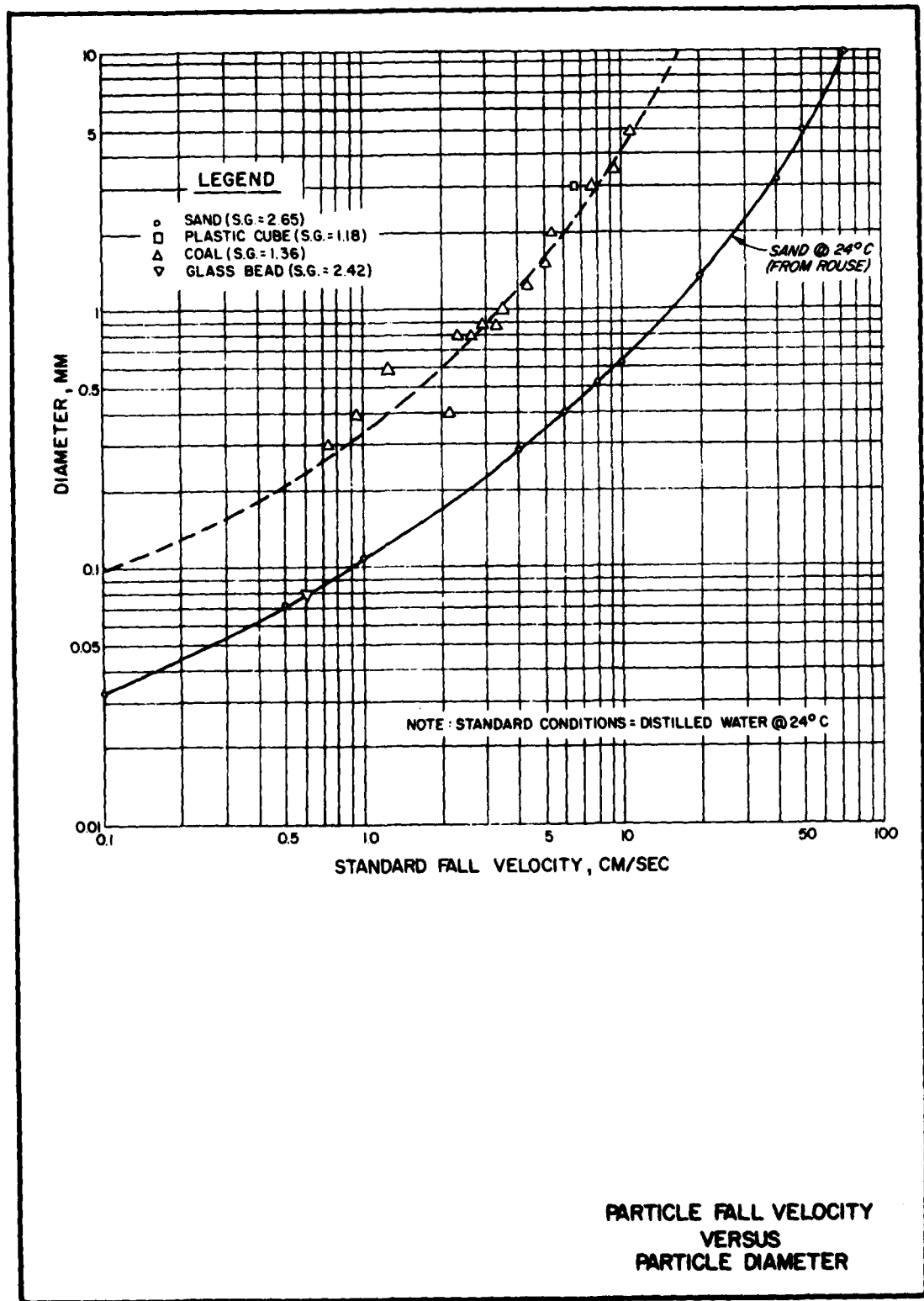
PLATE A4



ϕ = ANGLE OF REPOSE

MATERIAL USED	ϕ WET	ϕ DRY
1. SAND (0.25 mm)	31°	33°
2. GLASS BEADS (0.13 mm)	21°	24°
3. GLASS BEADS (0.08 mm)	19°	24°
4. COAL (1.00 mm)	35°	33°
5. COAL (0.50 mm)	26°	33°
6. PLASTIC (3.0 mm)	35°	35°

ANGLE OF REPOSE
FOR MATERIALS TESTED



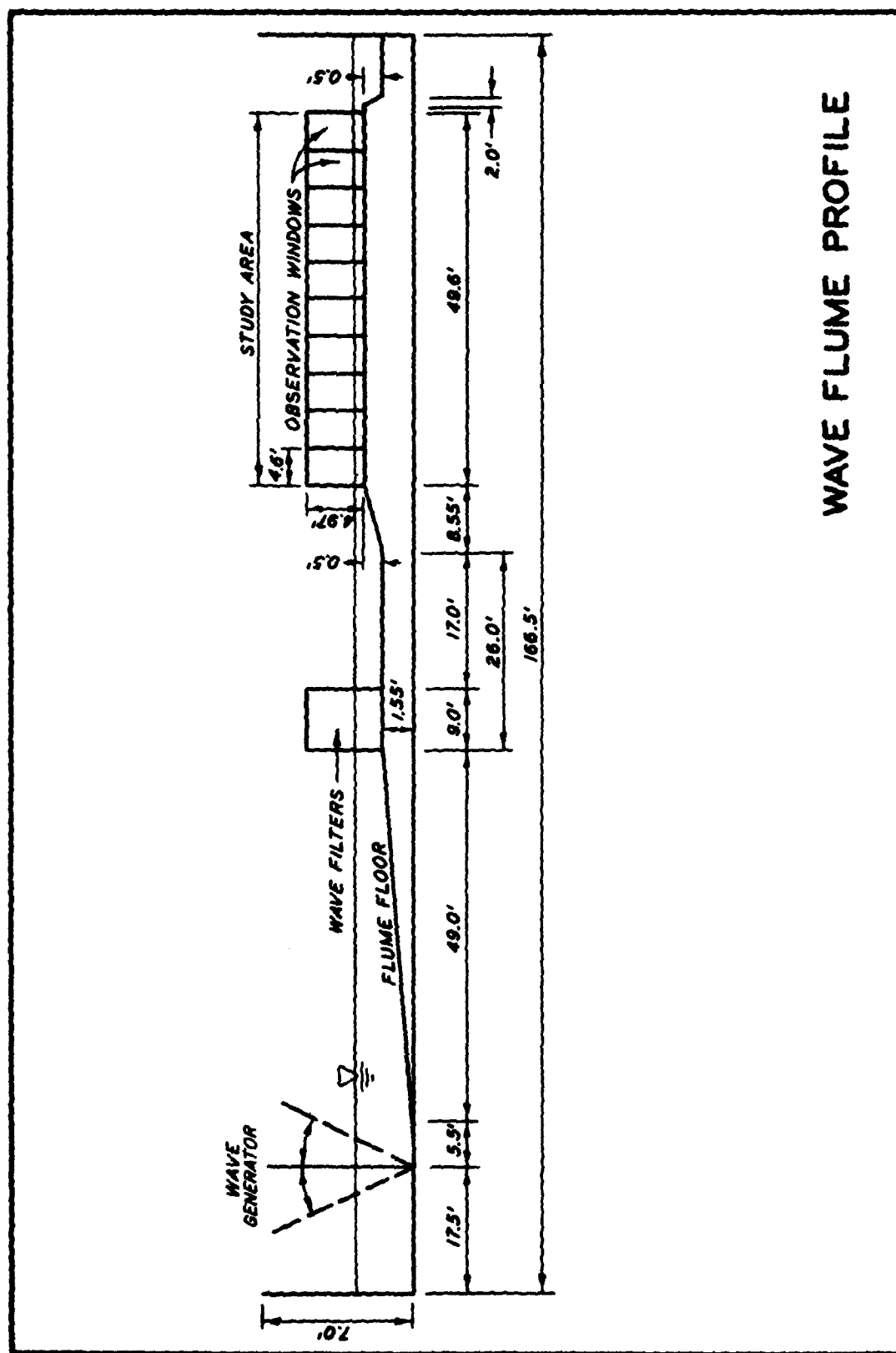
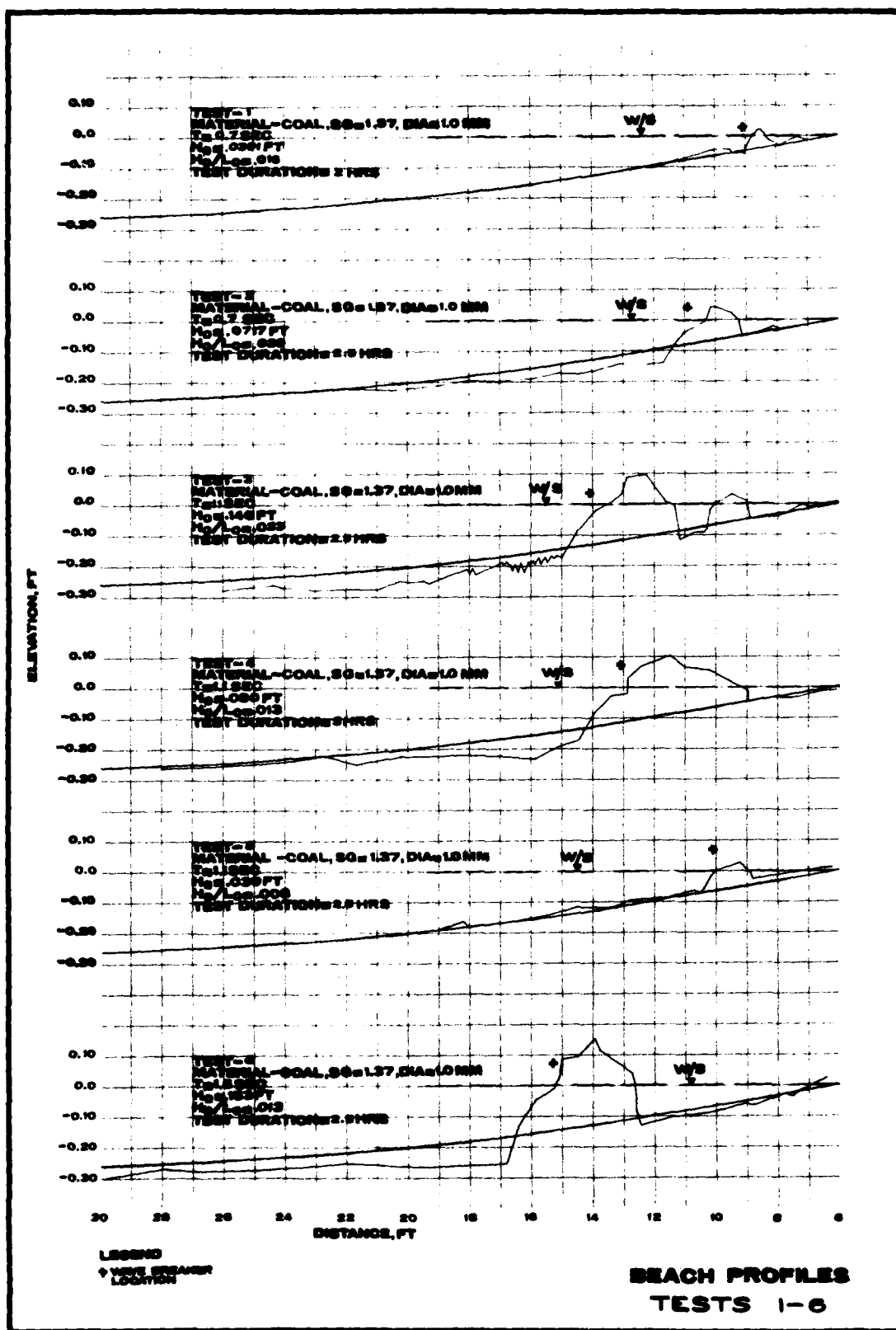
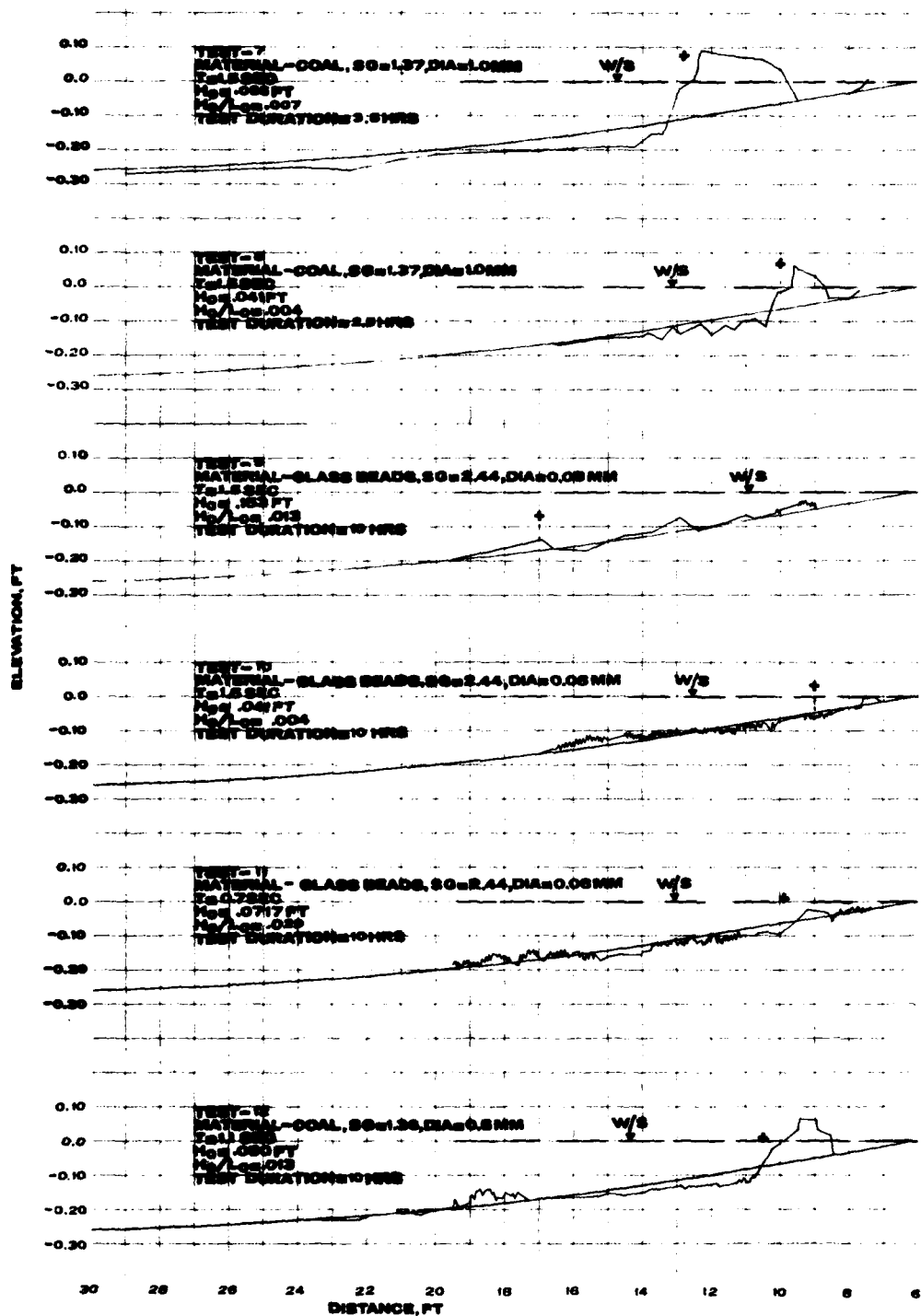


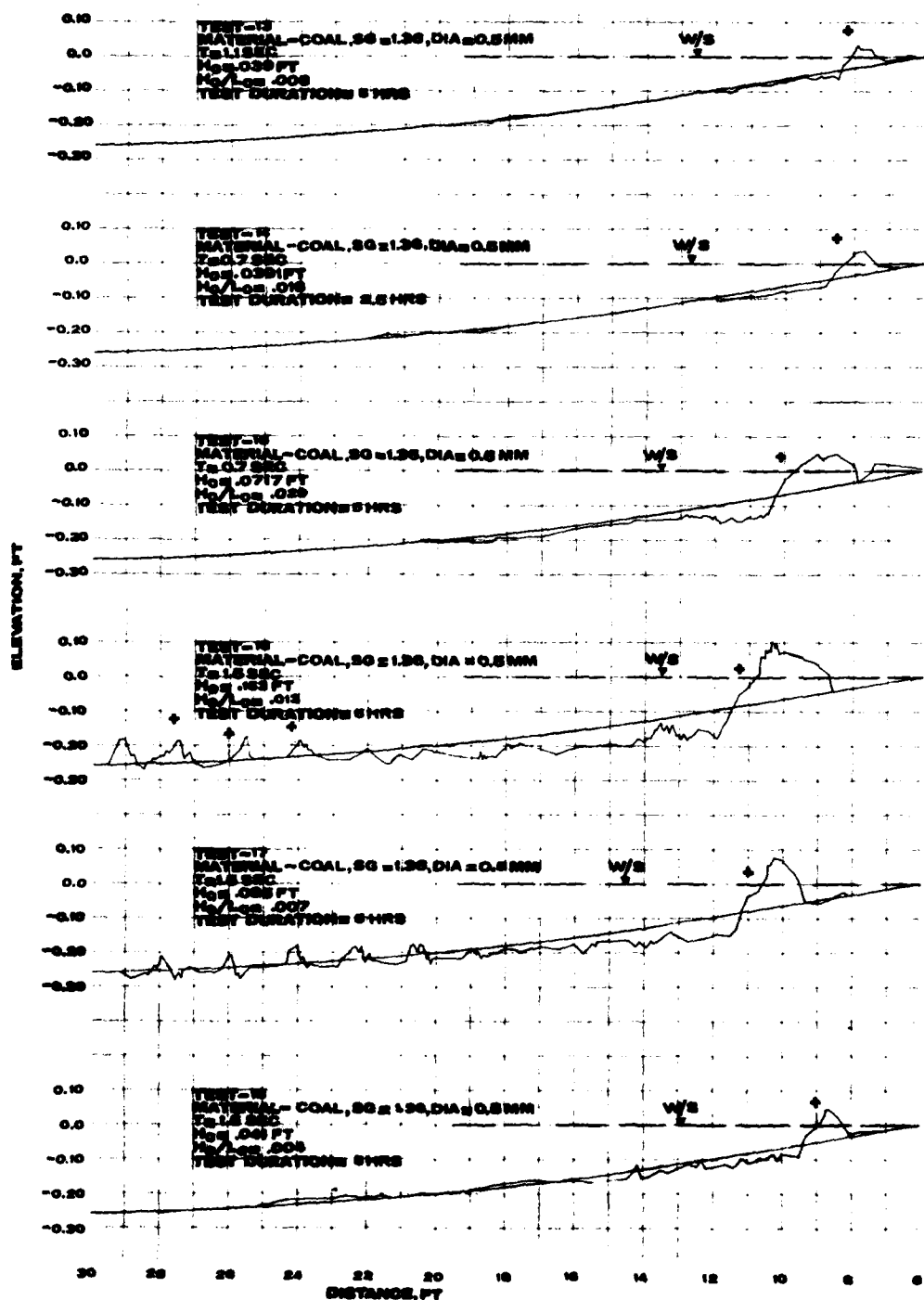
PLATE A8

WAVE FLUME PROFILE





BEACH PROFILES TESTS 7-12



**BEACH PROFILES
 TESTS 13-18**

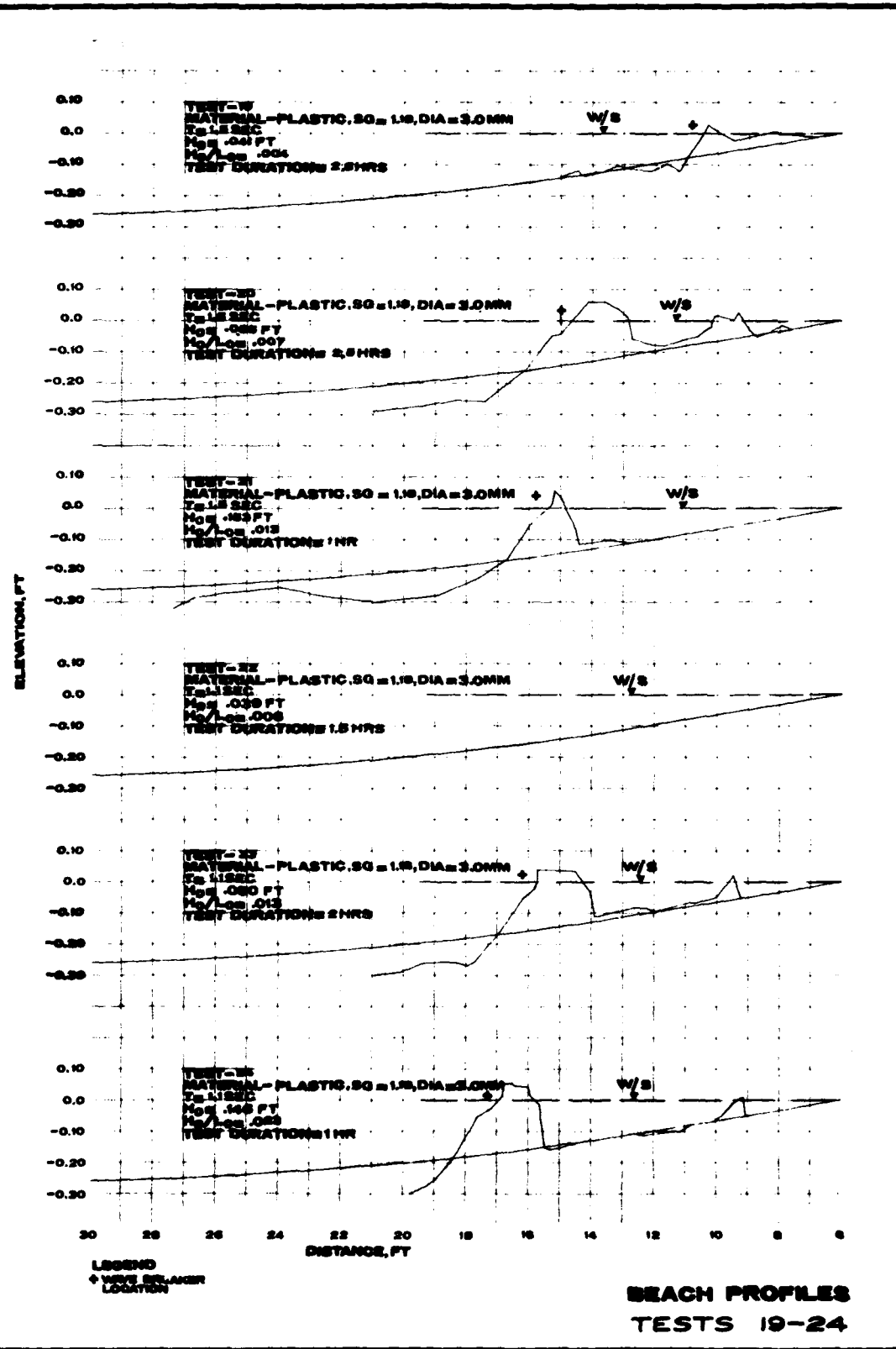
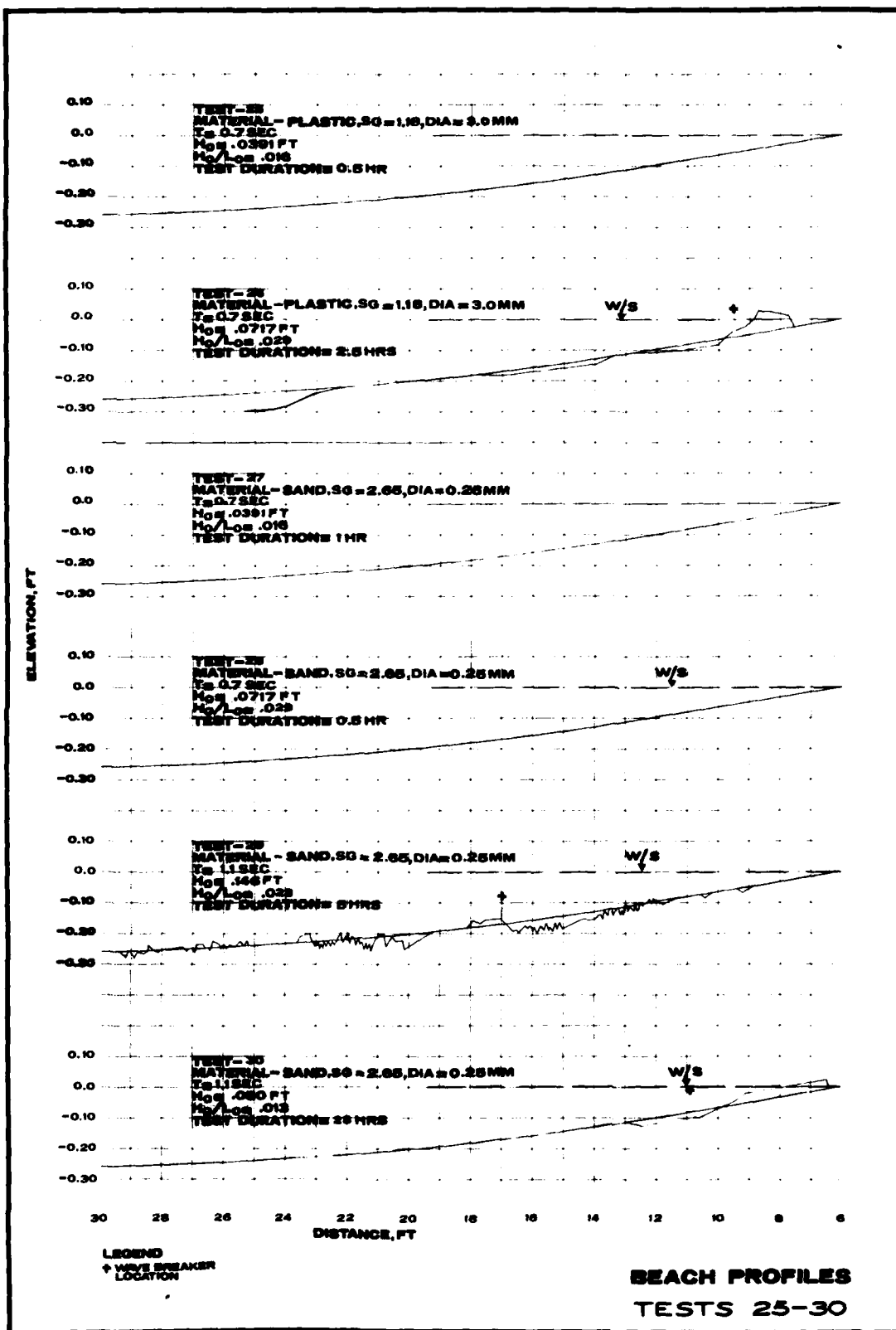


PLATE A12



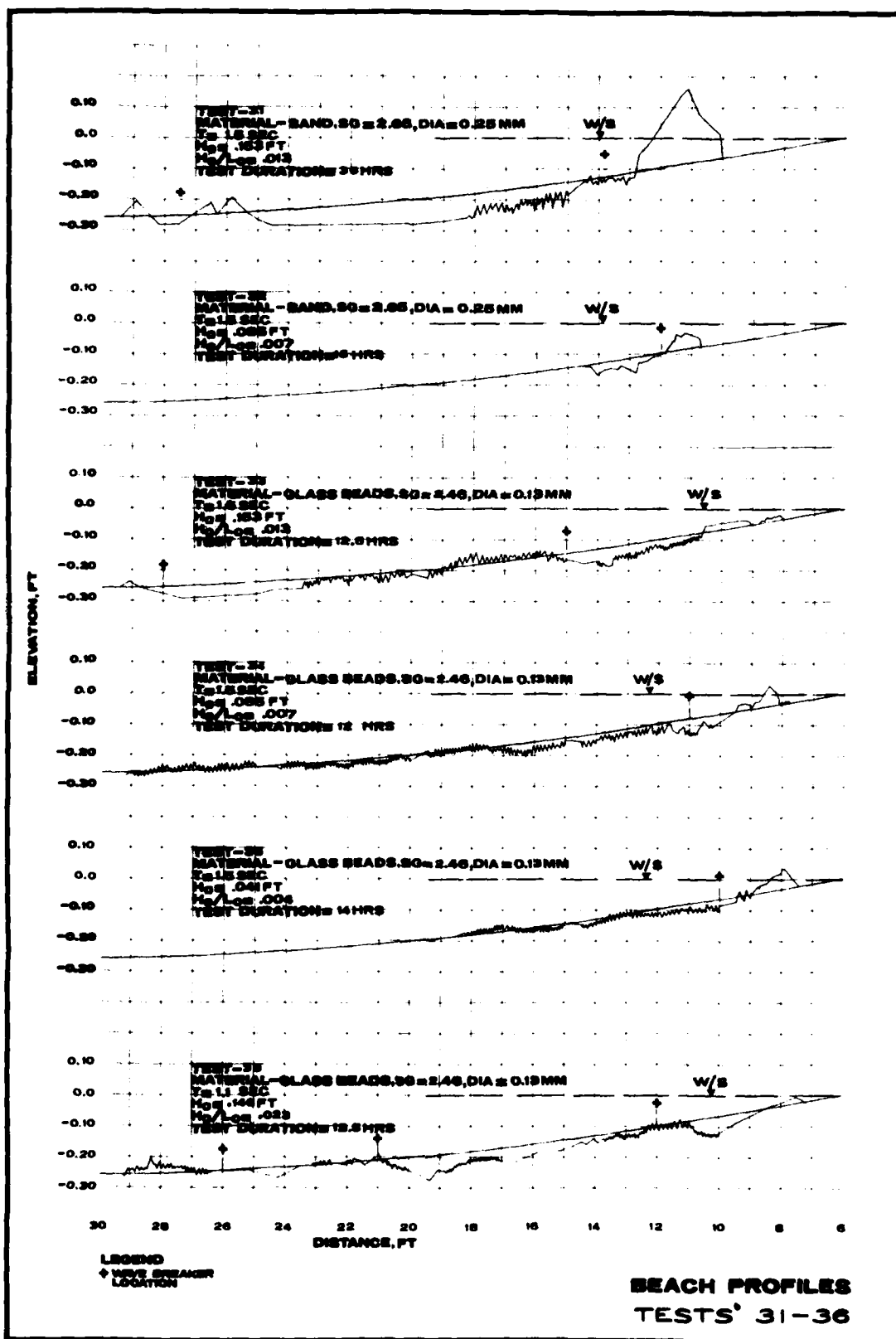
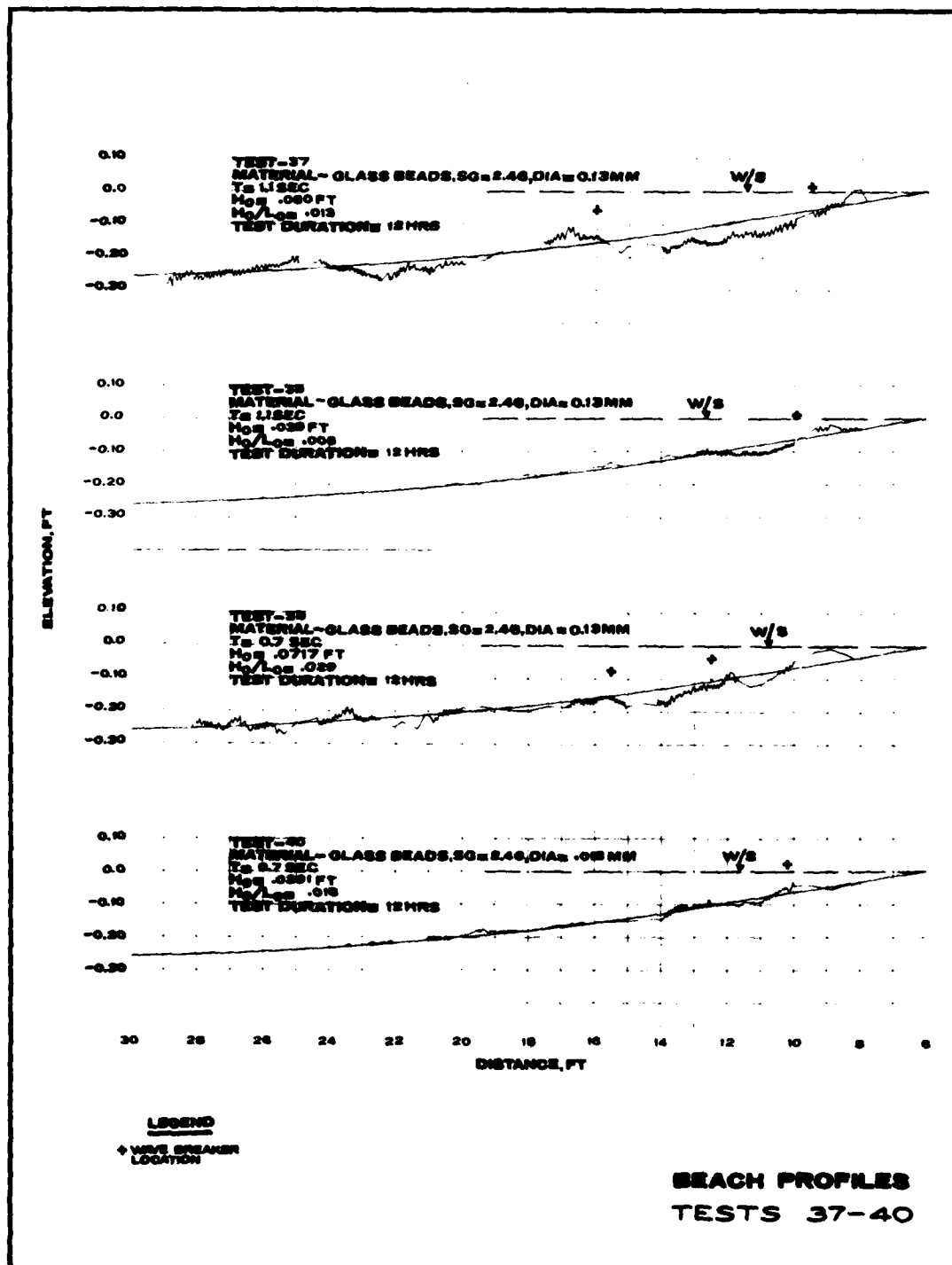


PLATE A14



APPENDIX B: NOTATION

a'	Correction factor for pore space
a_b	Bay tide amplitude, half range, ft
a_o	Ocean tidal amplitude, half range, ft
A_b	Surface area of bay, ft^2
A_c	Cross-sectional flow area of inlet, ft^2
A_{CE}	Equilibrium minimum cross-sectional flow area below mean sea level, ft^2
A_L	Incident wave amplitude, ft
A_{SC}	Short-crested wave amplitude, ft
A_1	Flow area between jetty tips at oceanward end of jetties, ft^2
A_2	Flow area at inlet gorge, equivalent to A_c , ft^2
C	Dimensionless number, function of Keulegan K
C_i	Incident wave celerity, fps
C_s	Short-crested wave celerity, fps
f	Darcy-Weisbach friction coefficient
F	Inlet impedance = $K_i + K_e + fL_c/4R_c$
g	Acceleration due to gravity, ft/sec^2
H	Wave height, ft
H_b	Breaker height, ft
H_o	Deepwater wave height, ft
I_1	Immersed weight transport rate, lb/sec
K	Keulegan repletion coefficient
K	Dimensionless constant in sediment transport formula
K_e	Inlet exit loss coefficient
K_i	Inlet entrance loss coefficient
K_r	Reflection coefficient of structure

L	Wave length, ft
L'	Crest length of short-crested wave, ft
L _c	Inlet channel length, ft
L _H	Horizontal length
L _i	Incident wave length, ft
L _O	Deepwater wave length, ft
L _s	Short-crested wave length, ft
L _v	Vertical length, ft
P	Tidal prism, ft ²
P _{ls}	Longshore energy flux factor, ft-lb/sec/linear ft of beach
q	Unit discharge over weir, ft ² /sec
Q	Longshore sediment transport rate, yd ³ /yr
Q _m	Maximum discharge, ft ³ /sec
R _c	Hydraulic radius of inlet channel flow area, ft
S _i	Volume transport rate, ft ³ /sec
T	Tidal period, wave period, sec
U _{MBL}	Maximum bottom velocity at a given depth for incident wave, fps
U _{MBSC}	Maximum bottom velocity at a given depth for short-crested wave, fps
V	Average velocity over weir, fps
V _m	Maximum average velocity, fps
V _{max}	Maximum average velocity over weir, fps
w	Fall velocity of sediment, cm/sec
W	Distance between maximum crestlines, ft
α	Acute angle between structure and shoreline
α _b	Breaker angle, deg
ΔH	Head difference across weir section, ft
θ	Acute angle between incident wave crest and structure, deg

θ_r Angle between reflected wave crest and shoreline, deg
 χ Width of circulation cell along shoreline, ft
 ϕ Angle between incident wave crest and structure, deg
 ϕ_f Intergranular friction coefficient
 ρ Water density, lb-sec²/ft⁴
 ρ_s Sediment density, lb-sec²/ft⁴

In accordance with letter from DAEN-RDC, DAEN-ASI dated 22 July 1977, Subject: Facsimile Catalog Cards for Laboratory Technical Publications, a facsimile catalog card in Library of Congress MARC format is reproduced below.

Seabergh, William C.

Weir jetty performance: hydraulic and sedimentary consideration : Hydraulic model investigation / by William C. Seabergh (Hydraulics Laboratory, U.S. Army Engineer Waterways Experiment Station). -- Vicksburg, Miss. : The Station ; Springfield, Va. : available from NTIS, 1983.

299 p. in various pagings, 120 p. of plates : ill. ; 27 cm. -- (Technical report ; HL-83-5)

Cover title.

"March 1983."

Final report.

"Prepared for U.S. Army Engineering Research Center, Fort Belvoir, Va."

Bibliography: p. 104-106.

Seabergh, William C.

Weir jetty performance: hydraulic and sedimentary ... 1983.
(Card 2)

1. Hydraulic models. 2. Hydraulic structures.
3. Inlets. 4. Jetties. 5. Sediment transport.
I. Coastal Engineering Research Center (U.S.).
II. U.S. Army Engineer Waterways Experiment Station.
Hydraulics Laboratory. III. Title IV. Series: Technical report (U.S. Army Engineer Waterways Experiment Station) ; HL-83-5.
TA7.W34 no.HL-83-5.

8
DTIC